

Oxidative Palladium(II)-Catalyzed Arene C–H Bond  
Functionalization And Progress Towards The Total  
Synthesis of 6-Deoxyerythronolide B

by

Nadine Borduas

A thesis submitted in conformity with the requirements  
for the degree of Master's of Science

Department of Chemistry  
University of Toronto

© Copyright by Nadine Borduas 2012

# Palladium(II)-Catalyzed Arene C–H Bond Functionalizations And Progress Towards The Total Synthesis of 6-Deoxyerythronolide B

Nadine Borduas

Master's of Science

Department of Chemistry  
University of Toronto

2012

## Abstract

To address the issue of unnecessary functional group transformations in synthesis, the direct functionalization of carbon-hydrogen (C–H) bonds presents itself as an efficient and atom economical process. In particular, palladium(II)-catalyzed oxidative functionalization of arene C–H bonds were investigated to yield intermolecular and intramolecular arylations. Kinetic studies and characterization of bimetallic palladium(II) complexes led to the discovery of two other palladium(II)-catalyzed processes: arene hydroxylation and selective chlorination of anilides.

Realizing the potential of biocatalysis and of transition-metal catalysis, we married these two fundamentally different methods to access complex molecules in rapid and step economical ways and chose popular synthetic target, 6-deoxyerythronolide B to showcase the efficiency of these stereoselective reactions. To form the 14-membered lactone, we employed a transition-metal catalyzed ring-closing metathesis. Two different fragments were assembled via traditional and reliable aldols, oxidations and reductions, crotylations and protective group chemistry.

## Acknowledgments

Thank you to my supervisor Vy Dong and all my colleagues who have helped me grow as a chemist and as a person. I have learned an incredible amount over my two years in the Dong Group and this is thanks to a challenging and stimulating environment. In particular, I would like to thank my collaborators on the oxidative cross-coupling project, Charles Yeung and Xiaodan Zhao. In addition, thank you to Peter Dornan, Kevin Kou and Tom Hsieh for their hard work and excellent skill on the total synthesis of 6-deoxyerythronolide B. Also, thank you to Prof. Rob Batey for his helpful comments in proof reading this thesis. I would like to acknowledge Dr. Alan Lough and Dr. Tim Burrows who have been very helpful with data interpretation.

I would also like to show my gratitude towards my husband, my family and my friends who never stop believing in my capabilities as a scientist. Their encouragement and support is priceless.

I would like to acknowledge the funding agencies that have greatly encouraged me through numerous prestigious awards: the Julie-Payette NSERC scholarship, the Andre Hamer Award and the Vanier Canada Graduate Scholarship. Their belief in my leadership skills has made me a stronger and a more devoted scientist and leader.

# Table of Contents

Acknowledgments.....	iii
Table of Contents.....	iv
List of Tables and Graphs.....	vii
List of Figures and Schemes.....	ix
Chapter 1 Pd(II)-Catalyzed C–H Bond Functionalization With Arenes .....	1
1 Pd(II)-Catalyzed Oxidative Cross-Coupling of Two Arenes.....	1
1.1 Introduction to C–H Bond Functionalization .....	1
1.2 Literature Precedence.....	2
1.2.1 Intermolecular Pd(II)-Catalyzed Oxidative Cross-Coupling .....	2
1.2.2 Intramolecular Pd(II)-Catalyzed oxidative cross-coupling.....	7
1.3 Development of an Intramolecular Pd(II)-Catalyzed Oxidative Arylation .....	11
1.3.1 Seven-membered lactams .....	11
1.3.2 Six-membered lactams.....	15
1.3.3 Preliminary Kinetic Studies .....	20
1.4 Experimental Data .....	26
Chapter 2 Synthesis, Characterization and Reactivity of Pd-Bimetallic Complexes .....	42
2 Cyclopalladation of <i>N</i> -Phenylbenzamides .....	42
2.1 Introduction.....	42
2.2 Synthesis of Palladium Complexes.....	43
2.3 Characterization of the Palladium Complexes.....	44
2.4 Stoichiometric Experiments of the Palladium Complexes .....	48
2.5 Catalytic Reactivity of the Palladium Complexes .....	49
2.6 Experimental.....	50
2.6.1 Crystallographic Data .....	50

2.6.2	Synthesis of Complexes .....	51
Chapter 3	Pd(II)-Catalyzed C–H Bond Functionalization With Peroxides .....	54
3	New Reactivities with Tetrabutylammonium Persulfate .....	54
3.1	The Uses of Tetrabutylammonium Persulfate .....	54
3.2	Reaction Discovery .....	56
3.3	Literature Relevance for Observed Byproducts .....	57
3.4	Reaction Optimization .....	59
3.5	Stoichiometric Experiments .....	62
3.6	Outlook .....	63
3.7	Experimental Data .....	64
Chapter 4	Pd(II)-Catalyzed C–H Bond Functionalization With Sodium Chlorite .....	68
4	Pd(II)-Catalyzed Benzamide Chlorination .....	68
4.1	Introduction .....	68
4.2	Literature Precedence .....	68
4.3	Reaction Condition Optimization .....	69
4.4	Reaction Scope .....	73
4.5	Outlook .....	74
4.6	Experimental Data .....	74
Chapter 5	Towards the Total Synthesis of 6-Deoxyerythronolide B .....	76
5	Biocatalysis and Transition-Metal Catalysis for Polyketide Synthesis .....	76
5.1	Introduction to Erythromycin .....	76
5.2	Biosynthesis of Erythromycin .....	77
5.2.1	The Polyketide Synthase .....	77
5.2.2	Post Polyketide Synthase Modifications .....	78
5.3	Total Synthesis of 6-Deoxyerythronolide B .....	79
5.3.1	Mission .....	79

5.3.2	Retrosynthetic Approach to 6-Deoxyerythronolide B .....	80
5.3.3	Biocatalysis – Amphotericin’s Ketoreductase .....	81
5.4	Synthetic Efforts Towards 6-Deoxyerythronolide B .....	82
5.4.1	Synthesis of 1,3,5-Tricarbonyl Compounds .....	82
5.4.2	Synthesis of the Western Fragment .....	84
5.4.3	The Eastern Fragments .....	95
5.4.4	Testing for the End Game .....	96
5.5	Experimental Section .....	98
5.5.1	Tricarbonyls .....	99
5.5.2	Intermediates Towards the Western Fragment .....	132
	References .....	179

## List of Tables and Graphs

Chapter 1 Pd(II)-Catalyzed C–H Bond Functionalization With Arenes .....	1
Table 1: Table of parameters explored while optimizing the reaction conditions .....	12
Graph 1: Conversion of starting material and yield of dibenzoazepinone as a function of time. ....	15
Table 2: Scope of the oxidative intramolecular two fold C–H activation .....	17
Table 3: Substrates with purification issues and GC yields are reported.....	19
Graph 2: Reaction profile of 3 identical oxidative cross-coupling reactions.....	22
Graph 3: Effect of TFA on yield and conversion.....	23
Graph 4: Effect of TFA on rate .....	24
Graph 5: effect of Pd(OAc) <sub>2</sub> on yield and conversion .....	25
Graph 6: effect of Pd(OAc) <sub>2</sub> on rate .....	25
Chapter 2 Synthesis, Characterization and Reactivity of Pd-Bimetallic Complexes .....	42
Table 5: Synthesis and characterization of the Pd-complexes .....	43
Table 6: Crystal data and structure refinement for crystal structures of Pd-complexes a, b and c. ....	45
Table 7: Selected bond lengths [Å] and bond angles [°] for 3a, 3b and 3c.....	47
Table 8: Stoichiometric reductive elimination reactions .....	49
Table 9: Comparison of Pd(II) catalysts in the oxidative intramolecular cross-coupling reaction.....	50
Chapter 3 Pd(II)-Catalyzed C–H Bond Functionalization With Peroxides .....	54
Table 10: Cross-coupling reaction optimization with TBAPS .....	59
Table 11: Cross-coupling reaction optimization at room temperature with TBAPS .....	60
Table 12: Reaction optimization without benzene for hydroxylation and carboxylation .....	61
Chapter 4 Pd(II)-Catalyzed C–H Bond Functionalization With Sodium Chlorite .....	68
Table 13: Reaction optimization for the <i>ortho</i> -chlorination of 3-methylanilides .....	71

Table 14: Reaction optimization for the <i>ortho</i> -chlorination of anilides .....	72
Chapter 5 Towards the Total Synthesis of 6-Deoxyerythronolide B.....	76
Table 15: Aldol screening parameters with methyl enone as the aldol donor .....	88
Table 16: Aldol optimization table with $\beta$ -amino ketone as the aldol donor.....	90



## List of Figures and Schemes

Chapter 1 Pd(II)-Catalyzed C–H Bond Functionalization With Arenes .....	1
Scheme 1: C—H activation leading to a variety of products.....	1
Scheme 2: Fagnou's selective C3 arylation of <i>N</i> -acylated indoles.....	3
Scheme 3: Pd-catalyzed C8 arylation of xanthenes .....	4
Scheme 4: Pd-catalyzed arylation of azoles.....	4
Scheme 5: Pd-catalyzed <i>ortho</i> -arylation of pyridine <i>N</i> -oxides with arenes and heteroarenes...	5
Scheme 6: Pd-catalyzed arylation of perfluorinated arenes with simple arenes and heteroarenes .....	5
Scheme 7: Sanford's <i>ortho</i> -arylation of benzo[ <i>h</i> ]quinoline with simple arenes.....	6
Scheme 8: Oxidative <i>ortho</i> -arylation with anilides as directing groups by Shi and Buchwald .....	7
Scheme 9: Intermolecular C–H bond functionalization of arenes .....	7
Scheme 10: Synthesis of carbazoles via an oxidative intramolecular cross-coupling by Fagnou and Menendez .....	8
Scheme 11: Synthesis of benzofurans via oxidative intramolecular cross-coupling .....	9
Scheme 12: Synthesis of 6H-isoindolo[2,1- <i>a</i> ]indolones via oxidative intramolecular cross-coupling.....	9
Scheme 13: Synthesis of triazole-tricyclic structures via oxidative intramolecular cross-coupling.....	10
Scheme 14: Synthesis of medium sized heterocycles via oxidative intramolecular cross-coupling.....	10
Scheme 15: Synthesis of dibenzoazepinone moiety .....	11
Scheme 16: Major byproduct formed in the presence of Pd(TFA) <sub>2</sub> .....	14
Scheme 17: Total synthesis of <i>N</i> -methylcrinasiadine via oxidative intramolecular cross-coupling.....	18
Figure 1: Unreactive substrates under oxidative cross-coupling reaction conditions.....	20
Scheme 18: Synthesis of dibenzofurans via oxidative intramolecular cross-coupling .....	20

Scheme 19: Optimized reaction conditions for the dehydrogenative cross-coupling of anilides and benzene used for kinetic studies .....	21
Chapter 2 Synthesis, Characterization and Reactivity of Pd-Bimetallic Complexes .....	42
Scheme 20: Reported Pd(II)-catalyzed intramolecular oxidative cross-coupling.....	42
Scheme 21: Possible palladacycles from N-phenylbenzamide.....	42
Figure 2: ORTEP plot of [(3-methoxy-N-methyl-N-phenylbenzamide)Pd( $\mu$ -TFA)] <sub>2</sub> (3a). All H atoms have been omitted for clarity. Anisotropic displacement ellipsoids are shown at the 50% probability level.....	46
Figure 3: ORTEP plot of [(3-methoxy-N-methyl-N-(o-tolyl)benzamide)Pd( $\mu$ -TFA)] <sub>2</sub> (3b). All H atoms have been omitted for clarity. Anisotropic displacement ellipsoids are shown at the 50% probability level.....	46
Figure 4: ORTEP plot of [(3,4-dimethoxy-N-methyl-N-phenylbenzamide)Pd( $\mu$ -TFA)] <sub>2</sub> (3c). All H atoms have been omitted for clarity. Anisotropic displacement ellipsoids are shown at the 50% probability level.....	47
Chapter 3 Pd(II)-Catalyzed C–H Bond Functionalization With Peroxides.....	54
Scheme 22: Oxidative phosphorylation of arene C–H bonds .....	54
Scheme 23: Cleavage of tosylhydrazones with TBAPS .....	55
Scheme 24: $\beta$ -masked formylation of cyclic $\alpha,\beta$ -unsaturated ketones.....	55
Scheme 25: TBAPS-initiated $\alpha$ -iodination of ketones .....	55
Scheme 26: Epoxidation of electron-deficient olefins with TBAPS and hydrogen peroxide..	56
Scheme 27: Synthesis of a soluble persulfate salt, TBAPS .....	56
Scheme 28: High reactivity of TBAPS in palladium-catalyzed cross-coupling reaction .....	57
Scheme 29: Yu's carboxylic acid directed and Pd-catalyzed ortho-hydroxylation.....	58
Scheme 30: Nagasawa's C-O forming reaction.....	58
Scheme 31: Synthesis of the dimeric palladacycle of N-(m-tolyl)pivalamide.....	62
Scheme 33: Reductive elimination with TBAPS without acid .....	63
Chapter 4 Pd(II)-Catalyzed C–H Bond Functionalization With Sodium Chlorite.....	68
Scheme 34: Sanford's Pd-catalyzed arene C–H bond halogenation reaction .....	68

Scheme 35: Chlorination of anilides with sodium chlorite as an unprecedented chlorinating agent.....	70
Figure 6: Preliminary scope of the chlorination reaction.....	73
Chapter 5 Towards the Total Synthesis of 6-Deoxyerythronolide B.....	76
Figure 7: Erythromycin A .....	76
Figure 9: Erythromycin's polyketide synthase .....	77
Figure 8: 6-deoxyerythronolide B .....	77
Scheme 36: Post-PKS biosynthesis of erythromycin A.....	78
Scheme 37: Retrosynthetic approach to 6-deoxyerythronolide B.....	80
Scheme 38: Envisioned biocatalytic approach to polyketide fragments.....	81
Scheme 39: Enzymatic reduction by AmpKR2, an isolated enzyme from amphotericin B's PKS .....	82
Scheme 40: Synthesis of 1,3,5-tricarbonyl ethyl ester via a Claisen condensation .....	83
Scheme 41: Synthesis of 1,3,5-tricarbonyl SNAC thioester .....	83
Scheme 42: Retrosynthetic approach to the western fragment .....	84
Scheme 43: Synthesis of Evans' oxazolidinone auxiliary .....	84
Scheme 44: Synthesis of the chiral aldehyde, the acceptor in the key aldol reaction.....	85
Scheme 45: Key aldol reaction and the four diastereomers generated .....	86
Scheme 46: Proposed transition state for the formation of the syn-aldol/anti-Felkin product .....	86
Scheme 47: Synthesis of aldol desired syn-aldol/anti Felkin aldol product by an analogous route to confirm Felkin stereochemistry .....	87
Scheme 48: Optimized reaction conditions for the aldol reaction with ethyl enone as the donor .....	91
Scheme 49: Attempted synthesis of the enone (top) and revised synthesis of the di-substituted olefin fragment (bottom) .....	92
Scheme 50: Synthesis of two analogous mono-substituted olefins for the western fragment .	94
Scheme 51: Alternate synthetic sequence towards an enone western fragment .....	95
Figure 10: Structures of the three eastern fragments synthesized.....	96

Scheme 52: Esterification and RCM yield the 14-membered core of erythronolide.....	96
Scheme 53: Proposed post-RCM synthetic steps to 6-deoxyerythronolide B .....	97

## Chapter 1

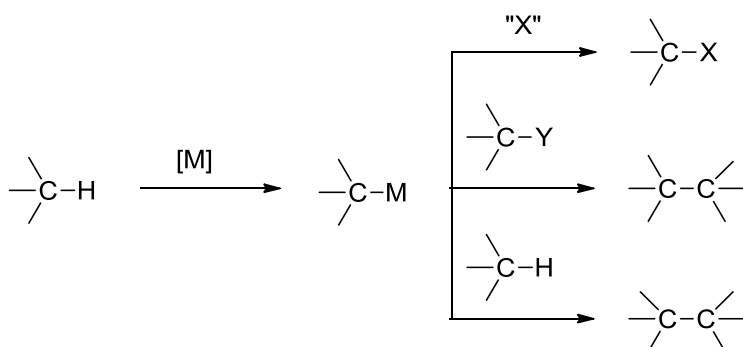
### Pd(II)-Catalyzed C–H Bond Functionalization With Arenes

## 1 Pd(II)-Catalyzed Oxidative Cross-Coupling of Two Arenes

### 1.1 Introduction to C–H Bond Functionalization

Organic synthesis is an ever-growing science with many challenges. Synthetic chemists aim to make the most complex molecules with the least amount of steps and with the highest possible yields. Synthesis involves the addition and transformation of functional groups to afford the desired product in a completely selective manner. The major issues in selectivity in synthesis include chemoselectivity, the control of reactivity towards a specific functional group, regioselectivity, the control of direction of the breaking or making of a chemical bond, and stereoselectivity, the control of the formation of a stereocenter.

To address the issue of addition and transformation of functional groups, the direct functionalization of carbon-hydrogen (C–H) bonds presents itself as an efficient and atom economical process. Since C–H bonds are ubiquitous in organic compounds, their functionalization can save steps in total syntheses by avoiding unnecessary functional group transformations and wasteful byproducts. The transition metal-catalyzed functionalization of C–H bonds can lead to many different types of products depending on the nature of the coupling partner (Scheme 1). The overall process involves the activation of a C–H bond via an oxidative



**Scheme 1: C–H activation leading to a variety of products**

addition onto a transition metal followed by transmetallation and finally by the reductive elimination to yield the desired new C—X bond, where X can be a heteroatom, a halogen, a carbon, etc. Furthermore, when X is carbon, the concomitant formation of a new C—C bond is undeniably very useful in synthesis for the building of molecular scaffolds. More specifically towards our research interest, when Y is hydrogen, then the process involves a tandem C—H bond activation to yield a new C—C bond. The formation of C—C bonds is unquestionably valuable in organic chemistry.

## 1.2 Literature Precedence

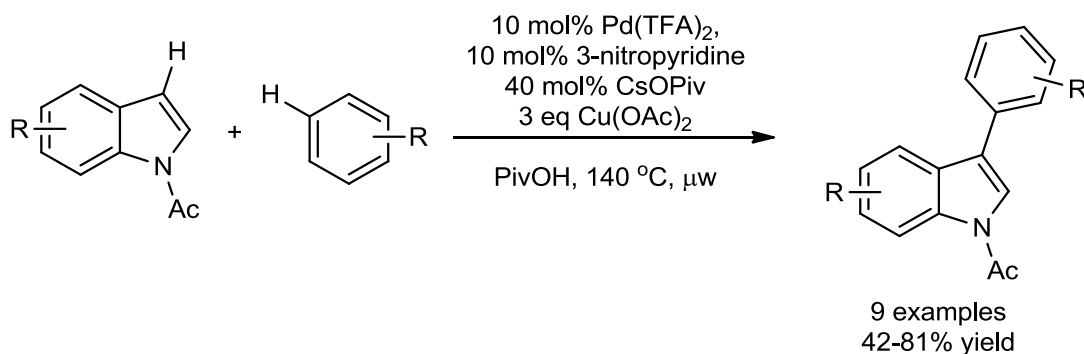
To address the issue of unnecessary functional group transformations in synthesis, the direct functionalization of carbon-hydrogen (C—H) bonds presents itself as an efficient and green alternative to traditional chemical reactions.<sup>1</sup> In particular, palladium(II)-catalyzed oxidative functionalization of arene C—H bonds yield a wide variety of biaryl motifs. Intermolecular reactions require two different coupling partners and must outcompete homocoupling reactions of either starting material. One approach to this problem involves using two electronically different arenes and heteroarenes which can intercept the catalytic cycle at different stages. The use of a directing functional group on one of the coupling partners is an alternative solution. Our lab has made contributions in this area by using amide-like directing groups. The work described in this chapter is the application of the developed intermolecular oxidative C—H bond cross-coupling to intramolecular systems where two tethered arenes generates relevant tricyclic structures via a ring closing reaction.

### 1.2.1 Intermolecular Pd(II)-Catalyzed Oxidative Cross-Coupling

#### 1.2.1.1 Without a Directing Group

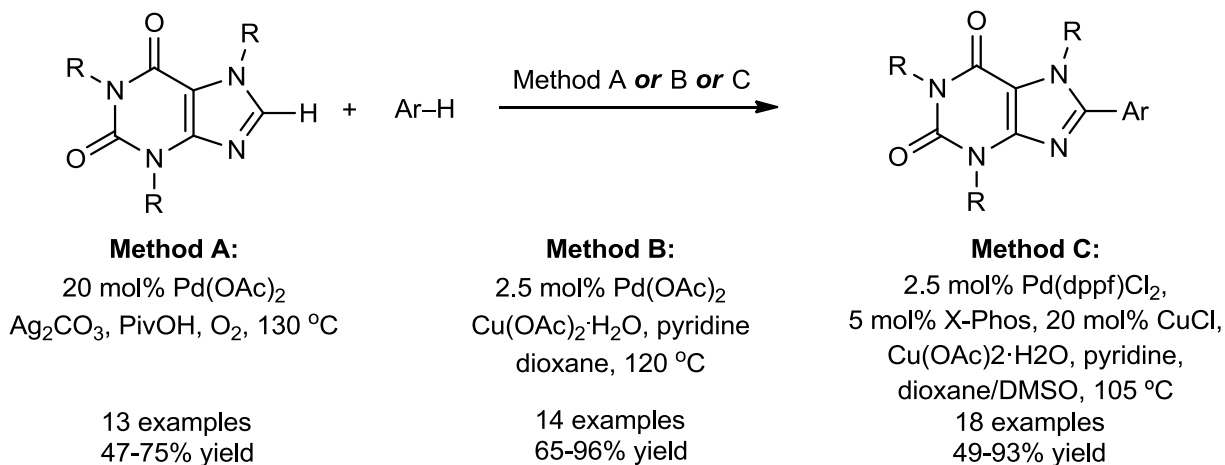
The examples listed in this section include oxidative palladium-catalyzed two-fold C—H bond activation where the chemoselectivity is governed by the electronics of each coupling partner. As such, no functional group is directing the catalyst to the C—H bond to be activated. Hence, we will use the term “without directing group”.

Pioneering work in the field of two-fold C–H bond activation was accomplished by the group of Prof. Keith Fagnou who developed a selective C3 arylation of *N*-acylated indoles (Scheme 2).<sup>2</sup> In the presence of copper salts as the terminal oxidant, *N*-acylated indoles react with simple arenes under palladium catalysis. Following this work, the complimentary reaction, C2 arylation of indoles was achieved using silver salts.<sup>3,4</sup> Then, *N*-alkyl indoles<sup>5</sup>, pyrroles<sup>6</sup> and benzofurans<sup>7</sup> were also reported to be efficient substrates for the oxidative cross-coupling with inactivated arenes.



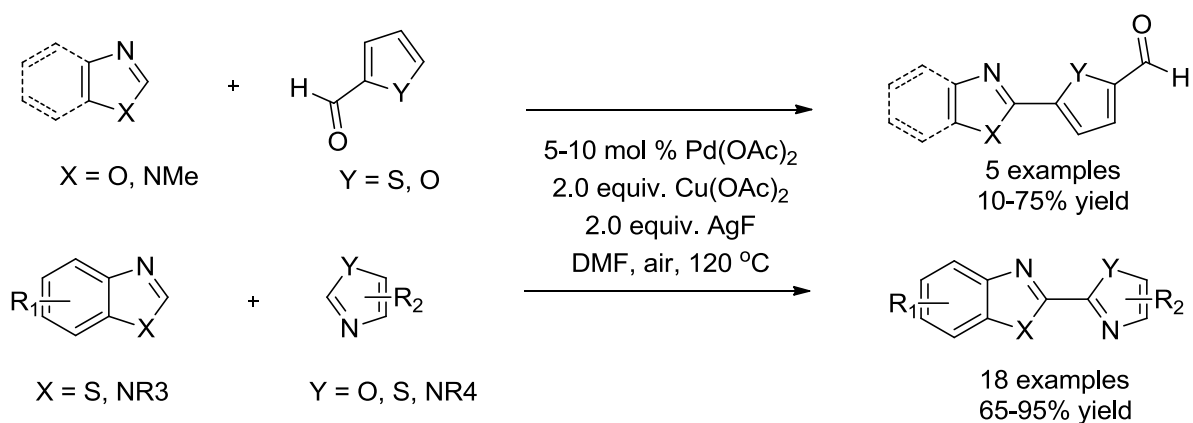
### Scheme 2: Fagnou's selective C3 arylation of *N*-acylated indoles

Azoles, such as xanthenes, are a class of pharmaceutically relevant compounds containing a number of reactive nitrogen atoms. These heterocycles possess an acidic proton and render azoles amenable to C–H bond activation. Functionalization of xanthenes can be accomplished with a number of arenes and heteroarenes using palladium catalysts (Scheme 3).<sup>8,9,10</sup> The use of copper and silver salts promotes these cross-couplings by acting as terminal oxidants themselves or by catalyzing oxygen reduction. Method A uses acidic reaction conditions whereas Method B required basic conditions, making both of these sets of conditions complimentary to each other. Method C highlights the interesting use of a ligand in the catalytic system to promote reactivity.



### Scheme 3: Pd-catalyzed C8 arylation of xanthenes

The selective cross-coupling of two different azoles bearing different heteroatoms can be achieved in the presence of palladium(II) acetate (Scheme 4).<sup>11,12</sup> Similarly to xanthine arylation, the most acidic C–H bond undergoes catalytic functionalization. Despite the similarity of the two C–H bonds present on both azole coupling partners, high levels of chemoselectivity are observed for the cross-coupling process over competing homocoupling.

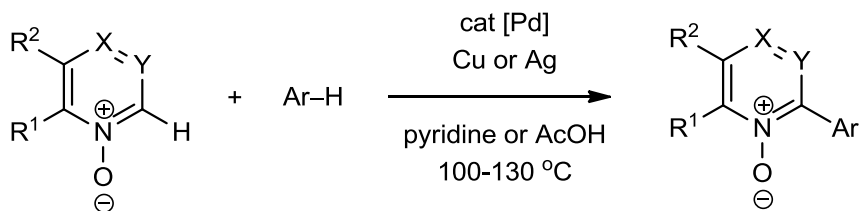


### Scheme 4: Pd-catalyzed arylation of azoles

Pyridines represent a difficult class of substrates in cross-coupling chemistry due to its ability to bind well with metals and hinder catalytic turnover. To circumvent this challenge, pyridine *N*-oxides have been useful surrogates for pyridines. Consequently, substituted pyridine *N*-oxides can be cross-coupled to a number of simple arenes and to a variety of heteroarenes in an efficient

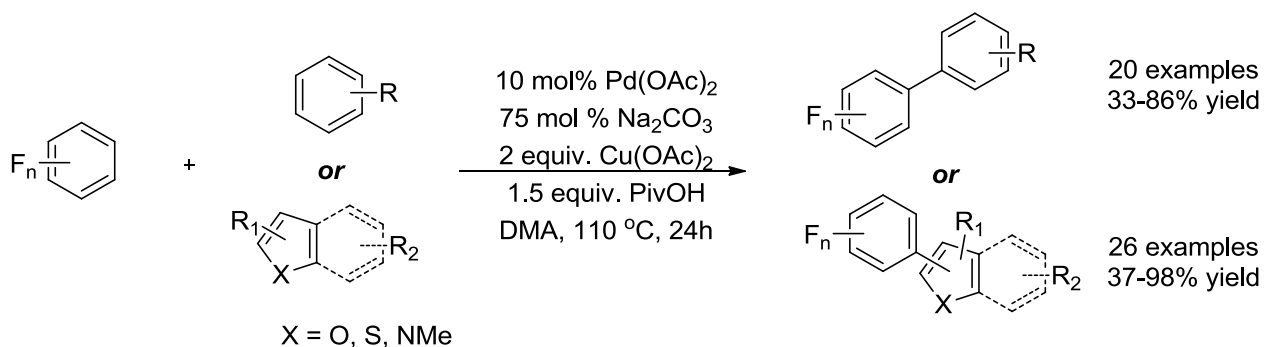


fashion (Scheme 5).<sup>13</sup> Since pyridine *N*-oxides serve as protected pyridines, they can easily be reduced using phosphorus trichloride in a short reaction time.



### Scheme 5: Pd-catalyzed *ortho*-arylation of pyridine *N*-oxides with arenes and heteroarenes

The strong electron-withdrawing effect of perfluorinated aryl groups induces a significant lowering of the HOMO and LUMO energy levels with respect to nonfluorinated arenes. Differentiation between a perfluorinated arene and other inactivated arenes, thus, allows for chemoselective cross-coupling between these two starting materials. Accordingly, palladium(II) acetate is an excellent catalyst for intermolecular double C–H activation for perfluorinated arene substrates (Scheme 6).<sup>14,15</sup> A wide range of inactivated arenes and heteroarenes can undergo oxidative coupling with perfluorinated arenes. In particular, Zhang and coworkers demonstrated that molecules containing the perfluoroarene-thiophene structure play a primary role as active materials in electronic devices, such as organic light-emitting diodes and field-effect transistors.<sup>14</sup>

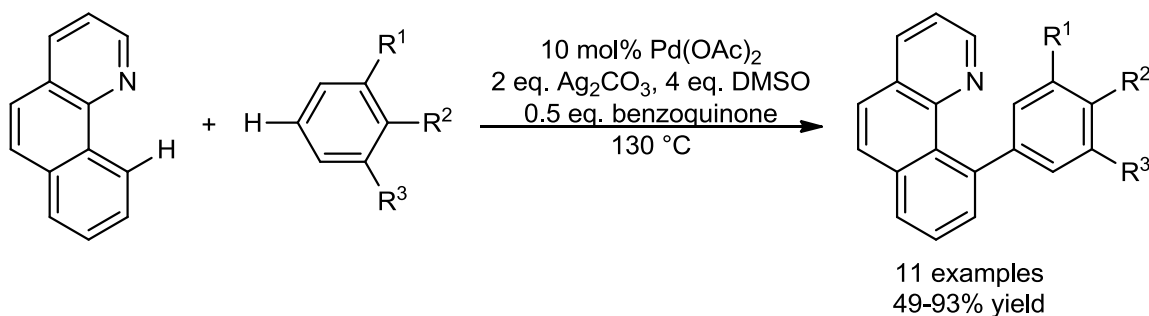


### Scheme 6: Pd-catalyzed arylation of perfluorinated arenes with simple arenes and heteroarenes

### 1.2.1.2 With a Directing Group

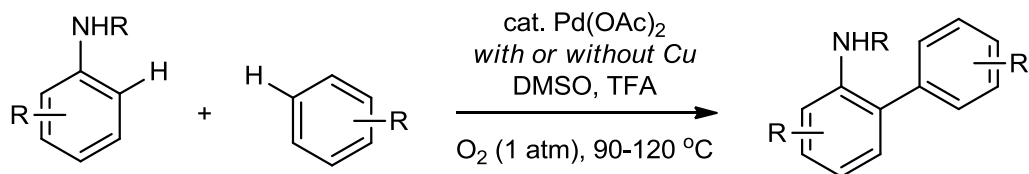
By choosing a suitable directing group, selective catalytic *ortho*-C–H functionalization can occur by chelating with the palladium catalyst. In two-fold C–H bond arylation,  $sp^2$  C–H bonds within proximity of Lewis basic functionalities benefit from enhanced regio- and chemoselectivity as well as improved reactivities.

Sanford and co-workers demonstrated in 2007 that a wide range of simple arenes undergo facile arylation of benzo[*h*]quinoline selectively at the *ortho* position (Scheme 7).<sup>16</sup> It is believed that the silver carbonate acts as the sole oxidizing agent, while benzoquinone serves as an ancillary ligand on palladium. As such, the observed regioselectivity of arylation on the unactivated arene component is impacted by using methyl-substituted benzoquinone derivatives. In the same account, the authors also reported the use of imines as efficient directing groups for oxidative *ortho*-arylation.



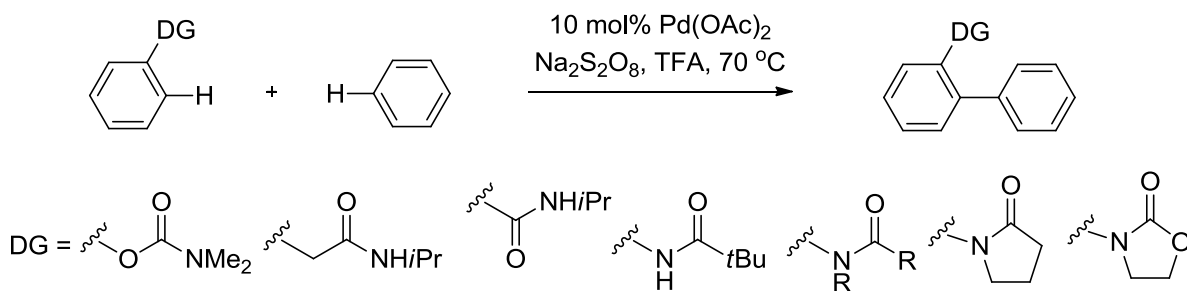
#### Scheme 7: Sanford's *ortho*-arylation of benzo[*h*]quinoline with simple arenes

Amides are very effective as directing groups for oxidative *ortho*-C–H bond arylation. In particular, anilides are excellent substrates for cross-coupling in the presence of palladium(II) acetate and copper(II) triflate as co-catalyst under aerobic conditions (Scheme 8).<sup>17</sup> In Shi's 2008 account, *N*-acyl-3,4-dihydroquinolines, a specific class of anilides, react with simple arenes to give biologically relevant structures. The authors also applied their developed methodology to *N*-acylanilides. The use of oxygen as the terminal electron acceptor is advantageous since the only byproduct formed is water. A related account by Buchwald demonstrated that a copper-free process could be realized in the presence of trifluoroacetic acid and a slight excess of the unactivated arene coupling partner.<sup>18</sup>



**Scheme 8: Oxidative *ortho*-arylation with anilides as directing groups by Shi and Buchwald**

Following these report on anilide's directing abilities, an intermolecular tandem C–H functionalization was developed by Dr. Xiaodan Zhao and Charles Yeung in our lab and involves the *ortho*-arylation of arenes directed by phenylacetamides, benzamides, *O*-phenylcarbamates and anilides. The reaction conditions include the use of catalytic palladium(II) acetate and stoichiometric sodium persulfate as the oxidant. The reaction works efficiently with the addition of trifluoroacetic acid at 70 °C.



**Scheme 9: Intermolecular C–H bond functionalization of arenes**

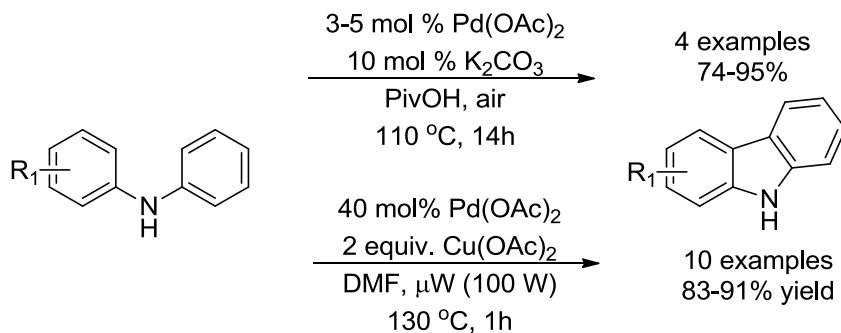
After our group's contributions were published, Yu and co-workers have extended the scope of the oxidative palladium cross-coupling with the benzamide derivatives.<sup>19</sup> As well, a cascade double C–H activation/oxidative C–N bond formation to provide an expeditious route to phenanthridinones from *N*-methoxybenzamides.<sup>20</sup>

### 1.2.2 Intramolecular Pd(II)-Catalyzed oxidative cross-coupling

Ring closing reactions are powerful strategies for making heterocycles, and even more so if the two coupling partners are brought together via double C–H bond activations. An advantage that intramolecular Pd-catalyzed oxidative couplings have over their intermolecular counterparts is

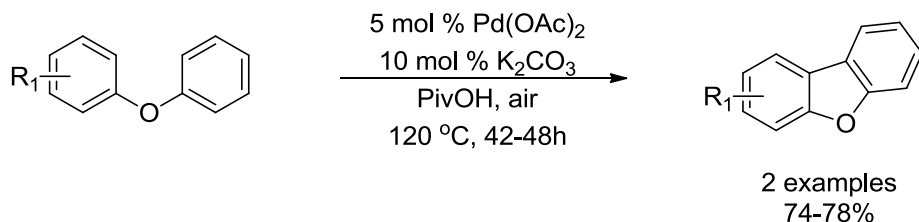
that the second coupling partner is tethered to the molecule, thereby avoiding the use of excess coupling partner. The application of this strategy has been demonstrated in one-pot sequences as well as in natural product synthesis. The size of the forming ring in these types of reactions has a large effect on reaction efficiency.

Carbazoles possess various pharmacological activities, including anti-HIV, anticancer, antibacterial and antifungal activities and are used in pigment production. Their synthesis traditionally calls for a Borsche-Drechsel cyclization or a Graebe-Ullmann reaction. The rapid assembly of carbazoles through oxidative intramolecular cross-coupling is made possible by palladium catalysis (Scheme 10). In this reaction, a double C–H activation occurs on adjacent aromatic rings tethered together with a single nitrogen linker. Fagnou developed the acidic reaction conditions and later Menendez improved the reaction time by using microwave irradiation.<sup>21,22</sup>



**Scheme 10: Synthesis of carbazoles via an oxidative intramolecular cross-coupling by Fagnou and Menendez**

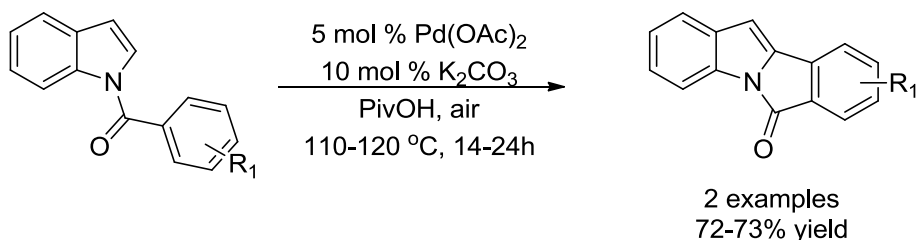
By changing the linker between the two aromatic rings from nitrogen to oxygen, intramolecular oxidative C–C coupling of diphenyl ethers affords dibenzofuran products. The cyclization to afford the five-membered ring product proceeds with high efficiencies, albeit limited scope (Scheme 11). Indeed, Fagnou’s team was able to apply the same reaction conditions developed for carbazoles to dibenzofurans.<sup>23</sup>



### Scheme 11: Synthesis of benzofurans via oxidative intramolecular cross-coupling

The C2 arylation chemistry previously described for intermolecular reactions of indole derivatives can also be applied to intramolecular cross-couplings. By tethering an aromatic group via an amide linker to the indole nitrogen atom, intramolecular cyclization affords a five-membered ring indole derivative termed 6*H*-isoindolo[2,1-*a*]indol-6-ones (Scheme 12).<sup>24</sup>

Regioselective coupling occurs at the C2 position of the indole ring.

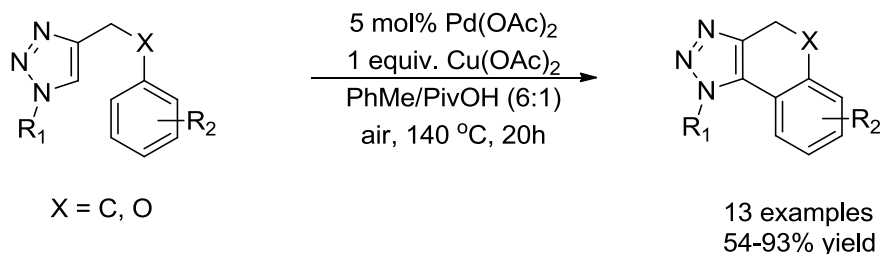


### Scheme 12: Synthesis of 6*H*-isoindolo[2,1-*a*]indolones via oxidative intramolecular cross-coupling

Among the examples of oxidative two fold C–H bond activation described up until now, the scope of the reaction still suffers from functional group compatibility, regioselectivity and harsh reaction conditions. Our group seized the opportunity to contribute to the field of oxidative cross-coupling by exploring a variety of directing group functionalities. Our goal was to develop broadly applicable reaction conditions by using milder reagents and reaction conditions and thus extend the substrate scope of two fold C–H bond activation reactions.

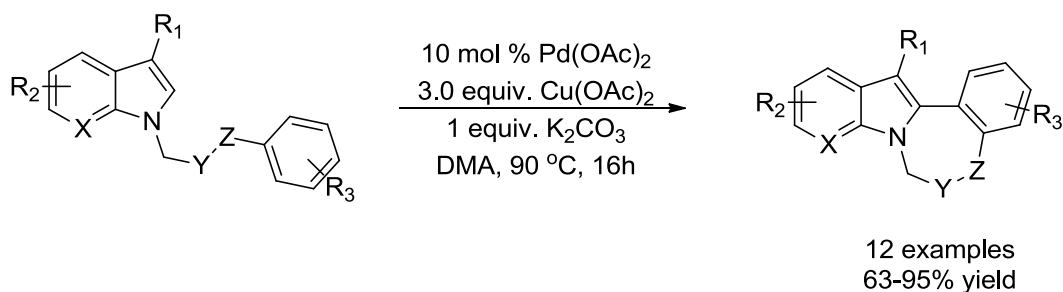
The intramolecular oxidative cross-coupling strategy that our group published in *Chemical Science* in 2010 was the first two-fold C–H bond activation method to make 6-membered rings. Following our report, two new methods have been added to the synthetic chemist's tool box to address the synthesis of tricyclic structures. The first was the ring closing reaction between an

arene and a heteroarene, namely a 1,2,3-triazole with the use of palladium as a catalyst and copper as the oxidant (Scheme 13).<sup>25</sup> A variety of heteroatom-containing six-membered rings were synthesized via this methodology and highly substituted substrates, which are normally difficult to access due to steric hindrance, were also prepared.



### Scheme 13: Synthesis of triazole-tricyclic structures via oxidative intramolecular cross-coupling

An account by Greaney and coworkers described the intramolecular Pd-catalyzed C2 arylation of indoles to medium-sized rings.<sup>26</sup> In analogy to five-membered annulations involving indole derivatives, a palladium(II)-catalyzed twofold C–H bond activation process generates seven- and eight-membered rings with a wide range of heteroatom-containing cycles. The optimal substrate requires an electron withdrawing group at the C3 position on the indole. In these reactions, copper(II) acetate is the sacrificial oxidant.

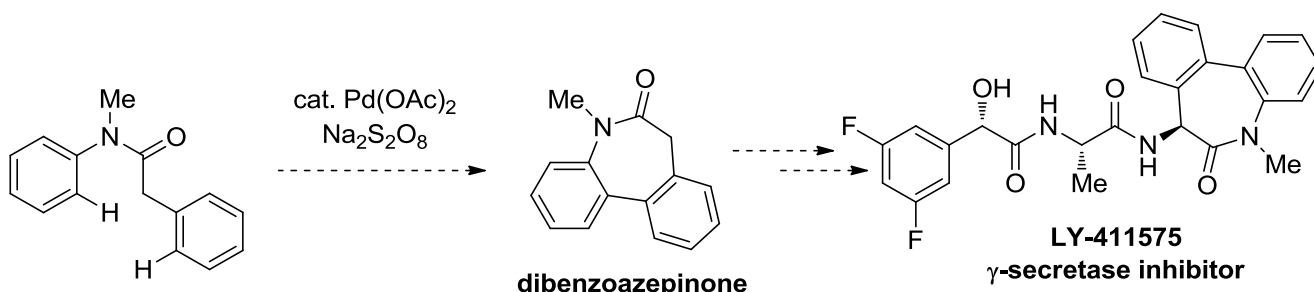


### Scheme 14: Synthesis of medium sized heterocycles via oxidative intramolecular cross-coupling

## 1.3 Development of an Intramolecular Pd(II)-Catalyzed Oxidative Arylation

### 1.3.1 Seven-membered lactams

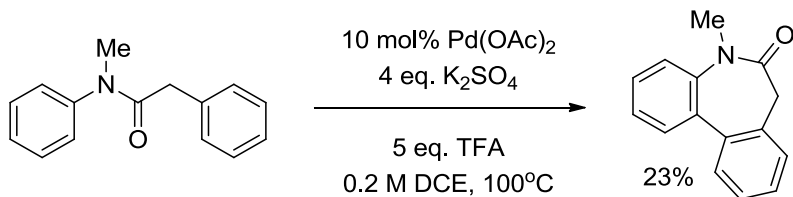
Originally, we envisioned applying the intramolecular two-fold C–H bond activation to synthesize 7-membered lactams which are biologically relevant scaffolds. With no known methods to make medium sized rings with oxidative cross-coupling methodologies, we sought a relevant application. Specifically, the LY-411575  $\gamma$ -secretase inhibitor drug candidate in therapeutics to treat Alzheimer's disease, appeared to be an attractive target (Scheme 15). There presently exists no efficient way of reaching this dibenzoazepinone moiety.



**Scheme 15: Synthesis of dibenzoazepinone moiety**

Borrowing the reaction conditions developed by Xiaodan Zhao and Charles Yeung in our lab, a summer student, Mengzhou Li had attempted the oxidative cross coupling (Scheme 15) and noticed some reactivity. I pursued this initial hit and aimed to optimize the reaction conditions by conducting a screen of all the reaction parameters.

To calculate the efficiency of the reaction, a calibration curve was obtained for *N*-methyl-*N*,2-diphenylacetamide and for 5-methyl-5H,7H-dibenzo[*b,d*]azepin-6-one on a gas chromatography flame ionization detector (GC-FID) using tetradecane as an internal standard. Some relevant results are tabulated in Table 1 where conversions and yields were quantified by the mentioned calibration curve.

**Table 1: Table of parameters explored while optimizing the reaction conditions**

parameter	reagent	Conversion	Yield <sup>a</sup>
oxidant	K <sub>2</sub> S <sub>2</sub> O <sub>4</sub>	Up to 97%	Up to 23%
	Na <sub>2</sub> S <sub>2</sub> O <sub>4</sub>	64%	11%
	Air	~6%	~2%
	O <sub>2</sub>	13%	5%
	AgOAc	0%	0%
	Ag <sub>2</sub> CO <sub>3</sub>	0%	0%
	oxone	70%	8%
	benzoquinone	62%	0%
catalyst	Pd(OAc) <sub>2</sub>	Up to 97%	Up to 23%
	Pd(dba) <sub>2</sub>	97%	7%
	PdCl <sub>2</sub>	3%	0%
	Pd(TFA) <sub>2</sub>	82%	16%
	No catalyst	0%	0%
acid	F <sub>3</sub> CCO <sub>2</sub> H	Up to 97%	Up to 23%
	Cl <sub>3</sub> CCO <sub>2</sub> H	Not quantified	trace
	Br <sub>3</sub> CCO <sub>2</sub> H	46%	0%
	Me <sub>3</sub> CCO <sub>2</sub> H	52%	4%
	Ph <sub>3</sub> CCO <sub>2</sub> H	21%	0%
	No acid	~0%	0%
solvent	DCE	Up to 97%	Up to 23%
	DMF	0%	0%
	DNP	0%	0%
	DMSO	0%	0%
	Acetic acid	99%	0%
	p-xylene	Not quantified	traces
	1,4-dioxane	86%	3%
	1,1,1-trichloroethane	97%	3%
	1,1,2,2,-tetrachloroethane	80%	25%
	glyme	69%	0%
	No solvent(after 13h)	>99%	~15%

<sup>a</sup> GC yields, with tetradecane as an internal standard.

Potassium persulfate remains the most effective oxidant, but it also seems to consume the starting material very quickly. It was important to verify whether the starting material was reactive towards the oxidant in the absence of a catalyst. As such, a control experiment was



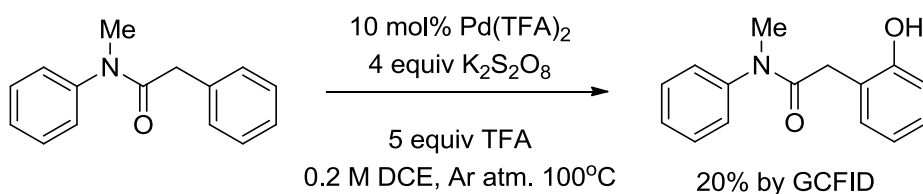
conducted without a catalyst and in the presence of four equivalents of potassium persulfate no decomposition of the starting material was observed. This result suggests that the oxidant does not consume the starting material and indeed a catalytic species activated by a persulfate salt is present. As discussed earlier, previous examples of intramolecular tandem C–H bond functionalization use molecular oxygen as the oxidant and this prompted us to try similar conditions. Oxygen decreased the conversion and yielded unsatisfactory formation of the desired product. Since the starting material appears to be stable under the oxidative reaction conditions, the high conversion and low product yield may indicate decomposition under catalysis. Other byproducts were also observed such as dimerization. Furthermore, it is also possible that the product is unstable under oxidative palladium catalysis.

Different acids were screened using five equivalents to the substrate. Trifluoroacetic acid remains the most effective acid for oxidative cross-coupling in analogy to the intermolecular reaction conditions. A solvent screen was also performed and aromatic solvents appeared to be reactive with the substrate. No byproduct was isolated to confirm this hypothesis but the quick formation of numerous byproducts observed by GC-FID suggests reactivity with the solvent. 2-Methylnaphthalene was also screened as an internal standard and its mass was found to decrease over time, again supporting the fact that aromatics are reactive in the presence of the substrate to yield an intermolecular functionalized product. This result is expected since intermolecular oxidative C–H bond functionalization was developed under identical reaction conditions. Interestingly, in this methodology inter- and intramolecular reactions are competitive.

Furthermore, in previously reported reaction conditions, the use of acetic acid as a solvent has been fruitful. Our attempts to run the reaction under acidic conditions at low (room temperature) and high (100 °C) temperatures resulted in a complex reaction mixture. 1,2-Dichloroethane is a relatively good solvent, but higher temperatures were found to be more effective and thus the boiling point of 1,2-dichloroethane (82.5-84.5 °C) became an issue. A similar solvent, 1,1,2,2-tetrachloroethane with a higher boiling point (147 °C) was screened and a slight increase in yield was detected. It is also important to highlight the experiment conducted without solvent. The reaction yielded ~15% of the desired product after only 13 hours, perhaps indicating that higher concentrations are favorable to accelerate the rate of the reaction. On the other hand, this observation may be counter-intuitive since intramolecular reactions are normally promoted by

high dilutions. To address this concern, higher dilutions of the reaction mixture were investigated in 1,2-dichloroethane but no improvement in yield was noticed.

In addition, the use of palladium(II) trifluoroacetate as the catalyst yielded an unknown major product. After isolation and characterization, the byproduct was found to be 2-(2-hydroxyphenyl)-*N*-methyl-*N*-phenylacetamide and formed via a hydroxylation reaction (Scheme 16). By  $^1\text{H}$  and  $^{13}\text{C}$  NMR, the hydroxyl group was determined to be on the benzamide ring.



### Scheme 16: Major byproduct formed in the presence of Pd(TFA)<sub>2</sub>

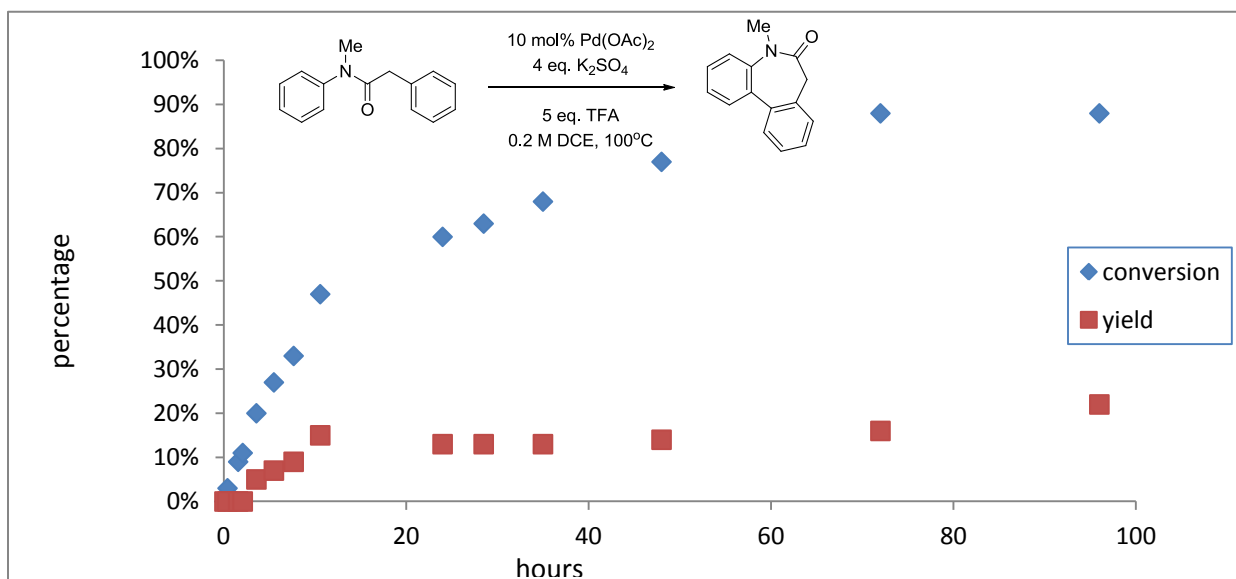
This experiment result is quite interesting since it implies the direct hydroxylation of aryls. The palladium-catalyzed direct acetoxylation of arenes has been developed by Sanford and coworkers<sup>27,28,29,30</sup> and is more common than hydroxylation. However, there are only a few reports of direct palladium-catalyzed C–H bond functionalization of arenes to form phenols.<sup>31,32</sup> The formation of this byproduct may be of significance and perhaps a methodology development for hydroxylation directed by amides can ensue from this discovery (see Chapter 3).

Further optimization led us to try different additives like 20 mol% DMSO, Sc(OTf)<sub>3</sub>, Cu(OAc)<sub>2</sub> and AgOAc, which were unfortunately inactive in our system. Basic reaction mediums were also tested but gave no conversion. Finally, the reactions were conducted under different atmospheres, notably, argon, air and oxygen and a slight increase in yield was observed in the presence of oxygen. Therefore, the reaction appears to be insensitive to anaerobic or anhydrous conditions, but is sensitive to acidic versus basic conditions.

Using tetradecane as an internal standard, a reaction with the optimized conditions was monitored over time by GC-FID. Taking aliquots at different intervals of time allowed us to gain some insight into the progression of the reaction. The conversion of the starting material and the yield of the desired product were plotted as a function of time (Graph 1). The graph is

characterized by an induction time of 2 to 3 hours where an increase in conversion but no formation of the final product is observed. Interestingly, no induction time was observed in the absence of solvent. An induction time may be explained by the formation of the active catalytic species. Notably, after 10 hours, the final product formation appears to stall. Possible causes include the poisoning of the catalyst by either the formation of a byproduct or of palladium black. The 7-membered lactam product is indeed stable under the reaction conditions and so no product inhibition is expected in this methodology.

**Graph 1: Conversion of starting material and yield of dibenzoazepinone as a function of time.**



However, in the pursuit of optimizing the reaction conditions, we faced the inherent difficulty of making 7-membered lactams. The best yield obtained was a mere 25%. Hence, we turned our attention to similar substrates which would lead to 6-membered lactams.

### 1.3.2 Six-membered lactams

Phenanthridones are important structural cores in natural products and pharmaceutically relevant compounds. Since palladium(II) acetate, sodium persulfate, and TFA proved to be an excellent combination for the functionalization of anilides and benzamides, the same reaction conditions were successful when extended to an intramolecular version. Namely, *N*-arylbenzamides undergo smooth cyclization to afford the six-membered phenanthridone products in synthetically

useful yields, effectively extending the single atom tether by one in comparison to carbazole and dibenzofuran synthesis. The electronics on the benzamide ring has an important effect on the efficiency of the cyclization.

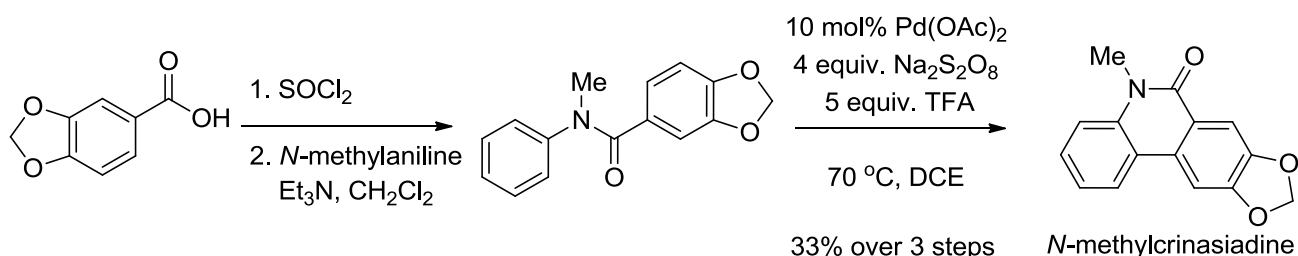
Numerous *N*-phenylbenzamides were synthesized via an amide bond coupling from an acyl chloride (commercially available or synthesized from the corresponding carboxylic acid) and an aniline. A table summarizing these results is shown below. The best substrates (Table 2, entry 1-3,8) are published in the first issue of *Chemical Science*.<sup>34</sup>

**Table 2: Scope of the oxidative intramolecular two fold C–H activation**

entry	substrate	product	yield
1			60%
2			33% (66% recovered starting material)
3			77%
4			55%
5			38%
6			46%
7			42%
8			63%

It became evident that the electronics of either arene of the phenanthridinone played an important role in this reaction, affecting greatly the yield. An electron donating group like a methoxy substituent on the anilide portion gave no reactivity; on the other hand the same group on the benzamide side increased the yield significantly. Furthermore the position of this electron rich substituent was crucial in promoting the reaction, where the *meta*- position was optimal.

Application of this twofold C–H bond intramolecular functionalization was extended to the total synthesis of the natural product *N*-methylcrinasiadine.



**Scheme 17: Total synthesis of *N*-methylcrinasiadine via oxidative intramolecular cross-coupling**

A list of failed/unpublished substrates was generated to highlight the limitations of the methodology. First, certain substitution patterns decreased the yields of the 6-membered lactam product or complicated their purifications (Table 3). A fluorine and an ethyl substitution on the anilide portion of the molecular has a deactivating effect (entries 1, 4). When the benzamide ring was substituted with a methyl in the ortho-position, the reaction was low yielding presumably due to a 1,3-allylic strain (entry 2). Indeed, the  $^1\text{H}$  NMR of the product indicated the presence of two rotamers. Also, the substitution pattern on the nitrogen of the anilide affected the reactivity of the system. The presence of a second phenyl group on the anilide may influence the electronics of the carbonyl, hindering its coordination to the palladium catalyst (entry 3).

**Table 3: Substrates with purification issues and GC yields are reported**

10 mol% Pd(OAc)<sub>2</sub>  
4 eq. Na<sub>2</sub>S<sub>2</sub>O<sub>8</sub>  
5 eq. TFA  
DCE, 70 °C, 72h

entry	substrate	product	yield
1			28% by GCFID
2			8% by GCFID
3			50% by GCFID difficult separation
4			full conversion by GCFID but highly impure product

Notably, only tertiary amides were effective under this chemistry and it is proposed that the methyl group on the amide affects the cis/trans conformation of the molecule.<sup>33</sup> The molecule with a tertiary anilide will predominantly lie in a cis conformation bringing the two arenes closer together. This hypothesis is further supported by the observation that mono-substituted anilides are excellent substrates in intermolecular oxidative cross-coupling reactions thereby proving their reactivity under the reaction conditions. Substrates which were completely unreactive under the optimized reaction conditions include indoline and tetrahydroquinoline derivatives (Figure 1).

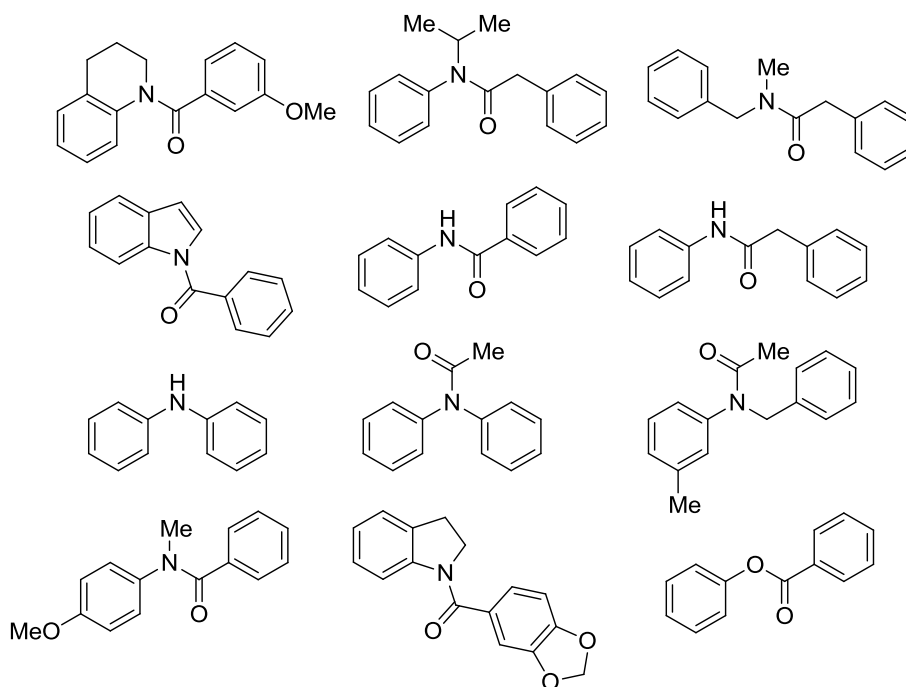
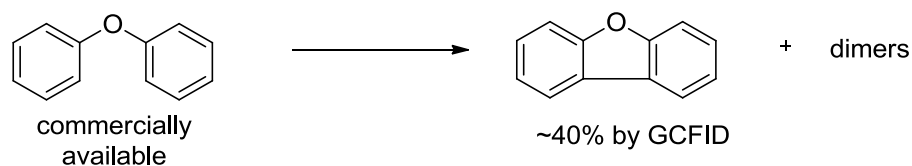


**Figure 1: Unreactive substrates under oxidative cross-coupling reaction conditions**

The oxidative cross-coupling product of diphenylether was observed and isolated along with its dimers (Scheme 18). However, this substrate has little relevance to our amide-type directing group and was therefore omitted. It nonetheless remains an interesting result analogous to Fagnou's results.



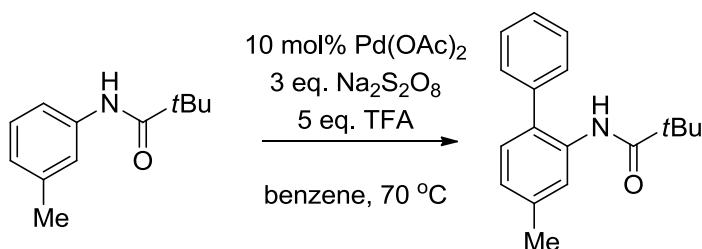
**Scheme 18: Synthesis of dibenzofurans via oxidative intramolecular cross-coupling**

### 1.3.3 Preliminary Kinetic Studies

Following the publication of our Pd-catalyzed dehydrogenative cross-coupling methodology<sup>34</sup>, we wanted to further our mechanistic understanding of the process by undertaking a kinetic study of the reaction parameters. The specific reaction conditions of the chosen system include *N*-(*m*-tolyl)pivalamide as the key substrate since it generated the product in a linear fashion (ie without



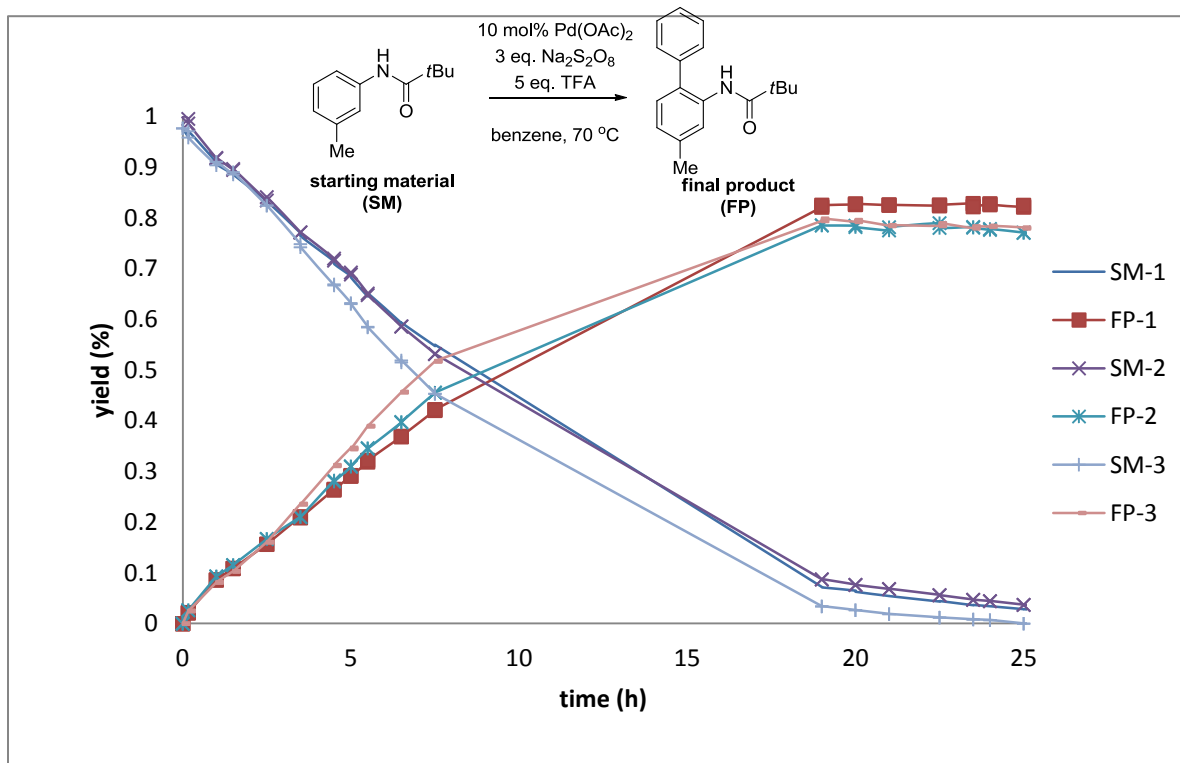
any byproducts originating from the starting material) and avoided diarylation, presumably due to steric hindrance (Scheme 19).



**Scheme 19: Optimized reaction conditions for the dehydrogenative cross-coupling of anilides and benzene used for kinetic studies**

With pure crystalline *N*-(*m*-tolyl)pivalamide in hand, a reaction profile was produced. Calibration curves for response factors were calculated for the starting material, *N*-(*m*-tolyl)pivalamide, for the product, *N*-(4-methyl-[1,1'-biphenyl]-2-yl)pivalamidebiphenyl and for the byproduct of the reaction, biphenyl. All relationships with the internal standard on the GC-FID were linear and indicated a linear response factor. The chosen internal standard was a simple unreactive aliphatic alkane, dodecane. Three identical reactions were run side by side and aliquots were sampled simultaneously to produce the reaction profile graph (Graph 2). Within experimental error, the reaction conversions and yields are reproducible. Importantly, the conversion of starting material and the yield of product appear to have linear dependencies on time. Of note, biphenyl was noticed after 18h of reaction time and never occurred in more than 2% yield. For the rest of the analysis, biphenyl is omitted from the results.

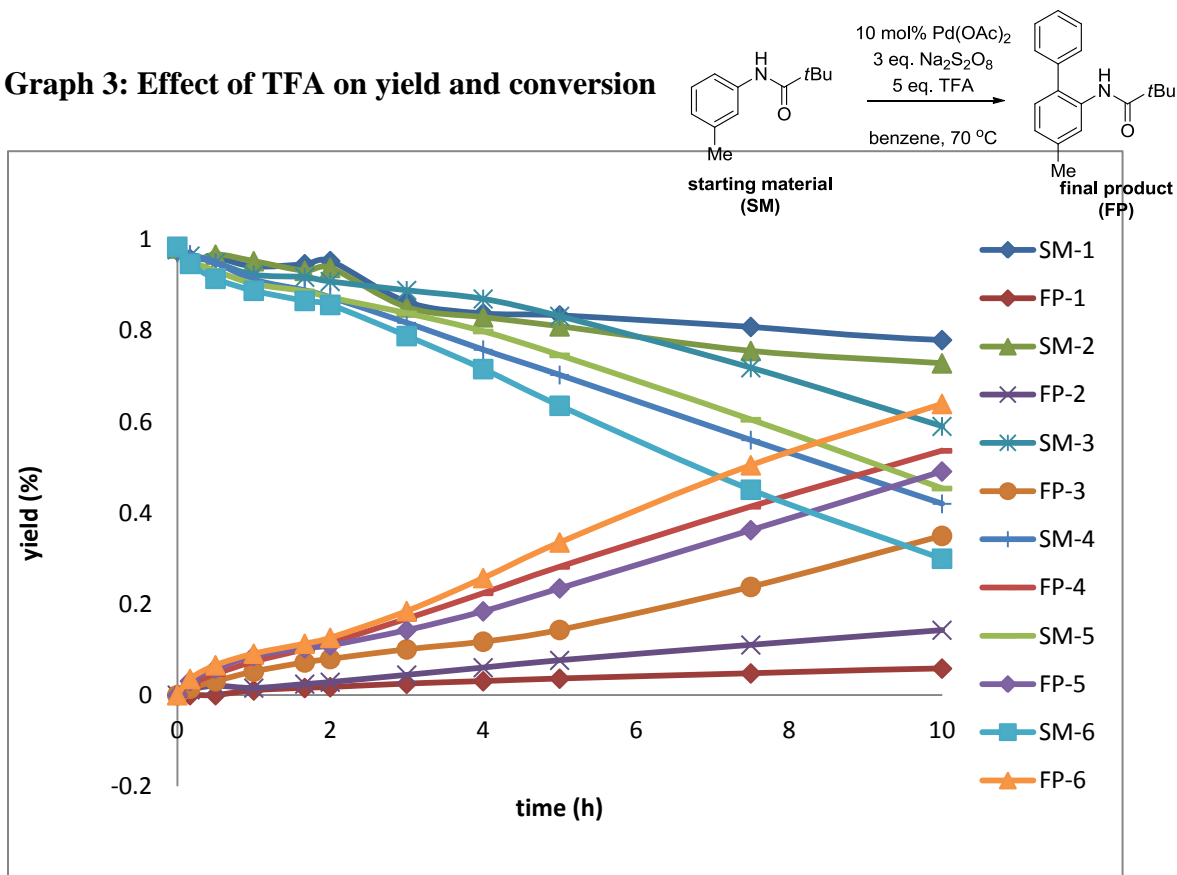
**Graph 2: Reaction profile of 3 identical oxidative cross-coupling reactions**



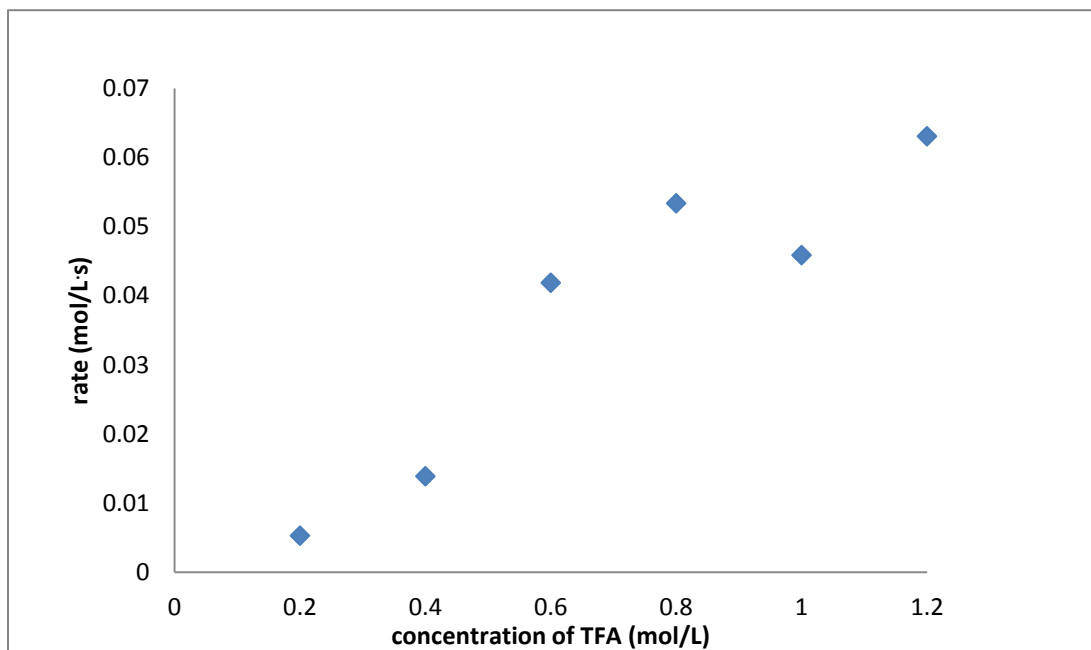
Overall the reaction profile appears to be consistent. To obtain each time point, the reaction was first taken off the reaction block (recorded time point) and left stirring while cooling for a timed 2 minutes. Then the cap was unscrewed and approximately 10  $\mu$ L was taken out of the reaction mixture and passed through a cotton-plugged pipette eluting with 1.5 mL of ethyl acetate into a GC vial. An optimized 5-minute GC-FID method was used to maximize the time between each analyzed sample. All three reactions were then placed back on the reaction block until the subsequent time point.

The first variable to be analyzed was the effect of trifluoroacetic acid (TFA) on the reaction rate. Six reactions were set up alongside each other, each with a different concentration of TFA: 1 equiv., 2 equiv., 3 equiv., 4 equiv., 5 equiv., and 6 equiv. (Graph 3). Of note, the volume was not corrected with the solvent, benzene, which implies that reaction #6, with 6 eq. of TFA, had a slightly larger volume, possibly affecting the concentration of acid.

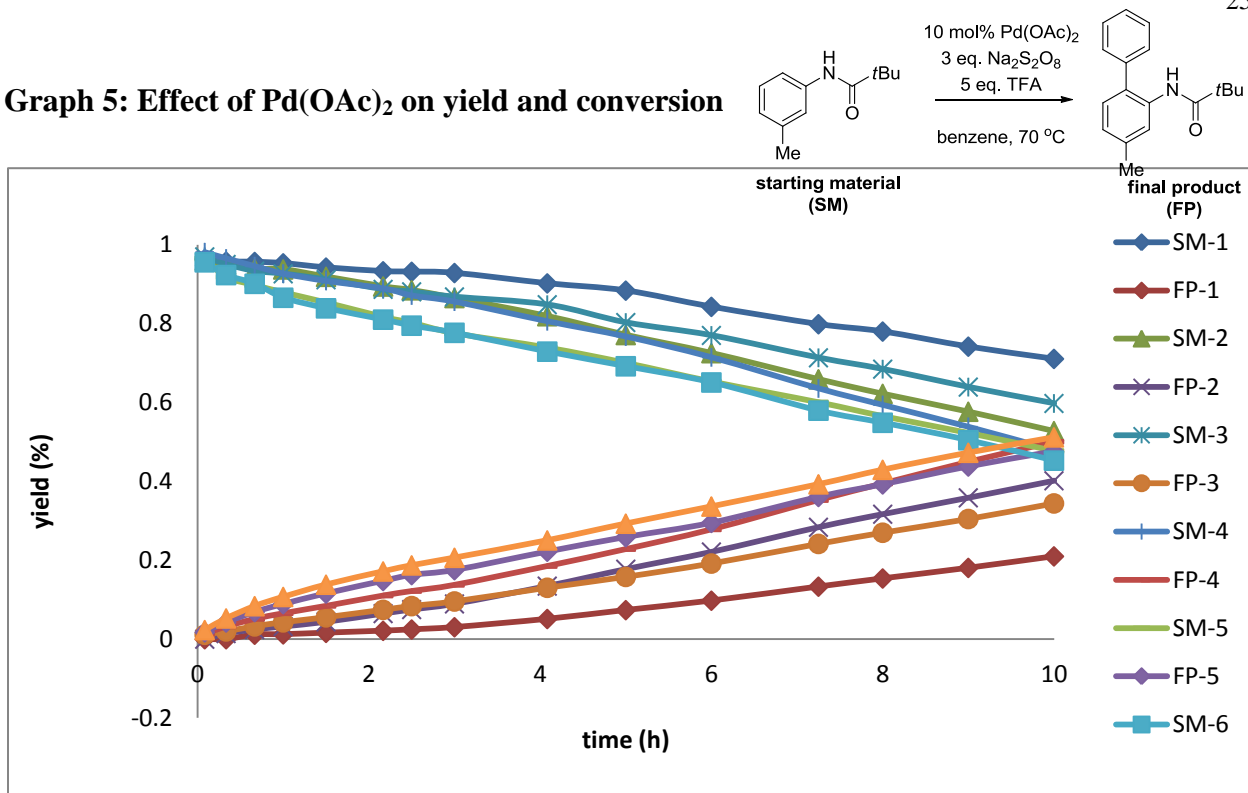
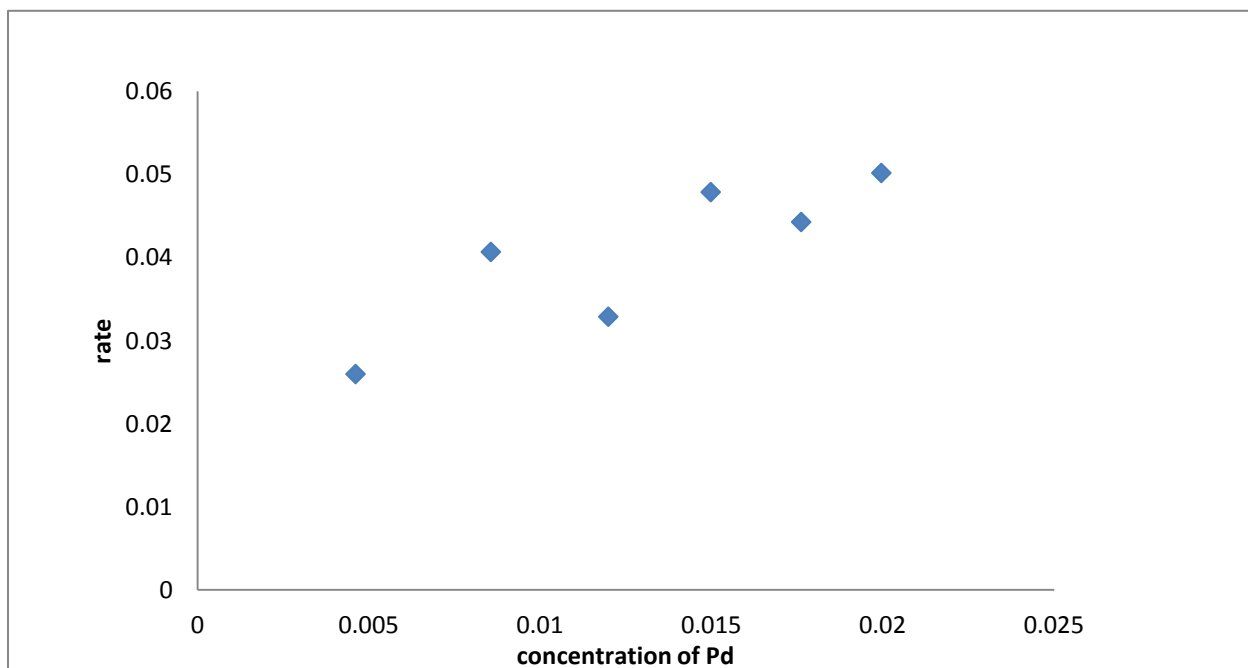
Graph 3: Effect of TFA on yield and conversion



The effect of TFA on rate was determined by first obtaining the linear relationship of the yield of *N*-(4-methyl-[1,1'-biphenyl]-2-yl)pivalamide as a function of time in the first 10-12 hours of the reaction (Graph 3). The slope of each line then gives the rate of the reaction at that specific concentration of acid. Hence, by having six reactions, and therefore six rates, six data points were obtained and plotted as a function of the concentration of TFA to determine its effect on the rate (Graph 4). Overall, the rate increases, but not necessarily in a linear fashion. An important equilibrium to keep in mind, is that  $\text{Pd(OAc)}_2 \rightleftharpoons \text{Pd(TFA)}_2$  and that only 10% palladium is used. In theory, we are using a large excess of TFA and this is only to push the equilibrium to the right and favour the formation of  $\text{Pd(TFA)}_2$ . Perhaps not much information can be drawn from an experiment where the concentration of TFA is varying from large excess to larger excess.

**Graph 4: Effect of TFA on rate**

Next, the effect of the number of equivalent of palladium was investigated in an analogous manner to the TFA experiment. A mother solution of  $\text{Pd}(\text{OAc})_2$  in benzene was used to add precisely the correct amount of palladium in each of the six reactions. Again, the volume of benzene was not corrected, but later taken into account in calculating the concentration for the rate graph (benzene volumes are additive). The six different equivalents probed were; 2.5 mol%; 5.0 mol%; 7.5 mol%; 10.0 mol%; 12.5 mol%; 15.0 mol% (Graph 5). The rate of the reaction with different equivalents of palladium as a function of its concentration generally increases as the concentration increases (Graph 6). Important points missing on the curve are rates at even lower concentrations of Pd. More data is required for a conclusion to be drawn from these experiments. Nonetheless, it would be expected to have the catalyst participate in the rate law.

Graph 5: Effect of Pd(OAc)<sub>2</sub> on yield and conversionGraph 6: Effect of Pd(OAc)<sub>2</sub> on rate

In summary, the kinetic information obtained through the listed experiments has helped gain some insight into the mechanism, but warrant further studies. From the profile curve, we observe a linear relationship between the conversion and the yield of the final product, suggesting a

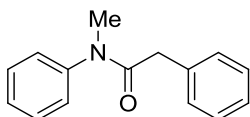
pseudo-zero order in substrate. This would be consistent with a rate limiting step involving a catalyst precursor. The rate as a function of TFA increases over higher concentrations of TFA presumably by favouring the equilibrium of the ligand on the metal centre. It is reasonable to say that the more TFA there is in the reaction, the easier it will displace the acetate ligands to form the reactive species. Some relevant experiments that would shine some more light on these results include running the reaction using  $\text{Pd}(\text{TFA})_2$  and adding some small amount of acetate (since the reaction does not proceed with  $\text{Pd}(\text{TFA})_2$  and hints towards an important role of the catalytic acetate ligand). Interesting findings by the Fagnou groups also points towards an important role of acetates in the concerted- metallation deprotonation mechanism.<sup>35</sup> More experiments with varying palladium concentration are required, especially at small catalyst loadings. An interesting experiment to try would be to use a substrate-palladacycle as a catalyst. Maybe this can aid in determining the active catalyst present in the catalytic cycle (see Chapter 2).

Finally, the reaction mixture is heterogeneous due to the insoluble sodium persulfate salt. It would therefore be difficult to obtain any rate dependence on this reagent. A soluble source of persulfate was indeed synthesized but revealed to be very reactive and therefore generated plenty of byproducts (see Chapter 3). Could the reactivity be tamed by synthesizing a persulfate oxidant with intermediate solubility? Modeling experiments are also ongoing with Peter Dornan and his collaboration with Prof. Tom Woo at University of Ottawa.

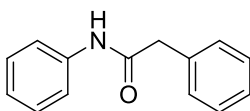
## 1.4 Experimental Data

**General procedure for the amide forming reaction:** In a flame-dried flask, N-methylaniline (1.08 mL, 5.00 mmol) was dissolved in dry dichloromethane (20 mL) at room temperature. Triethylamine (2.09 mL, 7.50 mmol) was added followed by benzoyl chloride (1.32 mL, 6.00 mmol). A small quantity of gas was observed and was evacuated with argon. The reaction was sealed and stirred at room temperature overnight. Then, the solvent was evaporated and the reaction mixture was redissolved in ethyl acetate. The organic layer was washed with a 1N HCl solution three times and then the aqueous layer was extracted three times with ethyl acetate. The combined organic phases were then washed with a sodium carbonate saturated solution three times and the aqueous layer was subsequently extracted with ethyl acetate three times. The

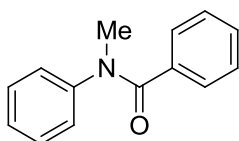
combined organic phases were washed twice with brine, dried with magnesium sulfate, filtered and concentrated. The crude reaction mixture was further purified by flash chromatography eluting with a mixture of ethyl acetate and hexanes (1:3).



**N-Methyl-N,2-diphenylacetamide:** A light yellow oil (0.580 g, 52%) was obtained. All spectral data are in agreement with reported literature data.<sup>36</sup> **<sup>1</sup>H NMR** (400 MHz, CDCl<sub>3</sub>) δ (ppm) 7.41-7.34 (m, 3H), 7.25-7.18 (m, 3H) 7.13-7.11 (m, 2H) 7.06-7.04 (m, 2H) 3.46 (s, 2H), 3.27 (s, 3H). **<sup>13</sup>C NMR** (100 MHz, CDCl<sub>3</sub>) δ (ppm) 171.0, 144.0, 135.4, 129.7, 129.0, 128.3, 127.9, 127.6, 126.5, 40.9, 37.6. **MS** (*m/z*,) 225 (M), 134, 107, 91.

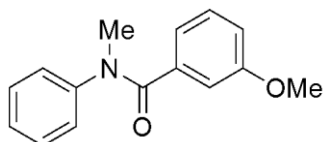


**N,2-Diphenylacetamide:** A light brown solid (1.100 g, 99%) was obtained. All spectral data are in agreement with reported literature data.<sup>37</sup> **mp** 116-118°C. **<sup>1</sup>H NMR** (400 MHz, CDCl<sub>3</sub>) δ (ppm) 7.42-7.24 (m, 9H), 7.08-7.06 (m, 1H), 3.70 (s, 2H). **<sup>13</sup>C NMR** (100 MHz, CDCl<sub>3</sub>) δ (ppm) 169.2, 137.7, 134.5, 129.5, 129.2, 128.9, 127.6, 124.4, 119.9, 44.8. **MS** (*m/z*) 211 (M), 119, 93, 77.

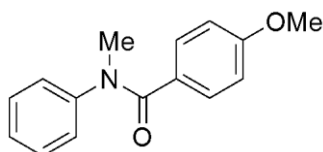


**N-Methyl-N-phenylbenzamide:** An orange oil was obtained (99%). All spectral data are in agreement with reported literature data.<sup>38</sup> **<sup>1</sup>H NMR** (400 MHz, CDCl<sub>3</sub>) δ 7.30-7.28 (m, 2H),

7.23-7.19 (m, 3H), 7.17-7.11 (m, 3H), 7.04-7.02 (m, 2H), 3.50 (s, 3H).  $^{13}\text{C}\{^1\text{H}\}$  NMR (100 MHz,  $\text{CDCl}_3$ )  $\delta$  170.7, 144.9, 135.9, 129.6, 129.1, 128.7, 127.7, 126.9, 126.5. **MS (ESI)**  $m/z$  212 (M+H), 234 (M+Na); **HRMS (ESI)**  $m/z$  calc'd for  $\text{C}_{14}\text{H}_{13}\text{NO}$   $[\text{M}+\text{H}]^+$ : 212.1069; found: 212.1080.

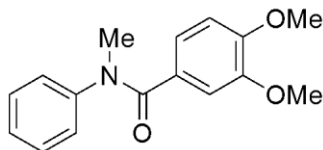


**3-Methoxy-N-methyl-N-phenylbenzamide:** A light yellow oil was obtained (99%), which became a white solid upon standing. All spectral data are in agreement with reported literature data.<sup>39</sup>  $^1\text{H}$  NMR (400 MHz,  $\text{CDCl}_3$ )  $\delta$  7.23 (t,  $J = 7.2$  Hz, 2H), 7.14 (t,  $J = 7.3$  Hz, 1H), 7.06-7.03 (m, 3H), 6.87-6.83 (m, 2H), 6.77 (dd,  $J = 2.2$  Hz,  $J = 8.2$  Hz, 1H), 3.65 (s, 3H), 3.49 (s, 3H).  $^{13}\text{C}\{^1\text{H}\}$  NMR (100 MHz,  $\text{CDCl}_3$ )  $\delta$  170.4, 158.9, 145.0, 137.1, 129.2, 129.2, 128.8, 126.8, 126.5, 121.2, 116.1, 113.7, 55.2, 38.4. **MS (ESI)**  $m/z$  242 (M+H), 264 (M+Na); **HRMS (ESI)**  $m/z$  calc'd for  $\text{C}_{15}\text{H}_{15}\text{NO}_2$   $[\text{M}+\text{H}]^+$ : 242.1175; found: 242.1180.

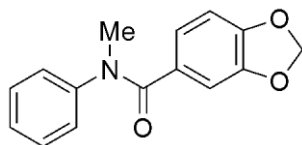


**4-Methoxy-N-methyl-N-phenylbenzamide:** A light yellow oil was obtained (99%). This compound has been reported in the literature.<sup>40</sup>  $^1\text{H}$  NMR (400 MHz,  $\text{CDCl}_3$ )  $\delta$  7.28-7.22 (m, 4H), 7.16-7.12 (m, 1H), 7.05-7.03 (m, 2H), 6.67-6.65 (m, 2H), 3.73 (s, 3H), 3.48 (s, 3H).  $^{13}\text{C}\{^1\text{H}\}$  NMR (100 MHz,  $\text{CDCl}_3$ )  $\delta$  170.2, 160.6, 145.5, 130.9, 129.2, 128.0, 126.9, 126.3, 113.0, 55.2, 38.6. **MS (ESI)**  $m/z$  242 (M+H), 264 (M+Na); **HRMS (ESI)**  $m/z$  calc'd for  $\text{C}_{15}\text{H}_{15}\text{NO}_2$   $[\text{M}+\text{H}]^+$ : 242.1175; found: 242.1181.

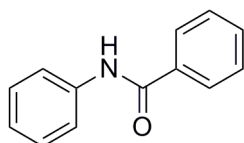




**3,4-Dimethoxy-N-methyl-N-phenylbenzamide:** A light yellow oil was obtained (99%). This compound has been reported in the literature.<sup>41</sup>  $^1\text{H NMR}$  (400 MHz,  $\text{CDCl}_3$ )  $\delta$  7.25 (t,  $J = 1.3$  Hz, 1H), 7.23 (t,  $J = 2.0$  Hz, 1H), 7.17-7.13 (m, 1H), 7.07-7.04 (m, 2H), 6.93 (dd,  $J = 2.0$  Hz,  $J = 8.4$  Hz, 1H), 6.85 (d,  $J = 2.0$  Hz, 1H), 6.63 (d,  $J = 8.4$  Hz, 1H), 3.81 (s, 3H), 3.64 (s, 3H), 3.49 (s, 3H).  $^{13}\text{C}\{^1\text{H}\}$  NMR (100 MHz,  $\text{CDCl}_3$ )  $\delta$  170.0, 150.2, 147.9, 145.6, 129.2, 127.8, 126.8, 126.3, 122.8, 112.4, 109.9, 55.8, 55.7, 38.6. **MS (ESI)**  $m/z$  272 (M+H), 294 (M+Na); **HRMS (ESI)**  $m/z$  calc'd for  $\text{C}_{16}\text{H}_{17}\text{NO}_3$  [M+H]<sup>+</sup>: 272.1281; found: 272.1272.

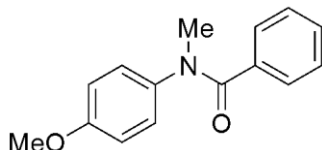


**N-Methyl-N-phenylbenzo[d][1,3]dioxole-5-carboxamide:** A light yellow oil was obtained (99%). This compound has been reported in the literature.<sup>42</sup>  $^1\text{H NMR}$  (400 MHz,  $\text{CDCl}_3$ )  $\delta$  7.27-7.23 (m, 2H), 7.16 (t,  $J = 7.4$  Hz, 1H), 7.04 (d,  $J = 7.7$  Hz, 2H), 6.83-6.81 (m, 2H), 6.56 (d,  $J = 7.9$  Hz, 1H), 5.90 (s, 2H), 3.47 (s, 3H).  $^{13}\text{C}\{^1\text{H}\}$  NMR (100 MHz,  $\text{CDCl}_3$ )  $\delta$  170.0, 148.7, 147.0, 145.3, 129.7, 129.2, 126.7, 126.4, 124.0, 109.5, 107.5, 101.3, 38.6. **MS (ESI)**  $m/z$  256 (M+H), 278 (M+Na); **HRMS (ESI)**  $m/z$  calc'd for  $\text{C}_{15}\text{H}_{13}\text{NO}_3$  [M+H]<sup>+</sup>: 256.0968; found: 256.0956.

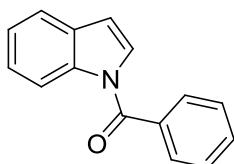


**N-Phenylbenzamide:** A light gray solid was obtained (99%). All spectral data are in agreement with reported literature data.<sup>43</sup> m.p. 159-161 °C.  $^1\text{H NMR}$  (400 MHz,  $\text{DMSO}-d_6$ )  $\delta$  10.24 (s, 1H)

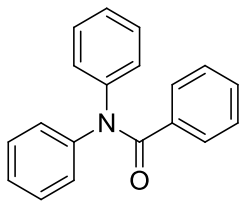
7.97-7.95 (m, 2H), 7.80-7.78 (m, 2H), 7.61-7.51 (m, 3H), 7.35 (t,  $J = 8.0$  Hz, 2H), 7.10 (t,  $J = 8.0$  Hz, 1H).  $^{13}\text{C}\{^1\text{H}\}$  NMR (100 MHz, DMSO- $d_6$ )  $\delta$  165.5, 139.1, 135.0, 131.5, 128.6, 128.4, 127.6, 123.6, 120.3. **MS (ESI)**  $m/z$  198 (M+H), 220 (M+Na); **HRMS (ESI)**  $m/z$  calc'd for  $\text{C}_{13}\text{H}_{11}\text{NO}$  [M+H] $^+$ : 198.0913; found: 198.0914.



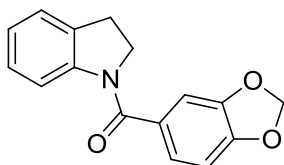
**N-(4-Methoxyphenyl)-N-methylbenzamide:** A light orange solid was obtained (99%). All spectral data are in agreement with reported literature data.<sup>44</sup> m.p. 77-79 °C.  $^1\text{H}$  NMR (400 MHz,  $\text{CDCl}_3$ )  $\delta$  7.29 (d,  $J = 7.0$  Hz, 2H), 7.24-7.14 (m, 3H), 6.95 (d,  $J = 8.7$  Hz, 2H), 6.73 (d,  $J = 8.9$  Hz, 2H), 3.73 (s, 3H), 3.45 (s, 3H).  $^{13}\text{C}\{^1\text{H}\}$  NMR (100 MHz,  $\text{CDCl}_3$ )  $\delta$  170.9, 170.9, 158.1, 138.0, 136.3, 129.6, 129.1, 129.0, 128.8, 128.4, 128.3, 127.9, 114.5, 55.6, 38.8.



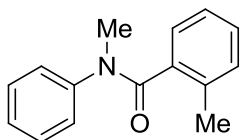
**(1H-Indol-1-yl)(phenyl)methanone:** A light yellow solid was obtained (88%). All spectral data are in agreement with reported literature data.<sup>45</sup> m.p. 58-60 °C.  $^1\text{H}$  NMR (400 MHz,  $\text{CDCl}_3$ )  $\delta$  8.40 (dd, 1H,  $J=0.8\text{Hz}$ ,  $J=8.2\text{Hz}$ ), 7.74 (m, 1H), 7.61 (m, 2H), 7.53 (tdd, 2H,  $J=1.5\text{Hz}$ ,  $J=6.6\text{Hz}$ ,  $J=8.2\text{Hz}$ ), 7.39 (m, 1H), 7.33 (dd, 1H,  $J=1.1\text{Hz}$ ,  $J=7.6\text{Hz}$ ), 7.30 (m, 1H).  $^{13}\text{C}\{^1\text{H}\}$  NMR (100 MHz,  $\text{CDCl}_3$ )  $\delta$  136.3, 134.8, 132.1, 131.0, 129.4, 128.8, 127.8, 125.1, 124.2, 121.1, 116.6, 108.8. **MS**  $m/z$  221 (M), 207, 130, 117, 105, 90, 77.



***N,N*-Diphenylbenzamide:** A white solid was obtained (92%) via trituration in hexanes. All spectral data are in agreement with reported literature data.<sup>46</sup> m.p. 179-181 °C. <sup>1</sup>H NMR (400 MHz, CDCl<sub>3</sub>) δ 7.46-7.44 (m, 2H), 7.30-7.25 (m, 5H), 7.22-7.14 (m, 8H). <sup>13</sup>C{<sup>1</sup>H} NMR (100 MHz, CDCl<sub>3</sub>) δ 170.6, 143.9, 136.1, 130.2, 129.2, 129.1, 127.9, 127.5, 126.4. MS (ESI) *m/z* 274 (M+H), 296 (M+Na); HRMS (ESI) *m/z* calc'd for C<sub>19</sub>H<sub>15</sub>NO [M+H]<sup>+</sup>: 274.1226; found: 274.1226.

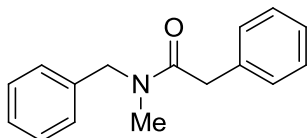


**Benzo[d][1,3]dioxol-5-yl(indolin-1-yl)methanone:** A pink solid was obtained (58%) via a CDI coupling procedure. All spectral data are in agreement with reported literature data.<sup>47</sup> m.p. 120-122 °C. <sup>1</sup>H NMR (400 MHz, CDCl<sub>3</sub>) δ 7.20 (d, 1H, *J* = 7.4Hz), 7.10 (dd, 2H, *J* = 1.7Hz, *J* = 8.0Hz), 7.04 (d, 1H, *J* = 1.6Hz), 7.00 (t, 1H, *J* = 7.5Hz), 6.85 (d, 1H, *J* = 8.0Hz), 6.03 (s, 2H), 4.10 (t, 2H, *J* = 8.3Hz), 3.11 (t, 2H, *J* = 8.2Hz). <sup>13</sup>C{<sup>1</sup>H} NMR (100 MHz, CDCl<sub>3</sub>) δ 168.5, 149.6, 147.9, 143.0, 132.6, 130.8, 127.4, 125.1, 124.0, 122.2, 117.1, 108.5, 108.3, 101.7, 50.9, 28.4. MS *m/z* 267 (M), 251, 149, 135, 117, 90, 65.

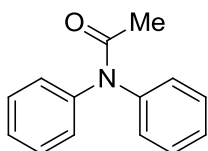


***N*,2-Dimethyl-*N*-phenylbenzamide:** A light yellow oil was obtained (99%). <sup>1</sup>H NMR (400 MHz, CDCl<sub>3</sub>) δ 7.13 (m, 9H), 3.48 (s, 3H), 2.33 (s, 3H). <sup>13</sup>C{<sup>1</sup>H} NMR (100 MHz, CDCl<sub>3</sub>) δ

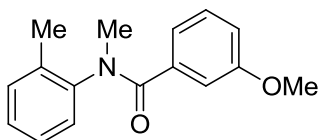
171.4, 144.1, 136.8, 135.0, 134.9, 130.4, 129.1, 128.8, 127.8, 127.7, 127.1, 126.8, 126.7, 125.3, 37.5, 19.7. **MS (ESI)**  $m/z$  226 (M+H), 248 (M+Na); **HRMS (ESI)**  $m/z$  calc'd for  $C_{15}H_{15}NO$  [M+H]<sup>+</sup>: 226.1226; found: 226.1223.



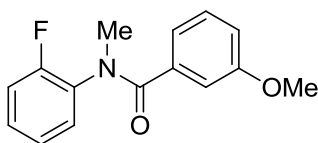
***N*-Benzyl-*N*-methyl-2-phenylacetamide:** A white solid was obtained (99%). All spectral data are in agreement with reported literature data.<sup>48</sup> m.p. 61-63°C. Characterized as a mixture of rotamers: **<sup>1</sup>H NMR** (400 MHz, CDCl<sub>3</sub>) Major rotamer: δ 7.34-7.21 (m, 9H, overlap), 7.10 (s, 1H), 4.61 (s, 2H), 3.79 (s, 2H), 2.90 (s, 3H). Minor rotamer: δ 7.34-7.21 (m, 9H, overlap), 7.09 (s, 1H), 4.53 (s, 2H), 3.75 (s, 2H), 2.95 (s, 3H). Assignment of the <sup>13</sup>C NMR to the each rotamer could not be accomplished: **<sup>13</sup>C{<sup>1</sup>H} NMR** (100 MHz, CDCl<sub>3</sub>) δ 171.5, 171.1, 137.3, 136.5, 135.1, 135.0, 128.9, 128.8, 128.8, 128.7, 128.6, 128.1, 127.6, 127.3, 126.8, 126.8, 126.4, 53.7, 51.0, 41.2, 40.9, 35.2, 34.0. **MS**  $m/z$  239 (M), 167, 120, 104, 91.



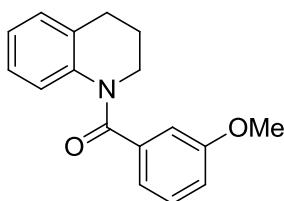
***N,N*-Diphenylacetamide:** A white solid was obtained (99%). Spectral data has been reported.<sup>49,50</sup> m.p. 97-98 °C. **<sup>1</sup>H NMR** (400 MHz, CDCl<sub>3</sub>) δ 7.45-7.15 (m, 5H), 7.28-7.26 (m, 5H), 2.06 (s, 3H). **<sup>13</sup>C{<sup>1</sup>H} NMR** (100 MHz, CDCl<sub>3</sub>) δ 170.7, 130.0-126.7 (broad peak), 24.1



**3-Methoxy-*N*-methyl-*N*-(*o*-tolyl)benzamide:** A yellow oil was obtained (99%).  $^1\text{H NMR}$  (400 MHz,  $\text{CDCl}_3$ )  $\delta$  7.13-7.07 (m, 3H), 7.04-7.00 (m, 2H), 6.85-6.83 (m, 2H), 6.75 (dd, 1H,  $J = 2.1$  Hz,  $J = 8.2$  Hz), 3.63 (s, 3H), 3.38 (s, 3H), 2.22 (s, 3H).  $^{13}\text{C}\{^1\text{H}\}$  NMR (100 MHz,  $\text{CDCl}_3$ )  $\delta$  170.4, 158.7, 143.6, 137.0, 134.8, 131.3, 128.6, 128.5, 127.7, 127.0, 120.8, 116.2, 113.3, 55.1, 37.6, 17.8. **MS (ESI)**  $m/z$  256 (M+H), 278 (M+Na); **HRMS (ESI)**  $m/z$  calc'd for  $\text{C}_{14}\text{H}_{13}\text{NO}$   $[\text{M}+\text{H}]^+$ : 256.1332; found: 256.1320.

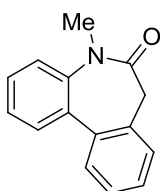


***N*-(2-Fluorophenyl)-3-methoxy-*N*-methylbenzamide:** A yellow oil was obtained (99%).  $^1\text{H NMR}$  (400 MHz,  $\text{CDCl}_3$ )  $\delta$  7.17 (dd, 1H,  $J = 6.1$  Hz,  $J = 12.7$  Hz), 7.08-6.97 (m, 4H), 6.90 (s, 1H), 6.86 (d, 1H,  $J = 7.2$  Hz), 6.79 (d, 1H,  $J = 7.8$  Hz), 3.68 (s, 3H), 3.42 (s, 3H).  $^{13}\text{C}\{^1\text{H}\}$  NMR (100 MHz,  $\text{CDCl}_3$ )  $\delta$  170.9, 159.0, 158.6, 156.2, 136.8, 129.6, 129.0, 128.9, 128.8, 124.7, 124.6, 120.4, 116.7, 116.5, 116.3, 112.9, 55.2, 37.5 (broad). **MS (ES+)**  $m/z$  259 (M); **HRMS (ES+)**  $m/z$  calc'd for  $\text{C}_{15}\text{H}_{14}\text{FNO}_2$   $[\text{M}]^+$ : 259.1009; found: 259.1009.

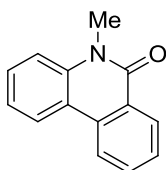


**(3,4-Dihydroquinolin-1(2H)-yl)(3-methoxyphenyl)methanone:** White crystals were obtained (99%). Mp 71-73°C.  $^1\text{H NMR}$  (400 MHz,  $\text{CDCl}_3$ )  $\delta$  7.15 (t, 2H,  $J = 7.8$  Hz), 6.99 (t, 1H,  $J = 7.5$  Hz), 6.95 (s, 1H), 6.90-6.86 (m, 3H), 6.77 (d, 1H,  $J = 6.9$  Hz), 3.90 (t, 2H,  $J = 6.5$  Hz), 3.73 (s, 3H), 2.84 (t, 2H,  $J = 6.6$  Hz), 2.05 (p, 2H,  $J = 6.6$  Hz).  $^{13}\text{C}\{^1\text{H}\}$  NMR (100 MHz,  $\text{CDCl}_3$ )  $\delta$  170.0, 159.3, 139.3, 137.6, 131.5, 129.1, 128.3, 125.8, 125.3, 124.6, 120.9, 116.3, 113.7, 55.3, 44.5, 26.9, 24.1. **MS (ESI)**  $m/z$  268 (M+H), 290 (M+Na); **HRMS (ESI)**  $m/z$  calc'd for  $\text{C}_{17}\text{H}_{17}\text{NO}_2$   $[\text{M}+\text{H}]^+$ : 268.1332; found: 268.1332.

**General procedure for the intramolecular tandem C—H functionalization reaction:** In a one-dram vial equipped with a Teflon cap was added *N*-methyl-*N*-phenylbenzamide (42.2 mg, 0.20 mmol), Pd(OAc)<sub>2</sub> (4.5 mg, 0.02 mmol, 10 mol%), Na<sub>2</sub>S<sub>2</sub>O<sub>8</sub> (190.0 mg, 0.8 mmol), and 1,2-dichloroethane (1 mL). Subsequently, trifluoroacetic acid (76 μL, 1 mmol) was added. The vial was sealed with a Teflon cap and stirred on a heating block at 70 °C for 96 h. After cooling to ambient temperature, the resulting mixture was diluted in EtOAc and washed with 2 mL sat'd NaHCO<sub>3</sub>. The aqueous phase was extracted with EtOAc. The combined organic extracts were concentrated *in vacuo* and the resulting residue was purified by preparative thin-layer chromatography (eluent: MeOH/CH<sub>2</sub>Cl<sub>2</sub> = 2:98, v/v) to afford the target product as an off-white solid (25.1 mg, 60%).



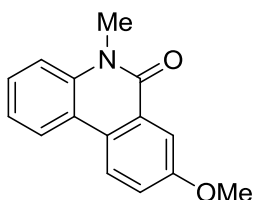
**5-Methyl-5H,7H-dibenzo[b,d]azepin-6-one:** A white solid (11.1 mg, 25%) was obtained. **mp** 144-146°C. **<sup>1</sup>H NMR** (400 MHz, CDCl<sub>3</sub>) δ (ppm) 7.59-7.57 (m, 2H), 7.46-7.28 (m, 2H), 3.58 (d, 1H, *J* = 12.8 Hz), 3.42 (d, 1H, *J* = 12.4 Hz), 3.32 (s, 3H). **<sup>13</sup>C{<sup>1</sup>H} NMR** (100 MHz, CDCl<sub>3</sub>) δ (ppm) 171.6, 141.8, 136.4, 135.5, 133.9, 130.0, 128.7, 128.4, 128.0, 127.8, 127.6, 125.2, 122.5, 42.1, 36.1. **IR** (neat) ν (cm<sup>-1</sup>) 2924, 1653 (s), 1422 (m), 1364 (m), 1105 (m). **MS** (*m/z*) 197 (M), 105, 93, 77.



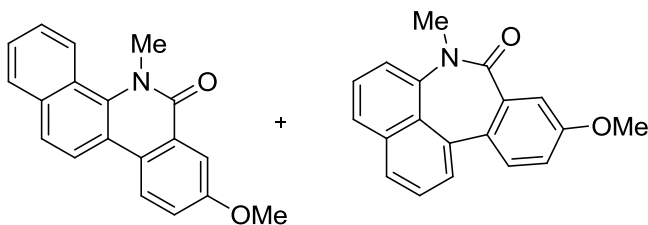
**5-Methylphenanthridin-6(5H)-one:** An off-white crystal was obtained (60%). **mp** 95-98°C. **<sup>1</sup>H NMR** (400 MHz, CDCl<sub>3</sub>) δ (ppm) 8.56 (d, 1H, *J* = 7.8 Hz), 8.30-8.28 (m, 2H), 7.76 (t, 1H, *J* =

7.3 Hz), 7.61-7.54 (m, 2H), 7.43 (d, 1H,  $J = 8.2$  Hz), 7.33 (t, 1H,  $J = 7.3$  Hz), 3.83 (s, 3H).

$^{13}\text{C}\{^1\text{H}\}$  NMR (100 MHz,  $\text{CDCl}_3$ )  $\delta$  (ppm) 161.7, 138.1, 133.6, 132.4, 129.6, 128.9, 128.0, 125.6, 123.2, 122.5, 121.6, 119.3, 115.1, 30.00. **MS** ( $m/z$ ) 209 (M), 178, 152.



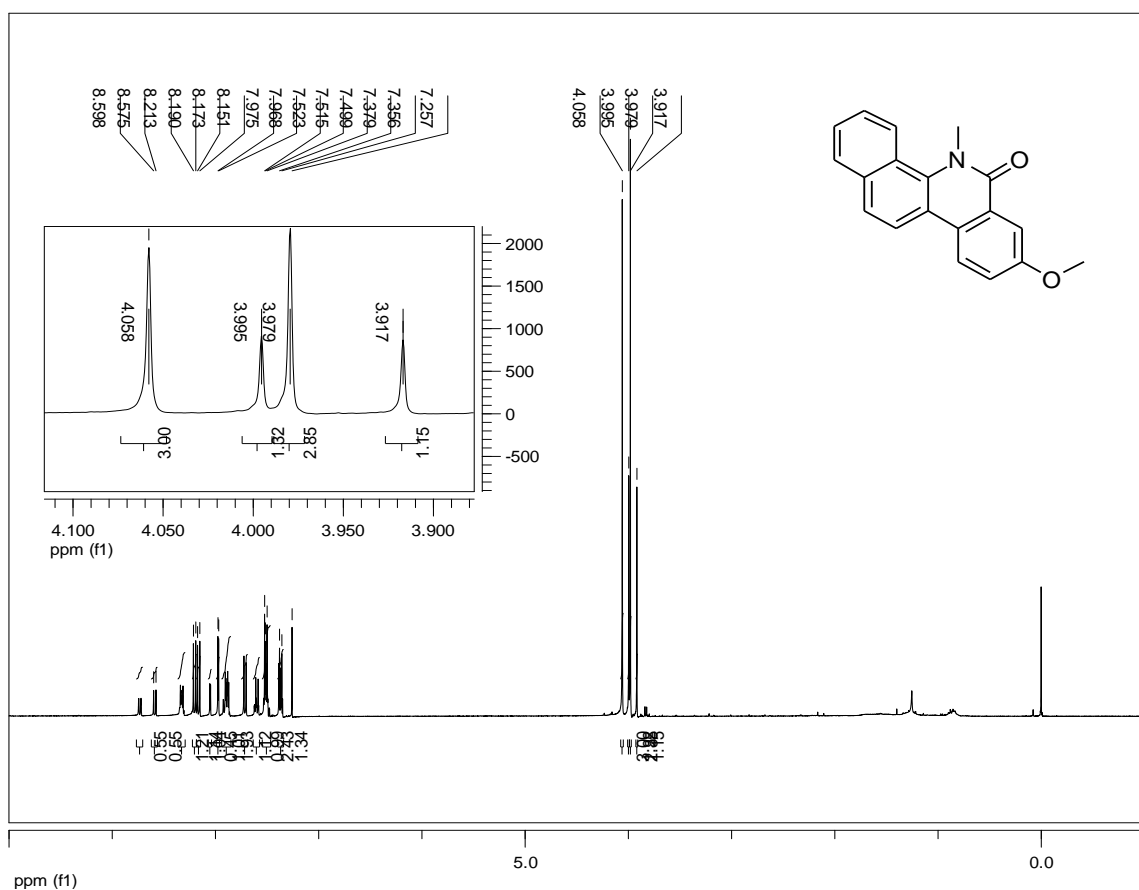
**8-Methoxy-5-methylphenanthridin-6(5H)-one:** An off-white solid was obtained (77%). m.p. 135-137 °C. All spectral data are in agreement with reported literature data.<sup>51</sup>  $^1\text{H}$  NMR (400 MHz,  $\text{CDCl}_3$ )  $\delta$  8.16-8.13 (m, 2H), 7.94 (d, 1H,  $J = 2.8$  Hz), 7.47 (ddd, 1H,  $J = 1.4$  Hz,  $J = 7.3$  Hz,  $J = 8.4$  Hz), 7.37 (d, 1H,  $J = 7.9$  Hz), 7.33-7.26 (m, 2H), 3.95 (s, 3H), 3.80 (m, 3H).  $^{13}\text{C}\{^1\text{H}\}$  NMR (100 MHz,  $\text{CDCl}_3$ )  $\delta$  161.4, 159.5, 137.0, 128.4, 127.1, 126.8, 123.4, 122.6, 122.5, 122.2, 119.4, 114.9, 109.2, 55.7, 30.1. **MS (EI)**  $m/z$  239 (M); **HRMS (EI)**  $m/z$  calc'd for  $\text{C}_{15}\text{H}_{13}\text{NO}_2$   $[\text{M}]^+$ : 239.0946; found: 239.0942.



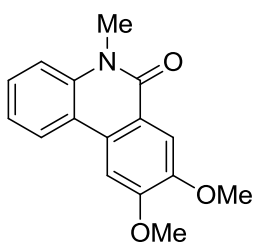
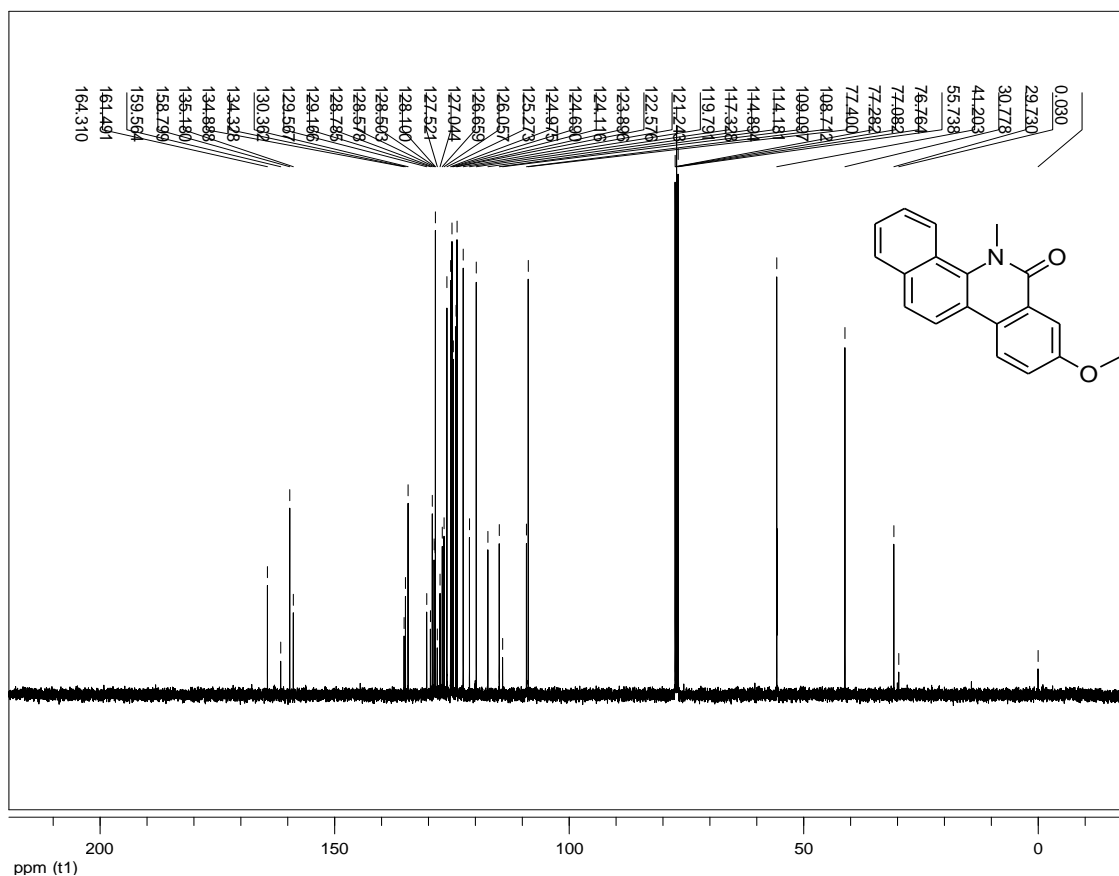
**8-Methoxy-5-methylbenzo[c]phenanthridin-6(5H)-one/7-methylbenzo[e]naphtho[1,8-bc]azepin-8(7H)-one:** An orange solid was obtained (63%). m.p. 111-115 °C. This compound was isolated as an inseparable mixture of two isomers in a 2.4:1 ratio (*phenanthridin-6(5H)-one:azepin-8(7H)-one*). The characterization of the major isomer is as follows:  $^1\text{H}$  NMR (400 MHz,  $\text{CDCl}_3$ )  $\delta$  8.35-8.30 (m, 1H), 8.20 (d,  $J = 9.0$  Hz, 1H), 8.16 (d,  $J = 8.8$  Hz, 1H), 7.97 (d,  $J = 2.8$  Hz, 1H), 7.90-7.87 (m, 1H, overlap), 7.71 (d,  $J = 8.6$  Hz, 1H), 7.52-7.49 (m, 2H, overlaps with minor isomer), 7.38-7.36 (m, 1H, overlaps with minor isomer), 4.06 (s, 3H), 3.98 (s, 3H).

Minor isomer:  $\delta$  8.73 (d,  $J = 8.6$  Hz, 1H), 8.59 (d,  $J = 9.0$  Hz, 1H), 8.05 (d,  $J = 2.9$  Hz, 1H), 7.90-7.87 (m, 1H, overlaps with major isomer), 7.62-7.59 (m, 2H), 7.52-7.49 (m, 2H, overlaps with major isomer), 7.38-7.36 (m, 1H, overlaps with major isomer), 4.00 (s, 3H), 3.92 (s, 3H).

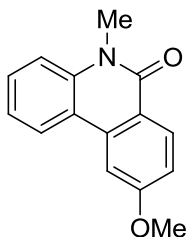
Assignment of the  $^{13}\text{C}$  NMR to the different isomers could not be accomplished:  $^{13}\text{C}\{^1\text{H}\}$  NMR (100 MHz,  $\text{CDCl}_3$ )  $\delta$  164.3, 161.5, 159.6, 158.8, 135.2, 134.9, 134.3, 130.4, 129.6, 129.2, 128.8, 128.6, 128.5, 128.1, 127.5, 127.0, 126.7, 126.1, 125.3, 125.0, 124.7, 124.1, 123.9, 122.6, 121.2, 119.8, 117.3, 114.9, 114.2, 109.1, 108.7, 55.7, 55.7, 41.2, 30.8. **MS (EI)**  $m/z$  289 (M); **HRMS (EI)**  $m/z$  calc'd for  $\text{C}_{19}\text{H}_{15}\text{NO}_2$   $[\text{M}]^+$ : 289.1103; found: 289.1110.



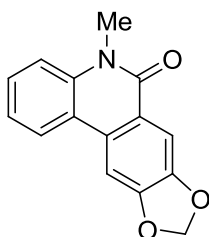




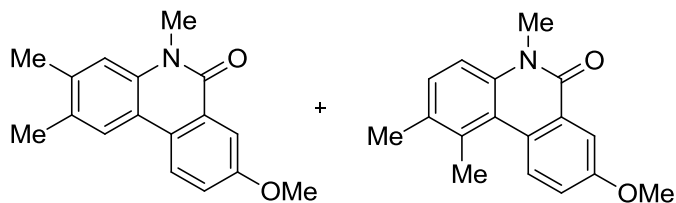
**8,9-Dimethoxy-5-methylphenanthridin-6(5H)-one:** An off-white solid was obtained (60%). m.p. 219-220 °C. All spectral data are in agreement with reported literature data.<sup>52</sup>  $^1\text{H NMR}$  (400 MHz,  $\text{CDCl}_3$ )  $\delta$  8.10 (dd,  $J = 1.2$  Hz,  $J = 8.1$  Hz, 1H), 7.88 (s, 1H), 7.53 (s, 1H), 7.51-7.47 (m, 1H), 7.38-7.36 (m, 1H), 7.31-7.26 (m, 1H), 4.07 (m, 3H), 4.02 (m, 3H), 3.79 (m, 3H).  $^{13}\text{C}\{^1\text{H}\}$  NMR (100 MHz,  $\text{CDCl}_3$ )  $\delta$  161.3, 153.4, 150.0, 137.7, 128.8, 128.4, 122.8, 122.4, 119.8, 119.3, 115.2, 109.2, 102.7, 56.4, 56.3, 30.1. **MS (EI)**  $m/z$  269 (M); **HRMS (EI)**  $m/z$  calc'd for  $\text{C}_{16}\text{H}_{15}\text{NO}_3$   $[\text{M}]^+$ : 269.1052; found: 269.1057.



**9-Methoxy-5-methylphenanthridin-6(5H)-one:** A pale yellow solid was obtained (33%). m.p. 135-137 °C. All spectral data are in agreement with reported literature data.<sup>53</sup> **<sup>1</sup>H NMR** (400 MHz, CDCl<sub>3</sub>) δ 8.49 (d, *J* = 8.9 Hz, 1H), 8.22 (d, *J* = 8.0 Hz, 1H), 7.66 (d, *J* = 2.2 Hz, 1H), 7.56 (t, *J* = 7.8 Hz, 1H), 7.42 (d, *J* = 8.4 Hz, 1H), 7.32 (t, *J* = 7.6 Hz, 1H), 7.16 (dd, *J* = 2.2 Hz, *J* = 8.9 Hz, 1H), 4.00 (s, 3H), 3.80 (s, 3H). **<sup>13</sup>C{<sup>1</sup>H} NMR** (100 MHz, CDCl<sub>3</sub>) δ 163.0, 161.5, 138.6, 135.5, 131.1, 129.7, 123.3, 122.2, 119.4, 119.2, 115.9, 115.1, 104.5, 55.6, 29.7. **MS (ESI)** *m/z* 240 (M+H), 262 (M+Na); **HRMS (ESI)** *m/z* calc'd for C<sub>15</sub>H<sub>14</sub>NO<sub>2</sub> [M+H]<sup>+</sup>: 240.1019; found: 240.1019.



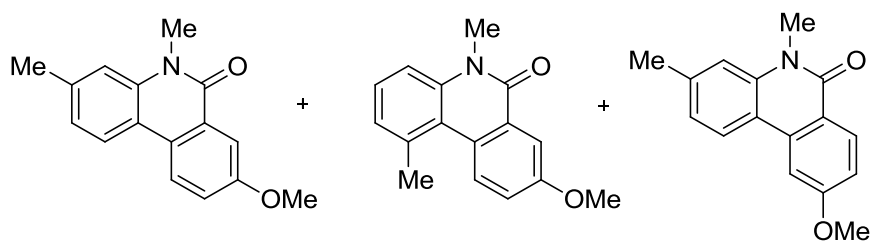
**5-Methyl-[1,3]dioxolo[4,5-j]phenanthridin-6(5H)-one:** A pale yellow solid was obtained (30%). m.p. 239-241 °C. All spectral data are in agreement with reported literature data.<sup>54</sup> **<sup>1</sup>H NMR** (400 MHz, CDCl<sub>3</sub>) δ 8.09 (dd, *J* = 1.3 Hz, *J* = 8.1 Hz, 1H), 7.91 (s, 1H), 7.61 (s, 1H), 7.51 (ddd, *J* = 1.4 Hz, *J* = 7.2 Hz, *J* = 8.5 Hz, 1H), 7.40 (d, *J* = 7.8 Hz, 1H), 7.32-7.28 (m, 1H), 6.12 (s, 2H), 3.80 (s, 3H). **<sup>13</sup>C{<sup>1</sup>H} NMR** (100 MHz, CDCl<sub>3</sub>) δ 161.0, 152.2, 148.4, 137.5, 130.4, 128.9, 122.9, 122.4, 121.4, 119.3, 115.0, 107.1, 102.0, 100.4, 30.0. **MS (ESI)** *m/z* 254 (M+H), 276 (M+Na); **HRMS (ESI)** *m/z* calc'd for C<sub>15</sub>H<sub>11</sub>NO<sub>3</sub> [M+H]<sup>+</sup>: 254.0811; found: 254.0799.



**8-Methoxy-2,3,5-trimethylphenanthridin-6(5H)-one/ 8-methoxy-1,2,5-**

**trimethylphenanthridin-6(5H)-one:** A yellow solid was obtained (42%). m.p. 239-241 °C. This compound was isolated as an inseparable mixture of two isomers in a 3:1 ratio (2,3,5-trimethyl/1,2,5-trimethyl). The characterization of the major isomer is as follows:  $^1\text{H NMR}$  (400 M Hz,  $\text{CDCl}_3$ )  $\delta$  8.13 (d, 1H,  $J = 8.9$  Hz), 7.94 (d, 1H,  $J = 2.8$  Hz), 7.90 (s, 1H), 7.30 (d, 1H,  $J = 2.9$  Hz), 7.16 (s, 1H), 3.95 (s, 3H), 3.79 (s, 3H), 2.40 (s, 3H), 2.38 (s, 3H). characterization of the minor isomer:  $\delta$  8.21 (d, 1H,  $J = 9.1$  Hz), 8.08 (d, 1H,  $J = 8.9$  Hz), 8.03 (d, 1H,  $J = 3.0$  Hz), 7.32 (d, 1H,  $J = 2.8$  Hz), 7.19 (s, 1H), 3.97 (s, 3H), 3.78 (s, 3H), 2.74 (s, 3H), 2.41 (s, 3H).

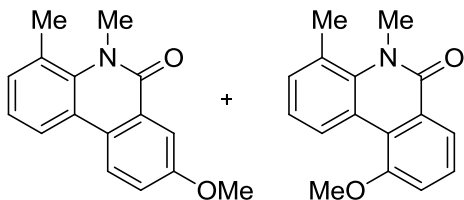
Assignment of the  $^{13}\text{C NMR}$  to the different isomers could not be accomplished:  $^{13}\text{C}\{^1\text{H}\}$  NMR (100 M Hz,  $\text{CDCl}_3$ )  $\delta$  161.4, 159.1, 158.5, 137.6, 135.2, 131.0, 129.1, 127.2, 126.5, 125.2, 123.3, 123.3, 123.2, 122.2, 122.2, 120.1, 119.4, 117.2, 115.9, 112.1, 109.4, 109.2, 108.8, 55.7, 40.1, 30.6, 30.1, 20.9, 20.4, 19.4, 19.1. **MS (EI)**  $m/z$  267 (M); **HRMS (ESI)**  $m/z$  calc'd for  $\text{C}_{17}\text{H}_{17}\text{NO}_2$   $[\text{M}]^+$ : 267.1259; found: 267.1256.



**8-Methoxy-3,5-dimethylphenanthridin-6(5H)-one/ 8-methoxy-1,5-dimethylphenanthridin-6(5H)-one/ 9-methoxy-3,5-dimethylphenanthridin-6(5H)-one:**

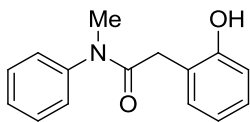
An orange solid was obtained (46%). m.p. 239-241 °C. This compound was isolated as an inseparable mixture of three isomers in a 3:2:2 ratio. The characterization of the major isomer is as follows:  $^1\text{H NMR}$  (400 M Hz,  $\text{CDCl}_3$ )  $\delta$  8.11 (d, 1H,  $J = 8.9$  Hz), 8.03 (d, 1H,  $J = 8.1$  Hz), 7.93 (d, 1H,  $J = 2.8$  Hz), 7.32-7.29 (m, 2H, overlap with other isomers), 7.18 (s, 1H), 3.95 (s, 3H), 3.79 (s, 3H), 2.49 (s, 3H).

Combined characterization of the two minor isomers:  $\delta$  8.36 (d, 1H,  $J = 9.2$  Hz), 8.15 (d, 1H,  $J = 8.9$  Hz), 8.11 (d, 1H,  $J = 9.0$  Hz), 8.06 (d, 1H,  $J = 3.0$  Hz), 8.00 (d, 1H,  $J = 8.1$  Hz), 7.95-7.94 (m, 2H, overlap), 7.90 (d, 1H,  $J = 2.8$  Hz), 7.38-7.29 (m, 3H), 7.14 (d, 1H,  $J = 7.2$  Hz), 7.10 (d, 1H,  $J = 8.2$  Hz), 3.97 (s, 3H), 3.94 (s, 3H), 3.81 (s, 3H), 3.79 (s, 3H), 2.90 (s, 3H), 2.46 (s, 3H). Assignment of the  $^{13}\text{C}$  NMR to the different isomers could not be accomplished:  $^{13}\text{C}\{^1\text{H}\}$  NMR (100 MHz,  $\text{CDCl}_3$ )  $\delta$  161.6, 161.4, 161.3, 159.4, 159.2, 158.6, 138.7, 138.1, 137.0, 135.4, 134.9, 132.8, 131.9, 129.4, 128.3, 128.2, 128.1, 127.5, 127.3, 127.0, 126.9, 126.7, 126.4, 126.1, 123.7, 123.7, 123.4, 123.2, 122.9, 122.8, 122.5, 122.3, 122.2, 122.1, 120.6, 120.5, 119.3, 119.2, 117.0, 115.3, 114.9, 113.3, 109.7, 109.2, 109.2, 108.8, 55.7, 55.6, 38.5, 31.0, 30.1, 26.5, 23.6, 21.9, 21.0. **MS (ES+)**  $m/z$  253 (M); **HRMS (ES+)**  $m/z$  calc'd for  $\text{C}_{16}\text{H}_{15}\text{NO}_2$   $[\text{M}]^+$ : 253.1103; found: 253.1100.



**8-Methoxy-4,5-dimethylphenanthridin-6(5H)-one/ 10-methoxy-4,5-dimethylphenanthridin-**

**6(5H)-one:** An orange solid was obtained (38%). m.p. 239-241 °C. This compound was isolated as an inseparable mixture of two isomers in a 5:1 ratio. The characterization of the major isomer is as follows:  $^1\text{H}$  NMR (400 M Hz,  $\text{CDCl}_3$ )  $\delta$  8.13 (d, 1H,  $J = 9.0$  Hz), 8.01 (d, 1H,  $J = 7.2$  Hz), 7.91 (d, 1H,  $J = 2.8$  Hz), 7.41-7.33 (m, 1H), 7.27-7.25 (m, 1H, overlap), 7.19 (t, 1H,  $J = 7.6$  Hz), 3.95 (s, 3H), 3.82 (s, 3H), 2.66 (s, 3H). Characterization of the minor isomer:  $\delta$  8.38 (d, 1H,  $J = 9.2$  Hz), 8.08 (d, 1H,  $J = 3.0$  Hz), 7.96 (d, 1H,  $J = 2.8$  Hz), 7.37 (m, 1H), 7.27-7.25 (m, 1H, overlap), 7.15 (d, 1H,  $J = 7.2$  Hz), 3.97 (s, 3H), 3.82 (s, 3H), 2.92 (s, 3H). Assignment of the  $^{13}\text{C}$  NMR to the different isomers could not be accomplished:  $^{13}\text{C}\{^1\text{H}\}$  NMR (100 M Hz,  $\text{CDCl}_3$ )  $\delta$  164.0, 159.4, 138.5, 135.4, 132.8, 128.4, 127.6, 127.3, 127.3, 126.7, 126.1, 123.7, 122.9, 122.3, 121.4, 120.7, 120.5, 113.3, 109.8, 108.9, 55.7, 55.6, 38.5, 31.0, 26.5, 23.6. **MS (ES+)**  $m/z$  253 (M); **HRMS (ES+)**  $m/z$  calc'd for  $\text{C}_{16}\text{H}_{15}\text{NO}_2$   $[\text{M}]^+$ : 253.1103; found: 253.1104.



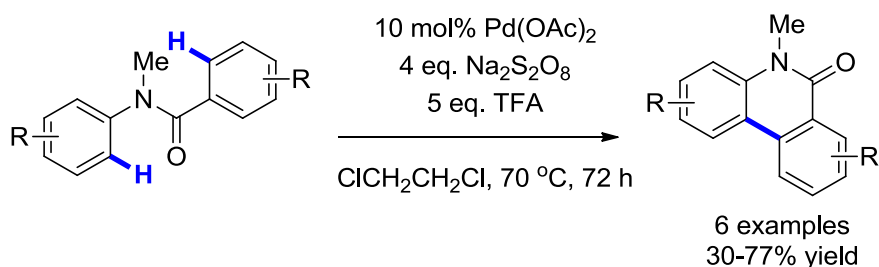
**2-(2-Hydroxyphenyl)-N-methyl-N-phenylacetamide:** A colourless oil (3.1 mg, 6%) was obtained. **<sup>1</sup>H NMR** (400 MHz, CDCl<sub>3</sub>) δ (ppm) 10.24 (s, 1H), 7.54-7.44 (m, 3H), 7.26-7.22 (m, 2H), 7.15 (td, 1H, *J* = 8.0, 1.6 Hz), 6.98 (dd, 1H, *J* = 8.1 Hz, 1.0 Hz), 6.73 (td, 1H, *J* = 7.4 Hz, 1.1 Hz), 6.50 (dd, 1H, *J* = 7.5 Hz, 1.3 Hz). **<sup>13</sup>C NMR** (100 MHz, CDCl<sub>3</sub>) δ (ppm) 172.5, 156.2, 142.3, 129.4, 129.0, 128.0, 127.7, 126.3, 120.1, 118.9, 117.2, 36.8, 36.5. **IR** (neat) ν (cm<sup>-1</sup>) 2931, 1732 (m), 1630 (m), 1591 (s), 1244 (s), 1114 (m). **MS** (*m/z*) 241 (M), 134, 107, 91, 77.

## Chapter 2 Synthesis, Characterization and Reactivity of Pd-Bimetallic Complexes

### 2 Cyclopalladation of *N*-Phenylbenzamides

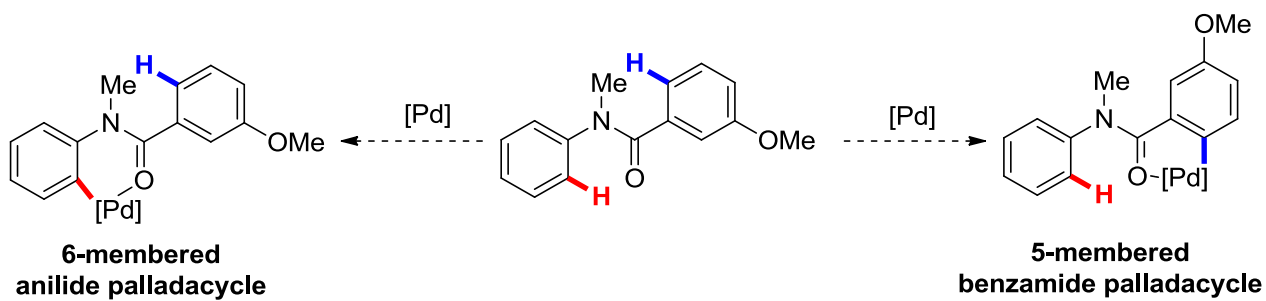
#### 2.1 Introduction

Intramolecular oxidative cross-coupling has emerged as an attractive strategy for generating cyclic architectures from relatively simple precursors (see Chap 1). This transition metal-catalyzed ring-closure involves C—C bond formation by the oxidation of two C—H bonds. Our group reported the palladium-catalyzed lactam synthesis by oxidative cyclization of *N*-phenylbenzamides using sodium persulfate ( $\text{Na}_2\text{S}_2\text{O}_8$ ) as a convenient oxidant (Scheme 20).<sup>55</sup>



#### Scheme 20: Reported Pd(II)-catalyzed intramolecular oxidative cross-coupling

To further study this process, we sought to isolate a Pd(II)-complex from the analogous stoichiometric reaction. *N*-methyl-*N*-phenylbenzamide could undergo initial *ortho* C—H bond activation by cyclopalladation to generate either a Pd(II) six-membered palladacycle or a Pd(II) five-membered palladacycle (Scheme 21).

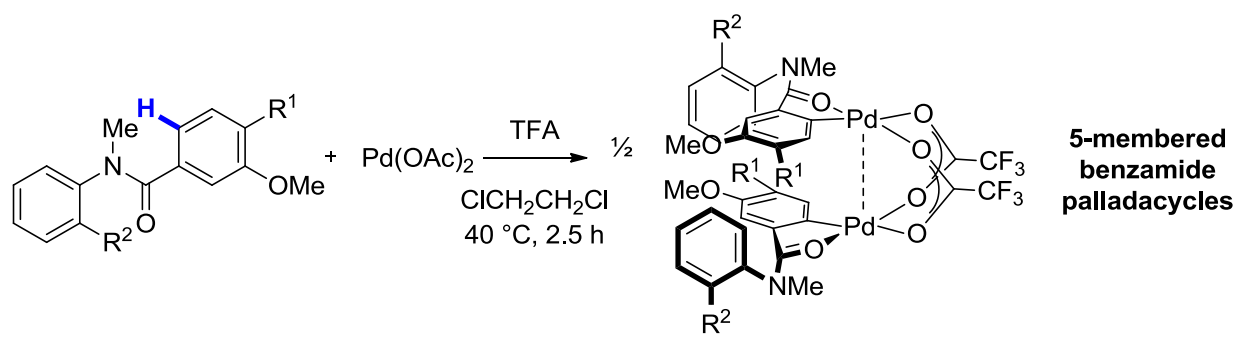


Scheme 21: Possible palladacycles from *N*-phenylbenzamide.

## 2.2 Synthesis of Palladium Complexes

Pd(II)-dimers have attracted interest due to their proposed role as precursors to Pd(III)-Pd(III) or Pd(II)-Pd(IV) intermediates in C–H bond functionalization.<sup>56</sup> For C–H bond activation of *N*-phenylbenzamides, either the six- or five-membered palladacycle could be possible (Scheme 21). To investigate the regioselectivity of the *ortho*-palladation, we submitted 3-methoxy-*N*-methyl-*N*-phenylbenzamide (**1a**) to stoichiometric Pd(OAc)<sub>2</sub> and trifluoroacetic acid (TFA) (Table 5, entry 1). Pd-complexes could also be obtained from the reaction of 1 equivalent of Pd(TFA)<sub>2</sub> and 3-methoxy-*N*-methyl-*N*-phenylbenzamide in 67% yield. The Pd(II)-dimer synthesized with Pd(TFA)<sub>2</sub> gave identical NMR data but was a greenish yellow solid. Recrystallization of the yellow solid followed by X-ray analysis of a single crystal allowed confirmation of a TFA-bridged dimeric Pd-complex (**2a**). Complexes **2b** and **2c** were obtained via an analogous method (Table 5, entries 2 and 3). In all three cases, we observed clean and smooth conversion to the kinetically favored five-membered palladacycle, presumably by C–H bond activation on the benzamide ring. In previous studies on intermolecular oxidative cross-couplings, six-membered palladacycles from the C–H bond activation of anilides were isolated. Attempts to isolate related five-membered palladacycles derived from *N*-alkyl-benzamides had been unsuccessful.

**Table 4: Synthesis and characterization of the Pd-complexes**



Entry	Substrate	R <sup>1</sup> , R <sup>2</sup>	Pd-complex	Yield	<sup>1</sup> H NMR (δ) for H <sub>ortho</sub>	<sup>19</sup> F NMR (δ)
1	<b>1a</b>	R <sup>1</sup> = H, R <sup>2</sup> = H	<b>2a</b>	58%	5.31 ppm	–74.78 ppm
2	<b>1b</b>	R <sup>1</sup> = H, R <sup>2</sup> = Me	<b>2b</b>	65%	5.29 ppm	–74.96 ppm
3	<b>1c</b>	R <sup>1</sup> = OMe, R <sup>2</sup> = H	<b>2c</b>	47%	5.28 ppm	–75.04 ppm

By  $^1\text{H}$  NMR analysis of Pd-complexes **2a**, **2b**, and **2c**, the *ortho*-benzamide protons have a chemical shift around 5.30 ppm, which is significantly more upfield than the benzamide protons in comparison to their respective starting material (chemical shifts between approximately 6.75-7.0 ppm). This characteristic upfield shift is indicative of an anionic arene and is in agreement with the X-ray crystal structure of the complexes which show a Pd–C single bond in the solid state.  $^{19}\text{F}$  NMR studies show that each complex possesses a single peak at slightly different chemical shifts.

The low solubility of the Pd-complexes **2a**, **2b** and **2c** in the majority of solvents prevented us from acquiring reliable photophysical data. These Pd(II)-dimers have some solubility in *N,N*-dimethylformamide and dimethylsulfoxide. All three palladacycles are bench-stable for months provided that they are kept away from light. Other substrates known to undergo oxidative cross-coupling under Pd(II) catalysis were tested, but failed to generate an isolable Pd-complex. Furthermore, these complexes were not observed to form in significant amounts within the reaction mixture based on *in situ* NMR studies. The substitution pattern on the arene rings of the benzamide appears to impact the stability of the corresponding palladacycle.

## 2.3 Characterization of the Palladium Complexes

Recrystallization from *N,N*-dimethylformamide and ether by diffusion technique gave a single crystal suitable for X-ray analysis. A perspective views of each complex **2a**, **2b** and **2c** with the pertinent atom-labeling scheme is shown in Figures 2, 3 and 4 respectively. Crystal data and refinement information for each structure is given in Table 6. Selected bond distances and angles are given in Table 7 for Pd-complexes **2a**, **2b** and **2c**.

In all cases, the palladium atom is coordinated in a slightly distorted square plane (i.e, clamshell geometry).<sup>57</sup> This geometry is further observed through the difference in bond angles between the  $\text{O}_{\text{benzamide}}\text{-Pd(1)-Pd(2)}$  and  $\text{O}_{\text{TFA}}\text{-Pd(1)-Pd(2)}$  where an increase in 14-22° is observed for the open-end of the clamshell. Of note, the two arenes of the ligand are perpendicular to each other and the two ligands are head to tail to one another. Furthermore, we observe that each palladacycle is a Pd(II)-bimetallic complex. The internuclear distance between the two palladium atoms in **2a**, **2b** and **2c** were determined to be 2.8945(6) Å, 2.8859(6) Å and 2.8959(6) Å respectively. In comparison to other Pd-complexes bearing bridging trifluoroacetate ligands, the bimetallic Pd-complex **2a** exhibits slightly shorter Pd–Pd bonds.<sup>58</sup>



**Table 5: Crystal data and structure refinement for crystal structures of Pd-complexes 2a, 2b and 2c.**

	<b>2a</b>	<b>2b</b>	<b>2c</b>
Empirical formula	C <sub>34</sub> H <sub>28</sub> F <sub>6</sub> N <sub>2</sub> O <sub>8</sub> Pd <sub>2</sub>	C <sub>36</sub> H <sub>32</sub> F <sub>6</sub> N <sub>2</sub> O <sub>10</sub> Pd <sub>2</sub>	C <sub>36</sub> H <sub>32</sub> F <sub>6</sub> N <sub>2</sub> O <sub>8</sub> Pd <sub>2</sub>
Formula weight	919.38	979.44	947.44
Temperature (K)	150(1)	150(1)	150(1) K
Wavelength (Å)	0.71073	0.71073 Å	0.71073 Å
Crystal system	Monoclinic	Monoclinic	Monoclinic
Space group	C 2/c	P 21/n	C2/c
a (Å)	20.7156(8)	12.4030(5)	19.6309(5)
b (Å)	13.0752(5)	14.8379(3)	12.8287(5)
c (Å)	15.1485(4)	20.6358(8)	17.0792(6)
α (°)	90	90	90
β (°)	124.5460(17)	97.2140(14)	124.0120(15)
γ (°)	90	90	90
Volume (Å <sup>3</sup> )	3379.6(2)	3767.6(2)	3565.4(2)
Z	4	4	4
Density (calculated) (Mg/m <sup>3</sup> )	1.807	1.727	1.765
Absorption coefficient (mm <sup>-1</sup> )	1.152	1.043	1.095
F(000)	1824	1952	1888
Crystal size (mm)	0.18 x 0.06 x 0.06	0.22 x 0.12 x 0.08	0.16 x 0.16 x 0.10
θ range for data collection (°)	2.74 to 27.50	2.75 to 27.55	2.86 to 27.53
Index ranges	-26 ≤ h ≤ 26 -16 ≤ k ≤ 16 -16 ≤ l ≤ 19	-16 ≤ h ≤ 16 -16 ≤ k ≤ 19 -21 ≤ l ≤ 26	-25 ≤ h ≤ 23 -16 ≤ k ≤ 16 -21 ≤ l ≤ 22
Reflections collected	11009	25472	15737
Independent reflections	3847 [R(int) = 0.0710]	8586 [R(int) = 0.0777]	4067 [R(int) = 0.0490]
Completeness to θ = 27.50°	99.2 %	98.8 %	98.9 %
Absorption correction		Semi-empirical from equivalents	
Max. and min. transmission	0.937 and 0.750	0.925 and 0.831	0.901 and 0.827
Refinement method		Full-matrix least-squares on F <sup>2</sup>	
Data / restraints / parameters	3847 / 0 / 237	8586 / 0 / 511	4067 / 0 / 247
Goodness-of-fit on F <sup>2</sup>	1.061	1.048	1.075
Final R indices [I > 2σ(I)]	R1 = 0.0471 wR2 = 0.1021	R1 = 0.0604 wR2 = 0.1246	R1 = 0.0459 wR2 = 0.1104
R indices (all data)	R1 = 0.0954	R1 = 0.1407	R1 = 0.0754

	wR2 = 0.1252	wR2 = 0.1621	wR2 = 0.1281
Largest diff. peak and hole (e.Å <sup>-3</sup> )	2.065 and -1.092	2.132 and -0.973	1.876 and -0.911

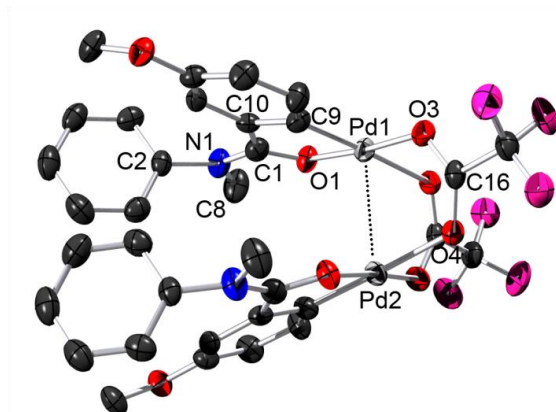


**Figure 2:** ORTEP plot of [(3-methoxy-*N*-methyl-*N*-phenylbenzamide)Pd( $\mu$ -TFA)]<sub>2</sub> (2a). All H atoms have been omitted for clarity. Anisotropic displacement ellipsoids are shown at the 50% probability level.

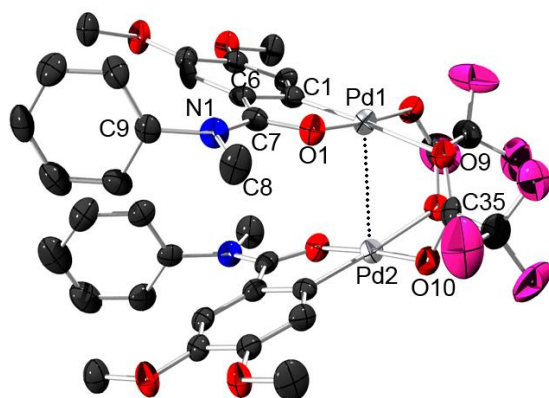


**Figure 3:** ORTEP plot of [(3-methoxy-*N*-methyl-*N*-(*o*-tolyl)benzamide)Pd( $\mu$ -TFA)]<sub>2</sub> (2b). All H atoms have been omitted for clarity. Anisotropic displacement ellipsoids are shown at the 50% probability level.

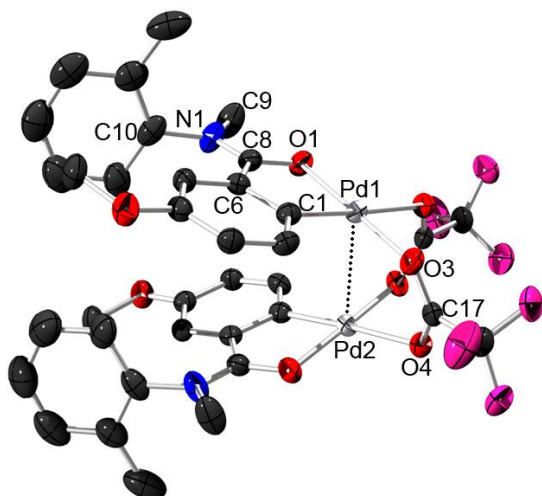


**Figure 4:** ORTEP plot of [(3,4-dimethoxy-*N*-methyl-*N*-phenylbenzamide)Pd( $\mu$ -TFA)]<sub>2</sub> (**2c**). All H atoms have been omitted for clarity. Anisotropic displacement ellipsoids are shown at the 50% probability level.

**Table 6:** Selected bond lengths [ $\text{\AA}$ ] and bond angles [ $^\circ$ ] for **2a**, **2b** and **2c**.

Bond lengths	<b>2a</b>	<b>2b</b>	<b>2c</b>
Pd(1)-Pd	2.8945(6)	2.8859(6)	2.8959(6)
Pd(1)-C	1.949(5)	1.931(6)	1.945(4)
Pd(1)-O <sub>benzamide</sub>	2.017(3)	2.008(4)	2.024(3)
Pd(1)-O <sub>TFA,trans to carbonyl</sub>	2.053(3)	2.040(4)	2.047(3)
Pd(1)-O <sub>TFA,trans to arene</sub>	2.181(3)	2.179(4)	2.192(3)
O <sub>carbonyl</sub> -C <sub>carbonyl</sub>	1.288(5)	1.294(7)	1.272(5)
C <sub>carbonyl</sub> -C <sub>arene</sub>	1.481(6)	1.450(8)	1.487(6)
C <sub>arene</sub> -C <sub>Pd</sub>	1.396(6)	1.411(8)	1.408(6)
C-Pd(1)-Pd	100.80(12)	102.37(17)	102.78(12)
O <sub>carbonyl</sub> -Pd(1)-Pd	102.55(8)	99.57(12)	98.41(9)
O <sub>TFA,trans to carbonyl</sub> -Pd(1)-Pd	80.83(8)	83.35(12)	84.16(8)
O <sub>TFA,trans to arene</sub> -Pd(1)-Pd	79.92(8)	78.12(11)	77.51(8)
O <sub>carbonyl</sub> -Pd(1)-O <sub>TFA,trans to carbonyl</sub>	175.16(12)	175.86(16)	175.73(11)
O <sub>carbonyl</sub> -Pd(1)-O <sub>TFA,trans to arene</sub>	92.81(12)	90.38(17)	93.34(11)
C-Pd(1)-O <sub>carbonyl</sub>	82.06(16)	81.9(2)	81.78(15)
O <sub>TFA,trans to carbonyl</sub> -C <sub>TFA</sub> -O <sub>TFA</sub>	130.3(4)	130.6(6)	130.5(4)
C-Pd(1)-O <sub>TFA,trans to carbonyl</sub>	93.95(16)	94.6(2)	94.35(15)
O <sub>TFA,trans to carbonyl</sub> -Pd(1)-O <sub>TFA,trans to arene</sub>	91.18(12)	93.10(17)	90.54(12)
C <sub>arene</sub> -C <sub>Pd</sub> -Pd(1)	114.1(3)	114.5(4)	114.7(3)

To further the study of these complexes and their possible role as catalysts in the studied cross-coupling reaction, cyclic voltammetry measurements were attempted. The Seferos Group kindly

let me use their cv instrument. Oxidation potentials were obtained for the three Pd-complexes described above. However this oxidation was irreversible in every case. This result is in contrast to Bercaw and coworkers' 2010 report on the synthesis and characterization of similar TFA-bridged Pd-complexes obtained via C–H bond insertion where they observed reductive potentials for every oxidation.<sup>59</sup> There can be multiple interpretations for this discrepancy. First, our Pd-complexes could be less stable under oxidation and simply decompose following a one-electron oxidation. Second, there could be an issue relating to the electrodes, the electrolyte, the solvent and the concentration of each sample. A control experiment was therefore performed with Bercaw's phenylpyridine complexes and unfortunately, the same irreversible spectrum was obtained. This lack of reproducibility may indicate a problem with the instrument and the experimental.

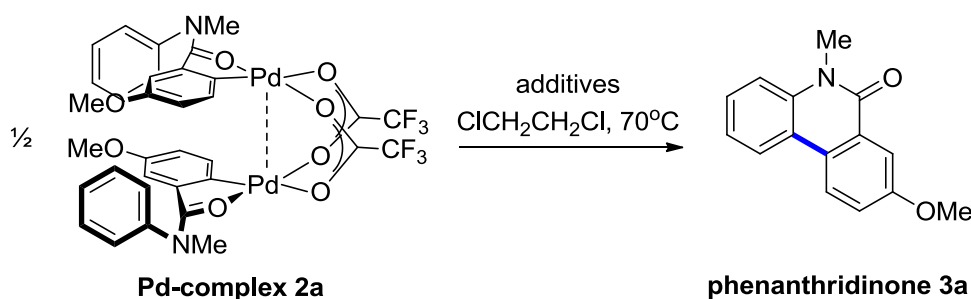
We found that the Pd-complexes are unstable in solution in the presence of electrolytes, since the complexes decompose in coordinating solvents in the presence of the electrolyte tetrabutylammonium hexafluorophosphate (TBAPF<sub>6</sub>) used in the cyclic voltammetry experiments. Dissolving the complexes in acetonitrile, for example, followed by the addition of TBAPF<sub>6</sub> resulted in decomposition to form Pd-black. The <sup>1</sup>H NMR of this solution indicated a complex mixture of products. The complex in acetonitrile-d<sub>3</sub> is stable as confirmed by repeated <sup>1</sup>H NMR.

## 2.4 Stoichiometric Experiments of the Palladium Complexes

With the dimeric palladium complex **2a** in hand, we sought to investigate its viability as an intermediate in the catalytic cycle. Previous work in our group has demonstrated that the mechanism of oxidative cross-coupling depends on the directing group and the oxidant (see Chapter 1). For instance, in the *ortho*-arylation of *O*-phenylcarbamates, reductive elimination from the Pd(II) dimers was observed at 70 °C in benzene without additives, while for anilides, the isolated palladacycles underwent reductive elimination solely in the presence of TFA and Na<sub>2</sub>S<sub>2</sub>O<sub>8</sub>. In the case of our intramolecular reaction, the coupling partner is part of the ligand. Therefore, for the anilide portion of the ligand to undergo C–H bond activation followed by reductive elimination, a rearrangement of the ligand, which perhaps involves dissociation of the TFA or of the carbonyl of the amide, is required.

In an attempt to observe reductive elimination directly from palladacycle **2a**, we heated a stoichiometric amount of this Pd-complex in 1,2-dichloroethane at 70 °C. The experiment generated none of the desired cross-coupled product within the time-frame of the corresponding catalytic process (24 hours) (Table 8, entry 1). On the other hand, if the reaction was stirred for 4 days at the same temperature, phenanthridinone **3a** could be detected by GC-FID (Table 8, entry 3). When both TFA and Na<sub>2</sub>S<sub>2</sub>O<sub>8</sub> were added to the reaction mixture, the reductive elimination product was detected within 24 hours, but in low yield (Table 8, entry 2). Product **3a** appears to be unstable under the reaction conditions over prolonged times (Table 8, entry 4). Therefore, reductive elimination is a viable process from complex **2a** and the efficiency varies depending on the reaction conditions.

**Table 7: Stoichiometric reductive elimination reactions**



Entry	Additive	Time	Yield <sup>a</sup>
1	None	24 h	-
2	TFA, Na <sub>2</sub> S <sub>2</sub> O <sub>8</sub>	24 h	21%
3	none	4 days	17%
4	TFA, Na <sub>2</sub> S <sub>2</sub> O <sub>8</sub>	4 days	9%

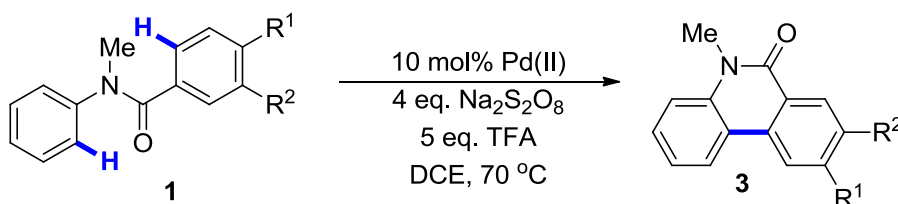
<sup>a</sup> The yield was determined by GC-FID analysis with C<sub>14</sub>H<sub>30</sub> as an internal standard.

## 2.5 Catalytic Reactivity of the Palladium Complexes

Next, Pd-complex **2a** was tested as a catalyst in oxidative cross-coupling reactions. When the palladacycle **2a** is used to catalyze the cyclization of substrate **1a**, (i.e, the substrate and ligand are of the same source), the reaction is complete within 24 h, whereas with Pd(OAc)<sub>2</sub>, the reaction progresses to only 54% yield (Table 9, entries 1 and 2). Complex **2a** also catalyzed the oxidative cross-coupling of other *N*-methyl-*N*-phenylbenzamide substrates. Of note, substrate **1c** yields 64% of the desired phenanthridinone in the presence of catalytic Pd(OAc)<sub>2</sub>, in contrast to yielding 99% with Pd-complex **2a**. (Table 9, entries 3 and 4). Pd-complex **2a** also catalyzed the

reaction with substrate **1d** faster than Pd(OAc)<sub>2</sub> (Table 9, entries 5 and 6). These results suggest that Pd-complex **2a** is a more reactive precatalyst than Pd(OAc)<sub>2</sub> and it appears that Pd(OAc)<sub>2</sub> requires a longer induction period than Pd-complex **2a**. Palladacycles **2b** and **2c** gave similar results as catalysts; they catalyze the intramolecular oxidative arylation more efficiently than Pd(OAc)<sub>2</sub>.

**Table 8: Comparison of Pd(II) catalysts in the oxidative intramolecular cross-coupling reaction.**



Entry	R <sup>1</sup> , R <sup>2</sup>	Substrate	Catalyst	Time	Yield <sup>a</sup>
1	R <sup>1</sup> = H, R <sup>2</sup> = OMe	<b>1a</b>	<b>2a</b>	24 h	90%
2	R <sup>1</sup> = H, R <sup>2</sup> = OMe	<b>1a</b>	Pd(OAc) <sub>2</sub>	24 h	54%
3	R <sup>1</sup> , R <sup>2</sup> = OMe	<b>1c</b>	<b>2a</b>	24 h	99%
4	R <sup>1</sup> , R <sup>2</sup> = OMe	<b>1c</b>	Pd(OAc) <sub>2</sub>	24 h	64%
5	R <sup>1</sup> , R <sup>2</sup> = H	<b>1d</b>	<b>2a</b>	24 h	60%
6	R <sup>1</sup> , R <sup>2</sup> = H	<b>1d</b>	Pd(OAc) <sub>2</sub>	24 h	33%

<sup>a</sup> The yield was determined by GC-FID analysis with C<sub>14</sub>H<sub>30</sub> as an internal standard.

In summary, three novel dimeric TFA-bridged palladium(II) complexes were isolated from an *ortho*-palladation reaction. Single crystal X-ray structures were obtained for Pd-complexes **2a**, **2b** and **2c** and these structures establish a regioselective C–H bond activation to form five-membered palladacycles. Pd-complex **2a** undergoes reductive elimination at 70°C to give phenanthridinone with low efficiency. Nonetheless, Pd-complex **2a** is an effective precatalyst for oxidative cross-coupling reactions.

## 2.6 Experimental

### 2.6.1 Crystallographic Data

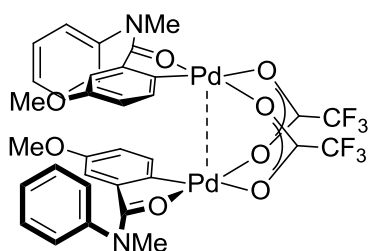
Data were collected on a Bruker-Nonius Kappa-CCD diffractometer using monochromated Mo-K $\alpha$  radiation and were measured using a combination of  $\phi$  scans and  $\omega$  scans with  $\kappa$  offsets, to fill the Ewald sphere. The data were processed using the Denzo-SMN package.<sup>60</sup> Absorption

corrections were carried out using SORTAV.<sup>61</sup> The structure was solved and refined using SHELXTL V6.1<sup>62</sup> for full-matrix least-squares refinement that was based on  $F^2$ . All H atoms were included in calculated positions and allowed to refine in riding-motion approximation with U~iso~ tied to the carrier atom.

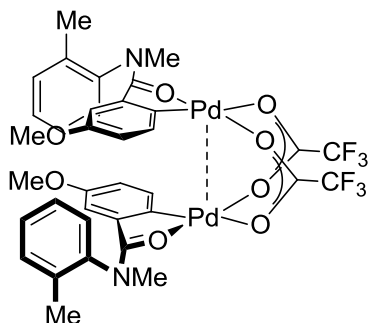
## 2.6.2 Synthesis of Complexes

### General procedure A:

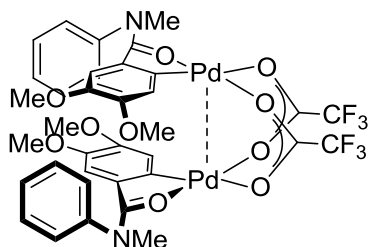
In a one-dram vial was added 3-methoxy-*N*-methyl-*N*-phenylbenzamide (**1a**) (48 mg, 0.20 mmol), Pd(OAc)<sub>2</sub> (45 mg, 0.20 mmol) and 1,2-dichloroethane (1 mL). The reaction mixture was stirred for 2 minutes and trifluoroacetic acid (16  $\mu$ L, 0.21 mmol) was subsequently added. The resulting solution was heated to 40 °C for 2.5 h under air. After cooling to ambient temperature, the reaction mixture was left to stand for several minutes until a yellow precipitate was observed. The mixture was filtered through a cotton-plugged pipette and the resulting yellow residue was washed (4 x 1 mL) with dichloromethane. The filtrate was then discarded. The yellow residue was suspended in dichloromethane and subsequently transferred into a tared vial and concentrated *in vacuo* to afford the bimetallic palladacycle **2a** as a yellow solid (53 mg, 58%).



**[(3-Methoxy-*N*-methyl-*N*-phenylbenzamide)Pd( $\mu$ -TFA)]<sub>2</sub> (**2a**):** A yellow solid (53 mg, 58%) was obtained. <sup>1</sup>H NMR (400 MHz, DMF-*d*<sub>7</sub>)  $\delta$  7.68-7.60 (m, 5H), 6.73 (d, 1H,  $J$  = 7.3 Hz), 6.62 (d, 1H,  $J$  = 8.1 Hz), 5.31 (d, 1H,  $J$  = 1.9 Hz), 3.51 (s, 3H), 3.24 (s, 3H). <sup>13</sup>C{<sup>1</sup>H} NMR (100 MHz, DMF-*d*<sub>7</sub>)  $\delta$  178.4, 156.2, 143.0, 139.1, 135.8, 132.2, 131.1, 130.0, 127.9, 118.2, 114.2, 54.7, 41.0. <sup>19</sup>F NMR (376 MHz, DMF-*d*<sub>7</sub>)  $\delta$  -74.78.



**[(3-Methoxy-*N*-methyl-*N*-(*o*-tolyl)benzamide)Pd( $\mu$ -TFA)]<sub>2</sub> (**2b**):** Prepared according to general procedure A, using 3-methoxy-*N*-methyl-*N*-(*o*-tolyl)benzamide (51 mg, 0.20 mmol) to afford the bimetallic palladacycle **2b** as a yellow solid (62 mg, 65%). <sup>1</sup>H NMR (400 MHz, DMF-*d*<sub>7</sub>)  $\delta$  7.55-7.48 (m, 4H), 6.75 (dd, 1H, *J* = 2.2 Hz, *J* = 8.4 Hz), 6.64 (d, 1H, *J* = 7.8 Hz), 5.29 (d, 1H, *J* = 2.8 Hz), 3.46 (s, 3H), 3.23 (s, 3H), 2.23 (s, 3H). <sup>13</sup>C{<sup>1</sup>H} NMR (100 MHz, DMF-*d*<sub>7</sub>)  $\delta$  178.4, 156.5, 141.5, 139.1, 135.8, 135.6, 132.5, 132.2, 130.4, 128.9, 128.2, 118.5, 113.0, 54.8, 39.8, 16.8. <sup>19</sup>F NMR (376 MHz, DMF-*d*<sub>7</sub>)  $\delta$  -74.96.



**[(3,4-Dimethoxy-*N*-methyl-*N*-phenylbenzamide)Pd( $\mu$ -TFA)]<sub>2</sub> (**2c**):** Prepared according to general procedure A, using 3,4-dimethoxy-*N*-methyl-*N*-phenylbenzamide (54 mg, 0.20 mmol) to afford the bimetallic palladacycle **2c** as a yellow solid (46 mg, 47%). <sup>1</sup>H NMR (400 MHz, DMF-*d*<sub>7</sub>)  $\delta$  7.68-7.64 (m, 2H), 7.60-7.56 (m, 3H), 6.24 (s, 1H), 5.28 (s, 1H), 3.71 (s, 3H), 3.48 (s, 3H), 3.06 (s, 3H). <sup>13</sup>C{<sup>1</sup>H} NMR (100 MHz, DMF-*d*<sub>7</sub>)  $\delta$  178.2, 150.6, 145.7, 143.1, 131.1, 129.9, 128.2, 112.7, 112.6, 112.5, 55.3, 54.8, 40.5 (one C peak overlapping). <sup>19</sup>F NMR (376 MHz, DMF-*d*<sub>7</sub>)  $\delta$  -75.04.

### General Procedure B:



Phenanthridinones **3a-d** were prepared based on a modified literature procedure.<sup>63</sup> In a one-dram vial was added 3-methoxy-*N*-methyl-*N*-phenylbenzamide (**1a**) (48 mg, 0.20 mmol), [(3-methoxy-*N*-methyl-*N*-phenylbenzamide)Pd( $\mu$ -TFA)] (**2a**) (9.2 mg, 0.01 mmol) or Pd(OAc)<sub>2</sub> (4.5 mg, 0.02 mmol), Na<sub>2</sub>S<sub>2</sub>O<sub>8</sub> (190 mg, 0.80 mmol), and 1,2-dichloroethane (1 mL). The mixture was stirred at room temperature for 2 minutes and subsequently, tetradecane (52  $\mu$ L, 0.20 mmol) and trifluoroacetic acid (77  $\mu$ L, 1.0 mmol) were added. The vial was sealed under air with a Teflon cap and stirred on a heating block at 70 °C for the indicated amount of time. The reactions were monitored by GC-FID.

## Chapter 3

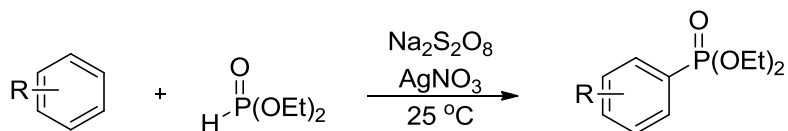
### Pd(II)-Catalyzed C–H Bond Functionalization With Peroxides

## 3 New Reactivities with Tetrabutylammonium Persulfate

### 3.1 The Uses of Tetrabutylammonium Persulfate

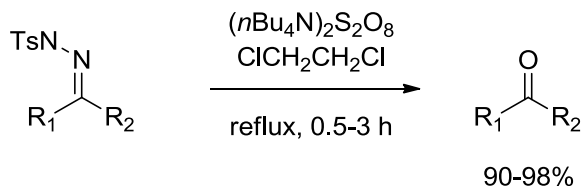
In the context of the kinetic studies on our oxidative palladium-catalyzed intermolecular cross-coupling reaction (see chapter 1), we aimed to determine the rate of reaction of the oxidant. Because the reaction mixture is heterogeneous due to the sodium persulfate salt, we couldn't obtain the rate of oxidant as a function of its concentration. Therefore, it was necessary to find a soluble alternative: a soluble source of persulfate. Tetrabutylammonium persulfate (TBAPS) had previously been reported in the literature and seemed like a promising oxidant for homogeneous kinetic studies.

Of interest, TBAPS is an uncommon reagent and only five articles report its use as an oxidant. In 1985, Kottman reported the use of TBAPS for the first time in the oxidative phosphorylation of arene C–H bonds (Scheme 22).<sup>64</sup> The optimized process required stoichiometric amounts of sodium persulfate and silver nitrate. Within the optimization process, TBAPS was shown to be effective and evidence for a radical mechanism was presented.



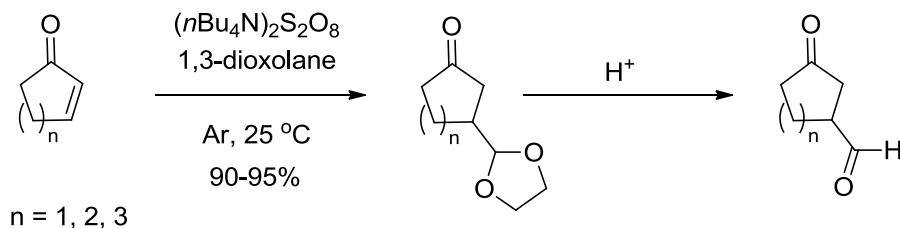
**Scheme 22: Oxidative phosphorylation of arene C–H bonds**

Following Kottman's initial report, Wan and coworkers employed TBAPS to cleave tosylhydrazones under mild conditions (Scheme 23).<sup>65</sup> Its use was stoichiometric in converting tosylhydrazones into the corresponding carbonyl compound in high yield.



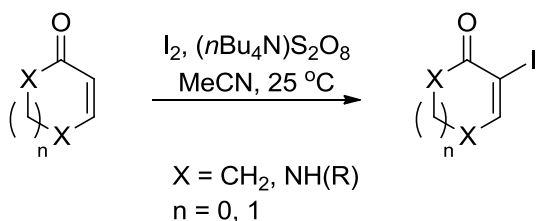
### Scheme 23: Cleavage of tosylhydrazones with TBAPS

The radical nature of TBAPS was also investigated by Choi in 1997 and his team applied the reagent for a  $\beta$ -masked formylation of cyclic  $\alpha,\beta$ -unsaturated ketones (Scheme 24).<sup>66</sup> The conjugate addition of acetals to cyclic ketones was observed in high yield in the presence of TBAPS, acting here as a radical initiator. Subsequent deprotection of the acetal reveals the corresponding aldehyde.



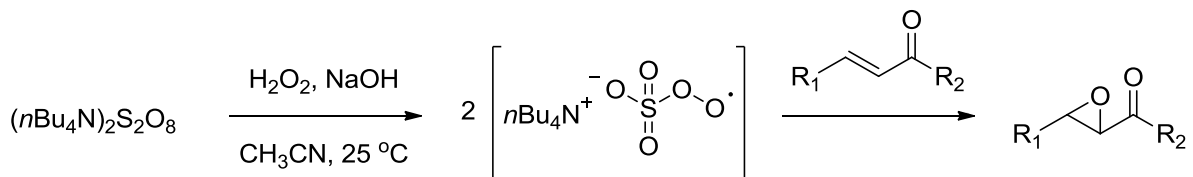
### Scheme 24: $\beta$ -masked formylation of cyclic $\alpha,\beta$ -unsaturated ketones

Shortly afterwards, TBAPS was also found to mediate the  $\alpha$ -iodination of functionalized ketones with iodine (Scheme 25).<sup>67</sup> TBAPS in this reaction mechanism oxidizes iodine to an iodonium radical which is thought to be the active species. The reactive iodonium radical then forms a iodonium three-membered ring with the electron deficient olefin. This iodonium then rearranges, loses a proton and generates the  $\alpha$ -iodo product.



### Scheme 25: TBAPS-initiated $\alpha$ -iodination of ketones

Most recently, Kim and coworkers applied TBAPS to the epoxidation of  $\alpha,\beta$ -unsaturated ketones.<sup>68</sup> In this reaction, TBAPS is itself oxidized by hydrogen peroxide under basic conditions to yield the reactive peroxy species (Scheme 26). The radical then reacts efficiently with electron-deficient olefins.

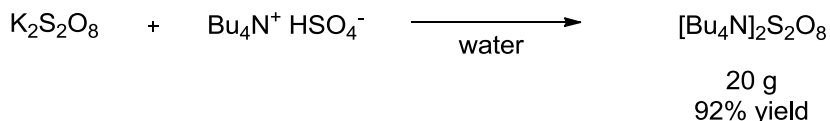


**Scheme 26: Epoxidation of electron-deficient olefins with TBAPS and hydrogen peroxide**

In all, TBAPS is an unexplored reagent in cross-coupling reactions. Its application to other oxidative transformations suggests TBAPS operates under radical conditions.

### 3.2 Reaction Discovery

TBAPS presented itself as an alternative to sodium persulfate, allowing the oxidant to be soluble and amenable to kinetic experiments. The synthesis of TBAPS is straightforward and high yielding (Scheme 27).

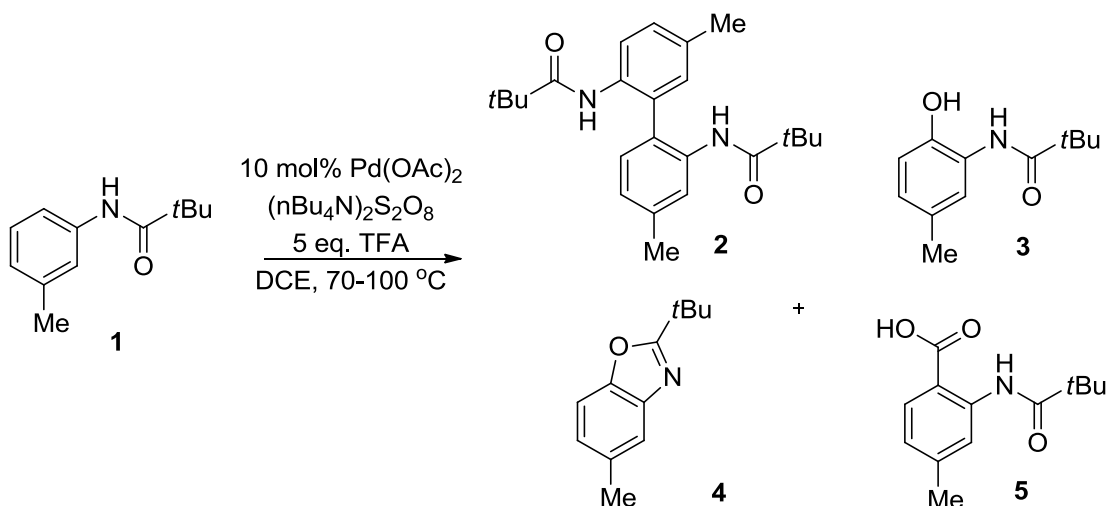


**Scheme 27: Synthesis of a soluble persulfate salt, TBAPS**

With our soluble source of oxidant in hand, we replaced  $\text{NaS}_2\text{O}_8$  by TBAPS in our standard reaction condition for the Pd-catalyzed dehydrogenative cross-coupling of anilides. To our surprise, the reaction with TBAPS was very fast; the cross-coupling was complete within 10 minutes (as opposed to 25-30h with  $\text{NaS}_2\text{O}_8$ )! With this interesting result in hand, we decided to move away from the kinetic studies and further explore the uncommon reactivity of this new oxidant.

By taking a closer look at the reaction mixture, the rate of the reaction was not the only factor to be affected by the soluble oxidant. In fact, the desired cross-coupling product with benzene was

observed as the major product, but at least four other byproducts were detected and subsequently identified by NMR and mass spectroscopy (Scheme 28). Running the reaction without benzene eliminated the possibility for cross-coupling reactions and allowed for a better understanding of the nature of the reaction mixture.



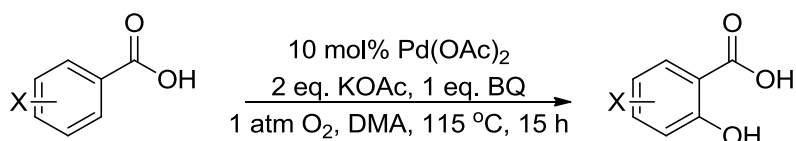
### Scheme 28: High reactivity of TBAPS in palladium-catalyzed cross-coupling reaction

After reaction optimization and purification, four distinct products were characterized: homocoupled product **2**, hydroxylated product **3**, C-O reductive elimination product **4** and carboxylated product **5**. Homocoupled product **2** had been observed in other oxidative Pd-catalyzed cross-coupling systems and thus is not uncommon. However, in the presence of sodium persulfate, homocoupling was never detected, highlighting the difference with TBAPS. No more than 10% of the homocoupled product was ever observed. The other three byproducts generated in the presence of TBAPS are of interest and optimization was pursued to better understand their formation.

### 3.3 Literature Relevance for Observed Byproducts

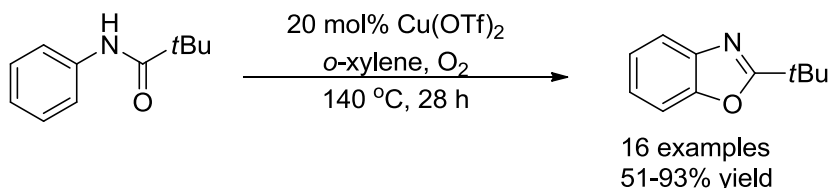
Hydroxylated product **3** is quite interesting since direct hydroxylation from a C-H bond is uncommon in the literature. A seminal example includes Jin Quan Yu's Pd-catalyzed and carboxylic acid directed ortho-hydroxylation (Scheme 29).<sup>69</sup> Hydroxylation of arenes can also be obtained through transition metal catalyzed acetoxylation and subsequent hydrolysis. A recent review by Alonso and Pastor thoroughly reviews arene hydroxylations and outlines the

challenges with this reaction.<sup>70</sup> This review also highlights methodologies for converting arylhalides to phenols. In the first reaction run with TBAPS, 22 % of the hydroxylated product was isolated. By GC-FID, up to 50% hydroxylation occurs under oxidative reaction conditions and further investigation is discussed further.



### Scheme 29: Yu's carboxylic acid directed and Pd-catalyzed ortho-hydroxylation

A C–O forming reaction has previously been reported by Nagasawa's group in two separate accounts.<sup>71</sup> The reaction conditions require 20 mol% of Cu(OTf)<sub>2</sub> in dichlorobenzene at 140 °C (Scheme 30). For *t*-butyl substrate, only 22% yield was reported. The structure of this product was confirmed by independent synthesis via Nagasawa's reported method and then comparing the two GCMS traces. <sup>1</sup>H NMR shifts did not correspond exactly and so the GCMS spectra were a definite piece of evidence for this byproduct.



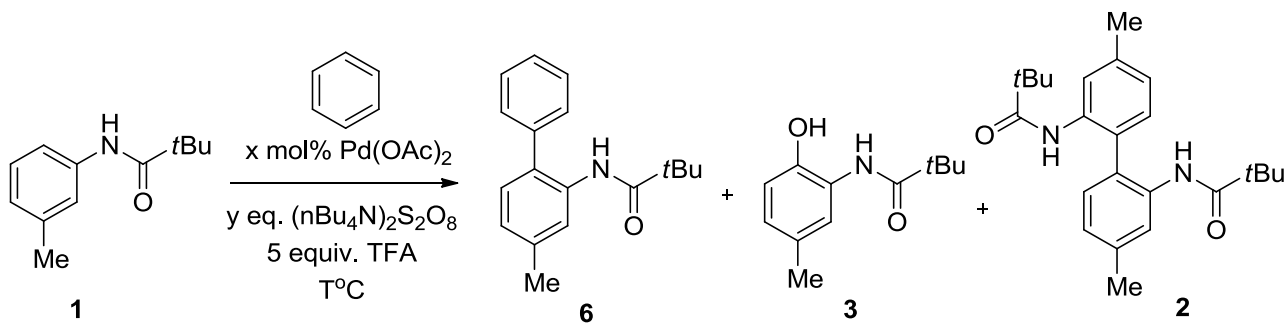
### Scheme 30: Nagasawa's C-O forming reaction

Carboxylated product **5** is intriguing since its generation is completely unexpected. To try and understand its formation, we needed to identify the origin of the carbon atom on the carboxylic group. An extensive acid screen revealed no definite trends in respect to the formation of this product (where it was proposed that the COOH, may be originating from TFA with CF<sub>3</sub> as a leaving group). Experiments ran under different atmospheres were also inconclusive. The carboxylated product is difficult to monitor, and can be seen only by LCMS (unfortunately it doesn't fly on the GC-FID).

### 3.4 Reaction Optimization

First, we sought to optimize the published reaction conditions to try to obtain quick reaction times with high selectivity for the biphenyl cross-coupling product. Different equivalents of oxidant and palladium were investigated (Table 10). As such, starting material **1** was consumed in 5 mins with 3 or 2 equivalents of  $(\text{Bu}_4\text{N})_2\text{S}_2\text{O}_8$  (Table 10, entries 2,3). With 1 equivalent of  $(\text{Bu}_4\text{N})_2\text{S}_2\text{O}_8$ , **1** was still present after 44 h but with the absence of other byproducts (Table 10, entry 4). It was also observed by GC-FID that the yield of the cross-coupled product **6** decreases overtime (Table 10, entry 2) indicating that the desired product is unstable under the reaction conditions. Biphenyl was also detected in the reaction mixture and originates from the cross-coupling of two benzene rings. This pathway doesn't contribute to the mass balance but may play a role in consuming the catalyst and the oxidant.  $\text{Pd}(\text{OAc})_2$  is a more efficient catalyst than  $\text{Pd}(\text{TFA})_2$ , requiring less time to reach maximum conversion (Table 10, entries 8 and 9).

**Table 9: Cross-coupling reaction optimization with TBAPS**



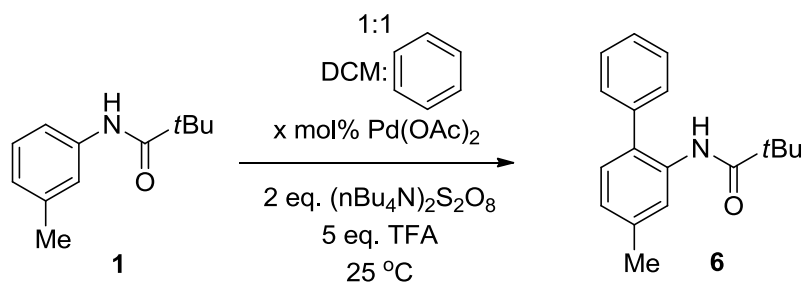
Entry	x	y	T °C	Conversion	Yield <sup>c</sup> <b>6</b>	Yield <b>3</b>	Yield <b>2</b>
1	10	3	70	>99% (1h)	62% (5mins) <sup>b</sup>	-	Trace
2	10	2	70	>99% (5mins)	88% (5mins) <sup>c</sup>	3% (5mins) <sup>b</sup>	Trace
3	10	1.2	70	74% (5mins) <sup>d</sup>	67% (5 mins) <sup>b</sup>	5% (1h)	Traces
4	10	1	70	79% (1h) <sup>g</sup>	53% (1h)	9% (15.5h)	Trace
5	10	2	25	>99% (~7h)	39% IY	-	-

6	1	2	70	>99% (~7h)	49% IY	-	-
7 <sup>a</sup>	10 <sup>f</sup>	2, no TFA	40	~20% (48)	~15%	-	-
8 <sup>a</sup>	5 <sup>f</sup>	2, 2eq. TFA	40	~70% (48h)	~40%	traces	traces
9 <sup>a</sup>	5	2, 2eq. TFA	40	~70% (19h)	~40%	traces	traces
10 <sup>a</sup>	5	2, no TFA	40	>99%	Complete decomposition		

<sup>a</sup> 0.5mL benzene. <sup>b</sup> The reaction stalls after the mentioned time. <sup>c</sup> but the yield decreases over time to 69% after 15.5h. <sup>d</sup> The reaction reaches 84% conversion after 15.5h. <sup>e</sup> IY indicated isolated yields, otherwise all yields all calculated by GCFID with a calibration curve. <sup>f</sup> Pd(TFA)<sub>2</sub>. <sup>g</sup> starting material was still present after 44h.

According to the results in Table 10, the reaction reached maximum conversion very rapidly, i.e., within minutes. Lower temperatures were therefore investigated to slow the reaction down in the hope of observing better selectivity (Table 11). Surprisingly, the oxidative cross-coupling proceeded smoothly at room temperature. This is an important result since few mild conditions exist in the literature for oxidative two fold C–H bond activation. Interestingly, reaction mixtures with different catalyst loadings all went to full conversion but in different time frames. The observation that the reaction was still progressing after more than week with only 1 mol% of Pd(OAc)<sub>2</sub> is indicative of a long life cycle of the catalyst system. The long reaction time also highlights the robustness of the catalyst system developed and high turnover frequencies.

**Table 10: Cross-coupling reaction optimization at room temperature with TBAPS**



Entry	Catalyst loading	Conversion of <b>1</b>	Time	Isolated yield <b>6</b>
1	10 mol % Pd(OAc) <sub>2</sub>	>99%	16h	20% <sup>a</sup>
2	5 mol % Pd(OAc) <sub>2</sub>	>99%	24h	23%
3	2.5 mol % Pd(OAc) <sub>2</sub>	>99%	10 days	24%



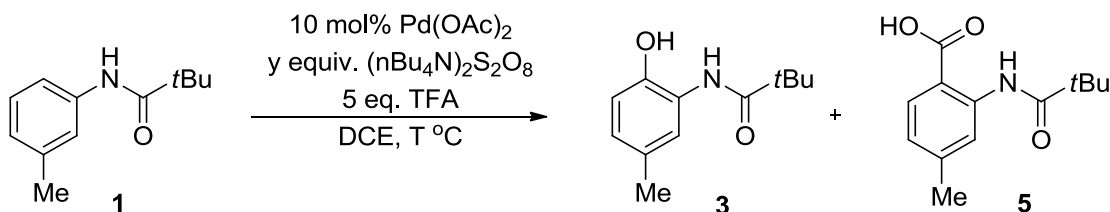
4	1 mol % Pd(OAc) <sub>2</sub>	>99%	16 days	24%
5	0.5 mol % Pd(OAc) <sub>2</sub>	>99%	18days	22%

<sup>a</sup> 15% of hydroxylated product was also isolated.

Next, we aimed to optimize the reaction conditions in favour of the hydroxylated product **3**.

Contributing to the field of arene C–H bond hydroxylation would be beneficial. To better probe the byproduct reactions and in particular the hydroxylation reaction, reactions were run without benzene thereby eliminating possible cross-coupling reactions (Table 12).

**Table 11: Reaction optimization without benzene for hydroxylation and carboxylation**



Entry	y	T °C	Conversion	Time	Yield <b>3</b>	Yield <b>5</b> <sup>a</sup>
1	2	70	>99%	7h	≤ 20%	NA
2	2	100	>99%	4h	≤ 20%	2%
3	3	70	>99%	4h	≤ 20%	NA
4	2	100	>99%	6h	5% <sup>c</sup>	5%
5	2	40	95%	7days	≤ 20%	NA
6	1.5	70	95%	7days	≤ 20%	6%
7	2	25	90%	7days	≤ 20%	NA
8 <sup>b</sup>	2	100, CO <sub>2</sub> atm	>99%	16h	4%	NA
9 <sup>b</sup>	2	50, CO <sub>2</sub> atm	92%	16h	2%	NA
10 <sup>b</sup>	2	100, Ar atm	>99%	16h	5%	NA

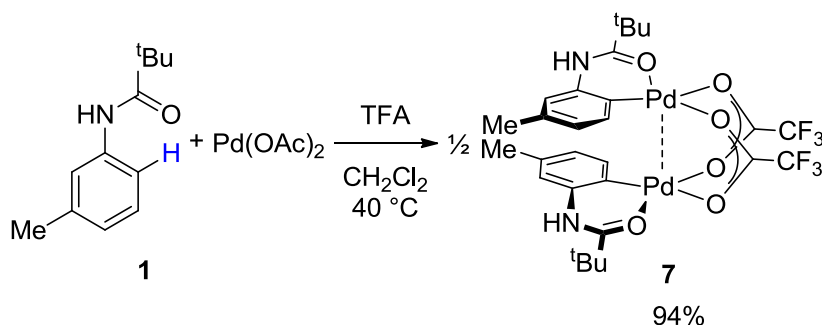
<sup>a</sup> Not detected by GC methods, only observed after purification. <sup>b</sup> 5mol% Pd(OAc)<sub>2</sub>. <sup>c</sup> Isolated yield

Of note, most reactions generate an appreciable amount of the C–O bond formation product **4**. However, **4** was difficult to isolate but could be easily detected by GC-FID. Furthermore, after some method development, these reactions were monitored by GC-FID where an internal standard (adamantane) indicating the relative yield. An undergraduate student, Sylvia Maule

worked on optimizing this reaction during a semester in our group. She was able to achieve a 36% isolated yield of the hydroxylated product **3** using chloroform as the solvent. The optimization of the hydroxylated reaction with TBAPS as the terminal oxidant requires further investigation.

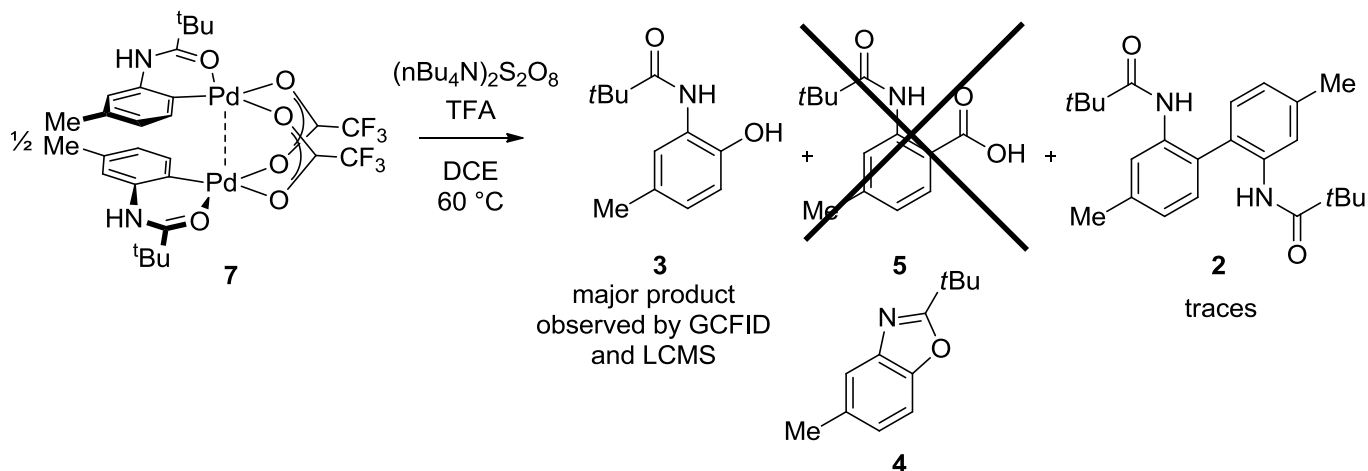
### 3.5 Stoichiometric Experiments

Stoichiometric experiments were undertaken to try and understand the origin of the hydroxylated **3** and carboxylated **5** byproducts observed in the oxidative cross-coupling reaction with TBAPS. The dimeric palladacycle of *N*-(*m*-tolyl)pivalamide was obtained in 94% yield (Scheme 31).



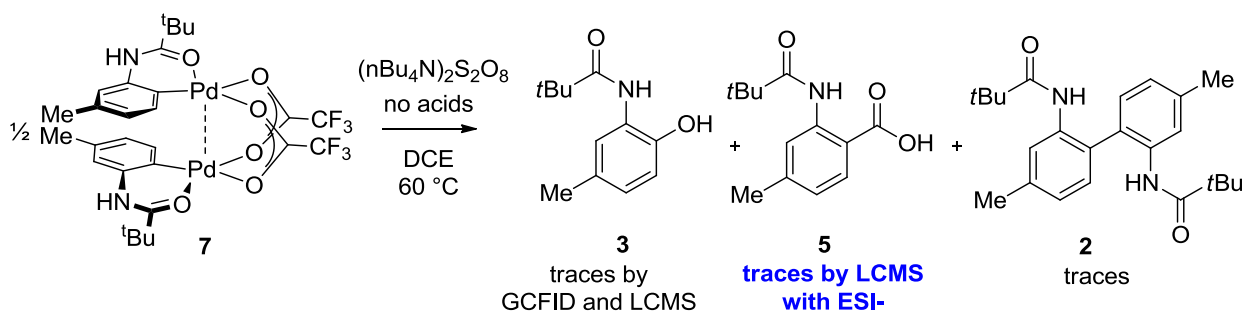
#### Scheme 31: Synthesis of the dimeric palladacycle of *N*-(*m*-tolyl)pivalamide

Pd(II)-dimer **7** was first submitted to TBAPS, TFA in dichloroethane at 60 °C with the intent of observing reductive elimination products. The major product detected from this reaction mixture was the hydroxylated product **3** (Scheme 32). In the absence of TBAPS, no hydroxylated product **3** was detected. It is therefore likely that the oxygen originates from the persulfate oxidant. Furthermore, under the same stoichiometric reaction conditions, benzoxazole **4** and homo-coupled product **2** were also observed, but none of the carboxylated product **5** was seen by GC or LCMS. Benzoxazole product **4** was detected in the presence of acid, however it appears to be consumed overtime (this observation is consistent with most reactions, where benzoxazole **4** GC-FID peak decreases over time). Is it possible benzoxazole **4** is an intermediate towards the generation of hydroxylated product **3**?



### Scheme 32: Reductive elimination with TBAPS and acid

Next, stoichiometric reactions were conducted in the absence of acid (Scheme 33). This time, only trace amounts of hydroxylated product **3** were observed, and conversely carboxylated product **5** was unambiguously detected from the reaction mixture and then isolated. Earlier in this study, it was proposed that the carboxylic functional group was derived from the acid, but this hypothesis must be rejected. Indeed, carboxylated product **5** is strictly formed in the absence of TFA in the stoichiometric experiments.



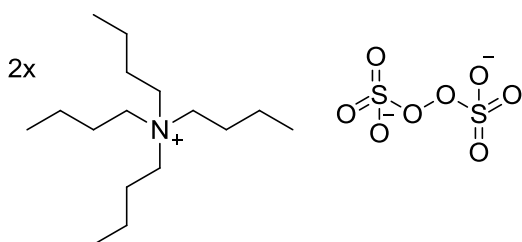
### Scheme 33: Reductive elimination with TBAPS without acid

## 3.6 Outlook

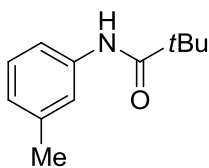
In conclusion, TBAPS displays unprecedented reactivity in oxidative cross-coupling reactions. First, this persulfate oxidant is very reactive and generates two fold C–H bond activation cross-coupling products within minutes in comparison to days with sodium or potassium persulfate oxidants. At room temperature, TBAPS allows for palladium loadings as low as 1 mol% and for

high turnover numbers. Due to the high reactivity of the homogeneous oxidant, interesting byproducts were observed and characterized. As such, an *ortho*-hydroxylation methodology and an *ortho*-carboxylation reaction were briefly investigated. Furthermore, benzoxazoles were also generated under TBAPS conditions and is complimentary to the Cu-catalyzed reaction previously published by Nagasawa. Lastly, further investigations are warranted for the development of a room temperature and low catalyst loading oxidative two fold C–H bond activation cross-coupling as well as for the *ortho*-hydroxylation of anilides.

### 3.7 Experimental Data



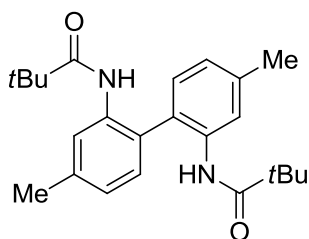
**Tetrabutylammonium persulfate (TBAPS):** Following a known procedure<sup>72</sup>, tetrabutylammonium hydrogen sulfate (21.73 g, 64.0 mmol) and potassium persulfate (8.65 g, 32.0 mmol) were dissolved in 140 mL of deionized water. The solution was stirred for 30 minutes at room temperature. The solution was then extracted with dichloromethane three times. The combined organic phases were washed with deionized water three times, dried over Na<sub>2</sub>SO<sub>4</sub>, filtered and evaporated. The colourless oil was dried under vacuum at room temperature for several hours. (Note: do not heat this compound, as it is heat sensitive.) A white solid (20.03 g, 92%) was obtained. <sup>1</sup>H NMR (400 MHz, CDCl<sub>3</sub>) δ (ppm) 3.34-3.30 (m, 2H), 1.68-1.60 (m, 2H), 1.49-1.42 (m, 2H), 0.98 (t, 3H, *J* = 7.3 Hz).



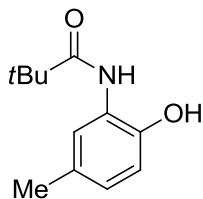
***N*-*m*-Tolylpivalamide (1):** According to a known procedure,<sup>71</sup> in a flame-dried flask, 3-methylaniline (3.25 mL, 30.0 mmol) was dissolved in dry dichloromethane (120 mL) at room temperature. At 0 °C, triethylamine (6.27 mL, 45.0 mmol) was added followed by acetyl chloride (4.43 mL, 36.0 mmol). A small quantity of gas was observed and was evacuated with argon. The

reaction was sealed and stirred at room temperature overnight. The reaction was quenched with 1M HCl and washed two more times with 1M HCl. The aqueous layer was extracted three times with dichloromethane. The combined organic phases were washed twice with brine, dried with magnesium sulfate, filtered and concentrated. The crude reaction mixture was further purified by recrystallization in hot ethylacetate and hexanes (1:1). The filtrate was recrystallized two more times to obtain 5.25 g (92%) of a white solid.  $^1\text{H NMR}$  (400 MHz,  $\text{CDCl}_3$ )  $\delta$  7.43 (s, 1H), 7.28 (d,  $J = 8.2$  Hz, 1H), 7.19 (t,  $J = 7.8$  Hz, 1H), 6.91 (d,  $J = 7.4$  Hz, 1H), 2.33 (s, 3H), 1.31 (s, 9H).  $^{13}\text{C}\{^1\text{H}\}$  NMR (100 MHz,  $\text{CDCl}_3$ )  $\delta$  176.7, 139.0, 138.1, 128.9, 125.1, 120.8, 117.1, 39.7, 27.8, 21.6.

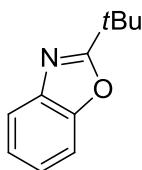
**General procedure for the intermolecular tandem C–H functionalization reaction:** In a one-dram vial equipped with a Teflon cap was added *N*-(*m*-tolyl)pivalamide (48.2 mg, 0.20 mmol),  $\text{Pd}(\text{OAc})_2$  (4.5 mg, 0.02 mmol),  $(n\text{Bu}_4\text{N})_2\text{S}_2\text{O}_8$  (271 mg, 0.40 mmol), and 1,2-dichloroethane (1 mL). Subsequently, trifluoroacetic acid (76  $\mu\text{L}$ , 1.00 mmol) was added. The vial was sealed with a Teflon cap and stirred on a heating block at 70  $^\circ\text{C}$ . After cooling to ambient temperature, the resulting mixture was diluted in EtOAc and washed with 2 mL sat'd  $\text{NaHCO}_3$ . The aqueous phase was extracted with EtOAc. The combined organic extracts were concentrated *in vacuo* and the resulting residue was purified by preparative thin-layer chromatography (eluent: EtOAc/hexanes = 3:7, v/v) to afford the target compound.



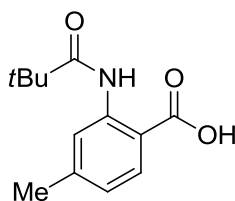
***N,N'*-(4,4'-Dimethyl-[1,1'-biphenyl]-2,2'-diyl)bis(2,2-dimethylpropanamide) (2):** An off-white solid was obtained.  $^1\text{H NMR}$  (400 MHz,  $\text{CDCl}_3$ )  $\delta$  (ppm) 8.22 (s, 2H), 7.18 (s, 2H), 7.08 (d, 2H,  $J = 7.6$  Hz), 7.03-7.01 (m, 2H), 2.42 (s, 6H), 1.01 (s, 18H).  $^{13}\text{C}\{^1\text{H}\}$  NMR (100 MHz,  $\text{CDCl}_3$ )  $\delta$  (ppm) 176.7, 139.7, 136.0, 129.8, 125.2, 124.6, 121.9, 39.7, 27.2, 21.6. **MS (ESI)**  $m/z$  381 (M+H), 403 (M+Na); **HRMS (ESI)**  $m/z$ . calc'd for  $\text{C}_{24}\text{H}_{32}\text{N}_2\text{O}_2$  [M+H] $^+$ : 381.2536; found: 381.2521.



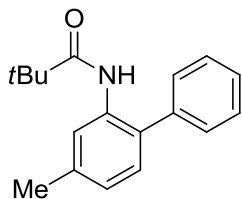
**N-(2-Hydroxy-5-methylphenyl)pivalamide (3):** An off-white solid was obtained.  $^1\text{H}$  NMR (400 MHz,  $\text{CDCl}_3$ )  $\delta$  (ppm) 8.52 (s, 1H), 7.53 (br, 1H), 6.92 (d, 2H,  $J = 2.6$  Hz), 6.81 (s, 1H), 2.26 (s, 3H), 1.35 (s, 9H).  $^{13}\text{C}\{^1\text{H}\}$  NMR (100 MHz,  $\text{CDCl}_3$ )  $\delta$  179.0, 146.7, 130.0, 127.9, 125.3, 122.7, 119.8, 39.7, 27.9, 20.6. **MS (ESI)**  $m/z$  208 (M+H), 230 (M+Na); **HRMS (ESI)**  $m/z$  calc'd for  $\text{C}_{12}\text{H}_{17}\text{NO}_2$  [M+H] $^+$ : 208.1332; found: 208.1330.



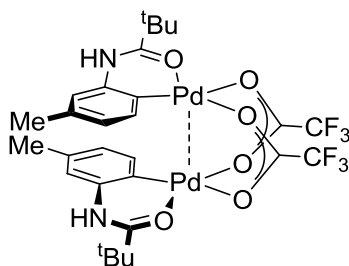
**2-(tert-butyl)benzo[d]oxazole (4):** An off-white solid was obtained. **MS (ES)**  $m/z$  175 (M) with identical retention time of an authentic sample.



**4-Methyl-2-pivalamidobenzoic acid (5):** An beige solid was obtained.  $^1\text{H}$  NMR (400 MHz,  $\text{CDCl}_3$ )  $\delta$  (ppm) 11.14 (s, 1H), 8.67 (s, 1H), 8.01 (d, 1H,  $J = 8.2$  Hz), 6.92 (dd, 1H,  $J = 0.9$  Hz,  $J = 8.1$  Hz), 2.41 (s, 3H), 1.34 (s, 9H).  $^{13}\text{C}\{^1\text{H}\}$  NMR (100 MHz,  $\text{CDCl}_3$ )  $\delta$  178.1, 171.7, 147.1, 142.5, 131.7, 123.4, 120.8, 111.2, 40.4, 27.6, 22.2. **MS (ESI)**  $m/z$  236 (M+H), 258 (M+Na); **HRMS (ESI)**  $m/z$  calc'd for  $\text{C}_{13}\text{H}_{17}\text{NO}_3$  [M+H] $^+$ : 236.1281; found: 236.1289.



***N*-(4-Methyl-[1,1'-biphenyl]-2-yl)pivalamide (6):** An off-white solid was obtained. Spectra are in accordance with the literature.<sup>73</sup>  $^1\text{H NMR}$  (400 MHz,  $\text{CDCl}_3$ )  $\delta$  (ppm) 8.24 (s, 1H), 7.48 (t, 3H,  $J = 7.3$  Hz), 7.40 (t,  $J = 7.4$  Hz, 1H), 7.35 (d,  $J = 6.8$  Hz, 2H), 7.14 (d,  $J = 7.7$  Hz, 1H), 6.98 (dd,  $J = 0.9$  Hz,  $J = 7.7$  Hz, 1H), 2.40 (s, 3H), 1.10 (s, 9H).  $^{13}\text{C}\{^1\text{H}\}$  NMR (100 MHz,  $\text{CDCl}_3$ )  $\delta$  176.4, 138.6, 138.2, 135.0, 129.6, 129.5, 129.1, 128.0, 124.8, 121.5, 39.9, 27.5, 21.6.



**Bimetallic palladium complex (7):** In a one-dram vial was added *N*-(*m*-tolyl)pivalamide (19.1 mg, 0.1 mmol),  $\text{Pd}(\text{OAc})_2$  (22.4 mg, 0.1 mmol), and dichloromethane (1 mL). Trifluoroacetic acid (7.7  $\mu\text{L}$ , 0.105 mmol) was subsequently added into the vial and the resulting solution was heated to 40  $^\circ\text{C}$  for 3 h. After cooling to ambient temperature, the reaction mixture was concentrated *in vacuo* and the resulting residue was suspended in a mixture of hexanes and  $\text{CHCl}_3$  (hexanes: $\text{CHCl}_3 = 9:1$ , v/v, 2 mL). The suspension was filtered through Celite and washed with 4 x 0.3 mL hexanes. The residue was washed with dichloromethane and the wash solution was subsequently collected and concentrated *in vacuo* to afford the bimetallic palladacycle as a yellow solid (38.6 mg, 94%).  $^1\text{H NMR}$  (400 MHz,  $\text{CDCl}_3$ )  $\delta$  7.58 (s, 1H), 7.03 (d,  $J = 8.1$  Hz, 1H), 6.72 (d,  $J = 8.0$  Hz, 1H), 6.33 (s, 1H), 2.24 (s, 3H), 0.89 (s, 9H).  $^{13}\text{C}\{^1\text{H}\}$  NMR (100 MHz,  $\text{CDCl}_3$ )  $\delta$  174.1, 135.3, 134.0, 130.1, 125.1, 115.8, 112.0, 38.9, 27.2, 20.6.  $^{19}\text{F NMR}$  (376 MHz,  $\text{CDCl}_3$ )  $\delta$  -73.6. MS (ESI)  $m/z$  296 ( $\text{C}_{12}\text{H}_{16}\text{NOPd}$ , i.e., monomer-TFA); HRMS (ESI)  $m/z$  calc'd for  $\text{C}_{12}\text{H}_{16}\text{NOPd}$ : 296.0261; found: 296.0255.

## Chapter 4

### Pd(II)-Catalyzed C–H Bond Functionalization With Sodium Chlorite

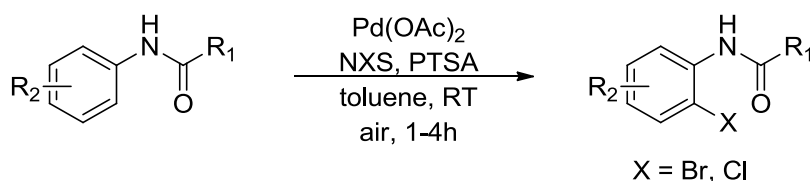
## 4 Pd(II)-Catalyzed Benzamide Chlorination

### 4.1 Introduction

Halogenated compounds are important pharmaceutical agents and hence can have enhanced biological activity.<sup>74</sup> In particular, aryl halides have also found application in cross-coupling methodologies and are therefore useful starting materials.<sup>75</sup> As such, direct halogenations of arenes are important synthetic reactions to diversify aromatic scaffolds which find application in materials science, pharmaceutical industry and agrochemical sector. As a result, the development of new regioselective, chemoselective and functional group tolerant approaches to the synthesis of halogenated molecules remains an important challenge.

### 4.2 Literature Precedence

Commonly used methods for the construction of aryl halides include electrophilic aromatic substitution (EAS)<sup>76</sup> and directed *ortho*-lithiation (DoL)<sup>77</sup>. Direct halogenation is a relatively new field for the construction of C–X bonds by C–H bond activation under palladium catalysis. Pioneering work by Prof. Melanie Sanford and coworkers has shown that reductive elimination reactions from Pd<sup>IV</sup> have very different electronic requirements than those from Pd<sup>II</sup> (Scheme 34).<sup>78</sup> This electronic difference indicates that the desired carbon–halogen coupling can be achieved via the higher oxidation state paving the way for catalytic methods.<sup>79</sup>



**Scheme 34: Sanford's Pd-catalyzed arene C–H bond halogenation reaction**



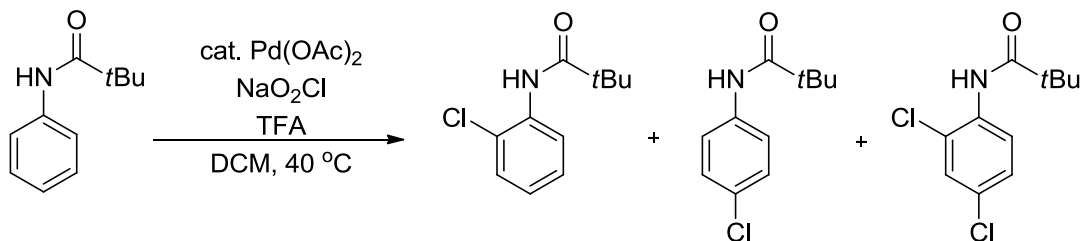
There is precedence in the literature for chlorinating aromatic rings with sodium chlorite. Over a decade ago, Hirano published the chlorination of a number of different anisoles while observing exclusively *para*-chlorination with NaO<sub>2</sub>Cl, moist kaolin and Mn(acac)<sub>3</sub> in dichloromethane.<sup>80</sup> As for Pd-catalyzed chlorination's of C–H bonds, Shi demonstrated in 2006 the highly *ortho*-selective chlorination of anilides.<sup>81</sup> Previous to this report, Sanford had shown a single example of the chlorination of benzoquinoline with NCS.<sup>82</sup> Following these reports, Sanford published a detailed study of the scope and selectivity of Pd-catalyzed directed C–H bond halogenations reactions observing that the presence of Pd affected the regioselectivity.<sup>83</sup> The difference in regioselectivity stems from an *ortho*-C–H bond palladium-catalyzed activation versus a Friedel-Crafts mechanism (which explains any *para*-selectivity). However, in Sanford's extensive oxidant screen, sodium chlorite was not reported. Furthermore, the scope remains limited to phenylpyridines. More recently, Bedford and co-workers have demonstrated the possibility of effecting C–H functionalization under solvent free-conditions.<sup>84</sup> They show chlorination with NCS or CuCl<sub>2</sub>/Cu(OAc)<sub>2</sub> of phenylpyridines, anilides, pyrrolidones and *O*-carbamates. The anilide substrates give 90% yields whereas the other substrates range from 35% to 60% with dichlorination as the major byproduct. Note that these are types of substrates similar to our methodology.

### 4.3 Reaction Condition Optimization

While optimizing the hydroxylation reactions (see chapter 3), an oxidant screen was performed to test different peroxides. Bleach (5% sodium hypochlorite) and sodium chlorite were tested and found to have completely different reactivities to TBAPS. In fact, instead of cross-coupling or hydroxylation products, chlorination of the anilide substrate was observed. Because of the importance of chlorination reactions, further optimization was pursued to develop a selective and complimentary method to Sanford's *N*-chlorosuccinamide. To the best of our knowledge, the cheap and user friendly oxidant, sodium chloride, has never been employed as a chlorinating agent before this project.

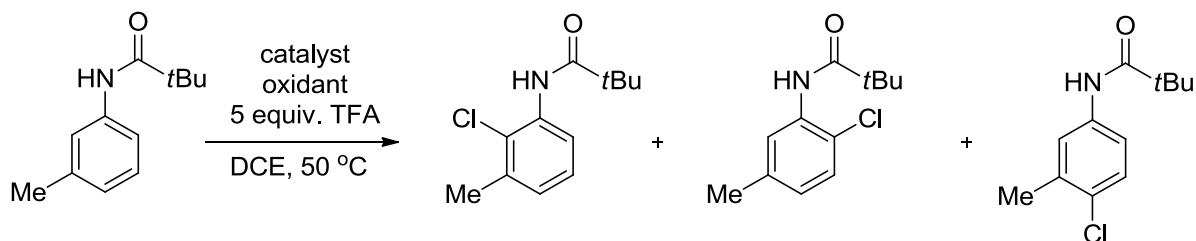
Investigation of the reaction conditions led to the discovery of a selective method with palladium. In the presence of a Pd-catalyst, *ortho*-chlorination is predominant due to the directing ability of the anilide functionality (Scheme 35). As expected, in the absence of

palladium, *para*-chlorination predominates through a Friedel-Crafts mechanism. Further screening allowed for the detection of the dichlorinated product, predominant after prolonged reaction times.



**Scheme 35: Chlorination of anilides with sodium chlorite as an unprecedented chlorinating agent.**

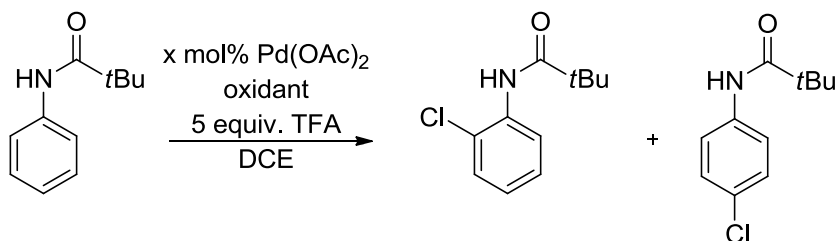
The same substrate, *N*-(*m*-tolyl)pivalamide, used for the kinetic studies (see Chap 1) was employed in the optimization of the chlorination reaction. Two types of chlorites were identified as potential oxidants, sodium hypochlorite (bleach) and sodium chlorite (Table 13). Bleach is actually a 5% aqueous solution of sodium hypochlorite, and despite the biphasic mixture, the selective chlorination reaction proceeds in the presence of dichloromethane as the co-solvent. However, a difference in the *ortho*-*para*-selectivity is not observed in the absence or presence of palladium (Table 13, entries 1,2,4), despite higher yields of the product. When bleach is used as the chlorinating agent, phase transfer compounds like *n*Bu<sub>4</sub>NHSO<sub>3</sub> appear to be necessary to obtain directed chlorination. With a phase transfer compound, high conversion was observed (Table 13, entry 2). On the other hand, most reactions suffered from a decreasing reactivity and eventually stalled after only 24 h. Sodium chlorite gave the best selectivity of 1 : 1.1 *ortho*- to *para*-selectivity albeit with 28% yield (Table 13, entry 3). Furthermore, the *ortho*-chlorinated product was isolated as a mixture of two isomers due to the presence of the *meta*-methyl which desymmetrizes the molecule. For further optimization, a symmetrical substrate, such as *N*-phenylpivalamide was chosen.

**Table 12: Reaction optimization for the *ortho*-chlorination of 3-methylanilides**

Entry	oxidant	additive	Conversion <sup>a</sup>	Yield of <i>ortho</i> - <sup>b</sup>	<i>ortho</i> - : <i>para</i> - <sup>c</sup>
1	NaOCl (bleach)	1% Pd(OAc) <sub>2</sub>	22%	-	1:2
2	NaOCl (bleach)	<i>n</i> Bu <sub>4</sub> NHSO <sub>3</sub> , 1% Pd(OAc) <sub>2</sub>	98%	50%	1:3.5
3	NaO <sub>2</sub> Cl	1% Pd(OAc) <sub>2</sub>	71%	28%	1:1.1
4	NaOCl (bleach)	no Pd	72%	-	1:1.4
5	NaO <sub>2</sub> Cl	no Pd	66%	-	1:1.3

<sup>a</sup> 72h. <sup>b</sup> a mixture of two *ortho*-Cl isomers was detected. <sup>c</sup> ratios are reported.

After more screening with a symmetrical substrate, sodium chlorite was found to be more effective than bleach (even in the presence of a phase transfer catalyst). The equivalents of sodium chlorite are important and selecting for mono-chlorination and enhancing reactivity (Table 14). It is noteworthy that the addition of 2 eq. of sodium chlorite after 1 h of reaction time at 40 °C resulted in the reaction catching fire. Three more identical reactions were set up to attempt to reproduce the fire and understand its origin, but without success. Nonetheless there is a definite build up of pressure within the reaction mixture and if the reaction is sealed for prolonged reaction times (i.e, 24h) then the reaction finally goes to completion with high selectivity. It appears that higher temperature and higher catalyst loadings favour the non-directed *para*-chlorination.

**Table 13: Reaction optimization for the *ortho*-chlorination of anilides**

Entry	oxidant	x	additive	T °C	Conversion	Time	Isolated yield of <i>ortho</i> -Cl	<i>ortho</i> -Cl : <i>para</i> -Cl (ratios)
1	NaO <sub>2</sub> Cl	5	-	40	~70%	5 days	53%	10 : 1
2	NaO <sub>2</sub> Cl	0	-	40	~40%	5 days	14%	1 : 1.5
3	5% NaOCl	5	-	40	~80%	5days	-	1 : 1.7
4	5% NaOCl	0	-	40	~90%	5days	-	1 : 1.3
5	5% NaOCl	5	<i>n</i> Bu <sub>4</sub> NHSO <sub>3</sub>	70	~53%	6.5h	-	1 : 2.7
6	5% NaOCl	5	<i>n</i> Bu <sub>4</sub> NHSO <sub>3</sub>	100	~75%	6.5h	-	1 : 2.5
7	Ca(OCl) <sub>2</sub>	5	-	70	~12%	6.5h	-	1 : 1.5
8	10% NaOCl	5	<i>n</i> Bu <sub>4</sub> NHSO <sub>3</sub>	70	~96%	6.5h	-	1 : 1.6
9	5% NaOCl	0	<i>n</i> Bu <sub>4</sub> NHSO <sub>3</sub>	70	~72%	6.5h	-	1 : 2.5
10 <sup>a</sup>	5% NaOCl	5	<i>n</i> Bu <sub>4</sub> NHSO <sub>3</sub>	70	N/A	-	-	1 : 1.9
11	NaO <sub>2</sub> Cl	5	-	70	~25%	6.5h	-	1.1 : 1
12 <sup>b</sup>	5% NaOCl	5	<i>n</i> Bu <sub>4</sub> NHSO <sub>3</sub>	70	0%	24h	-	-

<sup>a</sup> No solvent. <sup>b</sup> acetone as solvent.

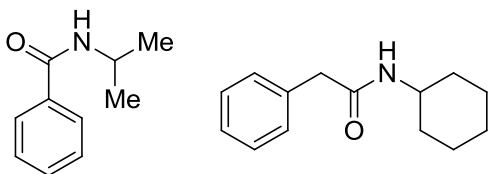
Finally, the best result was obtained with 10 mol% Pd and room temperature yielding up to 95% *ortho*-chlorination product by GC-FID in 25:1 regioselectivity! Control experiments with sodium chlorite in the absence of acid reveal no reactivity, thereby indicating the importance of acid in the reaction mixture.

## 4.4 Reaction Scope

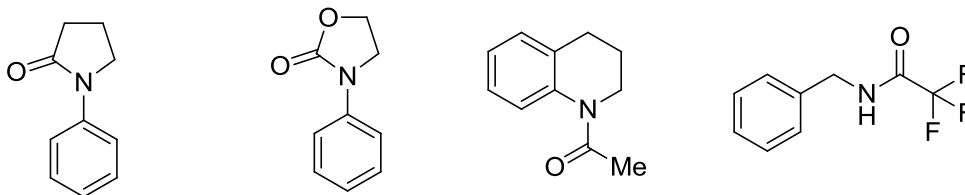
The scope of this chlorination was investigated and the reactions were monitored by GC-FID and GCMS. A hurdle in screening the scope of the chlorination was differentiating the *ortho*- and *para*-chloroanilide products, since the distinction between *ortho*-chlorination and *para*-chlorination can only be done by NMR.

A benzamide and a phenylacetamide were unreactive under the optimized reaction conditions (Figure 6). Some tertiary anilides showed no selectivity between *ortho*- and *para*-chlorination, displaying the Friedel-Crafts reaction as a competitive mechanism. *N*-Benzylamides also showed no selectivity in the absence or presence of a palladium catalyst. Compounds which gave encouraging reactivity and selectivity included differentially substituted anilides as well as *O*-carbamates. Finally, dichlorination was an issue with a phenylacetamide substrate and so the selectivity could not be determined.

*unreactive substrates towards chlorination:*



*reactive, but no difference in apparent selectivity in the presence/absence of Pd:*



*reactive and sensitive to the regioselectivity in the presence of Pd:*

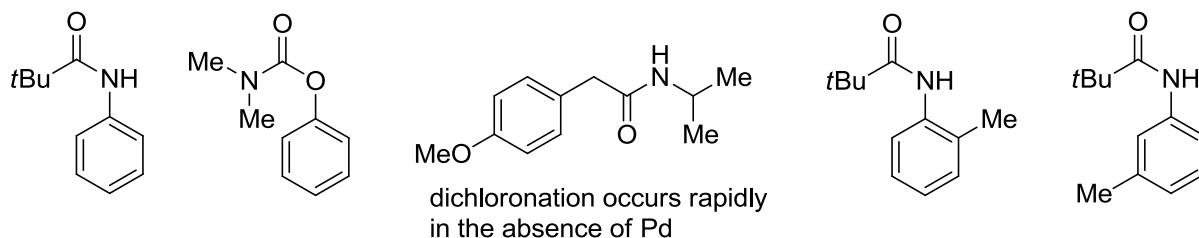
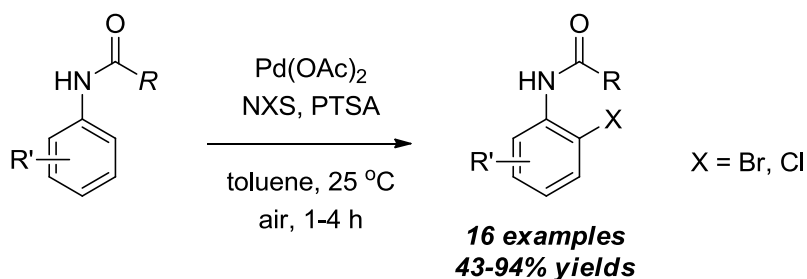


**Figure 5: Preliminary scope of the chlorination reaction**

## 4.5 Outlook

The project of the amide-directed and palladium-catalyzed chlorination with sodium chlorite is still in an early stage. Further reaction conditions need to be screened to optimize the chlorinating process. Different directing groups known to form *ortho*-complexes with palladium were somewhat successful under sodium chlorite conditions. Up to now, only a qualitative scope has been identified and further investigation is still warranted.

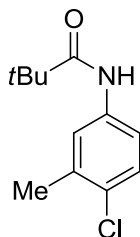
Shortly after we moved on from the palladium-catalyzed *ortho*-C–H bond chlorination of anilide, a relevant methodology was published by Bedford and coworkers (Scheme 36).<sup>85</sup>



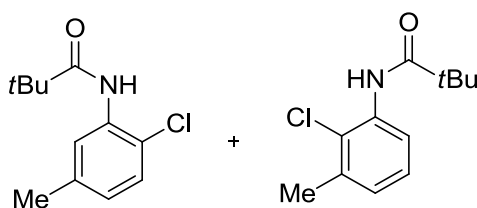
**Scheme 36: Bedford's *N*-halogen succinimide method for mild halogenation of anilides**

## 4.6 Experimental Data

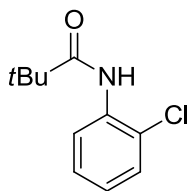
**General procedure for the chlorination of anilides:** In a vial equipped with a stir bar, *N*-phenylpivalamide (35.4 mg, 0.20 mmol), sodium chlorite 80% (45.2 mg, 0.40 mmol) and Pd(OAc)<sub>2</sub> were dissolved in 1 mL of dry DCM. TFA (77 mL, 1.00 mmol) was quickly added and the reaction was capped under air and stirred at 40 °C. It is important not to open the vial during the course of the reaction. The reaction is monitored by GC-FID. When complete, the reaction mixture was diluted in EtOAc and washed 3x with a saturated solution of NaHCO<sub>3</sub>. The aqueous layers were extracted three times with EtOAc and the combined organic phases were washed with brine, dried over Na<sub>2</sub>SO<sub>4</sub>, filtered and evaporated. The crude product was purified by Prep TLC eluting several times with 20% EtOAc/hexanes.



***N*-(4-Chloro-3-methylphenyl)pivalamide:** Bleach was used as the oxidant and a white solid (26 mg, 58%) was obtained.  $^1\text{H}$  NMR (400 MHz,  $\text{CDCl}_3$ )  $\delta$  (ppm) 7.48 (s, 1H), 7.27-7.25 (m, 2H), 2.34 (s, 3H), 1.31 (s, 9H).  $^{13}\text{C}\{^1\text{H}\}$  NMR (100 MHz,  $\text{CDCl}_3$ )  $\delta$  176.6, 136.6, 136.5, 129.4, 129.3, 122.4, 118.7, 39.6, 27.6, 20.2.



***N*-(2-Chloro-5-methylphenyl)pivalamide and *N*-(2-chloro-3-methylphenyl)pivalamide:** Isolated as a mixture of regioisomers (~3:1), a yellow solid (12.4 mg, 28%) was obtained.  $^1\text{H}$  NMR (400 MHz,  $\text{CDCl}_3$ )  $\delta$  (ppm) 8.27 (s, 1H), 8.26 (s, 1H), 8.09 (s, 1H), 7.97 (s, 1H), 7.23 (d, 1H,  $J = 8.2$  Hz), 7.17 (t, 1H,  $J = 7.9$  Hz), 6.98 (dd, 1H,  $J = 0.7$  Hz,  $J = 7.6$  Hz), 6.84 (ddd, 1H,  $J = 0.5$  Hz,  $J = 2.0$  Hz,  $J = 8.1$  Hz), 2.39 (s, 3H), 2.33 (s, 3H), 1.35 (s, 9H), 1.34 (s, 9H).



***N*-(2-Chlorophenyl)pivalamide:** Spectra are in agreement with the literature.<sup>86</sup>  $^1\text{H}$  NMR (400 MHz,  $\text{CDCl}_3$ )  $\delta$  (ppm) 8.41 (dd, 1H,  $J = 1.5$  Hz,  $J = 8.3$  Hz), 8.02 (s, 1H), 7.36 (dd, 1H,  $J = 1.4$  Hz,  $J = 8.0$  Hz), 7.29-7.25 (m, 1H), 7.02 (dt, 1H,  $J = 1.5$  Hz,  $J = 7.8$  Hz), 1.35 (s, 9H).

## Chapter 5 Towards the Total Synthesis of 6-Deoxyerythronolide B

### 5 Biocatalysis and Transition-Metal Catalysis for Polyketide Synthesis

#### 5.1 Introduction to Erythromycin

Polyketides are natural products derived from acetate and/or propionate units assembled in a linear fashion by the polyketide synthase. Their biosynthesis involves an iteration of decarboxylative condensations to form the polyketide backbone. Erythromycin A is a cyclic polyketide produced by the bacteria *Saccharopolyspora erythraea* and is a commonly prescribed macrolide antibiotic.

In particular, it is often administered to patients allergic to penicillin. Erythromycin and its prodrug (erythromycin ethylsuccinate for example) are also effective against skin infections, pneumonias, chlamydial infections and pharyngitis. Bacteria are becoming resistant to this drug and much ongoing research involves developing potent analogues of erythromycin.

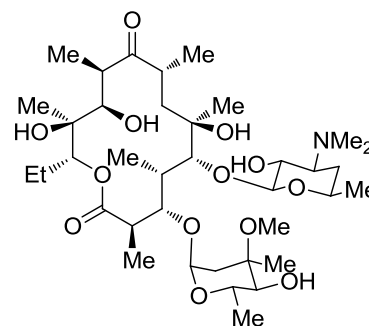


**Figure 6: Erythromycin A**

Erythromycin has a 14-membered lactone with ten stereocenters surrounding its backbone (Figure 7). It also has two appended sugars: L-cladinose and D-desosamine. Due to the presence of an amine on one of the deoxy-sugars, erythromycin is a basic molecule and has a pKa of 8.8. Novel derivatives have been synthesized to avoid bitterness upon oral administration of the drug. It is also a white solid and will readily form salts with acids.

Erythromycin is an unusually popular synthetic target, and has attracted the efforts of organic chemists for decades. Prof. Johann Mulzer at the University of Vienna summarizes this phenomenon, “The synthesis of the macrolide antibiotics, erythromycin A and B [...] is probably the most extensive single project in the history of synthetic organic chemistry.”<sup>87</sup>



## 5.2 Biosynthesis of Erythromycin

### 5.2.1 The Polyketide Synthase

The erythromycin polyketide synthase (PKS) is a catalytic machinery capable of assembling 6-deoxyerythronolide B in a processive and linear fashion (Figure 8 and 9).<sup>88,89</sup> The PKS includes three

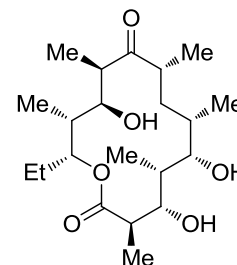


**Figure 7: 6-deoxyerythronolide B**

megaproteins abbreviated DEBS1, DEBS2 and DEBS3, where DEBS stands for 6-deoxyerythronolide B synthase. These megaproteins possess independent modules which hold different catalytic domains. One module is responsible for one iteration of the decarboxylative condensation and subsequent appropriate functional group modification. Furthermore, at the start of the PKS, a loading didomain (LDD) acts as a gateway for selectively introducing the primer unit, propionyl CoA. A thioesterase (TE) is present at the end of the polyketide synthase and catalyzes the macrolactonization of the *seco* acid attached to module 6 (Mod6).

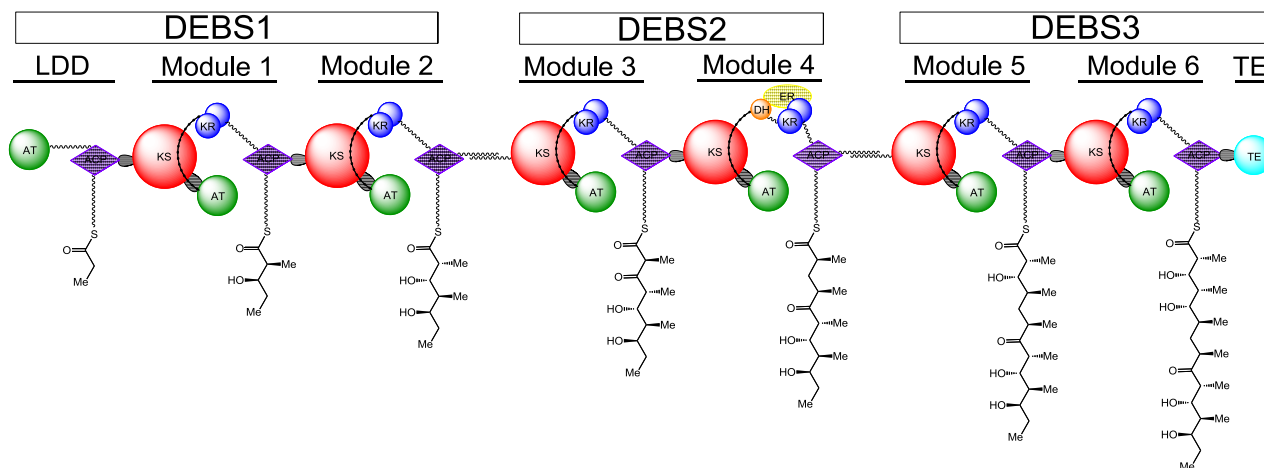


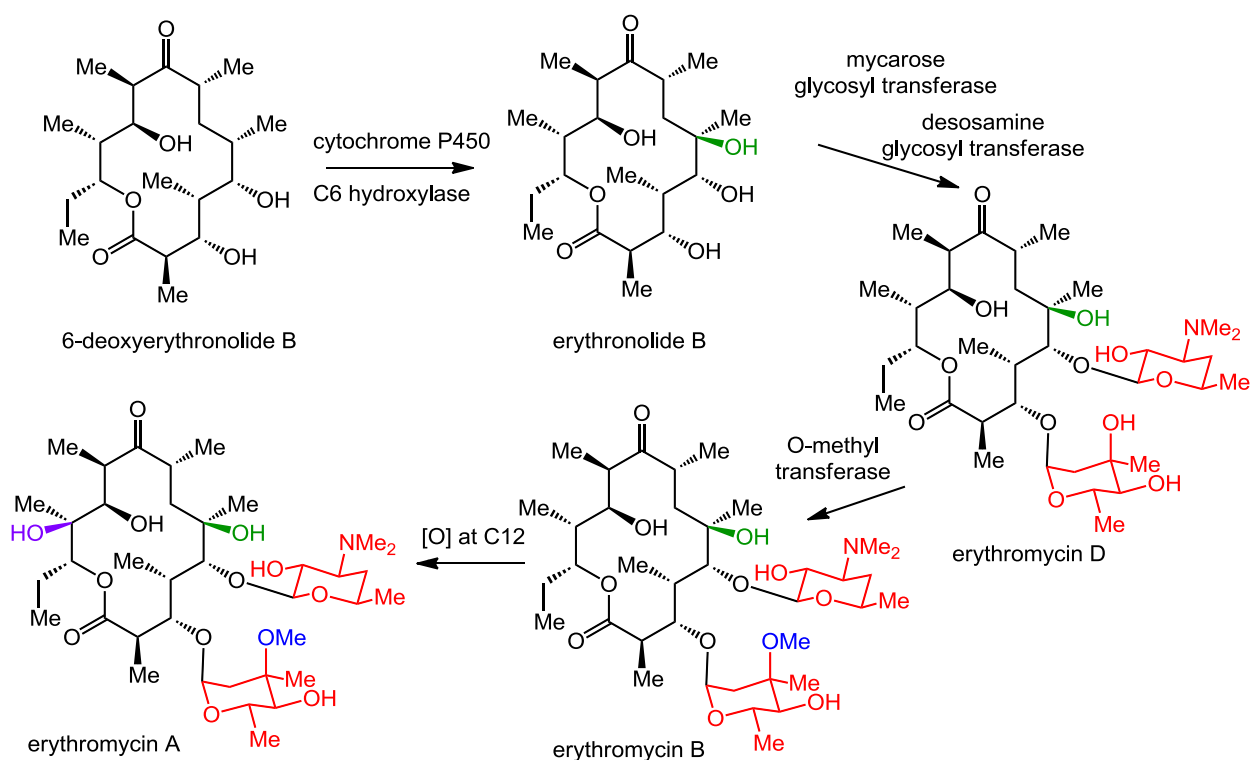
**Figure 8: Erythromycin's polyketide synthase**

Each DEBS megaprotein has two modules and consequently is responsible for adding two extending units to the growing polyketide chain. The catalytic domains which are present in every module include the acylcarrier protein (ACP), the ketosynthase (KS) and the acyl transferase (AT). There are also three optional tailoring domains, the NADH dependant ketoreductase (KR), the dehydratase (DH) and the NADH dependant enoylreductase (ER). Of note, Mod3 has an inactive KR which generates the C9 ketone functional group in 6-

deoxyerythronolide B. Also, Mod4 is the only module in the PKS to possess all three tailoring domains, closely resembling a fatty acid synthase (FAS) module. The presence of a KR, a DH and an ER generates the methylene group at the C7 position in 6-deoxyerythronolide B. Finally, the TE domain catalyses the macrocyclization of the lactone and subsequent cleavage from the PKS yields 6-deoxyerythronolide B. In all, the erythromycin polyketide synthase is a linear assembly line efficiently utilizing decarboxylative condensation reactions.

## 5.2.2 Post Polyketide Synthase Modifications

6-Deoxyerythronolide B is the first isolable intermediate of the erythromycin PKS. Indeed, previous to the cyclization, the growing seco acid is always bound to the enzyme. Nonetheless, post PKS modifications are required to transform 6-deoxyerythronolide B into erythromycin A (Scheme 37).<sup>90</sup>



**Scheme 37: Post-PKS biosynthesis of erythromycin A**

First, 6-deoxyerythronolide B is hydroxylated at the C6 position by a cytochrome P450 hydroxylase yielding erythronolide B. The L-mycarose and D-desosamine sugars are then appended by glycosyl transferases. This compound is called erythromycin D and leads to erythromycin B via an *O*-methyl transferase which methylates the axial hydroxyl group on the L-mycarose sugar to give the L-cladinose deoxy-sugar. Lastly, erythromycin B is converted into erythromycin A by a C12 hydroxylation.

## 5.3 Total Synthesis of 6-Deoxyerythronolide B

### 5.3.1 Mission

Setting multiple stereocenters asymmetrically in a single step is an unmet challenge. Nonetheless, it offers important advantages such as the rapid assembly of scaffolds and the generation of enantioselective product from achiral starting material. Perceived as elegant, transformations which generate more than one stereocenter in a single asymmetric step are extremely useful in total synthesis. Transition-metal catalysis with chiral ligands, organocatalysis and chiral auxiliary chemistry are amenable to multi-stereocenter single-step reactions. However, a powerful method which is somewhat underrepresented in total synthesis is biocatalysis. Although enzymes are often substrate specific, they can yield highly elaborated substrates by generating multiple stereocenters enantiomerically.

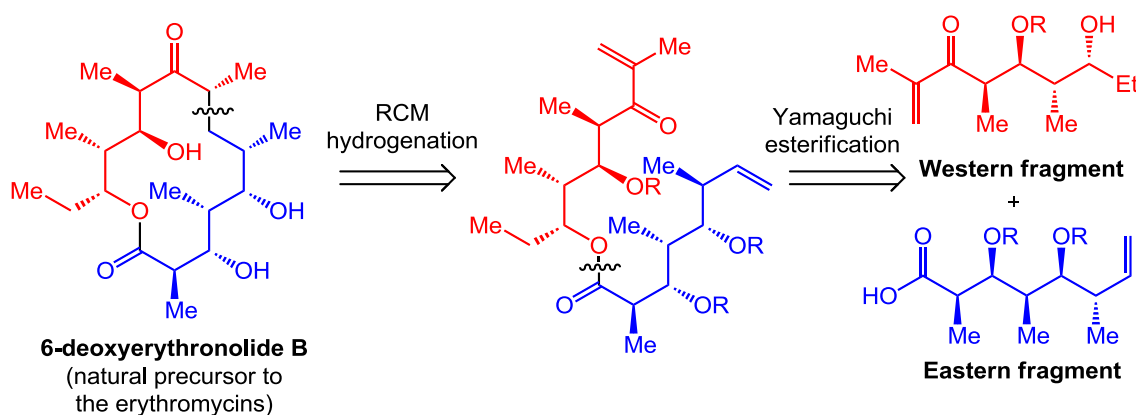
Our group has been active in exploring transition-metal-catalyzed asymmetric reactions. Realizing the potential biocatalysts can offer, we aim to marriage these two fundamentally different methods to access complex molecules in rapid and step economical ways. To showcase the efficiency of these stereoselective reactions, we envision their application to the total synthesis of a popular synthetic target, 6-deoxyerythronolide B. To date there are four reported total syntheses of 6-deoxyerythronolide B accomplished by Masamune in 1981,<sup>91</sup> by Danishefsky in 1990,<sup>92</sup> by Evans in 1998<sup>93</sup> and recently by White in 2009.<sup>94</sup> (Crimmins also published a formal synthesis of 6-deoxyerythronolide B in 2006.)<sup>95</sup>

Aware of over 20 total syntheses of erythromycin and its derivatives, we tried to disconnect this molecule in a completely novel manner. A unifying theme in the synthesis of erythronolide cores is the use of a macrolactonizations to form the 14-membered cycle. Conversely, we thought to

employ a transition-metal catalyzed ring-closing metathesis. To assemble the different fragments, we envisioned taking advantage of biocatalysts capable of setting multiple (three!) stereocenters simultaneously.

### 5.3.2 Retrosynthetic Approach to 6-Deoxyerythronolide B

The key disconnection envisioned in our retrosynthetic approach to 6-deoxyerythronolide B involves a ring-closing metathesis (RCM). This approach has never been explored for the erythronolide core. Indeed, previous syntheses have exclusively relied on macrolactonization to build the 14-membered lactone, including a late stage C–H oxidation by White.<sup>96</sup>



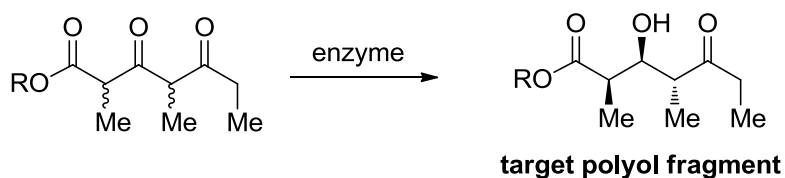
#### Scheme 38: Retrosynthetic approach to 6-deoxyerythronolide B

A RCM disconnection yields an ester intermediate with two terminal olefins, one of the olefins being an enone (Scheme 38). Ultimately, our goal is to access both fragments which have similar complexity with high efficiency via biocatalysis in collaboration with Prof. Adrian Keatinge-Clay at UT Austin. In the mean time, we want to test our late-stage RCM reaction and thus want to access the two polyol fragments in a most reliable way: Evans' well established aldol chemistry.

The RCM approach allows for a divergent and step economical synthesis of 6-deoxyerythronolide B. The long term goal is to go back and explore more efficient and elegant synthetic routes to the western and eastern fragments, including biosynthetic routes. The synthesis of the western fragment was allocated to Peter Dornan and me whereas the eastern fragment was assigned to Tom Hsieh and Kevin Kou.

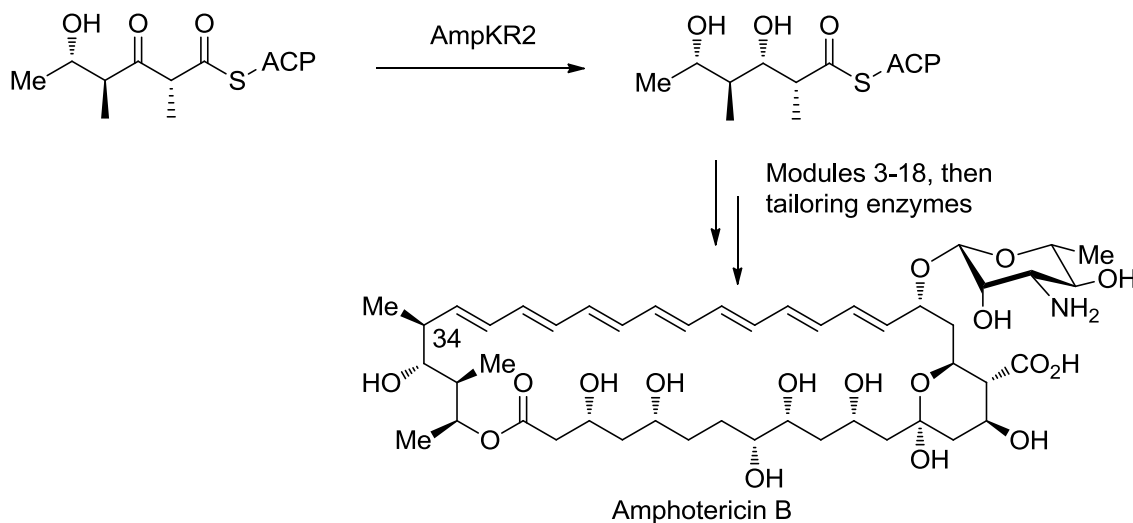
### 5.3.3 Biocatalysis – Amphotericin’s Ketoreductase

Exploiting biocatalysis as a means of setting numerous stereocenters simultaneously appears to be an efficient and attractive option towards generating polyols. In the context of our synthetic efforts towards 6-deoxyerythronolide B, we would like to use biocatalysis to reduce the ketone of a tricarbonyl substrate and set the  $\beta$ -hydroxyl and the  $\alpha$ - and  $\gamma$ -methyl stereocenters in one reaction. The target transformation is illustrated below (Scheme 39).



**Scheme 39: Envisioned biocatalytic approach to polyketide fragments**

After extensive literature searching, Peter Dornan found a potential candidate for our required stereoselective reduction: the ketoreductase of Mod2 of amphotericin (AmpKR-2). AmpKR-2 catalyzes the formation of a  $\beta$ -hydroxyl group of “S” stereochemistry at C-35 and a methyl group of “R” stereochemistry at C-34 in the complex polyketide amphotericin B (Scheme 40). Prof. Keatinge-Clay’s group at UT Austin was the first to publish the crystal structure of this enzyme and they combined their report with the scope of AmpKR-2 including different  $\beta$ -ketoesters with NAC derivatives.<sup>97</sup> It is important to highlight that the stereochemistry obtained after reduction with AmpKR-2 gives the exact stereochemistry required for the western fragment of 6-deoxyerythronolide B.



**Scheme 40: Enzymatic reduction by AmpKR2, an isolated enzyme from amphotericin B's PKS**

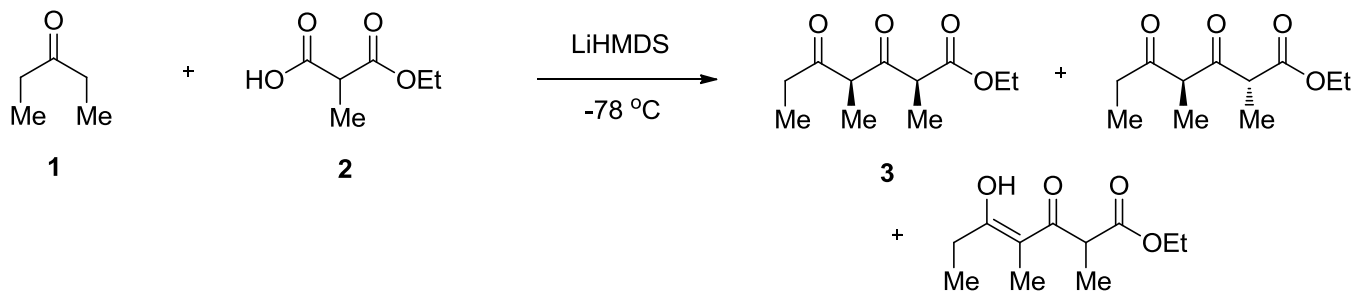
In light of Prof. Keatinge-Clay's result with AmpKR-2, we proposed that with a slightly modified substrate, a  $\beta,\delta$ -dicarbonyl compound instead of a  $\beta$ -carbonyl- $\delta$ -hydroxy, we would achieve high selectivity for the desired transformation. A collaboration was established with the Keatinge-Clay group in order to test  $\delta$ -keto- $\beta$ -keto-esters as substrates with their isolated ketoreductase enzyme.

## 5.4 Synthetic Efforts Towards 6-Deoxyerythronolide B

### 5.4.1 Synthesis of 1,3,5-Tricarbonyl Compounds

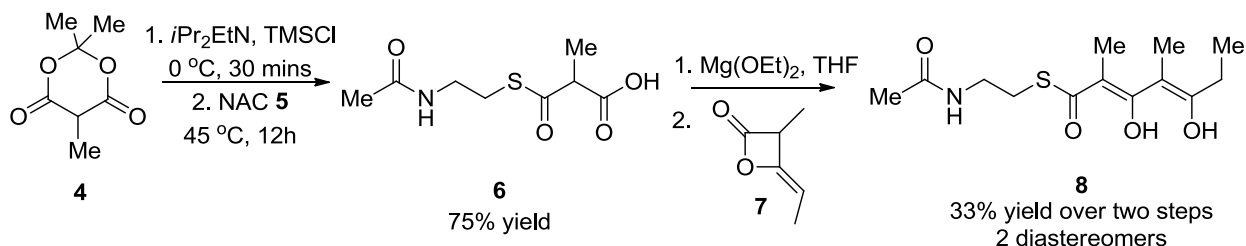
To get the biocatalytic route underway, four different 1,3,5-tricarbonyl substrates with different ester and thioester alkyl groups ( $-\text{OEt}$ ,  $-\text{OMe}$ ,  $-\text{OtBu}$ ,  $-\text{SMe}$ ) were sent to the collaborating student working on this project, Constance Bailey. After submitting the tricarbonyl substrates to the AmpKR2 enzyme, she obtained a promising hit with the ethyl ester tricarbonyl **3**.

Decarboxylative Claisen reactions and aldol/oxidation reactions were employed to make the  $\delta$ -keto- $\beta$ -keto-esters, but after optimization, larger quantities of the ethyl ester tricarbonyl **3** compound were synthesized via a cross-Claisen condensation. Careful purification of the Claisen reaction mixture yields between 10-30% of the desired 1,3,5-tricarbonyl ethyl ester **3** as a mixture of two diastereomers and one tautomer as determined by multiple NMR studies (Scheme 41).



**Scheme 41: Synthesis of 1,3,5-tricarboxyl ethyl ester **3** via a Claisen condensation**

Following Peter Dornan's computer modeling experiments at UCLA with Prof. Ken Houk of the native substrate in the enzyme pocket, he found that the *N*-acetylcysteamine (SNAC) derivative binds in a more selective fashion and may in part be responsible for the observed stereochemical outcome. If the tricarbonyl compound also had these specific binding properties, then enhancement of stereoselectivity may be observed. To address this hypothesis, a two step synthesis of SNAC tricarbonyl **8** was undertaken. The major issue encountered in this synthesis was the opening of methyl-Meldrum's acid **4** with SNAC **5**. To overcome the reactivity issue, SNAC **5** needed to be silylated, thereby generating a more nucleophilic thiol (Scheme 42).<sup>98</sup> The second synthetic step required the synthesis of freshly distilled methyl-diketene dimer **7** which was submitted to a decarboxylative Claisen condensation induced by magnesium ethoxide.

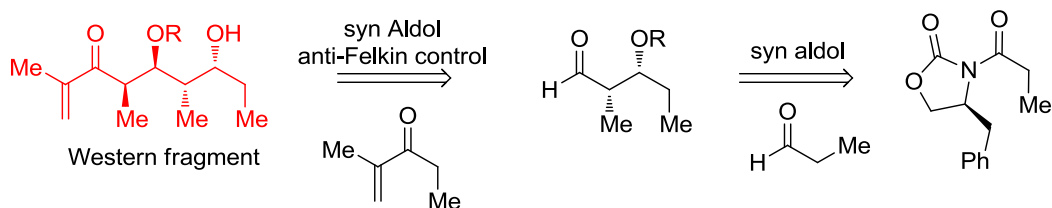


**Scheme 42: Synthesis of 1,3,5-tricarboxyl SNAC thioester **8****

The  $\delta$ -keto- $\beta$ -keto-ethyl ester **3** and the  $\delta$ -keto- $\beta$ -keto-SNAC thioester **8** are currently under investigation by Connie Bailey at UT Austin. She is encountering problems in her experiments relating to incomplete conversion and is having difficulty observing the desired product by NMR (but sees the reduced product by LCMS and TLC). She is currently considering evaluating the SNAC tricarbonyl **8** in more detail.

## 5.4.2 Synthesis of the Western Fragment

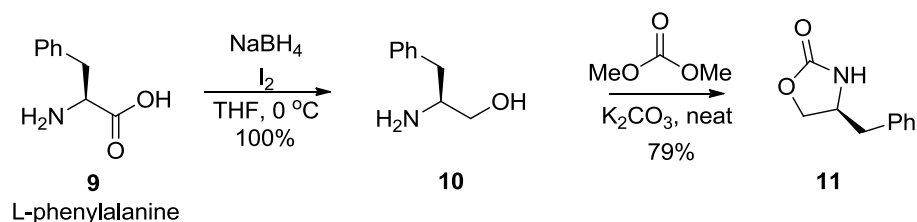
Our retrosynthetic plan for the western fragment involves a key aldol disconnection which renders the synthesis convergent. Teamed up with Peter Dornan, we considered an established approach to access the  $\beta$ -hydroxy aldehyde via Evans' aldol chemistry. The convergent aldol reaction would require optimizing but then protecting group manipulation would lead us to the western fragment in an efficient and reliable manner (Scheme 43).



**Scheme 43: Retrosynthetic approach to the western fragment**

### 5.4.2.1 Synthesis of the $\beta$ -Hydroxy Aldehyde

The synthesis of Evans' auxiliary **11** is straightforward and well documented in the literature (Scheme 44). L-phenylalanine **9** is reduced to the alcohol using  $\text{NaBH}_4$  and  $\text{I}_2$ , presumably forming the reactive reducing agent,  $\text{BH}_2\text{I}$ , in situ. The alcohol **10** was obtained in quantitative yield and then cyclized to the oxazolidinone **11** using dimethylcarbonate. Alternatively, oxazolidinone **11** can be purchased from Aldrich albeit at high cost.

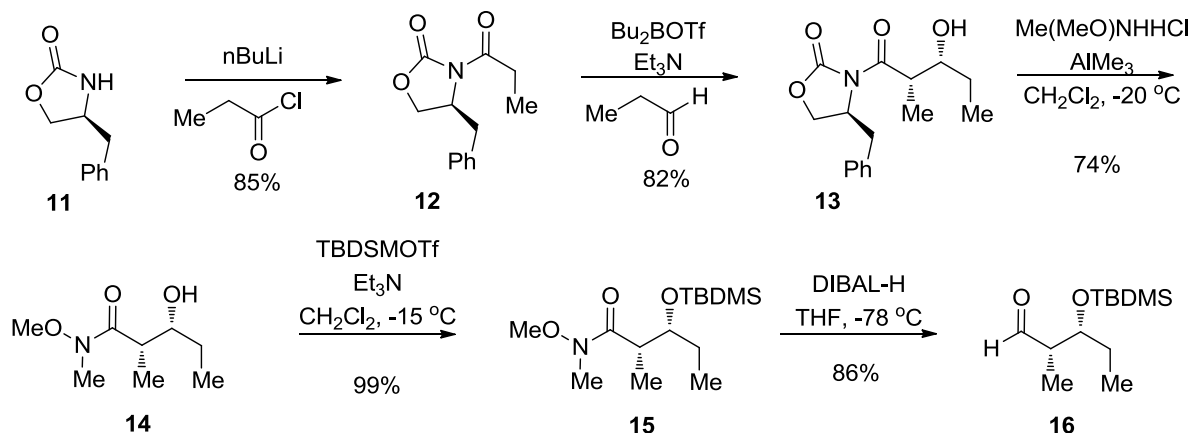


**Scheme 44: Synthesis of Evans' oxazolidinone auxiliary 11**

The oxazolidinone **11** is then carried through to the  $\beta$ -hydroxy aldehyde **16** in 5 steps and 44% overall yield (Scheme 45). The oxazolidinone auxiliary **11** is acylated using a strong base and freshly distilled propionyl chloride. The acylated oxazolidinone **12** is subjected to Evans' aldol reaction conditions involving dibutylboron triflate and triethylamine to generate the desired syn



aldol product **13**. This reaction is highly stereospecific and is amenable to large scale with good yield. The *tert*-butyl dimethylsilyl (TBDMS) protection of the  $\beta$ -hydroxyl group is easier once the oxazolidinone has been converted into the Weinreb amide **14**. The protected Weinreb amide **15** avoids over reduction with DIBAL-H reduction and generates aldehyde **16**.



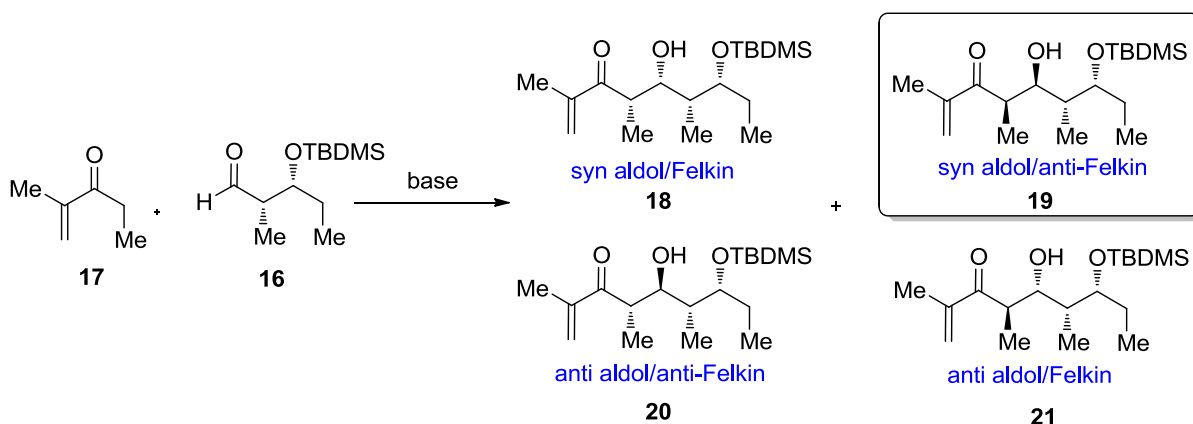
#### Scheme 45: Synthesis of the chiral aldehyde **16**, the acceptor in the key aldol reaction

This synthetic sequence has been attempted numerous times (each reaction performed 3-5 times) at different scales. Some problems encountered during the sequence include the coelution of the  $\beta$ -hydroxyl oxazolidinone **13** and the  $\beta$ -hydroxyl Weinreb amide **14**. Also, aldehyde **16** is unstable to preparative TLC purification but can be quickly chromatographed using basified silica gel. A recurring contaminant in the aldehyde intermediate **16** is the Weinreb amine analogue obtained via the imine (formed by the elimination of an Al-bound hydroxyl group after the first hydride addition). However this impurity was exclusively observed on scales larger than 2.00 mmol and was carried forward through the subsequent aldol reactions without any problems. Of note, the aldehyde **16** must be stored in the freezer and thus remains stable for at least two months. Over 3.00 g of compound **16** was synthesized.

#### 5.4.2.2 Optimizing the Aldol Reaction

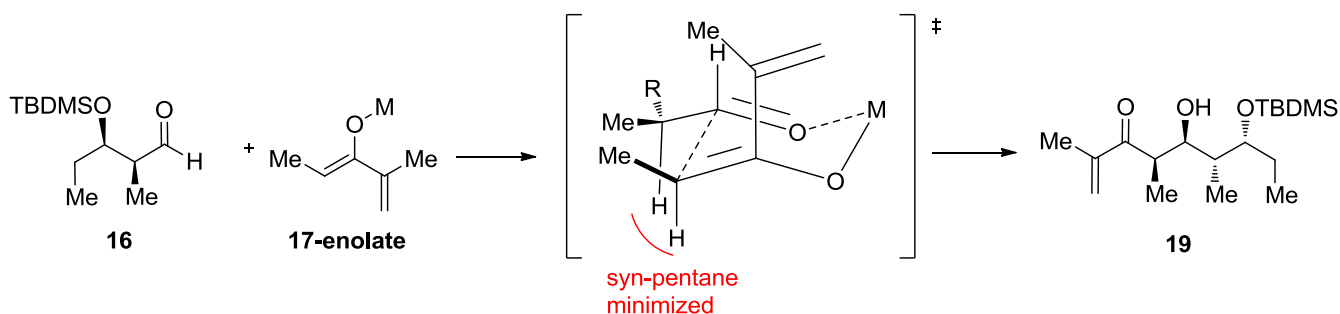
With large quantities of TBDMS-protected  $\beta$ -hydroxyl aldehyde **16** in hand; we were now ready to test our key aldol reaction with the  $\alpha,\beta$ -unsaturated ketone **17**. This aldol is expected to be diastereoselective but can nonetheless generate up to four different stereoisomers (Scheme 46).

The isomer of interest in the context of the total synthesis of 6-deoxyerythronolide B is the syn aldol/anti-Felkin product **19**.



### Scheme 46: Key aldol reaction and the four diastereomers generated

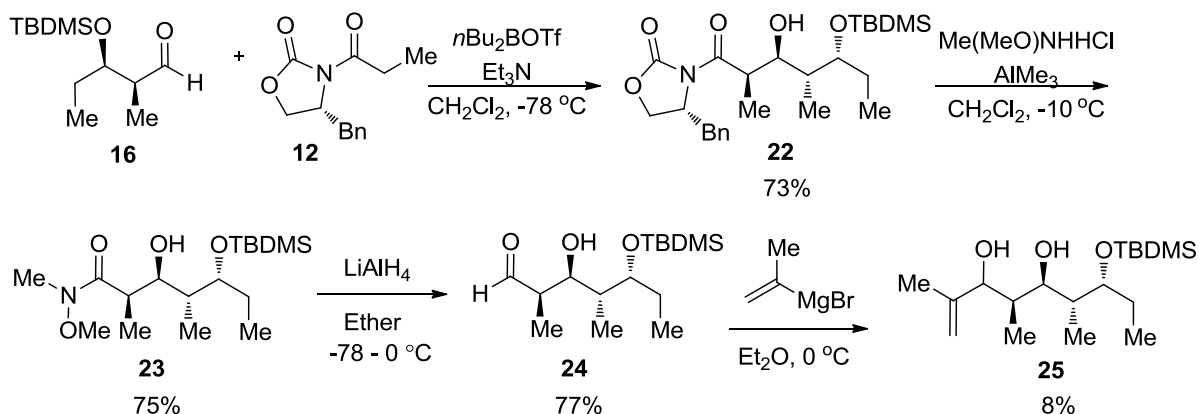
The use of a lithium base is preceded to favour a Zimmerman-Traxler transition state and yield the desired syn aldol.<sup>99</sup> The anti-Felkin selectivity stems from the  $\alpha$ -methyl stereocenter of aldehyde **16**. In the transition state, the  $\alpha$ -stereocenter will want to minimize syn-pentane interactions and preferentially generate the anti-Felkin product (Scheme 47). The transition state illustrated below should be lowest in energy since the syn-pentane interaction is minimized by placing the hydrogen in the axial position. The aldehyde will then attack the backside of the enolate since the methyl group is smaller than the R group giving the anti-Felkin selectivity.



### Scheme 47: Proposed transition state for the formation of the syn-aldol/anti-Felkin product 19

However, the use of lithium hexamethyldisilide (LiHMDS) generated all four possible stereoisomers, indicating low selectivity. In most reactions, the major diastereomer was indeed

the desired syn-aldol/anti-Felkin product **19**. Fortunately, all four isomers were separable and were fully characterized. A detailed  $^1\text{H}$ ,  $^{13}\text{C}$  and COSY NMR study helped differentiate the anti-aldol isomers from the syn-aldol isomers. This analysis was achieved assuming a hydrogen bond between the  $\beta$ -hydroxyl group and the ketone in a six-membered ring, thereby locking the configuration of the  $\alpha$ -methyl. A large coupling constant between the  $\alpha$ -hydrogen and the  $\beta$ -hydrogen is indicative of an anti-relationship.<sup>100</sup> By this analysis, the syn-aldol products had coupling constants of 3.9 Hz (syn-aldol/Felkin, **18**) and 3.0 Hz (syn-aldol/anti-Felkin, **19**) whereas the anti-aldol products had coupling constants of 7.2 Hz (anti-aldol/anti-Felkin, **20**) and 7.0 Hz (anti-aldol/Felkin, **21**). The Felkin and anti-Felkin relationship between the two syn-aldol isomers was confirmed by Peter Dornan via an independent synthesis using Evans's aldol chemistry (Scheme 48). The use of the oxazolidinone chiral auxiliary **11** will override the Felkin selectivity and selectively give the syn-aldol/anti-Felkin product **22**. Further manipulations and the addition of methylvinyl Grignard led to the aldol product **25** which was spectroscopically identical to the previously assigned aldol-product (**19**) once reduced. Of note, the Felkin selectivity for the anti-aldol/anti-Felkin **20** and anti-aldol/Felkin **21** products has not been verified. However, since the anti-aldol/Felkin triad generated by a (*Z*)-enolate is more common, it is likely that the major anti-aldol product obtained is the anti-aldol/Felkin diastereomer **21**.

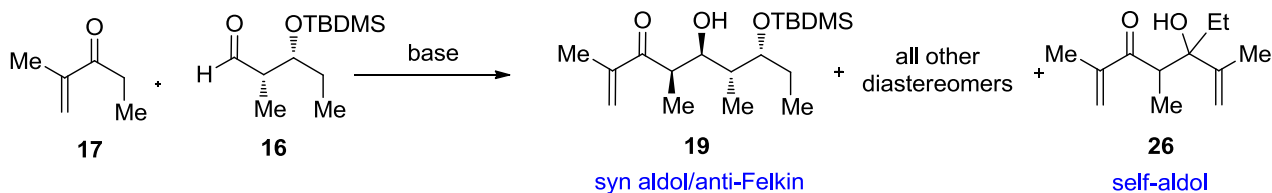


**Scheme 48: Synthesis of aldol desired syn-aldol/anti Felkin aldol product by an analogous route to confirm Felkin stereochemistry**

To optimize the selectivity of the aldol reaction in favour of the desired syn-aldol/anti Felkin isomer **19**, numerous reaction conditions were screened. Different bases, additives, solvents and

temperatures were evaluated for enhanced selectivity (Table 15). Lithium bases were first tested and the effect of different additives was investigated. Different equivalents of base yielded different selectivities and conversions (Table 15, entry 1 and 2). LDA gave the worst selectivity 1:4.3 (Table 15, entry 3) but when LDA and a titanium catalyst were added, the selectivity increased to 1:1.8 albeit the yield was much lower 3.5% (Table 15, entry 4). Other solvents and additives were screened with lithium bases but to no avail (Table 15, entries 5-9). Self-aldol **26** of enone **17** was observed as a by-product in certain cases. With a lithium base or an amine base, the self-aldol product **26** could be suppressed by using fewer equivalents of the enolate. However, in the presence of boron reagents, the formation of self-aldol product **26** could not be prevented. Dichlorophenylborane was the most selective reagent, giving moderate yields and moderate diastereoselectivity (5:1 where 1 represents all other diastereomers) (Table 15, entry 16). Nonetheless, the stoichiometric ratio between the enolate **17**, the aldehyde **16** and dichlorophenylborane was crucial in optimizing the selectivity (Table 15, entries 11-18). Also, the reaction doesn't proceed in the presence of triethylamine, highlighting the importance of Hunig's base in this system (Table 15, entry 15). Diphenylchloroborane is an unusual reagent in aldol reactions, but has successfully been employed in three previously described reports to yield a syn-aldol/anti Felkin product.<sup>101</sup>

**Table 14: Aldol screening parameters with methyl enone as the aldol donor**



#	base (equiv.)	<b>17</b> (equiv.)	additive (equiv.)	T <sup>o</sup>	solvent	Time (h)	conversion	dr <sup>a</sup>	Yield <b>19</b>
1	LiHMDS (1.5)	1.5		-78°C	THF	3	71%	1:1.9	9.5%
2	LiHMDS (2.6)	2.5		-75°C	THF	3	44%	1:2.4	15% <sup>b</sup>
3	LDA (2.2)	2.0		-78°C	THF	0.6	84%	1:4.3	16%
4	LDA (2.2)	2.0	Ti(OiPr) <sub>4</sub> (6.6)	-50°C	THF	0.3	8%	1:1.8	3.5%

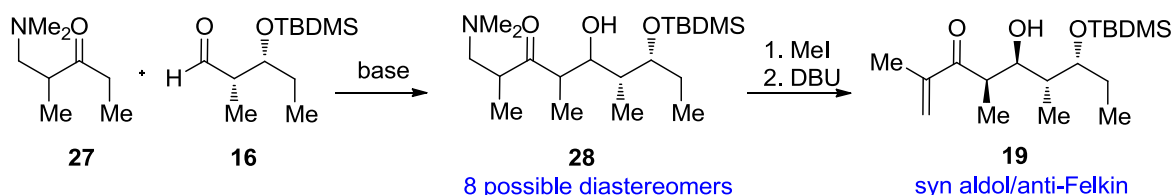
5	Et <sub>3</sub> N (1.6)	1.5	TiCl <sub>3</sub> (OiPr) (1.55)	0°C	CH <sub>2</sub> Cl <sub>2</sub>	3.3	32%	1:1.5	imp
6	LiHMDS (1.2)	1.0	HMPA (3.0)	-75°C	THF	4.5	84%	1:4.3	-
7	LiHMDS (1.2)	1.0	TMEDA (3.0)	-75°C	THF	4.5	76%	1:3.3	-
8	LiHMDS (1.2)	1.0		-75°C	Et <sub>2</sub> O	4.5	9%	1:2.4	-
9	LiHMDS (1.2)	1.0		-75°C	CH <sub>2</sub> Cl <sub>2</sub>	4.5	5%	1:2.0	-
10	iPr <sub>2</sub> NEt (1.3)	1.0	nBu <sub>2</sub> BOTf	0°C	CH <sub>2</sub> Cl <sub>2</sub>	4	0%	-	-
11	iPr <sub>2</sub> NEt (5.6)	2.0	PhBCl <sub>2</sub> (4.0)	0°C	CH <sub>2</sub> Cl <sub>2</sub>	4	85%	3.3:1	Imp <sup>b</sup>
12	iPr <sub>2</sub> NEt (1.3)	1.0	PhBCl <sub>2</sub> (1.2)	0°C	CH <sub>2</sub> Cl <sub>2</sub>	3.1	6.5%	1:1.1	Imp <sup>b</sup>
13	iPr <sub>2</sub> NEt (5.6)	2.0	PhBCl <sub>2</sub> (4.0)	0°C	CH <sub>2</sub> Cl <sub>2</sub>	2.5	85%	3.3:1	Imp <sup>b</sup>
14 <sup>c</sup>	iPr <sub>2</sub> NEt (2.8)	1.0	PhBCl <sub>2</sub> (2.0)	0°C	CH <sub>2</sub> Cl <sub>2</sub>	4.5	15%	1.2:1	4% <sup>b</sup>
15 <sup>c</sup>	Et <sub>3</sub> N (2.8)	1.0	PhBCl <sub>2</sub> (2.0)	0°C	CH <sub>2</sub> Cl <sub>2</sub>	4.5	0%	-	-
16	iPr <sub>2</sub> NEt (5.6)	2.0	PhBCl <sub>2</sub> (4.0)	0°C	CH <sub>2</sub> Cl <sub>2</sub>	1.5	92%	5:1	40% <sup>b</sup>
17	iPr <sub>2</sub> NEt (3.4)	1.2	PhBCl <sub>2</sub> (2.4)	0°C	CH <sub>2</sub> Cl <sub>2</sub>	1.5	34%	5:1	20% <sup>b</sup>
18 <sup>d</sup>	iPr <sub>2</sub> NEt (2.8)	1.0	PhBCl <sub>2</sub> (2.0)	0°C	CH <sub>2</sub> Cl <sub>2</sub>	1.5	28%	5:1	20% <sup>b</sup>

<sup>a</sup> Diastereoselectivity is represented as the desired diastereomer, syn-aldol/anti-Felkin **19**, to all other diastereomer (**18**, **20** and **21**). <sup>b</sup> Self-aldol product **26** was detected. <sup>c</sup> 1.5 equiv. of the aldehyde **16** was used. <sup>d</sup> 1.2 equiv. of the aldehyde **16** was used.

Further optimization led to exploring the use of a heteroatom in the  $\beta$ -position of the enolate. Enones are uncommon aldol donors and based on our observations (see Table 15), we found that they do not impart high levels of selectivity. Most successful aldols for syn aldol/anti-Felkin selectivity possess a heteroatom on the aldol donor. Perhaps the  $\beta$ -heteroatom coordinates to the reagent in the Zimmerman-Traxler cyclic transition state to give higher selectivities by blocking one face of the enolate.  $\beta$ -Amino ketone **27** was synthesized via a Mannich reaction with 3-pentanone, formaldehyde and dimethylamine to test this hypothesis. As predicted, the aldol reaction with a lithium base gave excellent conversions (Table 16). However, eight possible diastereomers of **28** could be produced and so the complex crude mixture was carried forward to

the next synthetic step for ease of analysis. The tertiary amine **28** was alkylated using methyl iodide and then the ammonium salt was eliminated using an organic base. The yields reported are over three synthetic steps, unfortunately rendering this sequence inefficient for the scale up of our synthesis. Even so, higher levels of selectivity were obtained in the presence of a lithium base with the  $\beta$ -amino ketone **27** in comparison to the methyl enone aldol donor **17** (Table 15 entry 1 and Table 16 entry 1). Interestingly, the optimized reaction conditions for the aldol reaction with the enone donor **17** completely inhibited the reaction with the  $\beta$ -amino ketone (Table 16, entries 5-7). It appears the aldol reaction conditions can be very substrate specific and in this case, incompatible with different reactants. This result supports the hypothesis that a coordinating atom enhances selectivity as well as explains the sparse use of enones in aldol reaction in the literature.

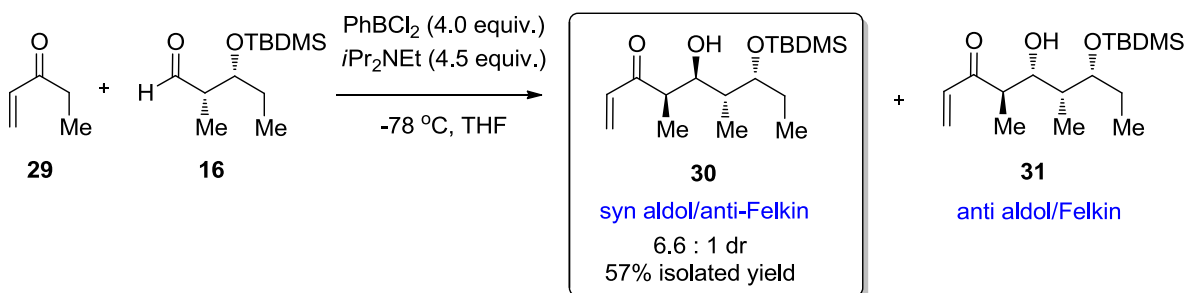
**Table 15: Aldol optimization table with  $\beta$ -amino ketone as the aldol donor**



#	base (equiv.)	ketone (equiv.)	T <sup>o</sup>	solvent	time	conversion	dr <sup>a</sup>	yield
1	LiHMDS (1.7)	1.50	-78°C	THF	3.0h	>95%	2.5:1	8%
2	LiHMDS (1.35)	1.25	-78°C	THF	4.5h	>90%	1.1:1	13%
3 <sup>c</sup>	LiHMDS (1.1)	1.00	-78°C	THF	4.5h	>90%	1.8:1	16%
4	LiHMDS (1.1)	1.00	-78°C	THF	4.5h	>85%	1.5:1	14%
5 <sup>b</sup>	iPr <sub>2</sub> NEt (5.6)	2.00	0°C	DCM	3.0h	trace	-	-
6 <sup>c</sup>	iPr <sub>2</sub> NEt (3.4)	1.20	0°C	DCM	3.0h	trace	-	-
7 <sup>d</sup>	iPr <sub>2</sub> NEt (2.8)	1.00	0°C	DCM	3.0h	trace	-	-

<sup>a</sup> Diastereoselectivity is represented as the desired diastereomer, syn-aldol/anti-Felkin **19**, to all other diastereomer (**18**, **20** and **21**). <sup>b</sup> 4.0 equiv. of PhBCl<sub>2</sub> was added. <sup>c</sup> 2.4 equiv. of PhBCl<sub>2</sub> was added. <sup>d</sup> 2.0 equiv. of PhBCl<sub>2</sub> and 1.20 equiv. of the aldehyde **16** were added. <sup>e</sup> 1.25 equiv. of the aldehyde **16** was used.

A third aldol donor was tested: vinyl ketone **29**. This experiment would tell us if the pending methyl on the enolate has a detrimental effect on the aldol selectivity. Further in the synthesis, the methyl could be installed at the C8 position of 6-deoxyerythronolide B via an alkylation reaction. Using the reaction conditions previously optimized for the ethyl methyl enone **17**, vinyl ketone **29** reacted with the β-hydroxy aldehyde **16** efficiently. Further screening of the ratios of boron-to-base led to the selection of the reaction conditions depicted below (Scheme 49). The desired syn-aldol/anti-Felkin adduct **30** was obtained in 57% isolated yield with a diastereomeric ratio of 6.6 : 1; the highest yield and diastereomeric ratio observed thus far. Also, only two of the four possible diastereoisomers were detected: the desired syn-aldol/anti-Felkin product **30** and the anti-aldol/Felkin product **31**. This result is indicative of a large enhancement in the anti-Felkin selectivity due solely by the absence of a α-methyl on the enolate.



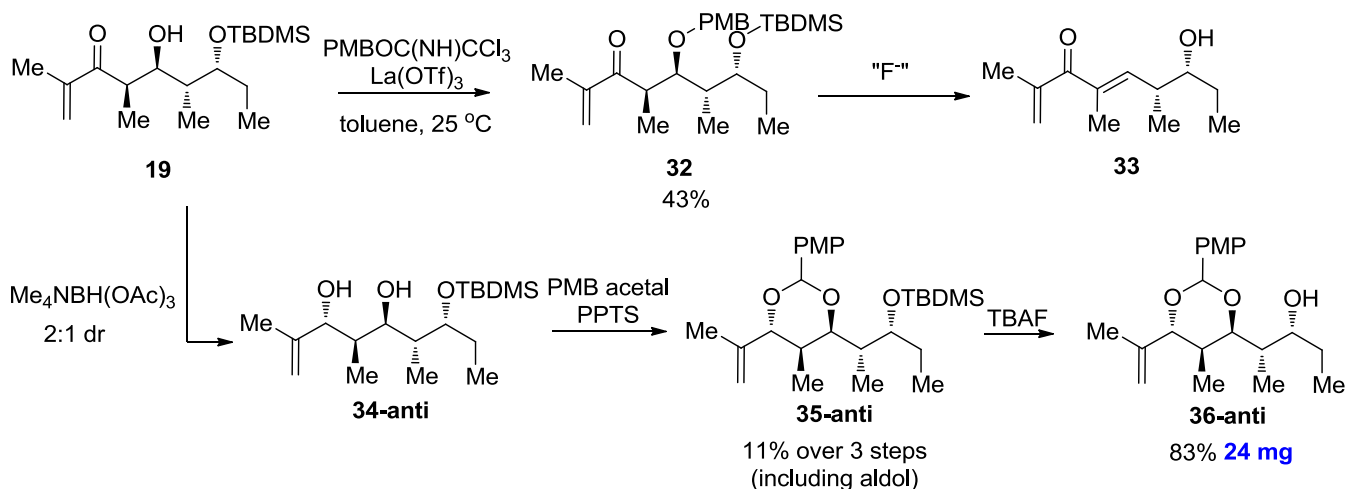
#### Scheme 49: Optimized reaction conditions for the aldol reaction with vinyl ketone **29** as the donor

The scale-up reactions of the dichlorophenylborane-mediated aldol were unfortunately problematic. Two aldol reactions with different aldol donors were performed: one with ethyl methyl enone **17** and the other with vinyl ketone **29**. The yields of these reactions were below 30% and the self-aldol product **26** of the ethyl methyl enone **17** was inseparable to the desired aldol adduct **19**. It is important to note that the diastereoselectivity is much better with the vinyl ketone aldol donor **29**. This result may be explained with the Zimmerman-Traxler cyclic transition state where the methyl group on the olefin could hinder the attack on the aldehyde,

affecting the Felkin selectivity. On the other hand, this extra methyl group could create steric hindrance and open up the cyclic transition state, again lowering the diastereoselectivity.

### 5.4.2.3 Taking the Aldol Product to the Western Fragment

To complete the synthesis of the western fragment of 6-deoxyerythronolide B from the aldol product, protecting group chemistry is required. The  $\beta$ -hydroxyl group must be orthogonally protected to the  $\delta$ -hydroxyl group for selective deprotection. In our retrosynthetic analysis, we wanted the western fragment to be a methyl enone. This would allow rapid conversion to the final natural product following the key RCM, but keeping in mind that the electron withdrawing nature of the enone could render the substrate challenging for the RCM. Nonetheless, we carried the aldol adduct **19** through and thus protected the  $\beta$ -hydroxyl with a *para*-methoxybenzyl group to give **32**. However, attempts to deprotect the  $\delta$ -hydroxyl silyl group with different fluoride sources were ineffective and gave elimination of the PMB-group instead, product **33** (Scheme 50).



**Scheme 50: Attempted synthesis of the enone **33** (top) and revised synthesis of the di-substituted olefin fragment **36** (bottom)**

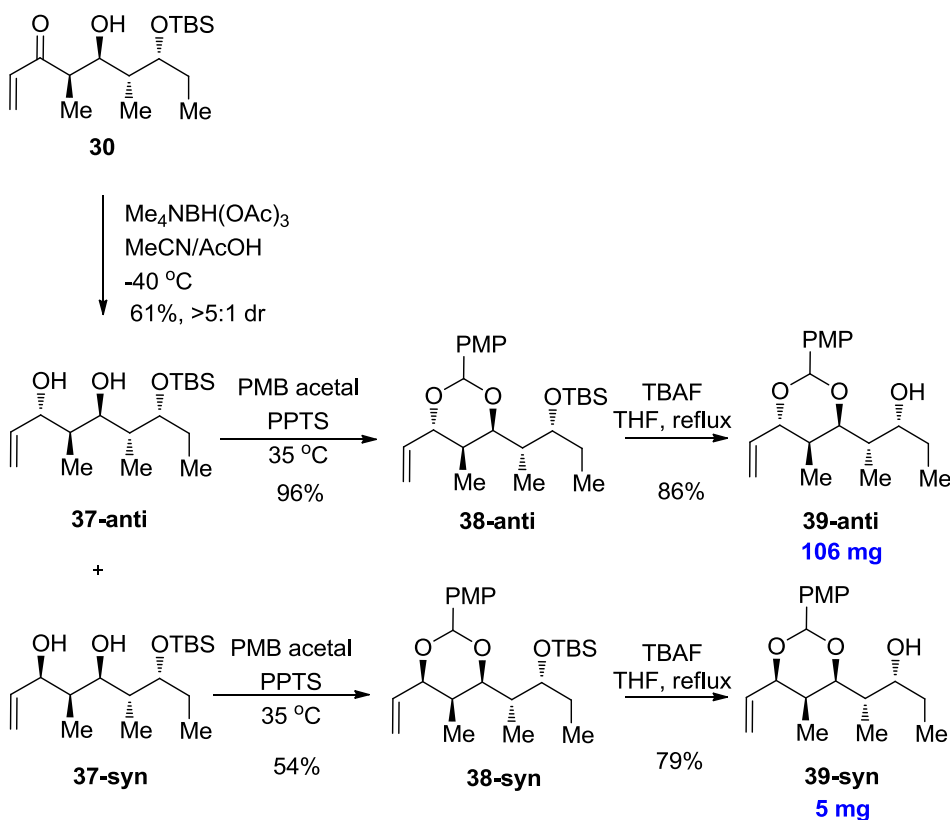


Following the difficulties with the TBDMS-deprotection, we revised the design of the western fragment (Scheme 50, bottom). A 1,3-directed reduction of the aldol adduct gave a diol **34** which was then protected as cyclic acetal **35**. This would avoid steric hindrance around the  $\delta$ -hydroxyl group, simultaneously enhancing the reactivity of the silyl group to fluoride attack. Of note, this sequence adds an extra step to the synthetic sequence.

A western fragment with a mono-substituted olefin **39** was also synthesized since the aldol with the vinyl ketone was most effective. Also, a substrate without the  $\alpha$ -methyl would generate a di-substituted olefin which is much easier to make via RCM than tri-substituted olefins. The key aldol reaction is modular and allowed incorporation of the mono-substituted olefin.

The synthesis of both fragments **36-anti** and **39-anti** are analogous (Scheme 50 bottom, Scheme 51 top). However, the directed 1,3-reduction of the mono-substituted olefin **19** and of the di-substituted olefin **30** proceeded quite differently. Firstly, the diastereoselectivity of the mono-substituted olefin is higher **37-anti**, presumably since the ketone is more accessible and facilitates the coordination of the boron atom. Also, the polarity of the anti- and of the syn-diastereomers is reversed in the two analogous reactions. In other words, the syn diastereomer **34-syn** is more polar than **34-anti** whereas the anti-diastereomer **37-anti** is more polar than **37-syn**. This result led to some confusion as to the correct assignment of the hydroxyl conformation. Therefore, to confirm the relative stereochemistry at C9, a syn directed 1,3-reduction was performed on **30**. The NMR analyses of the diols were not conclusive and so they were carried forward to the cyclic acetal to confirm the relative stereochemistry by COSY experiments.

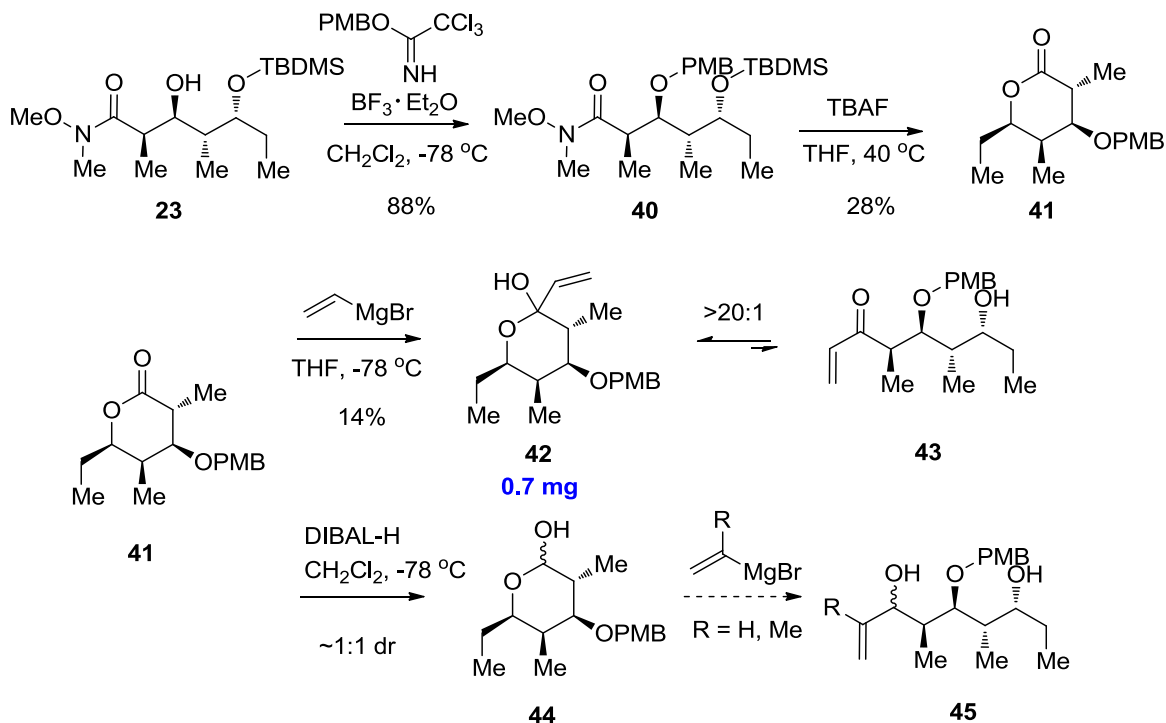
Furthermore, the C9 position of 6-deoxyerythronolide B is a ketone which implies that the allylic alcohol of **36** and **39** will need to be oxidized post-RCM. Because the stereochemistry of the C9 hydroxyl group is eventually lost, both hydroxyl isomers were synthesized **39-anti** and **39-syn** (Scheme 51). Woodward and co-workers have reported that the (*R*)-OH behaves differently to the (*S*)-OH in macrocyclization studies.<sup>102</sup> Although our disconnection is different, the stereochemistry of the C9-OH may favour a pre-cyclization confirmation which can impact the outcome of the RCM. This hypothesis remains to be tested, but both fragments have been synthesized in milligram quantities.



**Scheme 51: Synthesis of two analogous mono-substituted olefins 39-anti and 39-syn for the western fragment**

Having achieved the synthesis of three different western fragments **36-anti**, **39-anti** and **39-syn**, we remained interested in the synthesis of a western fragment with an enone instead of an allylic alcohol since the enone moiety would avoid synthetic steps post-RCM. With the previously encountered issues of  $\delta$ -silyl deprotection (from **32** to **33**), we thought of deprotecting the TBS-group from intermediate **23** instead (Scheme 52). This synthetic sequence is also modular to both enone fragments: with or without the methyl group. The same Weinreb amide intermediate **23** synthesized to confirm the Felkin selectivity (Scheme 48) was used as starting material. First, the  $\beta$ -hydroxyl group was protected with a PMB-group to yield **40**. Then, attempts to deprotect the TBS-group with a source of fluoride led to the formation of six-membered lactone **41**. Even though this product was unexpected, it can still serve as a useful intermediate in the synthesis of the modified western fragment. The vinyl Grignard reagent was successfully added to the lactone **41** and formed the lactol **42**. We hypothesized that intermediate **42** could exist in equilibrium

with the enone **43**, but unfortunately we were unable to detect the enone **43** by NMR. Also, we took the lactone **41** and reduced it to the lactol **44** with DIBAL-H. The intermediate **44** could lead to the synthesis of an allylic alcohol western fragment.



### Scheme 52: Alternate synthetic sequence towards an enone western fragment **43**

The cyclic allylic acetal fragment **42** was submitted to the esterification reaction conditions, and unfortunately no conversion was detected. The equilibrium with the open  $\delta$ -hydroxy enone from **43** seems lay to the cyclic allylic acetal **42**. No reaction was detected which also implies that the tertiary alcohol **42** is too hindered to react. The lactol compound **44** has yet to be tested in the esterification reaction.

#### 5.4.3 The Eastern Fragments

Three eastern fragments with different protecting group strategies were synthesized by Kevin Kou and Tom Hsieh (Figure 10). They employed traditional organic chemistry involving Evans' aldol and crotylation reactions.

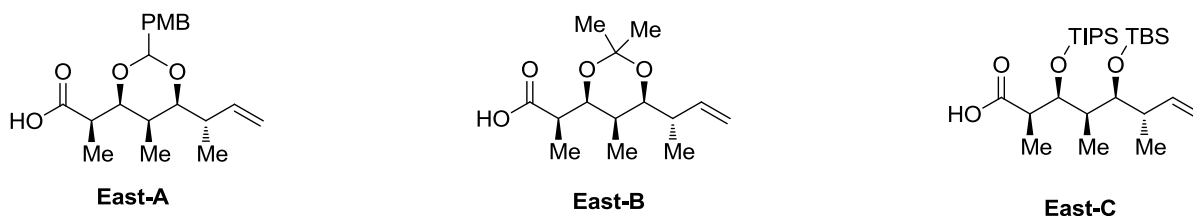
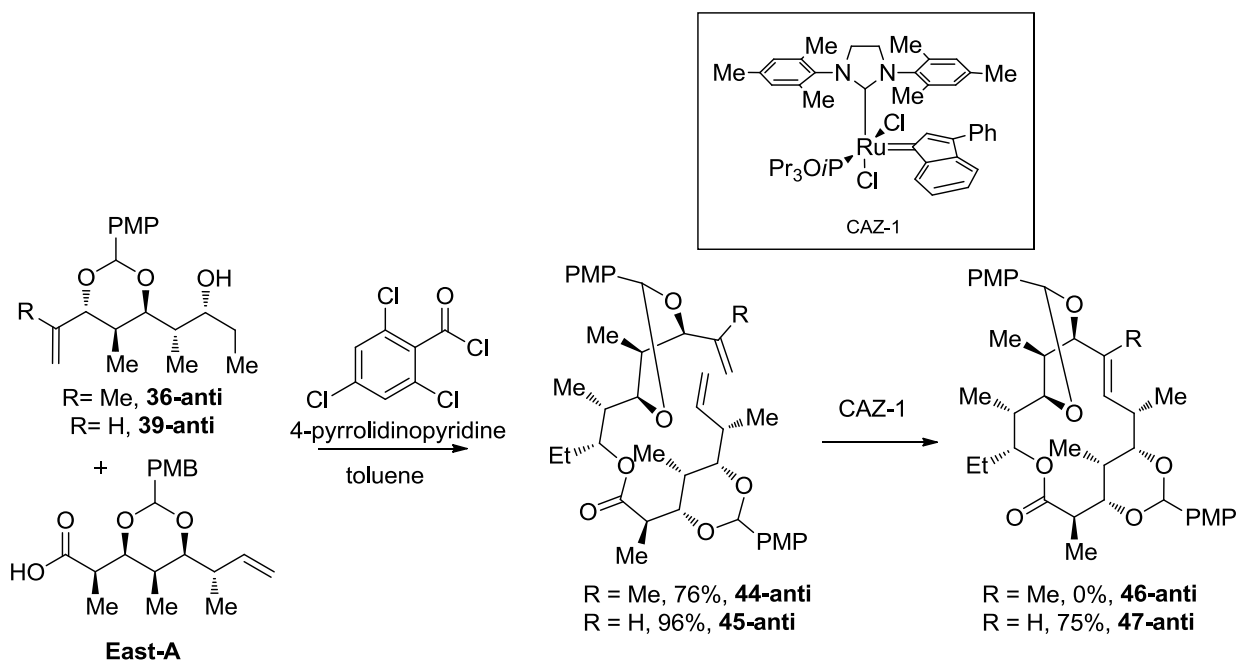


**Figure 9: Structures of the three eastern fragments synthesized**

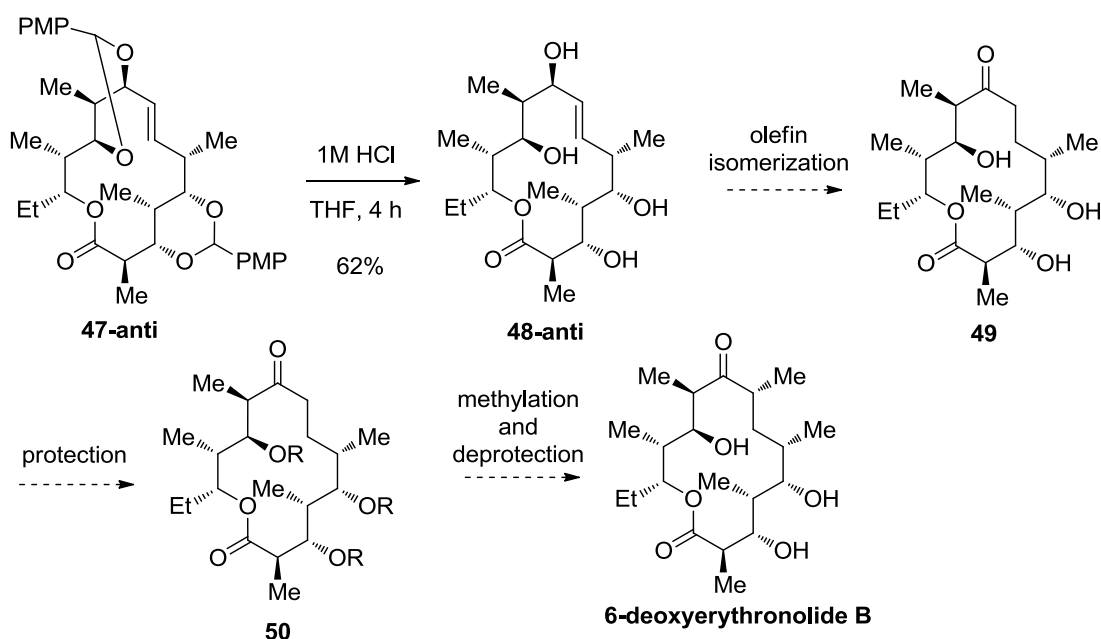
#### 5.4.4 Testing for the End Game

With the western and eastern fragments now synthesized, Peter Dornan was successfully able to optimize the esterification to form diene precursors **44-anti** and **45-anti** using a modified Yamaguchi procedure (Scheme 53). The key RCM was then ready to be attempted. Regrettably, the fragment with the methyl substituted olefin **44-anti** was unreactive. This was somewhat expected as forming tri-substituted olefins via a RCM is difficult and require unique catalysts.<sup>103,104</sup> There are presently only four reports of macrocyclic RCM which yield tri-substituted alkenes.<sup>105</sup> Professor Hoveyda at Boston College is an expert in the field, and we are currently collaborating with his group to identify a suitable catalyst which could cyclize the desired diene and form the tri-substituted alkene.



**Scheme 53: Esterification and RCM towards the 14-membered core of erythronolide**

In the meantime, we have synthesized the western fragment with a mono-substituted olefin **39-anti** which after esterification undergoes efficient RCM. To complete the total synthesis of 6-deoxyerythronolide B via intermediate **47-anti**, five more steps are required (Scheme 54). First, global deprotection of the PMB-acetals furnished tetraol **48-anti**. An olefin isomerization would avoid oxidation/reduction steps and give the C9-ketone **49**. The triol **49** would need to be protected (**50**) and then converted into the enolate and subsequently methylated. Finally, another global deprotection would give the desired natural product. We are in the process of exploring this sequence.



#### Scheme 54: Proposed post-RCM synthetic steps to 6-deoxyerythronolide B

The goal of this synthesis was to test the RCM and verify that our key disconnection is indeed viable. We employed classic auxiliary chemistry to impart chirality in the synthetic sequence. Aldol, oxidation and reduction, protecting group chemistry allowed us to successfully arrive at advance intermediates ready to be cyclized. Some insights were also gained through the RCM screening. As predicted, the generation of tri-substituted olefins via a metathesis reaction is challenging and failed in our hands. However, the western fragment containing the enone moiety **39-anti**, once coupled with the appropriate eastern fragment led to the successful synthesis of the 14-membered erythronolide core **47-anti**. The success of the RCM reaction confirmed the

viability of the retrosynthesis and now our goal is to rethink the synthesis of the eastern and western fragments. Ideally, the incorporation of a biocatalytic methodology would help make this synthesis of erythronolide B, the shortest synthesis to date.

## 5.5 Experimental Section

### General Method:

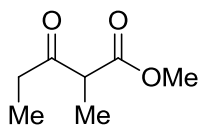
Reactions were carried out under an atmosphere of dry argon using standard Schlenk technique, unless specified otherwise. Anilines and acyl chloride were purchased from Aldrich or Acros and used as received. Pd(OAc)<sub>2</sub> was purchased from Strem. Reactions were monitored using thin-layer chromatography (TLC) on EMD Silica Gel 60 F<sub>254</sub> plates. Visualization of the developed plates was performed under UV light (254 nm) or KMnO<sub>4</sub> stain. Organic solutions were concentrated under reduced pressure on a Büchi rotary evaporator. Column chromatography was performed using Silicycle Silicagel 60 (0.043-0.06 mm).

### Analytical Methods:

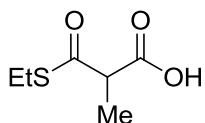
<sup>1</sup>H, <sup>13</sup>C{<sup>1</sup>H}, and <sup>19</sup>F NMR spectra were recorded on a Varian Mercury 300, Varian Mercury 400, VRX-S (Unity) 400, or Bruker AV-III 400 spectrometer at ambient temperature. All NMR spectra are referenced to TMS or the residual solvent signal. Data for <sup>1</sup>H NMR are reported as follows: chemical shift (δ ppm), multiplicity (s = singlet, d = doublet, t = triplet, q = quartet, m = multiplet, br = broad), coupling constant (Hz), integration. Data for <sup>13</sup>C{<sup>1</sup>H} NMR is reported as follows: chemical shift (δ ppm). Data for <sup>19</sup>F NMR are reported as follows: chemical shift (δ ppm), multiplicity (s = singlet, d = doublet, t = triplet, q = quartet, m = multiplet, br = broad), coupling constant (Hz), integration.

Mass spectra (MS) were recorded on a Sciex Qstar Mass Spectrometer. High resolution mass spectra (HRMS) were recorded on a micromass 70S-250 spectrometer (EI) or an ABI/Sciex Qstar Mass Spectrometer (ESI). Melting point ranges were determined on a Gallenkamp melting point apparatus (uncorrected). Column chromatography was carried out on Silicycle Silica-P Flash Silica Gel (40-63 μm). Preparative layer chromatography was performed on EMD Silica Gel 60 F<sub>254</sub> plates (254 μm).

### 5.5.1 Tricarbonyls

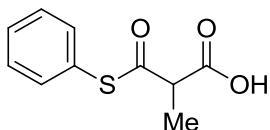


**Methyl 2-methyl-3-oxopentanoate:** In a flame-dried flask, methyl 3-oxopentanoate (1.88 mL, 15.0 mmol) was dissolved in 20 mL of dry acetone. Potassium carbonate (1.93 g, 14.0 mmol) was added and the reaction was stirred for 5 mins at room temperature. Methyl iodide (1.14 mL, 18.4 mmol) was added via syringe and the reaction mixture was refluxed for 6 h. Then, 0.6 mL of methyl iodide was added again to push the reaction to completion. The reaction was stirred overnight at reflux. The reaction mixture was diluted in ether and filtered to remove solids. The solvent was evaporated. The crude product was purified by silica gel flash chromatography eluting with a gradient of 5-15% ethylacetate/hexanes. 1.53 g (71%) of a colourless oil was obtained. The spectra are in agreement with reported literature data.<sup>106</sup>  $^1\text{H NMR}$  (400 MHz,  $\text{CDCl}_3$ )  $\delta$  (ppm) 3.73 (s, 3H), 3.55 (q, 1H,  $J = 7.2$  Hz), 2.67-2.47 (m, 2H), 1.35 (d, 3H,  $J = 7.2$  Hz), 1.08 (t, 1H,  $J = 7.2$  Hz) Note that the enol form is detected.  $^{13}\text{C}\{^1\text{H}\}$  NMR (100 MHz,  $\text{CDCl}_3$ )  $\delta$  (ppm) 206.4, 171.2, 52.4, 52.4, 34.7, 12.9, 7.7. MS (EI)  $m/z$  155 (M).



**3-(Ethylthio)-2-methyl-3-oxopropanoic acid:** In a flame-dried flask, methyl-Meldrum's acid (1.582g, 10.0 mmol, 1.00 eq) was dissolved in 10 mL of dry MeCN. The flask was placed in an ice bath (0 °C) and diisopropylethylamine (1.92 mL, 11.0 mmol, 1.10 eq) followed by TMSCl (1.40 mL, 11.0 mmol, 1.10 eq) were added. Upon addition of the TMSCl, a white gas was observed and evacuated with argon. The mixture was stirred at 0 °C for 30 mins (colourless solution). Ethylthiol (0.786 mL, 10.5 mmol, 1.05 eq) was then slowly added with a constant flow of argon to evacuate the gas formed. The reaction was stirred at 43 °C for 20 h. A solution of 0.3 M HCl was added to quench the reaction. The aqueous layer was extracted three times with ether. The combined organic layers were extracted three times with a solution of saturated

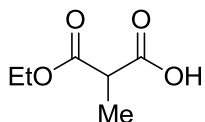
NaHCO<sub>3</sub>. The combined aqueous phases were acidified with a solution of 4 M HCl to a pH=0. This aqueous phase was extracted three times with ether. The combined organic phases were washed with brine, dried over MgSO<sub>4</sub> and evaporated. The crude product was purified by silica gel flash chromatography eluting with a gradient of 5-30% ethylacetate/hexanes. 1.418 g (87%) of a colourless oil was obtained. <sup>1</sup>H NMR (400 MHz, CDCl<sub>3</sub>) δ (ppm) 11.20-10.80 (br s, 1H), 3.68 (q, 1H, *J* = 7.2 Hz), 2.94 (q, 2H, *J* = 7.4 Hz), 1.47 (d, 3H, *J* = 7.2 Hz), 1.28 (t, 3H, *J* = 7.4 Hz). <sup>13</sup>C{<sup>1</sup>H} NMR (100 MHz, CDCl<sub>3</sub>) δ 195.9, 175.0, 53.6, 23.9, 14.3, 14.2. MS (ESI+) *m/z* 163 (M+H), 185 (M+Na); HRMS (ESI+) *m/z* calc'd for C<sub>6</sub>H<sub>10</sub>O<sub>3</sub>SNa [M+Na]<sup>+</sup>: 185.0242; found: 185.0252.



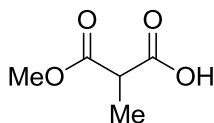
**2-Methyl-3-oxo-3-(phenylthio)propanoic acid:** In a flame-dried flask, recrystallized (from ethanol) methyl-Meldrum's acid (2.000 g, 12.6 mmol, 1.00 eq) was dissolved in 15 mL of dry MeCN. The flask was placed in an ice bath (0 °C) and diisopropylethylamine (2.42 mL, 13.9 mmol, 1.10 eq) followed by TMSCl (1.76 mL, 13.9 mmol, 1.10 eq) were added. Upon addition of the TMSCl, a white gas was observed and evacuated with argon. The mixture was stirred at 0 °C for 30 mins (yellow solution). Thiophenol (1.35 mL, 13.2 mmol, 1.05 eq) was then slowly added with a constant flow of argon to evacuate the gas formed. The reaction was stirred at 43 °C for 20 h. A solution of 0.3 M HCl was added to quench the reaction. The aqueous layer was extracted three times with ether. The combined organic layers were extracted three times with a solution of saturated NaHCO<sub>3</sub>. The combined aqueous phases were acidified with a solution of 4 M HCl to a pH=0. This aqueous phase was extracted three times with ether. The combined organic phases were washed with brine, dried over MgSO<sub>4</sub> and evaporated. The crude product was purified by silica gel flash chromatography eluting with a gradient of 5-30% ethylacetate/hexanes. 1.539 g (58%) of a white solid was obtained. All spectral data are in agreement with reported literature data.<sup>107</sup> m.p. 45-49 °C. <sup>1</sup>H NMR (400 MHz, CDCl<sub>3</sub>) δ (ppm) 11.40-11.00 (br s, 1H) 7.45-7.40 (m, 5H), 3.81 (q, 1H, *J* = 7.2 Hz), 1.54 (d, 3H, *J* = 7.2 Hz).



$^{13}\text{C}\{^1\text{H}\}$  NMR (100 MHz,  $\text{CDCl}_3$ )  $\delta$  193.9, 174.9, 134.5, 129.9, 129.4, 126.6, 53.3, 14.2. MS (ESI+)  $m/z$  211 (M+H), 233 (M+Na); HRMS (ESI+)  $m/z$  calc'd for  $\text{C}_{10}\text{H}_{11}\text{O}_3\text{S}$  [M+H] $^+$ : 211.0423; found: 211.0430.



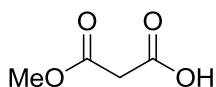
**3-Ethoxy-2-methyl-3-oxopropanoic acid (2):** Diethyl 2-methylmalonate (1.787 g, 10.3 mmol, 1.00 eq) was dissolved in 17 mL of THF and 170 mL of water. The reaction mixture was cooled to 0 °C and 49 mL of a 0.25 M solution of NaOH was added. The reaction was stirred for 1 h while warming to 15 °C. A cold 1 M HCl solution was used to acidify the mixture to pH=3. Then NaCl was added until saturation and immediately extracted four times with ethylacetate. The combined organic phases were dried over  $\text{MgSO}_4$ , filtered and evaporated. The crude product was purified by silica gel flash chromatography eluting with a gradient of 25-100% ethylacetate/hexanes. 1.279 g (85%) of a colourless oil was obtained. All spectral data are in agreement with reported literature data.  $^{108}\text{ }^1\text{H}$  NMR (400 MHz,  $\text{CDCl}_3$ )  $\delta$  (ppm) 11.40-10.50 (br s, 1H), 4.23 (q, 2H,  $J = 7.1$  Hz), 3.48 (q, 1H,  $J = 7.3$  Hz), 1.47 (d, 3H,  $J = 7.3$  Hz), 1.29 (t, 3H,  $J = 7.0$  Hz).  $^{13}\text{C}\{^1\text{H}\}$  NMR (100 MHz,  $\text{CDCl}_3$ )  $\delta$  191.2, 170.2, 62.0, 46.0, 14.2, 13.8. MS (ESI+)  $m/z$  147 (M+H), 169 (M+Na); HRMS (ESI+)  $m/z$  calc'd for  $\text{C}_6\text{H}_{11}\text{O}_4$  [M+H] $^+$ : 147.0651; found: 147.0654.



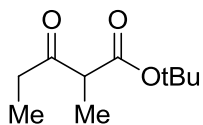
**3-Methoxy-2-methyl-3-oxopropanoic:** Dimethyl 2-methylmalonate (1.500 g, 10.3 mmol, 1.00 eq) was dissolved in 17 mL of THF and 170 mL of water. The reaction mixture was cooled to 0 °C and 49 mL of a 0.25 M solution of NaOH was added. The reaction was stirred for 1 h while warming to 15 °C. A cold 1 M HCl solution was used to acidify the mixture to pH=3. Then NaCl

was added until saturation and immediately extracted four times with ethylacetate. The combined organic phases were dried over  $\text{MgSO}_4$ , filtered and evaporated. The crude product was purified by silica gel flash chromatography eluting with a gradient of 25-100% ethylacetate/hexanes.

1.051 g (78%) of a colourless oil was obtained. All spectral data are in agreement with reported literature data.  $^{109} \text{^1H NMR}$  (400 MHz,  $\text{CDCl}_3$ )  $\delta$  (ppm) 11.40-11.00 (br s, 1H), 3.78 (s, 3H), 3.51 (q, 1H,  $J = 7.3$  Hz), 1.47 (d, 3H,  $J = 7.3$  Hz).  $^{13}\text{C}\{\text{^1H}\}$  NMR (100 MHz,  $\text{CDCl}_3$ )  $\delta$  175.7, 170.5, 53.0, 45.9, 13.8. MS (ES+)  $m/z$  could not be found (decarboxylates).

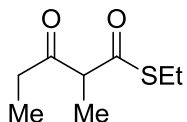


**3-Methoxy-3-oxopropanoic acid:** Dimethyl malonate (5.73 mL, 50.0 mmol, 1.00 eq) was dissolved in 83 mL of THF and 830 mL of water. The reaction mixture was cooled to 0 °C and 240 mL of a 0.25 M solution of NaOH was added. The reaction was stirred for 1 h while warming to 15 °C. A cold 4 M HCl solution was used to acidify the mixture to pH=2. Then NaCl was added until saturation and immediately extracted four times with ethylacetate. The combined organic phases were dried over  $\text{MgSO}_4$ , filtered and evaporated. The crude product was purified by silica gel flash chromatography eluting with a gradient of 25-100% ethylacetate/hexanes. 5.057 g (86%) of yellow oil was obtained. All spectral data are in agreement with reported literature data.  $^{110} \text{^1H NMR}$  (400 MHz,  $\text{CDCl}_3$ )  $\delta$  (ppm) 9.90-9.50 (br s, 1H), 3.78 (s, 3H), 3.45 (s, 2H). MS (ESI+)  $m/z$  119 (M+H), 141 (M+Na); HRMS (ESI+)  $m/z$  calc'd for  $\text{C}_4\text{H}_7\text{O}_4$  [M+H] $^+$ : 119.0338; found: 119.0344.



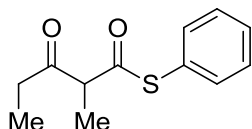
**tert-Butyl 2-methyl-3-oxopentanoate:** In a flame-dried flask, diisopropylethylamine (9.04 mL, 64.5 mmol, 4.30 eq) was dissolved in 67 mL of dry THF. The solution was cooled to 0 °C and

*n*butyl lithium (53.5 mL of a 1.206 M solution in hexanes, 64.5 mmol, 4.30 eq) was added dropwise. An argon balloon was installed and the reaction was cooled to  $-79\text{ }^{\circ}\text{C}$ . *t*butyl propionate (7.24 mL, 48.0 mmol, 3.20 eq) was added dropwise to the LDA solution. A precooled (at  $-70\text{ }^{\circ}\text{C}$ ) solution of methyl 3-hydroxybutanoate (1.772 g, 15.0 mmol, 1.00 eq) in 18 mL of dry THF was added in one shot, right after the enolate was formed. The reaction was left to warm to room temperature over 1h30. Then, a solution of 2 M HCl in brine was added to the solution. The aqueous phases were extracted three times with ether. The combined organic phases were washed with brine, dried over  $\text{Na}_2\text{SO}_4$ , filtered and evaporated. The crude product was purified by silica gel flash chromatography eluting with a gradient of 0-30% ethylacetate/hexanes. 3.156 g (byproduct; self-Claisen) of a colourless oil was obtained. The  $^{13}\text{C}$  NMR is in agreement with reported literature data.<sup>111</sup>  $^1\text{H}$  NMR (400 MHz,  $\text{CDCl}_3$ )  $\delta$  (ppm) 3.45 (q, 1H,  $J = 7.1$  Hz), 2.69-2.46 (m, 2H), 1.46 (s, 9H), 1.28 (d, 3H,  $J = 7.1$  Hz), 1.08 (t, 1H,  $J = 7.3$  Hz).  $^{13}\text{C}\{^1\text{H}\}$  NMR (100 MHz,  $\text{CDCl}_3$ )  $\delta$  206.6, 169.7, 81.4, 53.5, 34.5, 27.8, 12.6, 7.6. MS (ESI+)  $m/z$  187 (M+H); HRMS (ESI+)  $m/z$  calc'd for  $\text{C}_9\text{H}_{15}\text{O}_4$  [M+H] $^+$ : 187.0964; found: 187.0973.

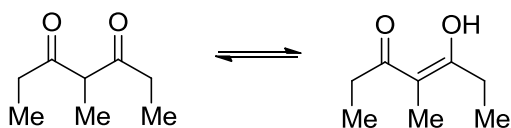


**S-Ethyl 2-methyl-3-oxopentanethioate:**  $\text{Mg}(\text{OEt})_2$  (0.286 g, 2.50 mmol) was added to a solution of 3-(ethylthio)-2-methyl-3-oxopropanoic acid (0.811 g, 5.00 mmol) in 12 mL of THF. The mixture was stirred at room temperature for 24 h. The solvent was evaporated and the salt was used as is. Propanoic acid (48  $\mu\text{L}$ , 0.65 mmol, 1.00 eq) and carbonyldiimidazole (0.116 g, 0.715 mmol, 1.10 eq) were dissolved in 2 mL of dry THF and stirred for 20 h at room temperature under argon. Then the magnesium salt of 3-(ethylthio)-2-methyl-3-oxopropanoate (0.248 g, 0.715 mmol, 1.10 eq) described above was added and the mixture was stirred for another 35 h. Then, a saturated solution of ammonium chloride was added and it was extracted three times with ether. The combined organic phases were dried over  $\text{MgSO}_4$ , filtered and evaporated. The crude product was purified by silica gel flash chromatography eluting with a gradient of 2-35% ethylacetate/hexanes. 60.5 mg (54%) of a yellow oil was obtained.  $^1\text{H}$  NMR

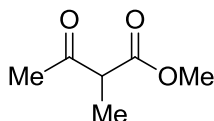
(400 MHz, CDCl<sub>3</sub>)  $\delta$  (ppm) 3.74 (q, 1H,  $J = 7.0$  Hz), 2.92 (q, 2H,  $J = 7.4$  Hz), 2.67-2.46 (m, 2H), 1.37 (d, 3H,  $J = 7.0$  Hz), 1.27 (t, 3H,  $J = 7.4$  Hz), 1.06 (t, 3H,  $J = 7.2$  Hz). <sup>13</sup>C{<sup>1</sup>H} NMR (100 MHz, CDCl<sub>3</sub>)  $\delta$  205.4, 196.9, 61.3, 34.7, 23.7, 14.5, 13.6, 7.7. MS (ESI+)  $m/z$  175 (M+H), 197 (M+Na); HRMS (ESI+)  $m/z$  calc'd for C<sub>8</sub>H<sub>14</sub>O<sub>2</sub>SNa [M+Na]<sup>+</sup>: 197.0606; found: 197.0604.



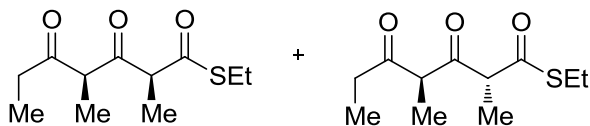
**S-Phenyl 2-methyl-3-oxopentane-1-thioate:** Mg(OEt)<sub>2</sub> (0.286 g, 2.50 mmol) was added to a solution of 3-(thiophenol)-2-methyl-3-oxopropanoic acid (1.051 g, 5.00 mmol) in 12 mL of THF. The mixture was stirred at room temperature for 24 h. The solvent was evaporated and the salt was used as is. Propanoic acid (56  $\mu$ L, 0.75 mmol, 1.00 eq) and carbonyldiimidazole (0.134 g, 0.83 mmol, 1.10 eq) were dissolved in 4.5 mL of dry THF and stirred for 18 h at room temperature under argon. Then the magnesium salt of 3-(ethylthio)-2-methyl-3-oxopropanoate (0.248 g, 0.715 mmol, 1.10 eq) described above was added and the mixture was stirred for another 24 h. Then, a saturated solution of ammonium chloride was added and it was extracted three times with ether. The combined organic phases were dried over MgSO<sub>4</sub>, filtered and evaporated. The crude product was purified by silica gel flash chromatography eluting with a gradient of 2-35% ethylacetate/hexanes. 24.5 mg (15%) of a light yellow oil was obtained. Not fully characterized in the literature. <sup>1</sup>H NMR (400 MHz, CDCl<sub>3</sub>)  $\delta$  (ppm) 7.44-7.41 (m, 5H), 3.86 (q, 1H,  $J = 7.1$  Hz), 2.71-2.51 (m, 2H), 1.45 (d, 3H,  $J = 7.1$  Hz), 1.09 (t, 3H,  $J = 7.2$  Hz). <sup>13</sup>C{<sup>1</sup>H} NMR (100 MHz, CDCl<sub>3</sub>)  $\delta$  205.2, 195.2, 134.6, 130.0, 129.5, 129.4, 127.1, 61.1, 35.0, 13.9, 7.9. MS (ESI+)  $m/z$  223 (M+H), 245 (M+Na); HRMS (ESI+)  $m/z$  calc'd for C<sub>12</sub>H<sub>15</sub>O<sub>2</sub>S [M+H]<sup>+</sup>: 223.0787; found: 223.0784.



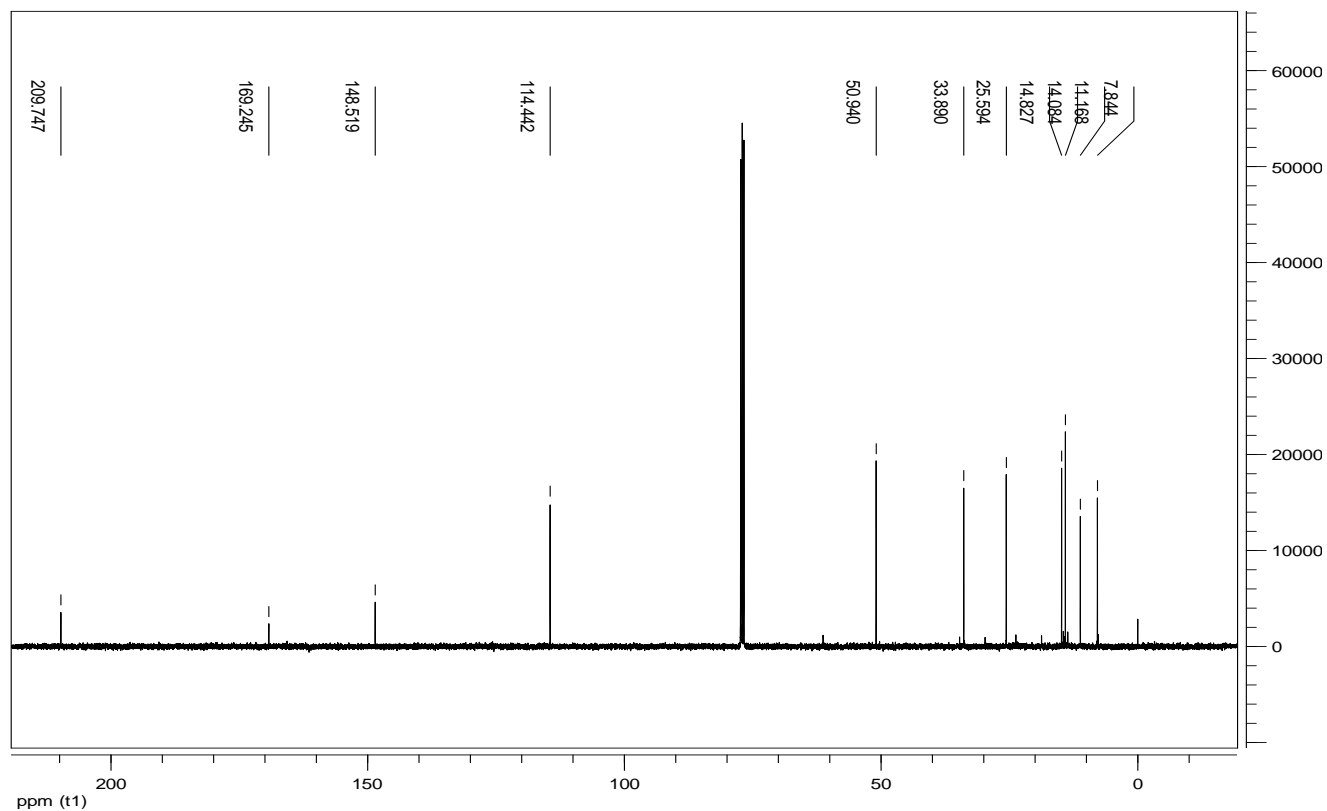
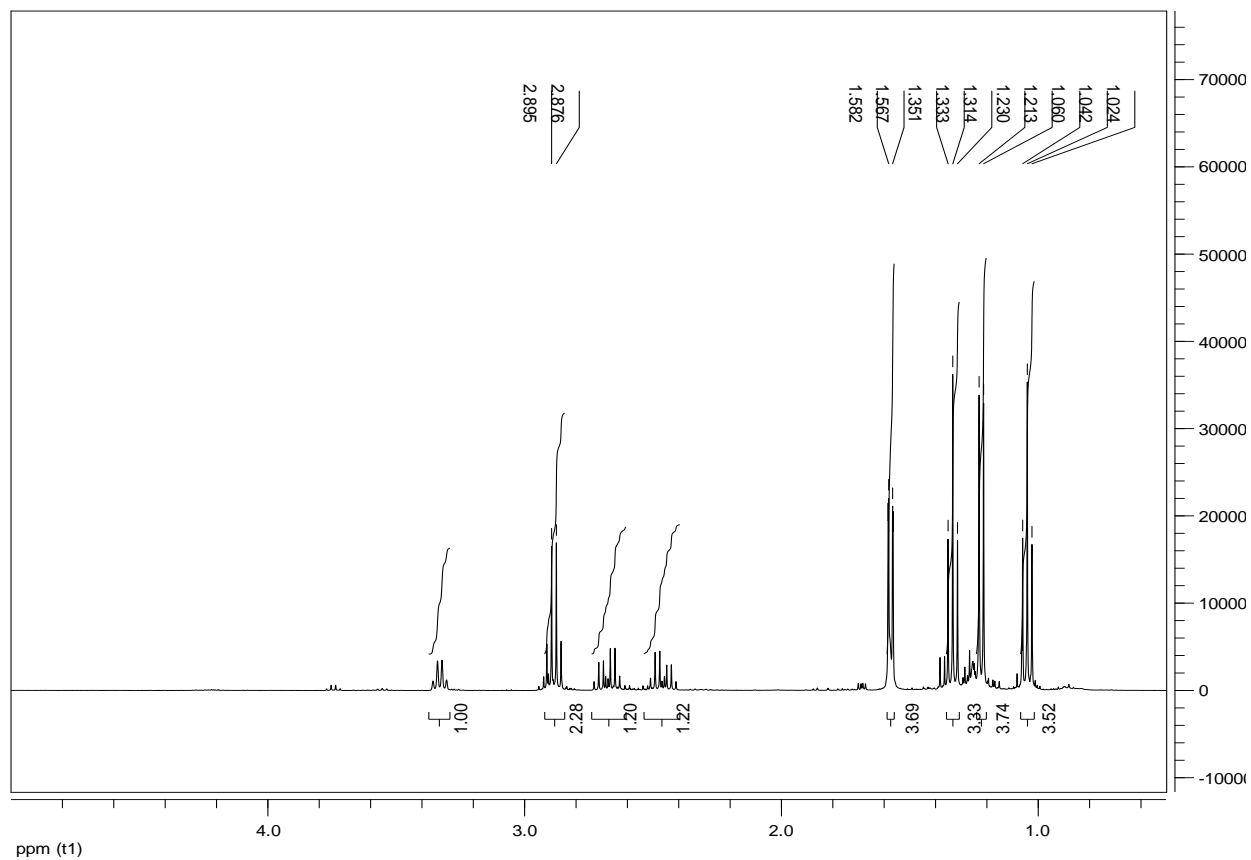
**4-Methylheptane-3,5-dione:** Sodium hydride (0.480 g, 20.0 mmol, 1.00 eq) was dissolved in 12 mL of dry ether at 0 °C. 3-pentanone (2.12 mL, 20.0 mmol, 1.00 eq) was added. After 10 mins, ethyl propanoate (2.30 mL, 20.0 mmol, 1.00 eq) was added and the solution was stirred at room temperature for 18 h. The reaction was then poured into a cold 1 M HCl solution and extracted three times with ether. The combined organic phases were dried over MgSO<sub>4</sub>, filtered and evaporated. The crude product was purified by silica gel flash chromatography eluting with a gradient of 0-10% ethylacetate/hexanes. Further purification was attempted by Kugelrohr. 0.115 g (4%) of a colourless oil was obtained. All spectral data for the diketone tautomer are in agreement with reported literature data.<sup>112</sup> Diketone to enol ratio: 6:1. For the diketone: <sup>1</sup>H NMR(400 MHz, CDCl<sub>3</sub>) δ (ppm) 3.70 (q, 1H, *J* = 7.1 Hz), 2.58-2.40 (m, 4H), 1.32 (d, 3H, *J* = 7.1 Hz), 1.05 (t, 6H, *J* = 7.2 Hz). <sup>13</sup>C{<sup>1</sup>H} NMR (100 MHz, CDCl<sub>3</sub>) δ 208.0, 60.5, 35.0, 13.1, 7.8. For the enol form: <sup>1</sup>H NMR(400 MHz, CDCl<sub>3</sub>) δ (ppm) 2.58-2.40 (m, 4H), 1.83 (s, 3H), 1.14 (t, 6H, *J* = 7.4 Hz). <sup>13</sup>C{<sup>1</sup>H} NMR (100 MHz, CDCl<sub>3</sub>) δ 193.9, 57.6, 29.4, 12.0, 9.5.

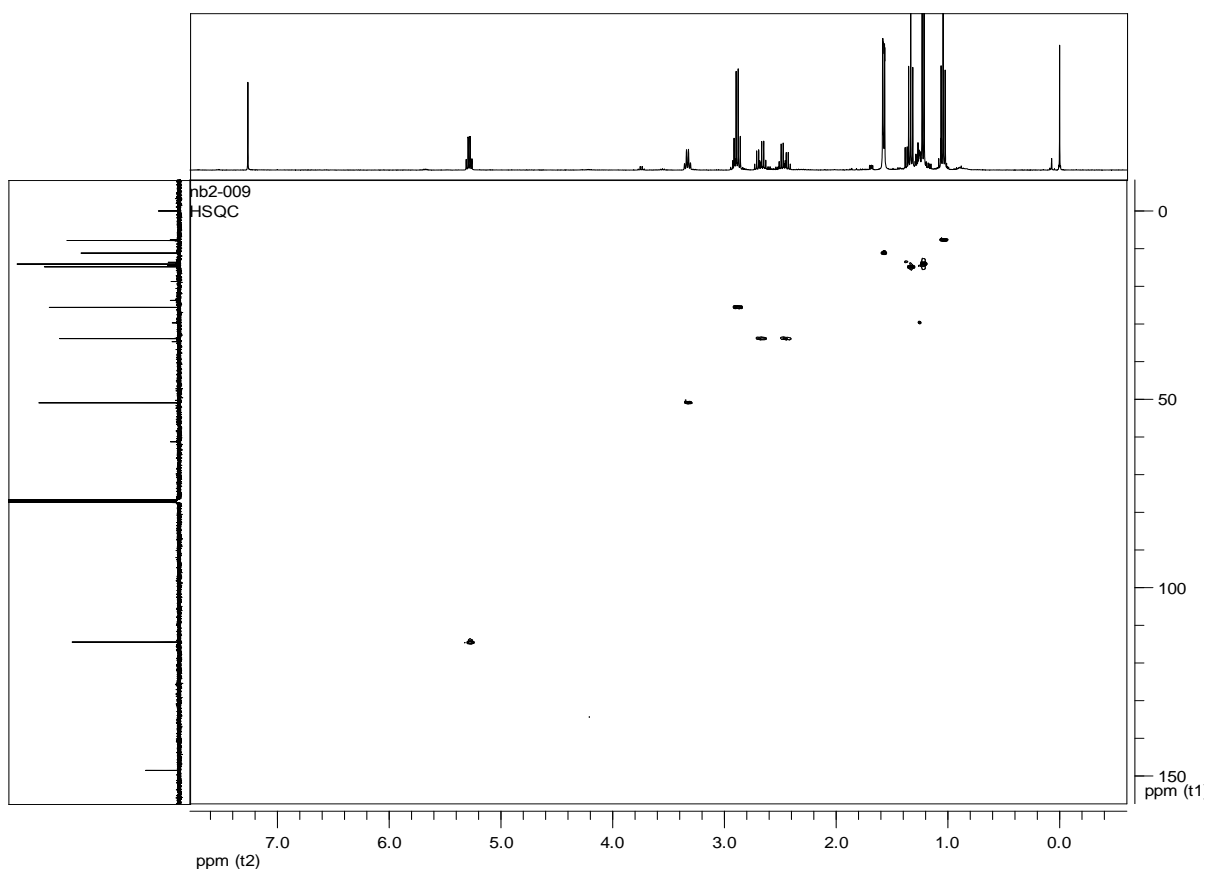
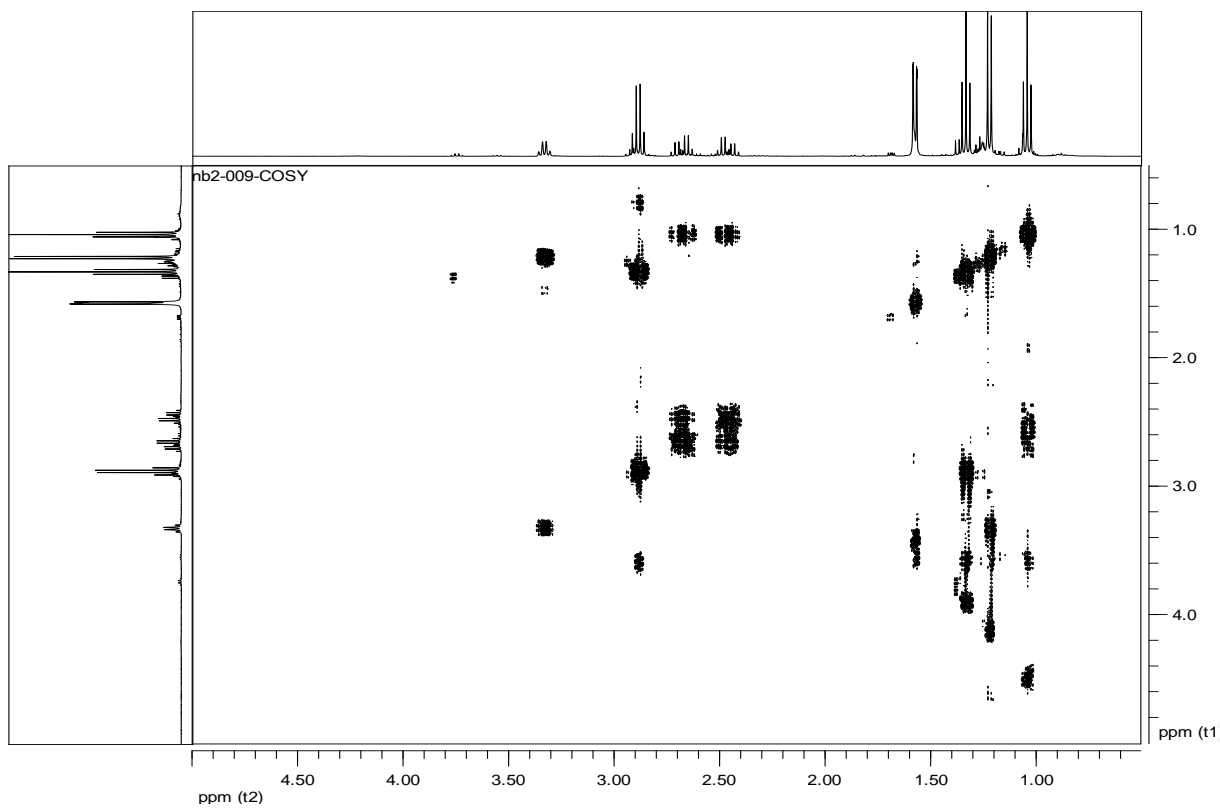


**Methyl 2-methyl-3-oxobutanoate:** In 100 mL of benzene, methyl 3-oxobutanoate (5.40 mL, 50.0 mmol, 1.00 eq) and DBU (7.47 mL, 50.0 mmol, 1.00 eq) were dissolved. Then, methyl iodide (3.11 mL, 50.0 mmol, 1.00 eq) in 50 mL of benzene was added to the solution. The resulting mixture was stirred at room temperature for 24 h. More methyl iodide was added to push the reaction to completion. Finally, the mixture was filtered under vacuum. The filtrate was washed with water, dried over MgSO<sub>4</sub>, filtered and evaporated. The crude product was purified by silica gel flash chromatography eluting with a gradient of 0-10% ethylacetate/hexanes. 1.600 g (25%) of a colourless oil was obtained. All spectral data are in agreement with reported literature data.<sup>113</sup> <sup>1</sup>H NMR (400 MHz, CDCl<sub>3</sub>) δ (ppm) 3.75 (s, 3H), 3.53 (q, 1H, *J* = 7.2 Hz), 2.25 (s, 3H), 1.36 (d, 3H, *J* = 7.2 Hz). <sup>13</sup>C{<sup>1</sup>H} NMR (100 MHz, CDCl<sub>3</sub>) δ 203.6, 171.0, 53.4, 52.4, 28.4, 12.8. MS (ESI+) *m/z* 131 (M+H), 153 (M+Na); HRMS (ESI+) *m/z* calc'd for C<sub>6</sub>H<sub>11</sub>O<sub>3</sub> [M+H]<sup>+</sup>: 131.0702; found: 131.0697.

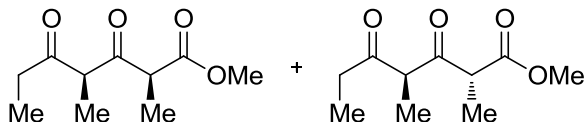


**Ethyl 2,4-dimethyl-3,5-dioxoheptanethioate:**  $\text{Mg}(\text{OEt})_2$  (0.143 g, 1.25 mmol) was added to a solution of 3-(ethylthiol)-2-methyl-3-oxopropanoic acid (1.051 g, 5.00 mmol) in 6.5 mL of THF. The mixture was stirred at room temperature for 18 h. The solvent was evaporated and the salt was used as is. Methyl diketone dimer (0.064 g, 0.568 mmol, 1.00 eq) was dissolved in 2.0 mL of dry THF and subsequently, magnesium 3-(ethylthiol)-2-methyl-3-oxopropanoate (0.217 g, 0.625 mmol, 1.10 eq) dissolved in 0.5 mL of THF was added. Then, a saturated solution of ammonium chloride was added and it was extracted three times with ether. The combined organic phases were dried over  $\text{MgSO}_4$ , filtered and evaporated. The crude product was purified by silica gel flash chromatography eluting with a gradient of 2-50% ethylacetate/hexanes. 17.3 mg (13%) of a light yellow oil was obtained. New compound characterized as a mixture of diastereomers (but only one set of peaks by  $^{13}\text{C}$  NMR). Traces of tautomers are detected.  $^1\text{H}$  NMR (400 MHz,  $\text{CDCl}_3$ )  $\delta$  (ppm) 5.28 (q, 1H,  $J = 6.8$  Hz), 3.33 (q, 1H,  $J = 7.0$  Hz), 2.89 (q, 2H,  $J = 7.4$  Hz), 2.68 (qd, 1H,  $J = 7.3$  Hz,  $J = 18.0$  Hz), 2.46 (qd, 1H,  $J = 7.2$  Hz,  $J = 18.0$  Hz), 1.57 (dd, 3H,  $J = 0.8$  Hz,  $J = 6.9$  Hz), 1.33 (t, 3H,  $J = 7.4$  Hz), 1.22 (d, 3H,  $J = 7.0$  Hz), 1.04 (t, 3H,  $J = 7.3$  Hz).  $^{13}\text{C}\{^1\text{H}\}$  NMR (100 MHz,  $\text{CDCl}_3$ )  $\delta$  209.7, 169.2, 148.5, 114.4, 50.9, 33.9, 25.6, 14.8, 14.1, 11.2, 7.8. MS (ESI+)  $m/z$  231 (M+H), 253 (M+Na) (2 distinct peaks by GCMS); HRMS (ESI+)  $m/z$  calc'd for  $\text{C}_{11}\text{H}_{19}\text{O}_3\text{S}$  [M+H] $^+$ : 231.1049; found: 231.1057.

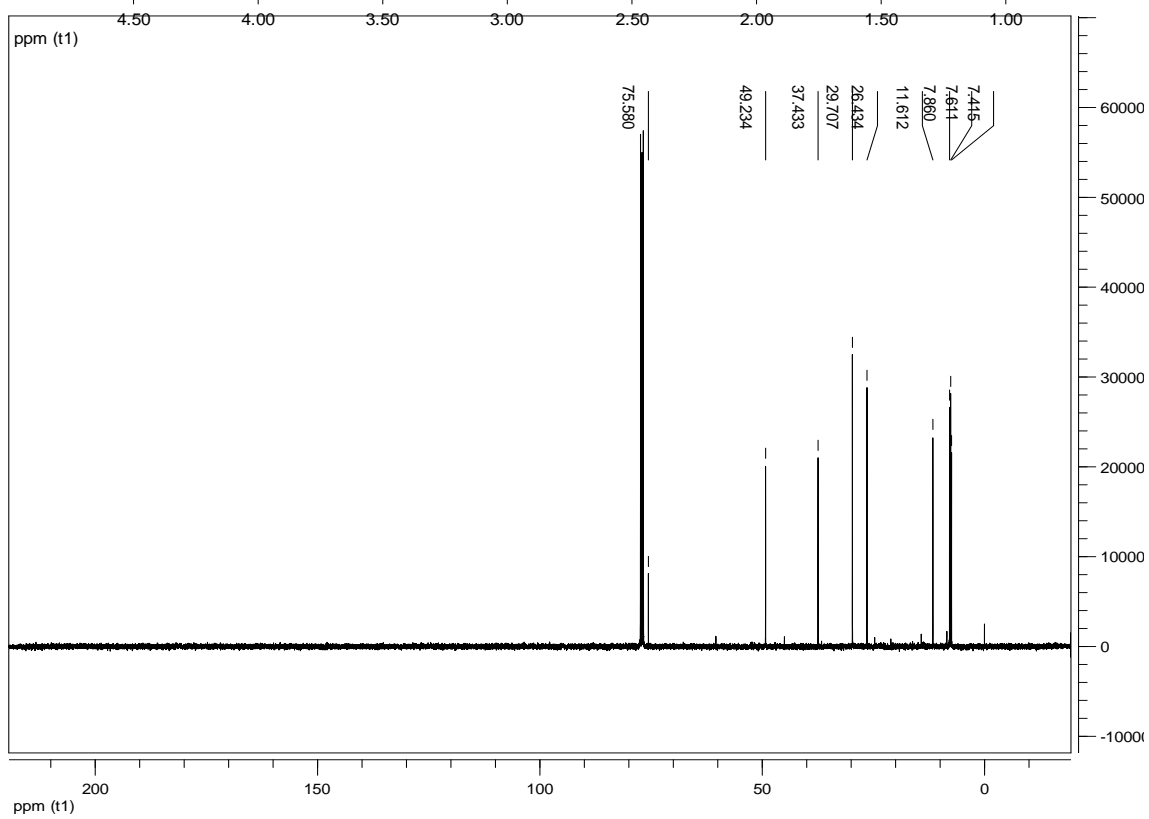
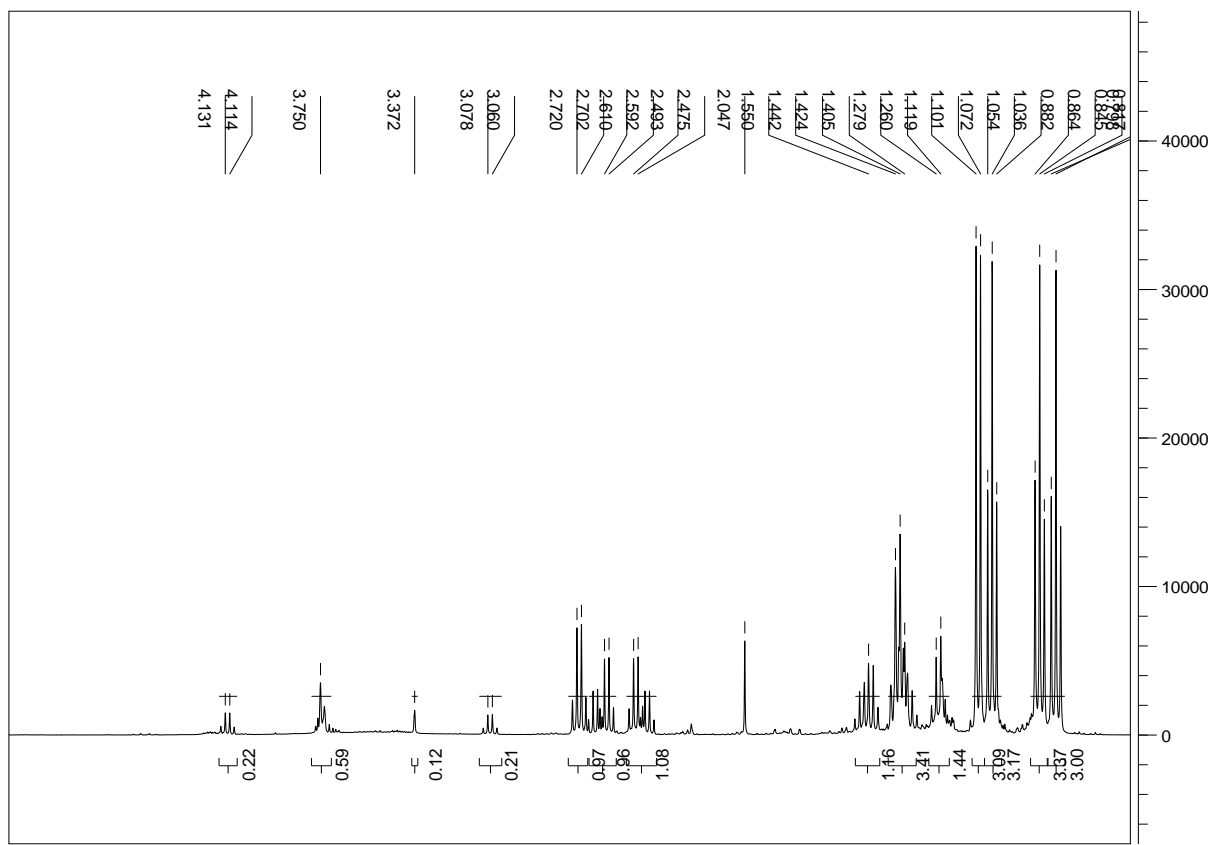


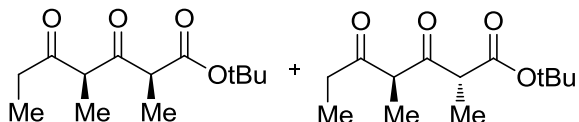




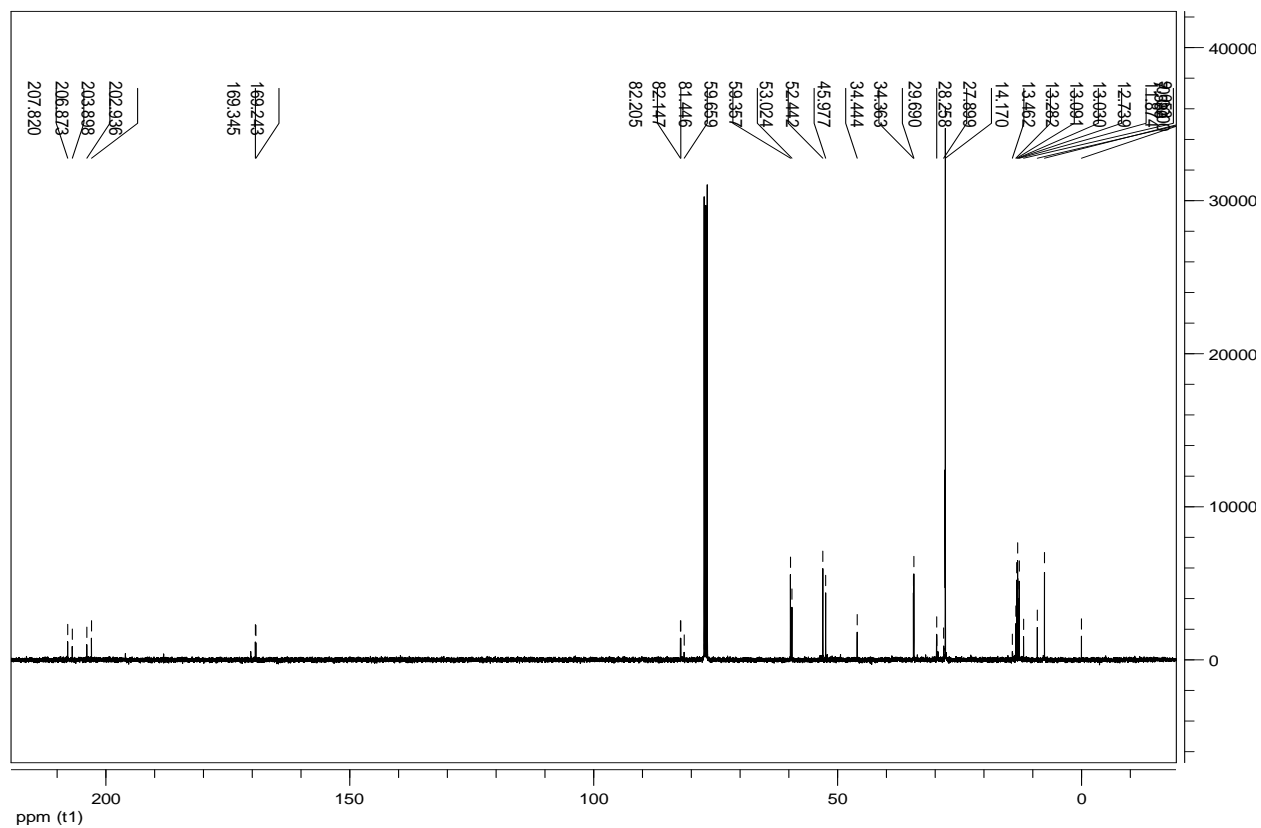
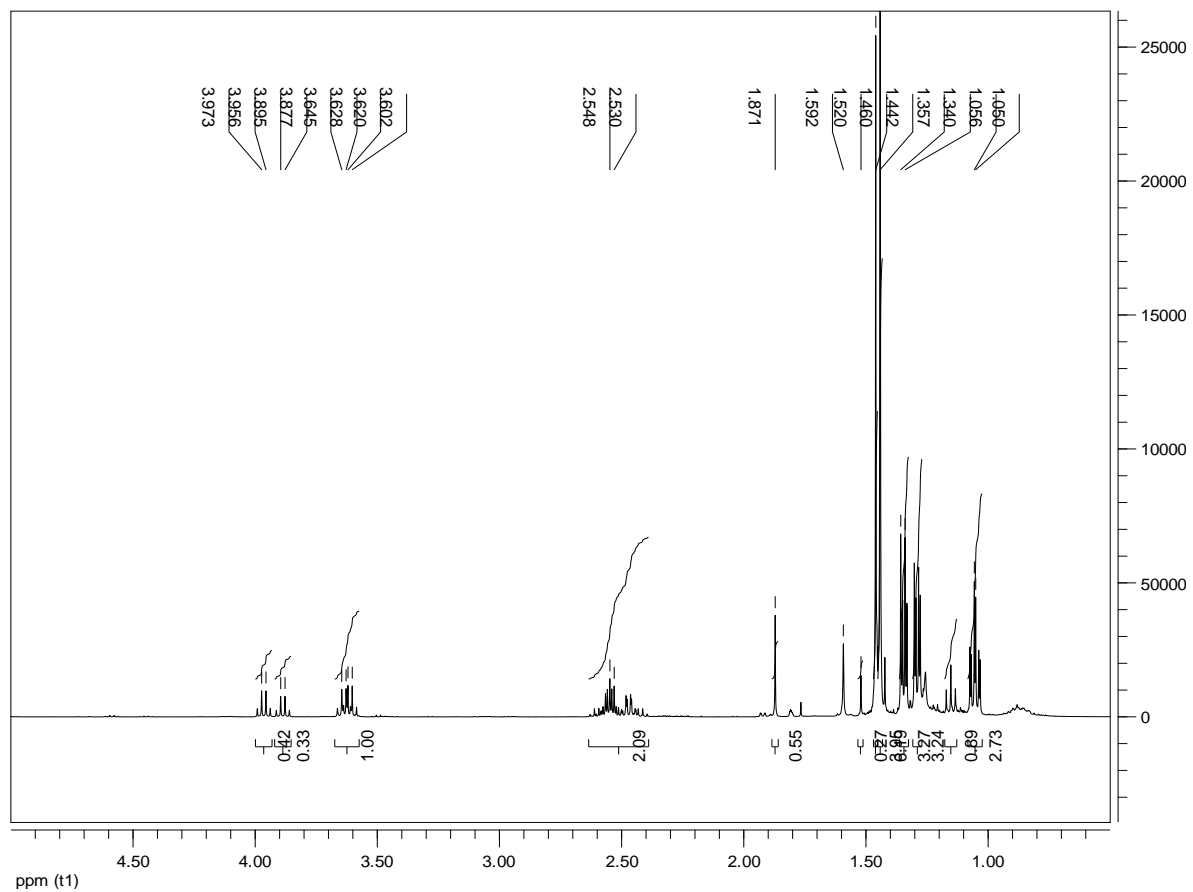


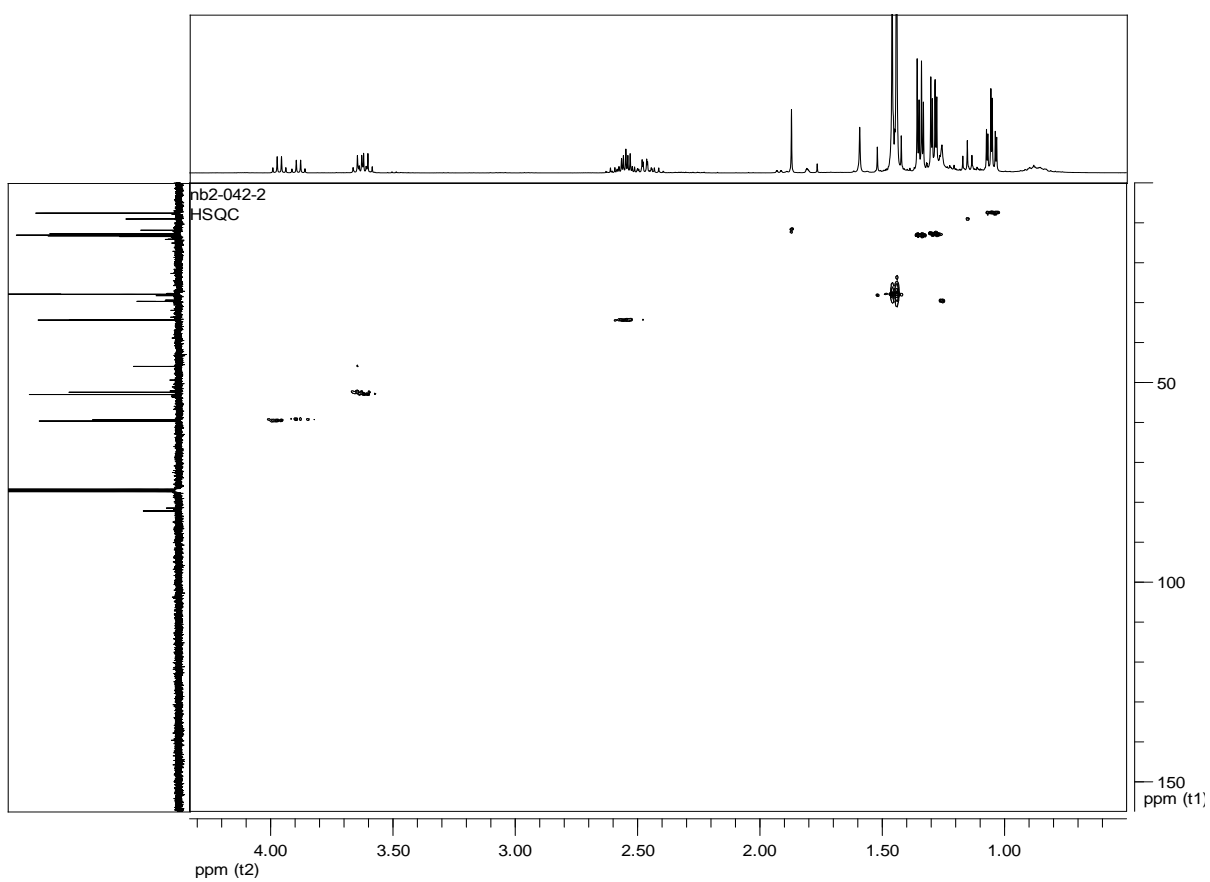
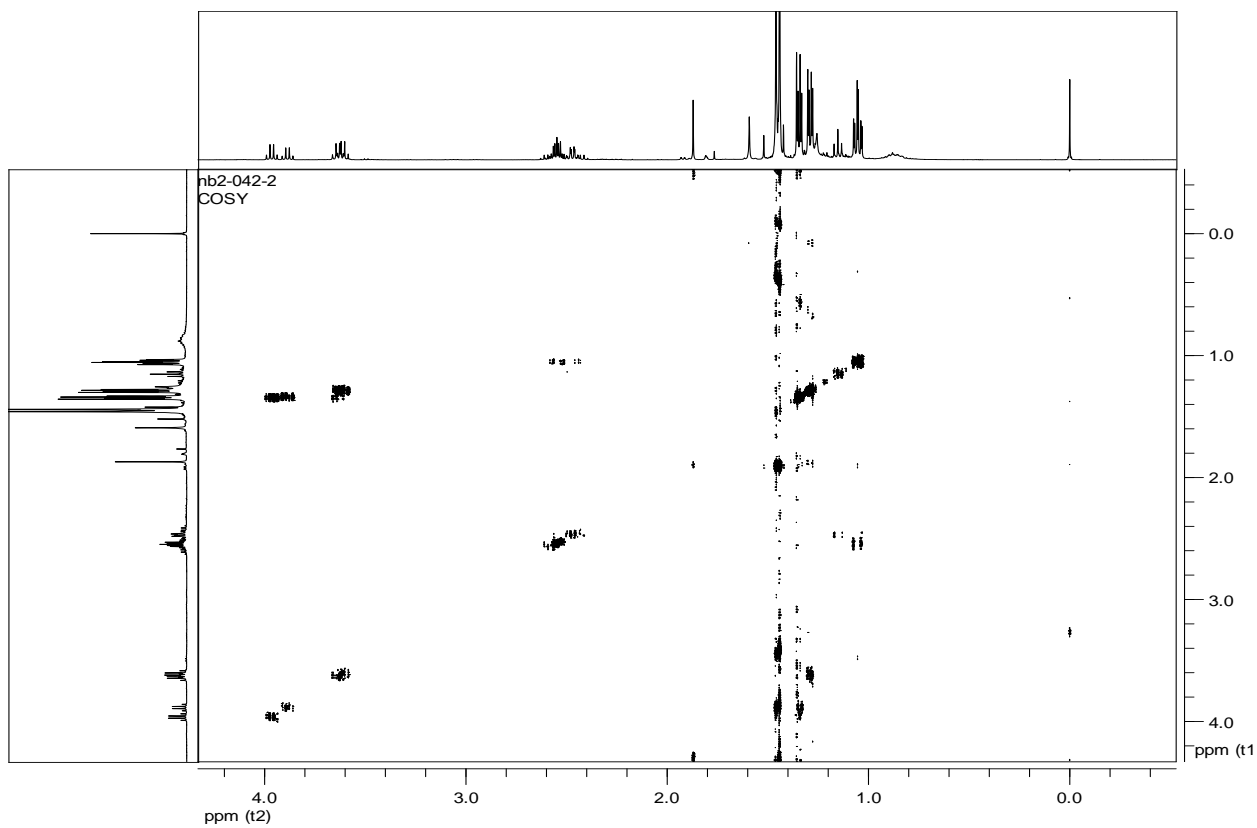
**Ethyl 2,4-dimethyl-3,5-dioxoheptanoate:** 3-methoxy-2-methyl-3-oxopropanoic acid (0.900 g, 6.8 mmol, 1.00 eq) was dissolved in 60 mL of dry DCM. DMF (52  $\mu$ L, 0.68 mmol, 2.00 eq) was added via pipette and the solution was purged with argon and cooled to 0 °C. Then, while monitoring the evolution of gas, oxalyl chloride (1.17 mL, 13.6 mmol, 2.00 eq) was slowly added. The mixture was stirred at 0 °C and warmed to room temperature until the gas ceased to evolve. The mixture was then concentrated under vacuum and used as is. 3-pentanone (0.21 mL, 2.0 mmol, 2.00 eq) was dissolved in 1 mL of dry THF and then lithium hexamethyldisilyl (1.9 mL of a 1M solution in hexanes, 1.9 mmol, 1.90 eq) was added at -78 °C under argon. After stirring for 30 mins at -78 °C, the acyl chloride made above (0.157 g, 1.0 mmol, 1.00 eq) dissolved in 1 mL of THF was added to the reaction and it was stirred at -78 °C for 30 mins and then slowly warmed to room temperature. The reaction was left to stir for 16 h. Then, the reaction mixture was diluted in ether and washed with a saturated solution of ammonium chloride. The aqueous phase was extracted three times with ether and the combined organic phases were dried over MgSO<sub>4</sub>, filtered and evaporated. The crude product was purified by silica gel flash chromatography eluting with a gradient of 0-100% ethylacetate/hexanes and drops of triethylamine. 39.5 mg (20%) of a light yellow oil was obtained. New compound characterized as a mixture of diastereomers. Important amounts of tautomers are present. <sup>1</sup>H NMR (400 MHz, CDCl<sub>3</sub>) see spectrum. <sup>13</sup>C{<sup>1</sup>H} NMR (100 MHz, CDCl<sub>3</sub>) see spectrum.

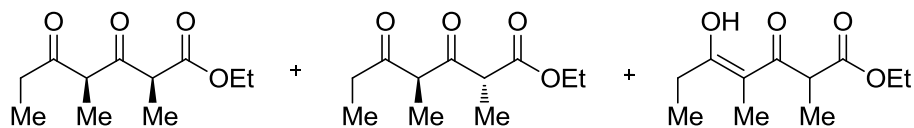




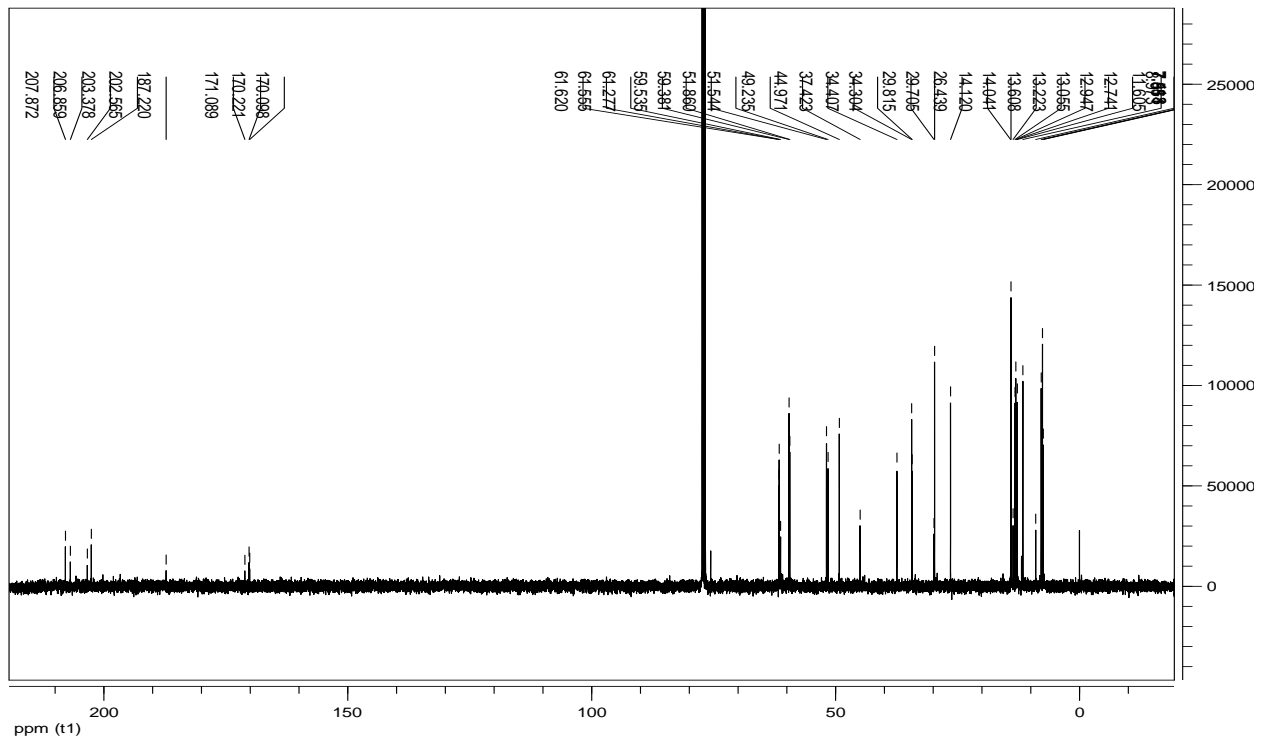
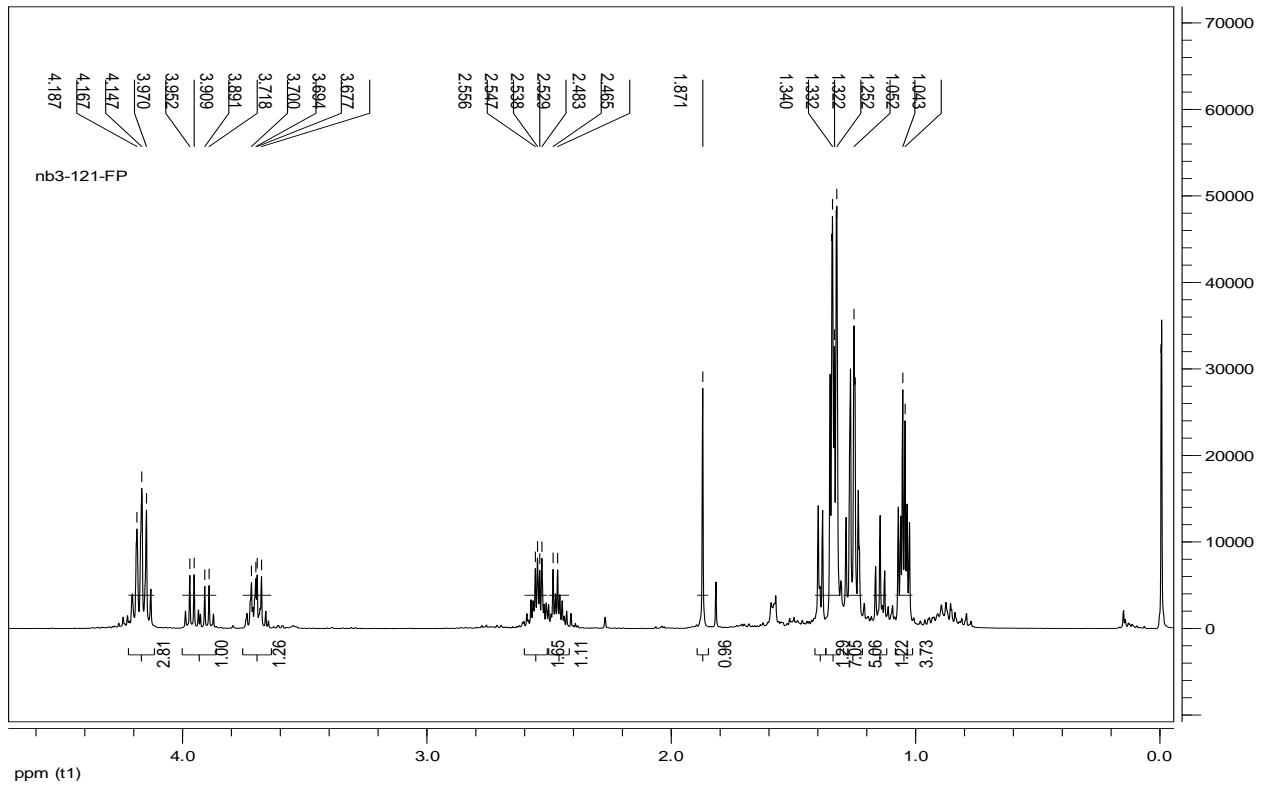
**tert-Butyl 2,4-dimethyl-3,5-dioxoheptanoate:** In a flame dried flask, sodium hydride (48 mg, 1.2 mmol, 1.20 eq) was dissolved in 2 mL of dry THF at 0 °C. tert-butyl 2-methyl-3-oxopentanoate (186 mg, 1.0 mmol, 1.00 eq) was slowly added dropwise.. The colourless solution was stirred for 15 mins at 0 °C. *n*-Butyl lithium (0.47 mL of a 2.36 M solution in hexanes, 1.1 mmol, 1.10 eq) was added and the light yellow solution was stirred for 20 mins at 0 °C and warmed to room temperature. The reaction was then cooled in a dry ice-bath and then methyl propanoate (0.11 mL, 1.1 mmol, 1.10 eq) was added in one shot and subsequently stirred for 5 mins at -60 °C and then for another 3 h at room temperature. Then, 1 mL of water was added to quench the reaction. It was extracted with ether and washed with a saturated solution of NaHCO<sub>3</sub>. The aqueous phase was extracted with ether three times and the combined organic phases were washed with brine, dried over MgSO<sub>4</sub>, filtered and evaporated. The crude product was purified by silica gel flash chromatography eluting with a gradient of 0-20% ethylacetate/hexanes. 38.4 mg (16%) of a light yellow oil was obtained. New compound characterized as a mixture of diastereomers. Traces of tautomers are present.. <sup>1</sup>H NMR (400 MHz, CDCl<sub>3</sub>) see spectrum. <sup>13</sup>C{<sup>1</sup>H} NMR (100 MHz, CDCl<sub>3</sub>) see spectrum. MS (ESI+) *m/z* 265 (M+Na); HRMS (ES+) *m/z* calc'd for C<sub>13</sub>H<sub>22</sub>O<sub>4</sub>Na [M+Na]<sup>+</sup>: 265.1410; found: 265.1412.

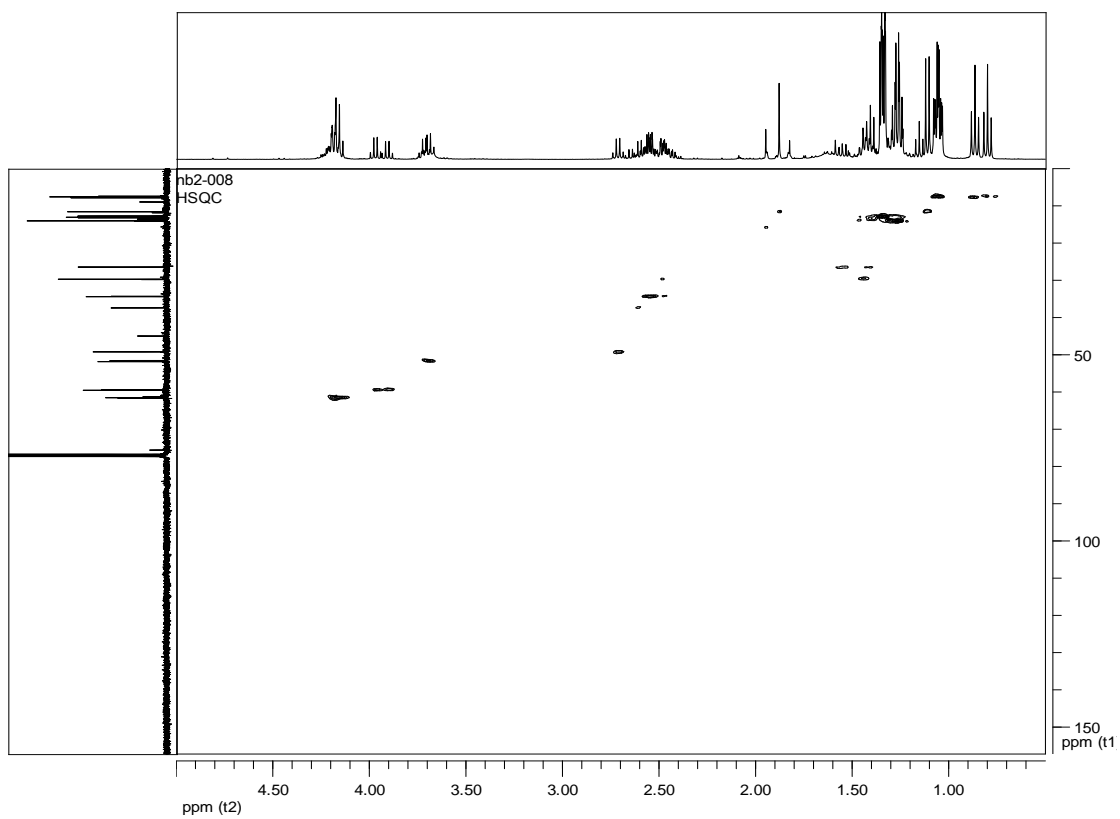
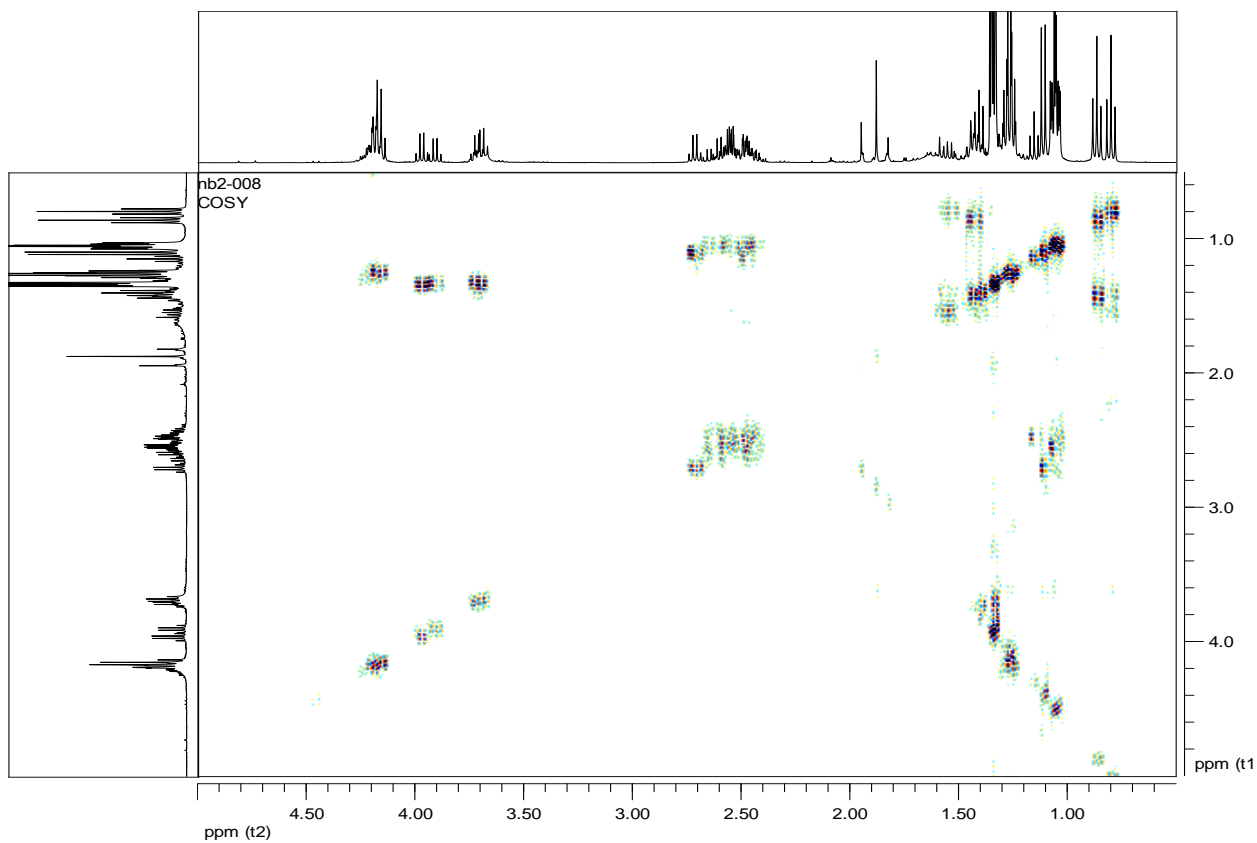




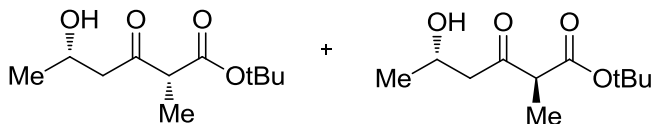


**Ethyl 2,4-dimethyl-3,5-dioxoheptanoate (3):** In a flame dried flask, 3-ethoxy-2-methyl-3-oxopropanoic acid (0.438 g, 3.0 mmol) was dissolved in 0.44 mL of  $\text{SOCl}_2$  and stirred at  $40\text{ }^\circ\text{C}$  for 4 h.<sup>114</sup> The excess  $\text{SOCl}_2$  was removed under vacuum and the obtained yellow liquid was used as is. 3-pentanone (0.64 mL, 6.0 mmol) was dissolved in 5 mL of dry THF and then lithium hexamethyldisilyzide (5.7 mL of a 1M solution in hexanes, 5.7 mmol) was added at  $-78\text{ }^\circ\text{C}$  under argon. After stirring for 30 mins at  $-78\text{ }^\circ\text{C}$ , the crude acyl chloride (0.427 g, 2.6 mmol) dissolved in 3 mL of dry THF was added dropwise via a small cannula to the reaction and it was stirred at  $-78\text{ }^\circ\text{C}$  for 90 mins and then quenched with sat.  $\text{NH}_4\text{Cl}_{(\text{aq})}$  at  $-78\text{ }^\circ\text{C}$ . Then, the reaction mixture was diluted in ether and washed with sat.  $\text{NH}_4\text{Cl}_{(\text{aq})}$  and then with water. The aqueous phase was extracted three times with ether and the combined organic phases were dried over  $\text{Na}_2\text{SO}_4$ , filtered and evaporated. The crude product was purified by silica gel flash chromatography eluting with a gradient of 10-20% ethylacetate/hexanes. 0.326 g (59%) of a clear oil was obtained. New compound characterized as a mixture of diastereomers.  $^1\text{H NMR}$  (400 MHz,  $\text{CDCl}_3$ ) see spectra. **MS** (ESI+)  $m/z$  215 (M+H), 237 (M+Na); **HRMS** (ESI+)  $m/z$  calc'd for  $\text{C}_{11}\text{H}_{19}\text{O}_4$  [M+H]<sup>+</sup>: 215.1277; found: 215.1287.

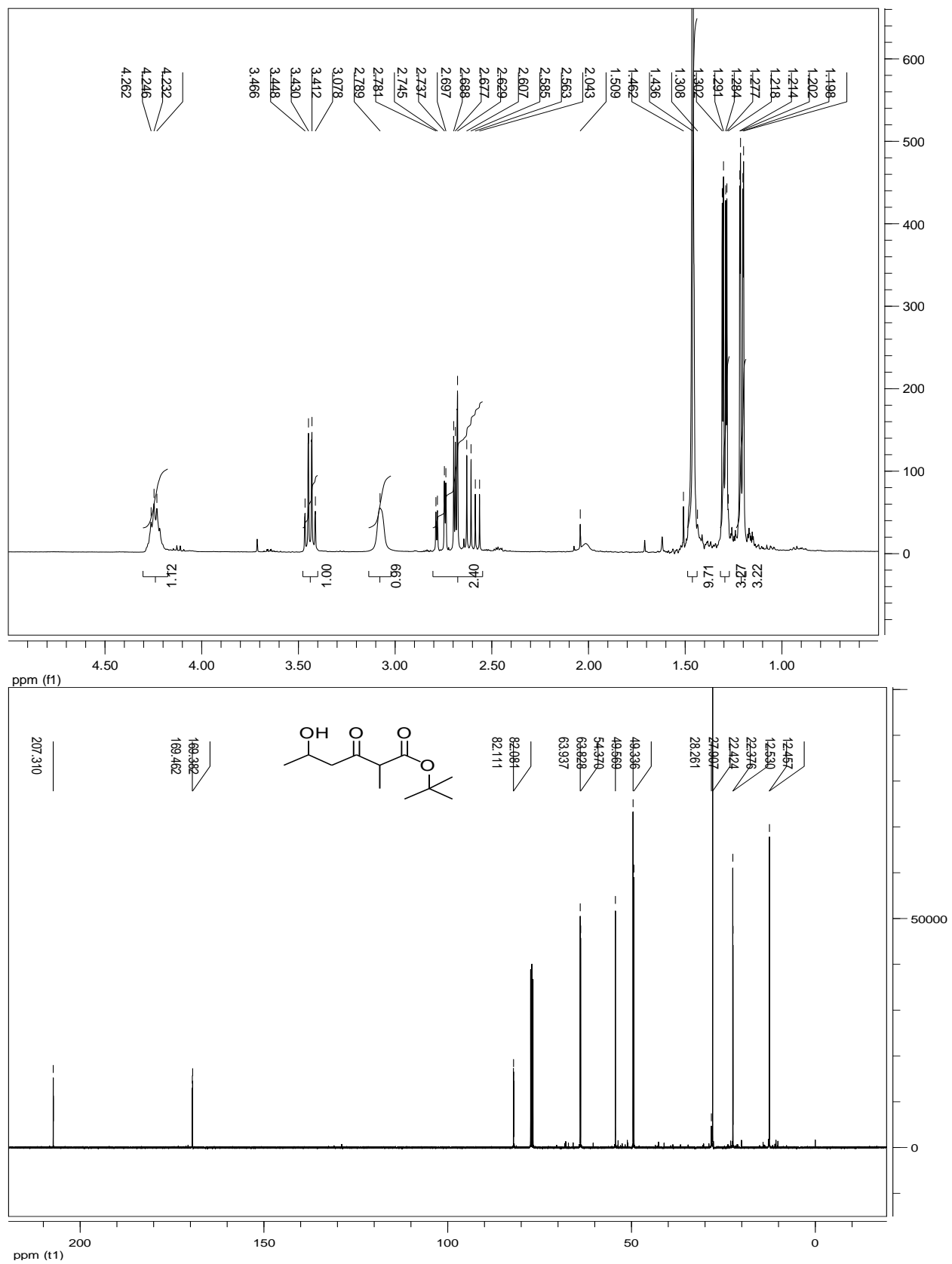


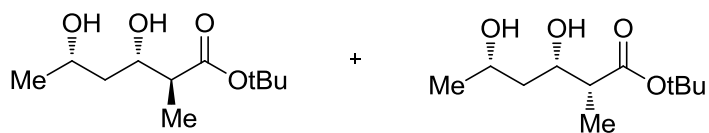
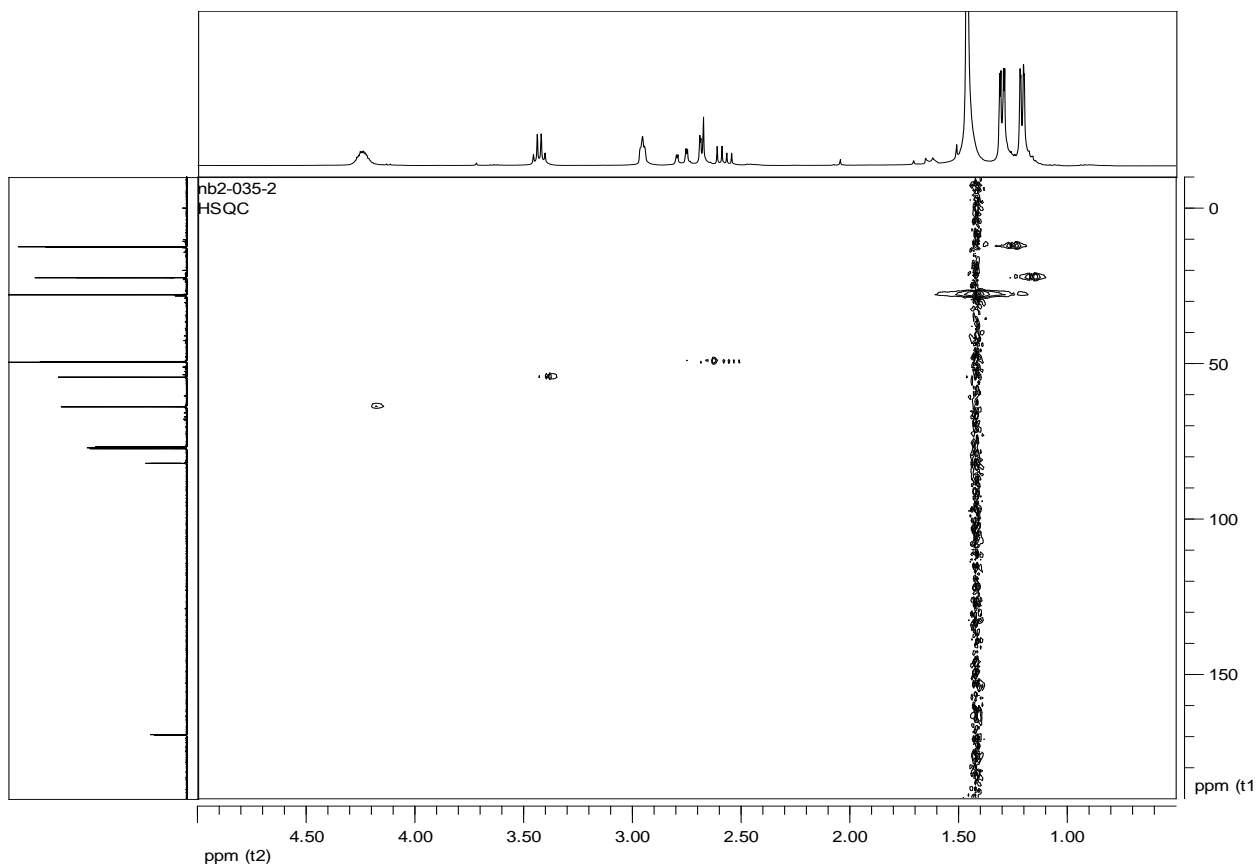






**tert-Butyl 5-hydroxy-2-methyl-3-oxohexanoate:** In a flame-dried flask, diisopropylethylamine (9.04 mL, 64.5 mmol, 4.30 eq) was dissolved in 67 mL of dry THF. The solution was cooled to 0 °C and *n*-butyl lithium (53.5 mL of a 1.206 M solution in hexanes, 64.5 mmol, 4.30 eq) was added dropwise. An argon balloon was installed and the reaction was cooled to -79 °C. *t*-butyl propionate (7.24 mL, 48.0 mmol, 3.20 eq) was added dropwise to the LDA solution. A precooled (at -70 °C) solution of methyl 3-hydroxybutanoate (1.772 g, 15.0 mmol, 1.00 eq) in 18 mL of dry THF was added rapidly, right after the enolate was formed. The reaction was left to warm to room temperature over 90 mins. Then, a solution of 2 M HCl in brine was added to the solution. The aqueous phases were extracted three times with ether. The combined organic phases were washed with brine, dried over Na<sub>2</sub>SO<sub>4</sub>, filtered and evaporated. The crude product was purified by silica gel flash chromatography eluting with a gradient of 0-30% ethylacetate/hexanes. 1.113 g (34%) of a light yellow oil was obtained. The <sup>13</sup>C NMR is in agreement with reported literature data.<sup>115</sup> Compound characterized as a mixture of diastereomers (1:1). <sup>1</sup>H NMR (400 MHz, CDCl<sub>3</sub>) δ (ppm) 4.28-4.21 (m, 1H), 3.44 (q, 1H, *J* = 7.1 Hz), 3.08 (br s, 1H), 2.79-2.56 (m, 2H), 1.46 (s, 9H), 1.30 (2 overlapping d, 3H, *J* = 7.1 Hz), 1.21 (2 overlapping d, 3H, *J* = 6.3 Hz). <sup>13</sup>C{<sup>1</sup>H} NMR (100 MHz, CDCl<sub>3</sub>) δ 207.3, 169.5, 169.4, 82.1, 82.0, 63.9, 63.8, 54.4, 49.6, 49.3, 28.3, 27.9, 22.4, 22.4, 12.5, 12.4. MS (ESI+) *m/z* 217 (M+H), 239 (M+Na); HRMS (ESI+) *m/z* calc'd for C<sub>11</sub>H<sub>20</sub>O<sub>4</sub>Na [M+Na]<sup>+</sup>: 239.1253; found: 239.1261.

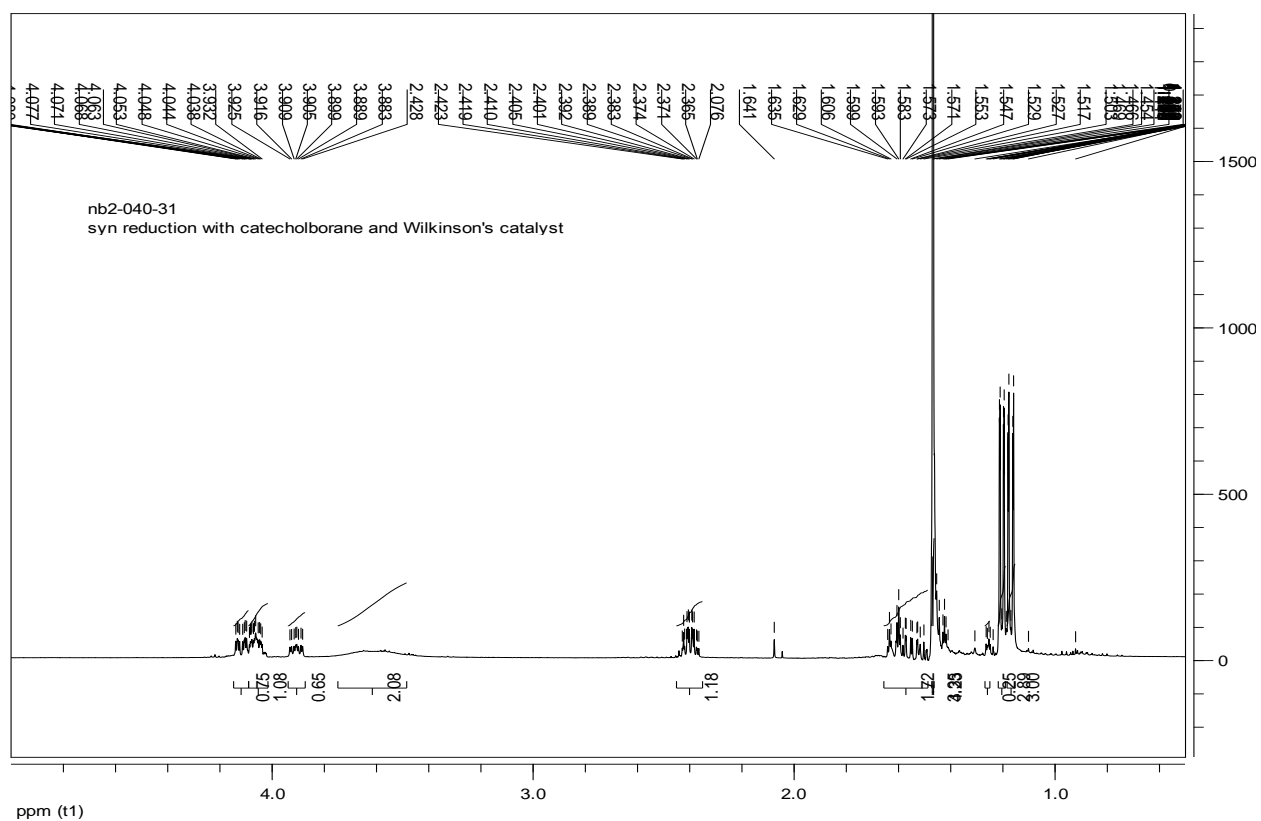


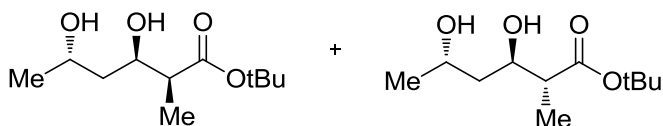
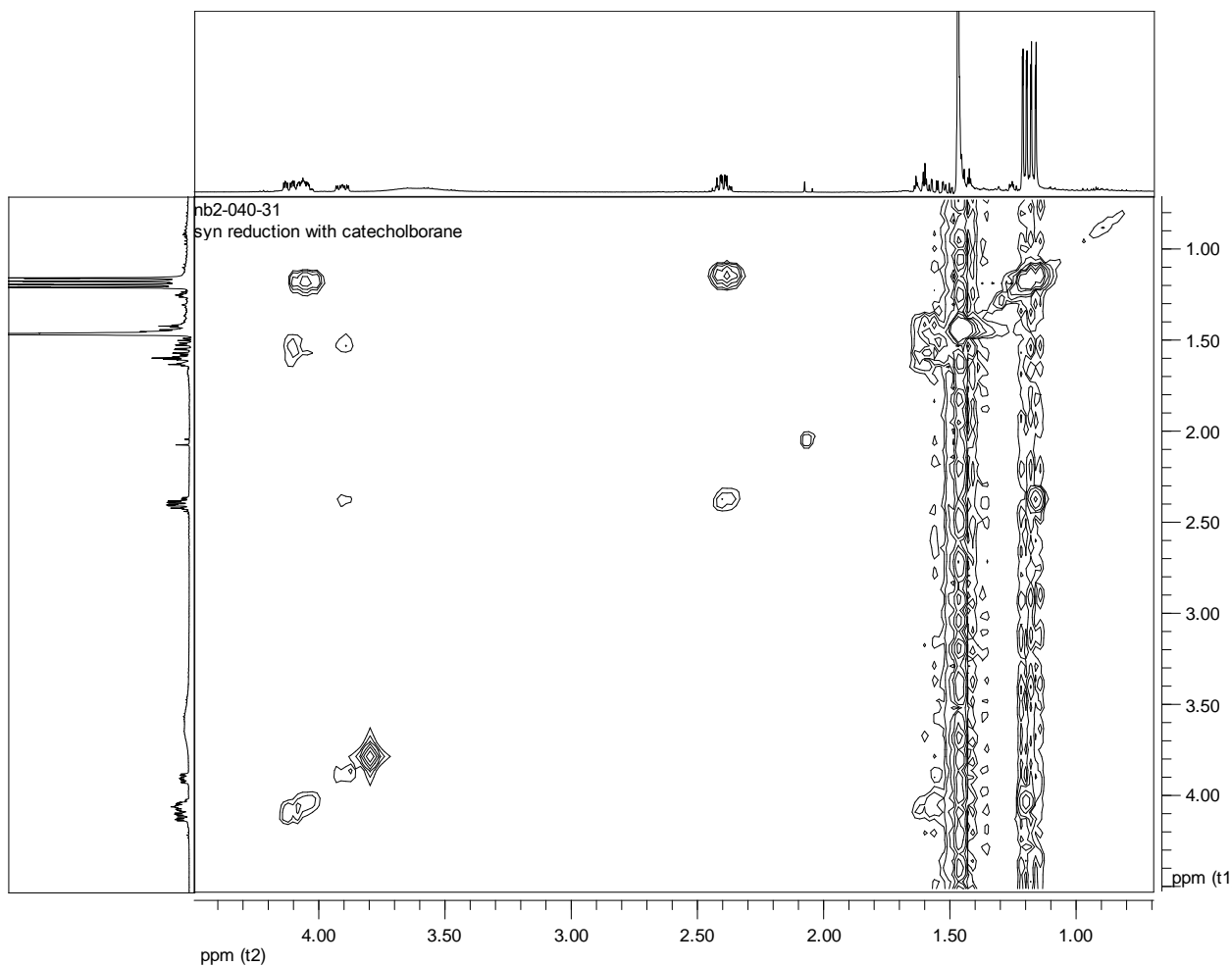


**(3S,5S)-tert-Butyl 3,5-dihydroxy-2-methylhexanoate:** In a flame-dried flask, tert-butyl 5-hydroxy-2-methyl-3-oxohexanoate (21.6 mg, 0.10 mmol, 1.00 eq) was dissolved in 0.8 mL of dry THF and in 0.2 mL of methanol. The solution was cooled to  $-78\text{ }^{\circ}\text{C}$  and diethylmethoxyborane (14.5  $\mu\text{L}$ , 0.11 mmol, 1.10 eq) was added dropwise. The resulting mixture was stirred for 20 mins. To this cloudy solution, sodium borohydride (4.2 mg, 0.11 mmol, 1.10 eq) was added slowly over 5 mins. The resulting suspension was stirred for 4 h at  $-78\text{ }^{\circ}\text{C}$ . 0.1 mL of acetic acid was added to quench the reaction. The solution was diluted in ethylacetate and washed with a solution of  $\text{NaHCO}_3$ . The aqueous phase was extracted three times with ethylacetate and the combined organic phases were washed with brine, dried over  $\text{Na}_2\text{SO}_3$ , filtered and evaporated. The crude mixture was purified by preparative TLC eluting with 20%

ethylacetate/hexanes. 3.4 mg (16%) of a light yellow oil was obtained. New syn-diol compound characterized as a mixture of diastereomers.  $^1\text{H NMR}$  (400 MHz,  $\text{CDCl}_3$ ) see spectrum .

$^{13}\text{C}\{^1\text{H}\}$  NMR (100 MHz,  $\text{CDCl}_3$ ) see spectrum. 10.8 mg (33%); 1:1 ratio of syn diastereomers; 12:1 dr for syn:anti. **MS** (ESI+)  $m/z$  241 ( $\text{M}+\text{Na}$ ); **HRMS** (ESI+)  $m/z$  calc'd for  $\text{C}_{11}\text{H}_{22}\text{O}_4\text{Na}$   $[\text{M}+\text{Na}]^+$ : 241.1410; found: 241.1412.

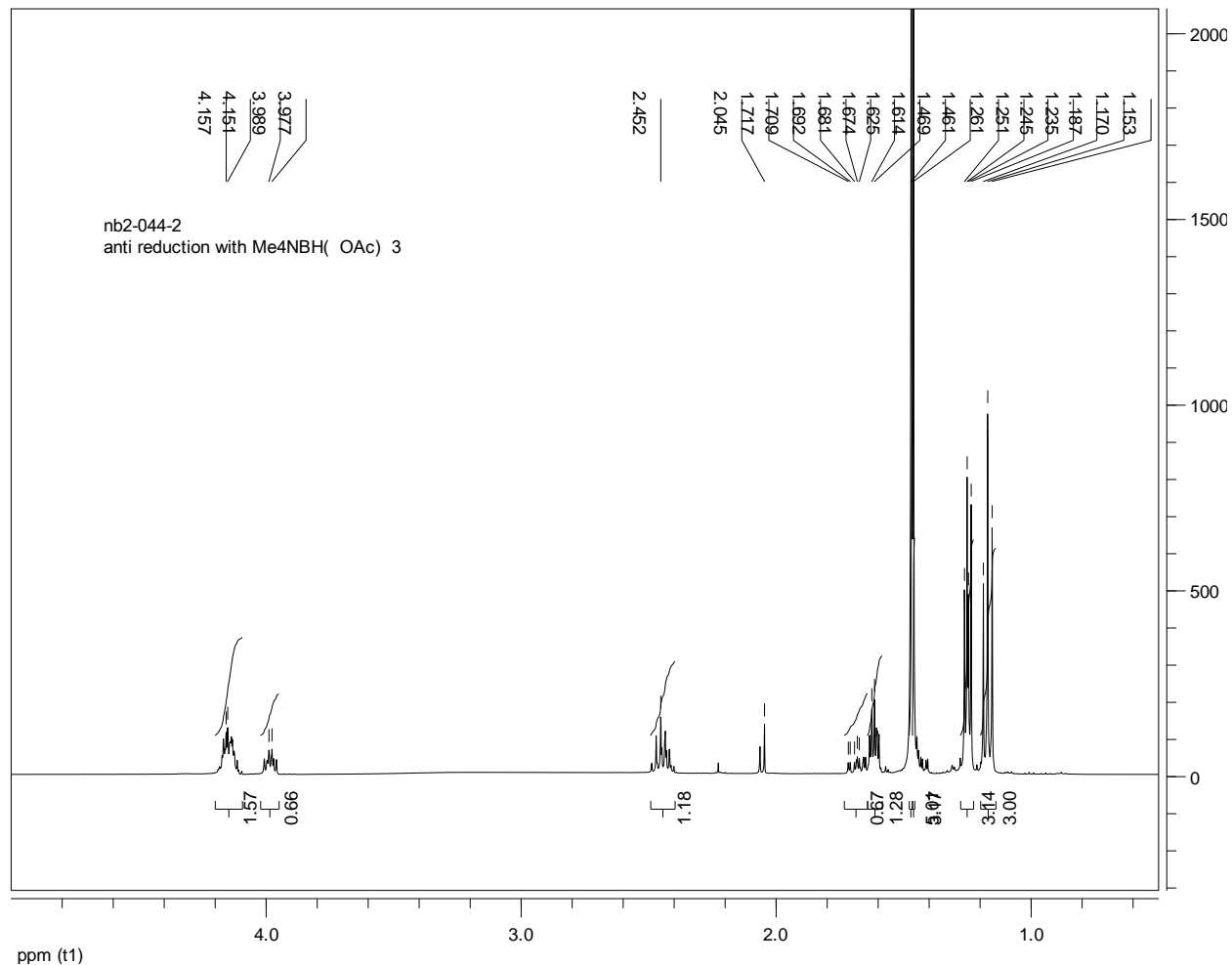


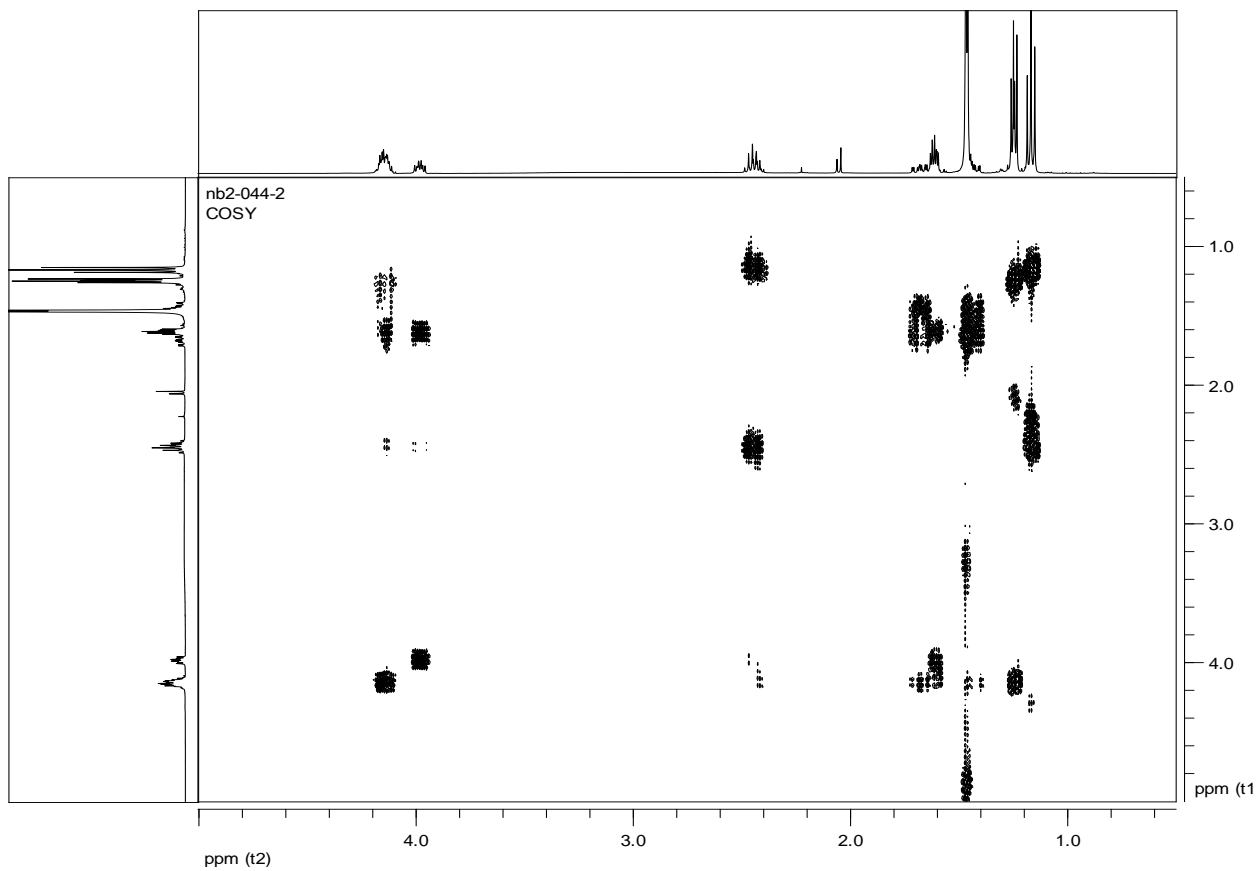
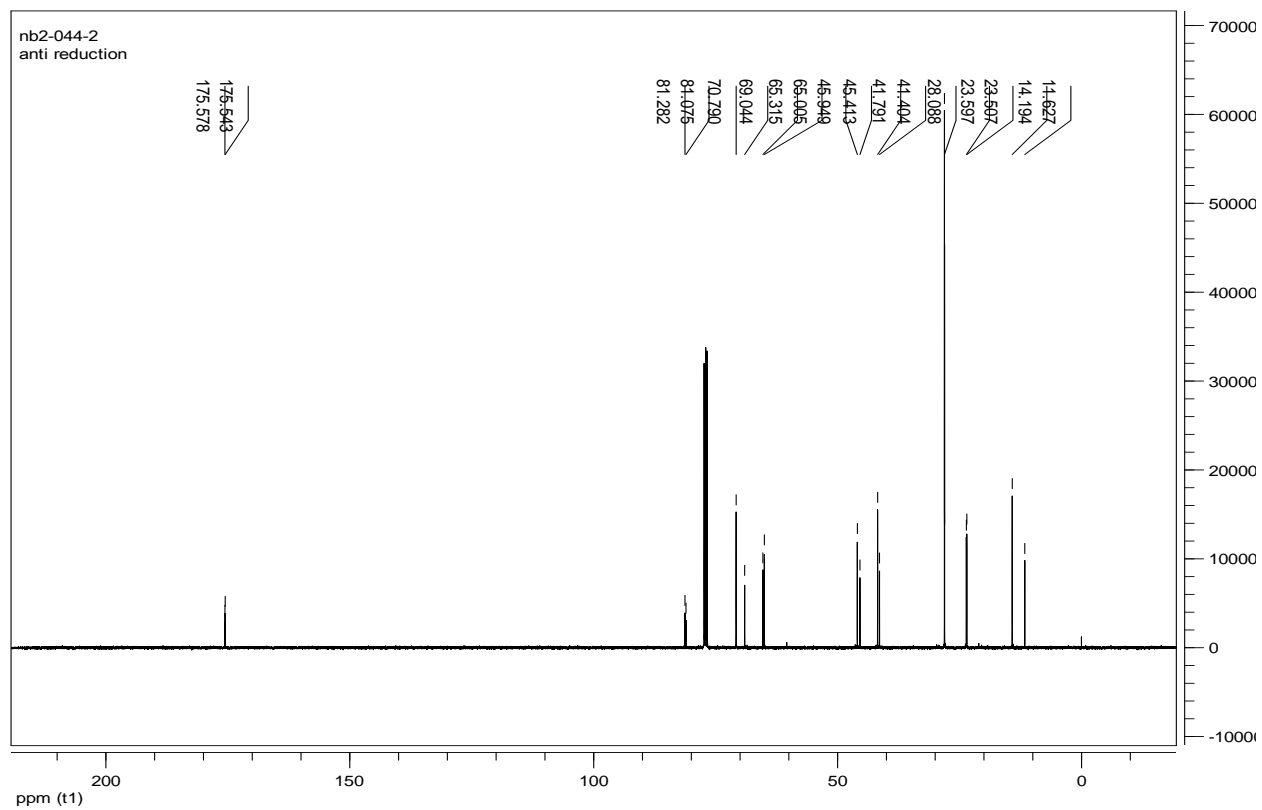


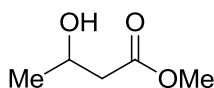
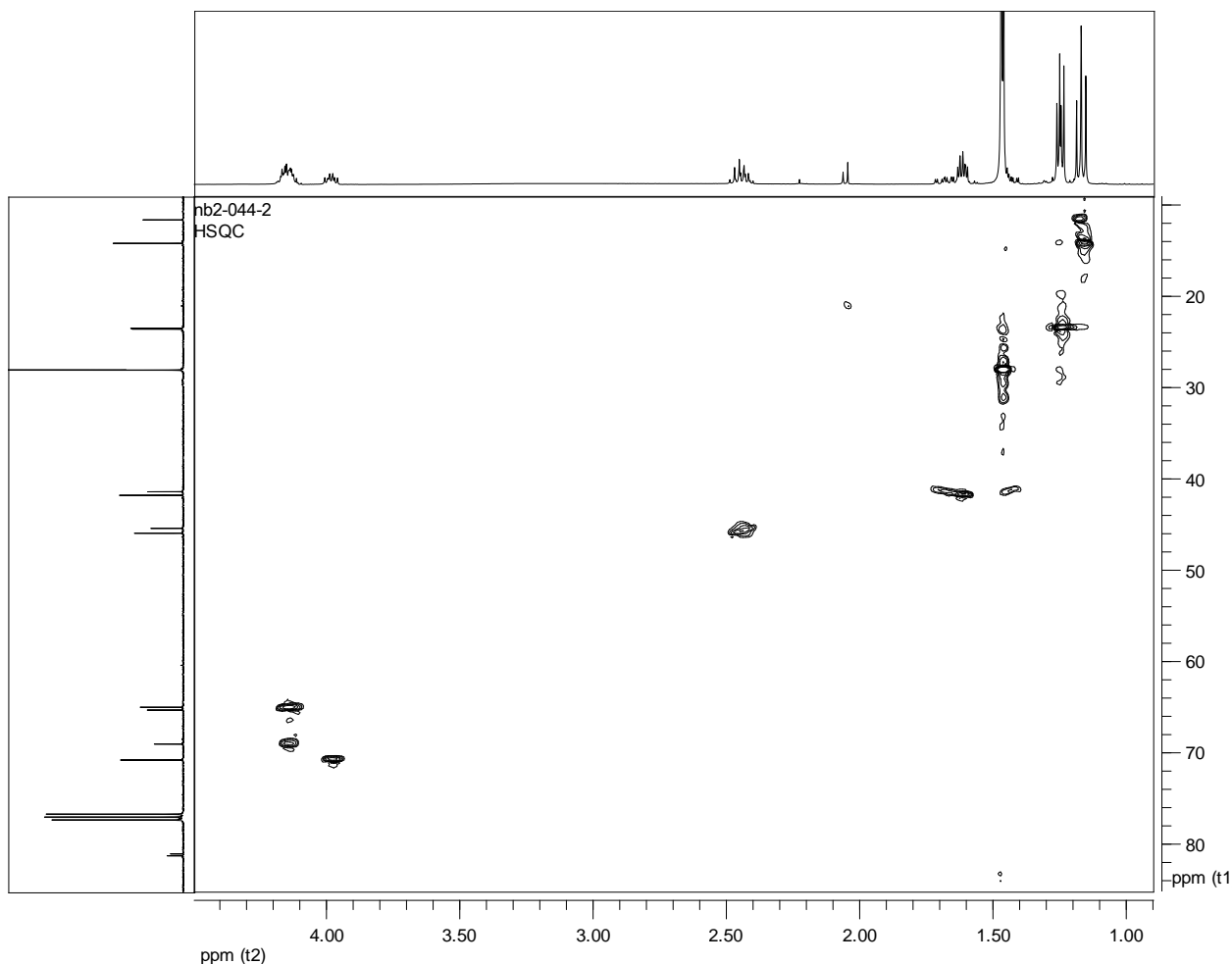
**(3R,5S)-*tert*-Butyl 3,5-dihydroxy-2-methylhexanoate:** In a flame-dried flask, to a solution of tetramethylammonium triacetoxyborohydride (0.316 g, 1.2 mmol, 8.00 eq) in 0.7 mL of dry MeCN was added acetic acid (0.66 mL, 11.6 mmol, 77 eq). This mixture was cooled to  $-40\text{ }^{\circ}\text{C}$  (using the Julabo) and *tert*-butyl 5-hydroxy-2-methyl-3-oxohexanoate (32.4 mg, 0.15 mmol, 1.00 eq) dissolved in 0.3 mL of dry MeCN was added via canula. The mixture was stirred at  $-40\text{ }^{\circ}\text{C}$  for 12.5 h. The reaction was quenched with 2 mL of 0.5 M of a sodium potassium tartrate solution. The mixture was diluted in DCM and washed with a saturated solution of  $\text{NaHCO}_3$ . The aqueous layer was extracted three times with DCM (twice). The final organic layers were dried over  $\text{MgSO}_4$ , filtered and evaporated. The crude mixture was purified by preparative TLC

eluting with 20% ethylacetate/hexanes. 18.9 mg (58%) of a light yellow oil was obtained. New anti-diol compound characterized as a mixture of diastereomers. 18.9 mg (58%); 5:3 ratio of anti/syn; high dr for anti  $^1\text{H NMR}$  (400 MHz,  $\text{CDCl}_3$ ) see spectrum (diastereomers overlap).

$^{13}\text{C}\{^1\text{H}\}$  NMR (100 MHz,  $\text{CDCl}_3$ )  $\delta$  175.6, 175.5, 81.3, 81.1, 70.8, 69.0, 65.3, 65.0, 45.9, 45.4, 41.8, 41.4, 28.1 (overlap of the diastereomers), 23.6, 23.5, 14.2, 11.6. **MS** (ESI+)  $m/z$  241 (M+Na); **HRMS** (ESI+)  $m/z$  calc'd for  $\text{C}_{11}\text{H}_{22}\text{O}_4\text{Na}$  [M+Na] $^+$ : 241.1410; found: 241.1411.



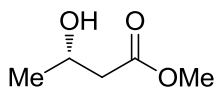




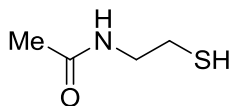
**Methyl 3-hydroxybutanoate:** In a flame dried flask, methyl acetoacetate (3.24 mL, 30.0 mmol, 1.00 eq) was dissolved in 300 mL of HPLC grade methanol. Then, ammonium chloride (9.628 g, 180 mmol, 6.00 eq) was added and the solution was cooled to 0 °C. Sodium borohydride (2.270 g, 60.0 mmol, 2.00) was subsequently added under argon and left to stir for 10 h. The solvent was evaporated to a small volume and the solution was washed with 1M HCl and extracted three times with ethylacetate. The combined organic phases were washed with brine, dried over MgSO<sub>4</sub>, filtered and evaporated. 2.433 g (69%) of a colourless liquid was obtained. All spectral data are in agreement with reported literature data. <sup>1</sup>H NMR (400 MHz, CDCl<sub>3</sub>) δ (ppm) 4.25-4.18 (m, 1H), 3.72 (s, 3H), 2.51 (dd, 1H, *J* = 3.6 Hz, *J* = 16.5 Hz), 2.44 (dd, 1H, *J* = 8.6 Hz, *J* = 16.5 Hz), 1.24 (d, 3H, *J* = 6.3 Hz). <sup>13</sup>C{<sup>1</sup>H} NMR (100 MHz, CDCl<sub>3</sub>) δ 173.4, 64.3, 51.8,



42.5, 22.4. **MS** (ESI+)  $m/z$  119 (M+H), 141 (M+Na); **HRMS** (ESI+)  $m/z$  calc'd for C<sub>5</sub>H<sub>11</sub>O<sub>3</sub> [M+H]<sup>+</sup>: 119.0702; found: 119.0704.

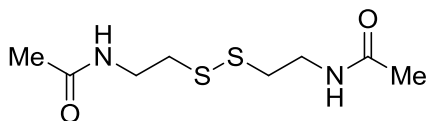
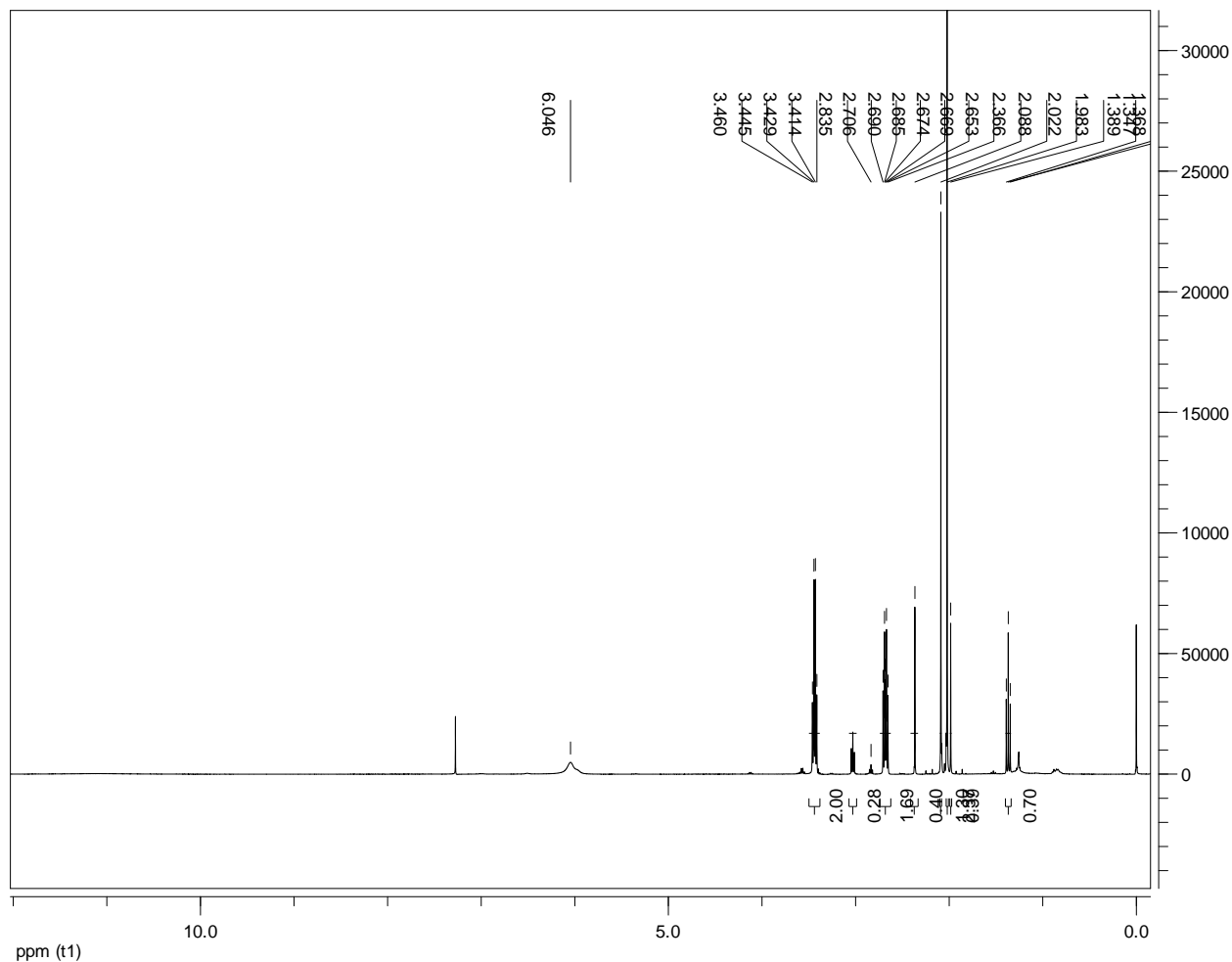


**Methyl 3-hydroxybutanoate:** The procedure was conducted as is from the literature.<sup>117</sup> 1.431 g (39%) of a colourless liquid was obtained with ~33% ee by polarimetry. All spectral data are in agreement with reported literature data.<sup>24</sup> **<sup>1</sup>H NMR** (400 MHz, CDCl<sub>3</sub>)  $\delta$  (ppm) 4.25-4.18 (m, 1H), 3.72 (s, 3H), 2.51 (dd, 1H,  $J = 3.6$  Hz,  $J = 16.5$  Hz), 2.44 (dd, 1H,  $J = 8.6$  Hz,  $J = 16.5$  Hz), 1.24 (d, 3H,  $J = 6.3$  Hz). **<sup>13</sup>C{<sup>1</sup>H} NMR** (100 MHz, CDCl<sub>3</sub>)  $\delta$  173.4, 64.3, 51.8, 42.5, 22.4. **MS** (ESI+)  $m/z$  119 (M+H), 141 (M+Na); **HRMS** (ESI+)  $m/z$  calc'd for C<sub>5</sub>H<sub>11</sub>O<sub>3</sub> [M+H]<sup>+</sup>: 119.0702; found: 119.0704.

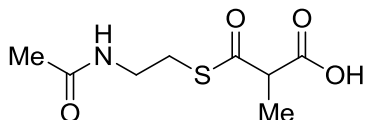


**N-Acetylcysteamine (5):** According to a modified procedure,<sup>118</sup> in 125 mL of deionized water, cysteamine hydrochloride (2.84g, 25.0 mmol), potassium hydroxide (1.40 g, 25.0 mmol) and sodium bicarbonate (6.30 g, 75.0 mmol) were added and a clear solution was obtained. Acetic anhydride (2.13 mL, 22.5 mmol) was then added dropwise and bubbles were observed. The solution was stirred for 10 mins at room temperature. The reaction was quenched with approximately 15 mL of 12N HCl<sub>(aq)</sub> or until a pH < 6 was obtained. The resulting mixture was separated and the aqueous phase, saturated with NaCl<sub>(s)</sub>, was extracted three times with ethyl acetate. The combined organic phases were dried over Na<sub>2</sub>SO<sub>4</sub>, filtered and evaporated. To remove the unavoidable presence of the diacetylated compound, the crude was diluted in 22 mL of methanol and 6 mL of a 25% sodium methoxide solution was added. This solution is stirred for 30 minutes at room temperature and was quenched with acetic acid. The resulting mixture was separated and the aqueous phase was extracted three times with ethyl acetate. The combined

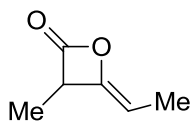
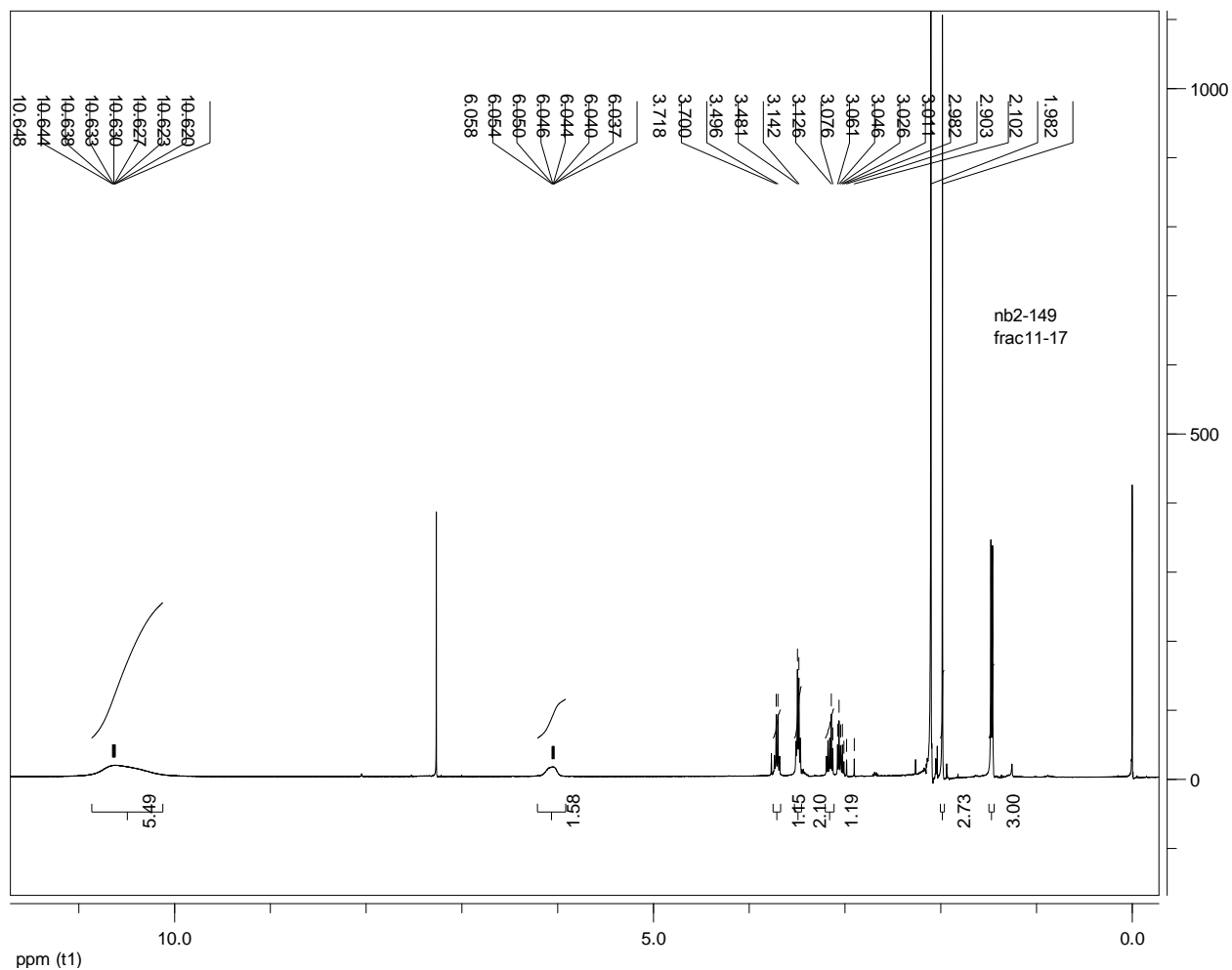
organic phases were dried over  $\text{Na}_2\text{SO}_4$ , filtered and evaporated. 2.20 g of a colourless liquid was obtained.  $^1\text{H NMR}$  (400 MHz,  $\text{CDCl}_3$ )  $\delta$  (ppm) 5.93 (br s, 1H), 3.44 (q, 2H,  $J = 6.2\text{Hz}$ ), 2.68 (td, 2H,  $J = 6.4\text{Hz}$ ,  $J = 8.4\text{Hz}$ ), 2.02 (s, 3H), 1.36 (t, 1H,  $J = 8.5\text{Hz}$ ).



***N,N'*-(Disulfanediy)bis(ethane-2,1-diy)diacetamide:** Inseperable byproduct of the above reaction <10%.  $^1\text{H NMR}$  (400 MHz,  $\text{CDCl}_3$ )  $\delta$  (ppm) 6.37 (br s, 2H), 3.57 (q, 4H,  $J = 6.3\text{Hz}$ ), 2.84 (t, 4H,  $J = 6.4\text{Hz}$ ), 2.10 (s, 6H).

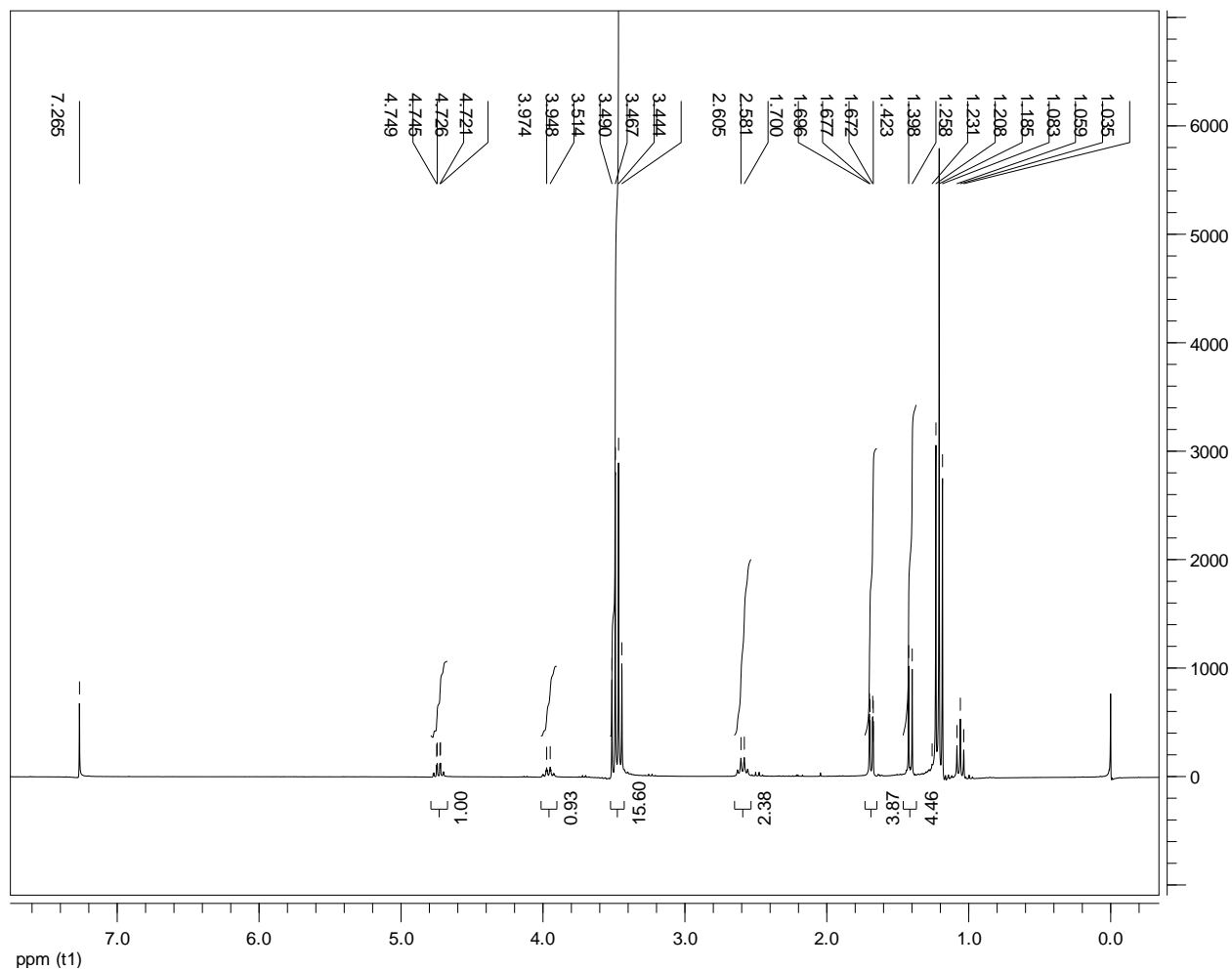


**3-((2-Acetamidoethyl)thio)-2-methyl-3-oxopropanoic acid (6):** According to a modified procedure,<sup>119</sup> in a flame-dried flask under Ar, trimethylsilylimidazole (0.49 mL, 3.4 mmol) was inserted via syringe, followed by *N*-acetylcysteamine (0.88 g, 6.7 mmol) and by trimethylsilyltriflate (0.33 mL, 1.7 mmol). Immediately, a white precipitate was formed with release of heat. The gas was evacuated with a flow of Ar. Methyl-Meldrum's acid (0.53 g, 3.4 mmol) dissolved in 5 mL of dry CH<sub>2</sub>Cl<sub>2</sub> was added to the flask via cannula at 0°C. The reaction mixture was stirred at room temperature. After a few hours, more trimethylsilyltriflate was added to drive the reaction to completion. The reaction was quenched with 1M HCl. The resulting mixture was separated and the aqueous phase was evaporated to a minimal volume (compound remains in the aqueous phase). The aqueous phase was extracted five times with CH<sub>2</sub>Cl<sub>2</sub>. The combined organic phases were dried over Na<sub>2</sub>SO<sub>4</sub>, filtered and evaporated. The crude mixture was purified by chromatography on silica gel eluting with 5% MeOH/ CH<sub>2</sub>Cl<sub>2</sub>. 0.522 g (71%) of a colourless oil was obtained. <sup>1</sup>H NMR (400 MHz, CDCl<sub>3</sub>) δ (ppm) 10.20-10.80 (br, 1H), 6.04-6.06 (br, 1H), 3.71 (q, 1H, *J* = 7.2 Hz), 3.49 (q, 2H, *J* = 6.1 Hz), 3.19-3.01 (m, 2H), 1.98 (s, 3H), 1.47 (d, 3H, *J* = 7.2 Hz). <sup>13</sup>C{<sup>1</sup>H} NMR (100 MHz, CDCl<sub>3</sub>) δ (ppm) 197.1, 173.9, 172.2, 54.1, 39.7, 28.8, 23.1, 14.2. MS (ESI-) *m/z* 218 (M-H).



**4-Ethylidene-3-methyloxetan-2-one (7):** In a flame-dried flask and under strictly anhydrous conditions, freshly distilled propanoyl chloride (8.7 mL, 100 mmol) was dissolved in 30 mL of dry ether (3.4M). Using an addition funnel under argon, freshly distilled triethylamine (13.9 mL, 100 mmol) dissolved in 200 mL of dry ether was added dropwise over one hour to the solution at 0 °C (Observation: upon the addition of the first drops of Et<sub>3</sub>N, the solution turned white and a white gas was formed. Et<sub>3</sub>NCl forms very quickly and contaminates the slowly dropping Et<sub>3</sub>N). The mixture was then warmed to room temperature and stirred overnight. The reaction mixture was filtered through a Schlenk filter under argon and washed 3 times with dry ether. The light

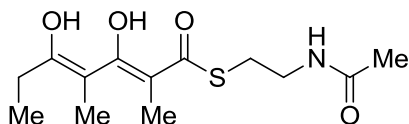
yellow solution was evaporated. NOTE: never heat this product above room temperature. The crude product was purified by distillation on a Kugelrohr under full vacuum at room temperature. 2.61 g (47%) of a colourless liquid was obtained. The spectra are in agreement with reported literature data.<sup>120</sup>  $^1\text{H NMR}$  (400 MHz,  $\text{CDCl}_3$ )  $\delta$  (ppm) 4.74 (dq, 1H,  $J = 1.4$  Hz,  $J = 7.0$  Hz), 3.99-3.93 (m, 1H), 1.69 (dd, 3H,  $J = 1.2$  Hz,  $J = 7.0$  Hz), 1.41 (d, 3H,  $J = 7.8$  Hz).



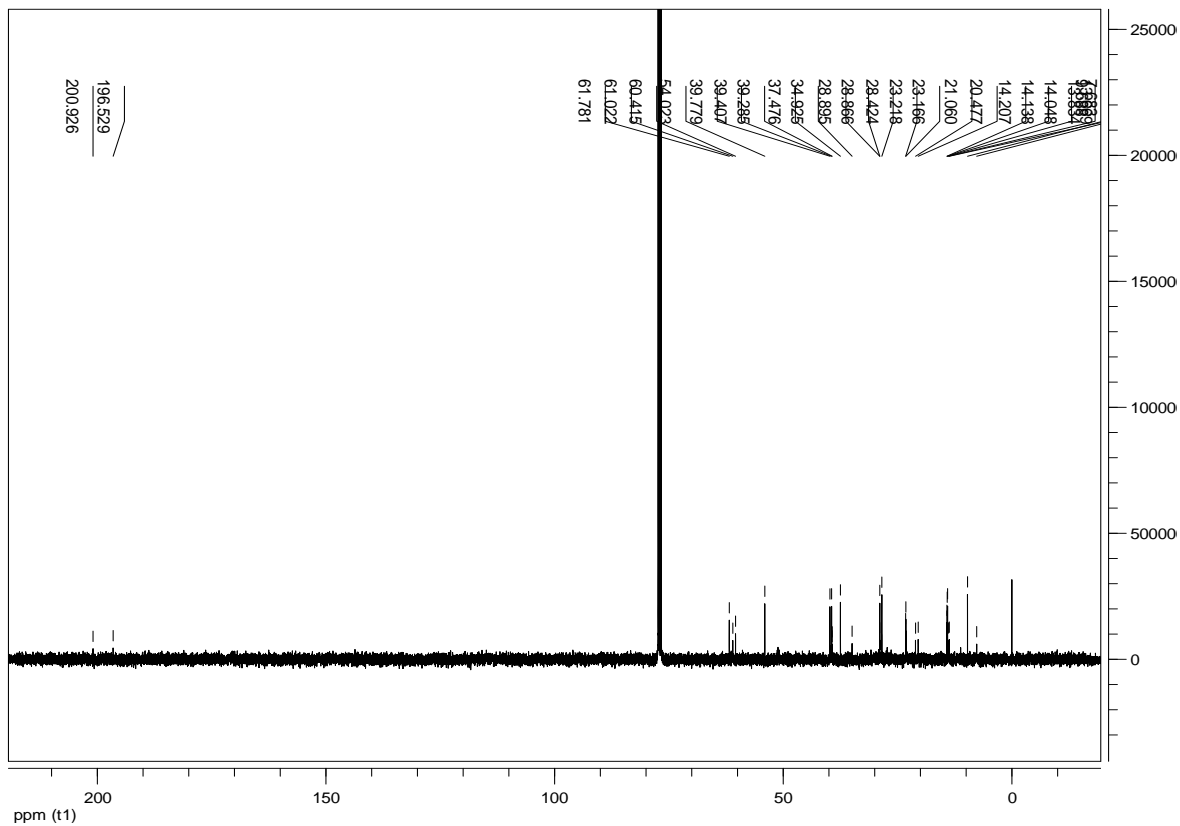
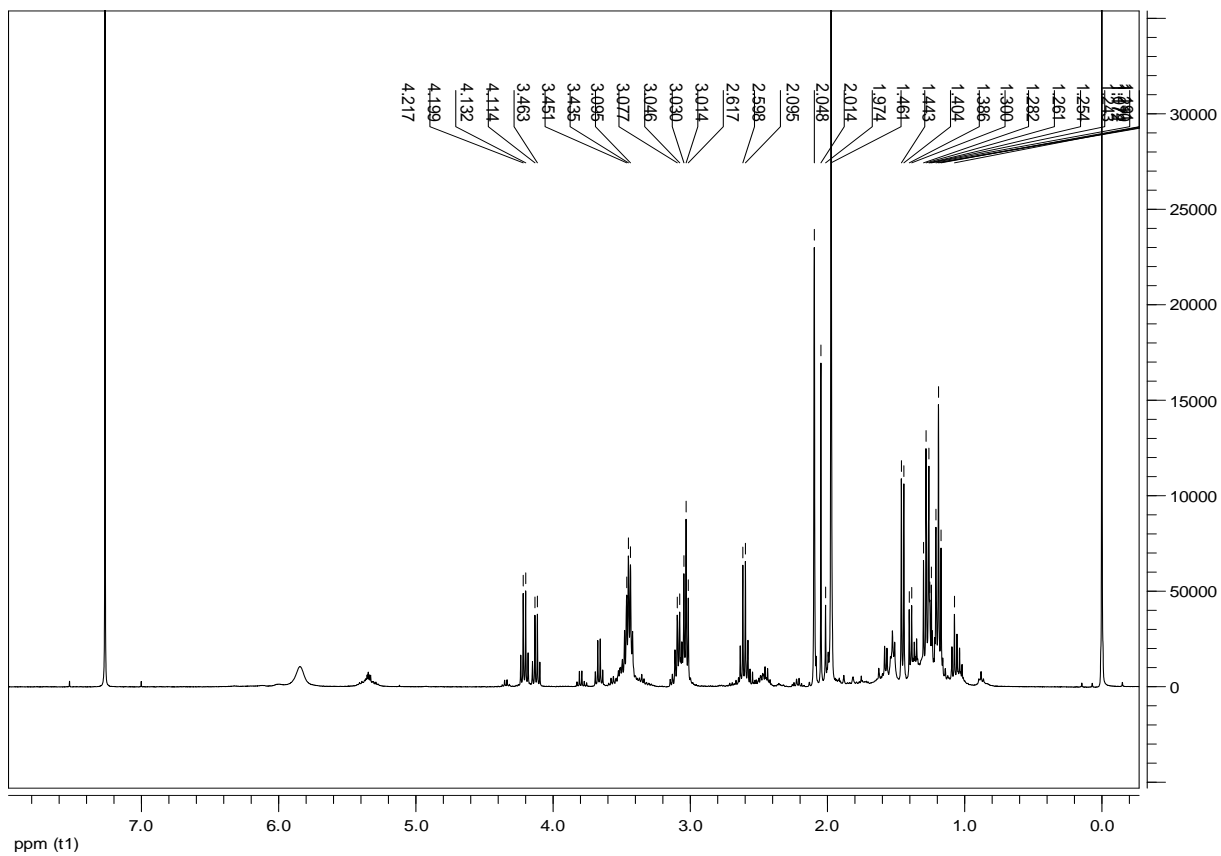
$\text{Mg}(\text{OEt})_2$

**Magnesium ethoxide:** According to a patent,<sup>121</sup> under anhydrous conditions, N-chlorosuccinamide (0.27 g, 2.0 mmol) and magnesium (0.24 g, 10.0 mmol) were dissolved in 4.0 mL of absolute ethanol. The solution was stirred at 40 °C and after 2 mins, hydrogen was generated. After the hydrogen evolution stopped (approx 20 mins), the reaction was stirred at 40 °C for 2 h. Then, the reaction was heated to 70 °C for another 2 h. The residue grey was washed

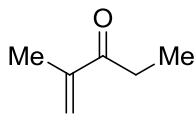
three times at 50 °C with hexanes. The solid was dried under vacuum for several hours. 0.38 g (33%) of a white/grey powder was obtained.



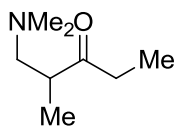
**S-(2-Acetamidoethyl) 2,4-dimethyl-3,5-dioxoheptanethioate (8):** Mg(OEt)<sub>2</sub> (29 mg, 0.25 mmol) was added to a solution of 3-((2-acetamidoethyl)thio)-2-methyl-3-oxopropanoic acid (0.11 g, 0.50 mmol) in 5 mL of dry THF. The mixture was stirred at room temperature under argon for 1h. The solvent was evaporated and the insoluble salt was used as is. Under anhydrous conditions, methyl diketene dimer (65 mg, 0.58 mmol) was dissolved in 2.5 mL of dry THF and subsequently added to a mixture of magnesium 3-((2-acetamidoethyl)thio)-2-methyl-3-oxopropanoic acid (115 mg, 0.25 mmol) dissolved in 2.5 mL of THF. The mixture was stirred at room temperature under argon for 36 h, at 40 °C for 36 h and then at 70 °C for another 36 h. Then, a saturated solution of ammonium chloride was added and it was extracted three times with ethyl acetate. The combined organic phases were dried over Na<sub>2</sub>SO<sub>4</sub>, filtered and evaporated. The crude product was purified by preparative TLC eluting with a gradient of 2% MeOH/CH<sub>2</sub>Cl<sub>2</sub>. 40 mg (28%) of a colourless oil was obtained. New compound characterized as a mixture of diastereomers. Tautomers are detected in significant amounts. **<sup>1</sup>H NMR** (400 MHz, CDCl<sub>3</sub>) δ (ppm) see spectra. **<sup>13</sup>C{<sup>1</sup>H} NMR** (100 MHz, CDCl<sub>3</sub>) δ see spectra. **MS** (ESI+) *m/z* 288 (M+H), 310 (M+Na); **HRMS** (ESI+) *m/z* calc'd for C<sub>13</sub>H<sub>21</sub>NO<sub>4</sub>S [M+H]<sup>+</sup>: 288.1264; found: 288.1254.



## 5.5.2 Intermediates Towards the Western Fragment



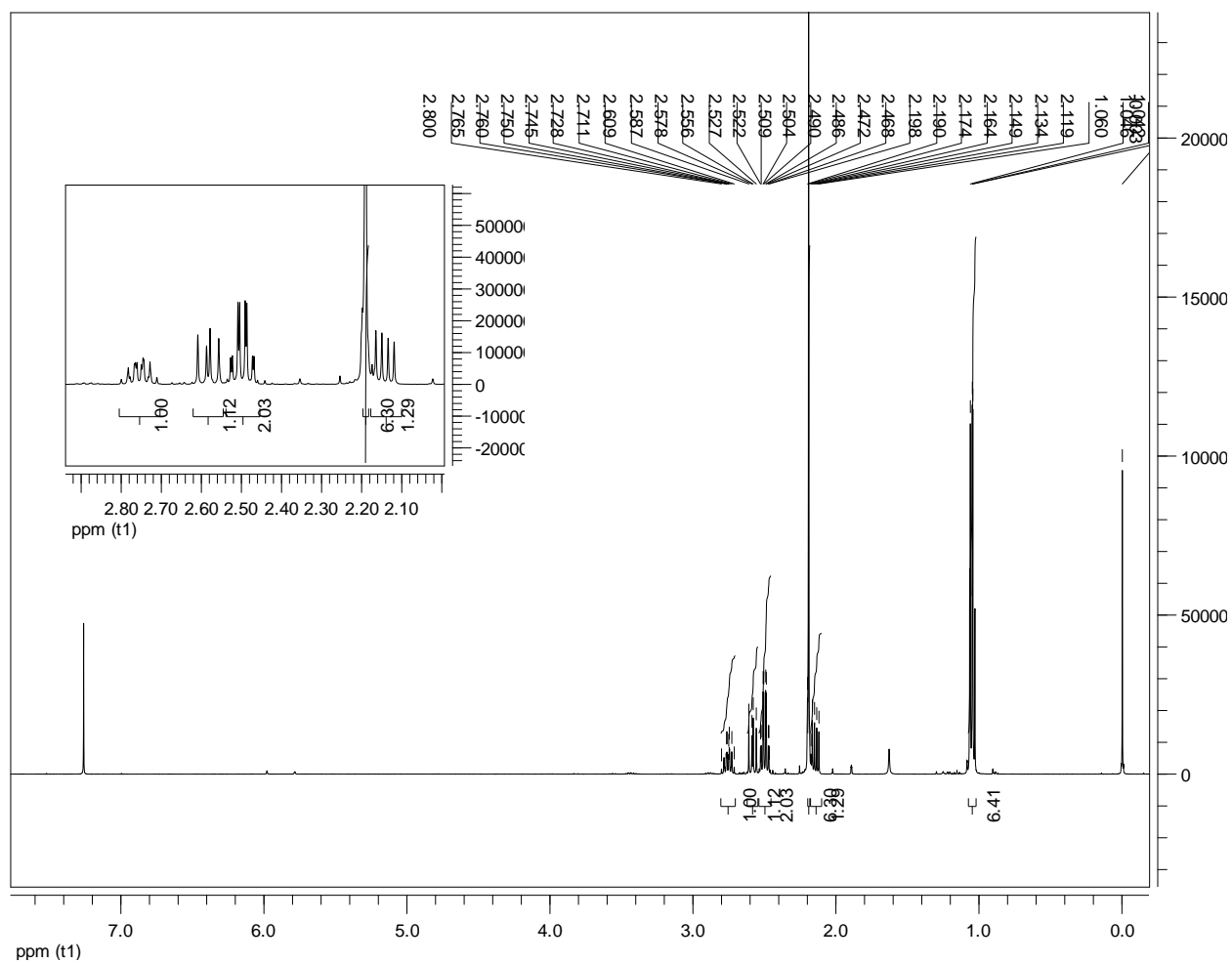
**2-Methylpent-1-en-3-one (17):** According to a patent procedure,<sup>122</sup> a solution of 3-pentanone (2.1 mL, 20 mmol), dimethylamine hydrochloride (0.82 g, 10 mmol) and 37% formaldehyde (0.75 mL, 10mmol) in water was adjusted to a pH=1 with a 1M HCl solution. The reaction mixture was refluxed overnight. The reaction was cooled to room temperature and the biphasic mixture was separated. The yellow aqueous phase was washed twice with diethyl ether and the aqueous phase was evaporated under reduced pressure and at 65 °C. Then 80 mg of hydroquinone was added to this orange crude mixture and it was refluxed for 2 h at 180 °C. The product was obtained by distillation of the crude mixture (but was contaminated with 3-pentanone). <sup>1</sup>H NMR (400 MHz, CDCl<sub>3</sub>) δ (ppm) 5.95 (s, 1H), 5.75 (s, 1H), 2.72 (q, 2H, *J* = 7.3Hz), 1.88 (s, 3H), 1.10 (t, 3H, *J* = 7.3Hz).

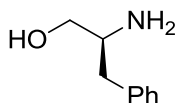
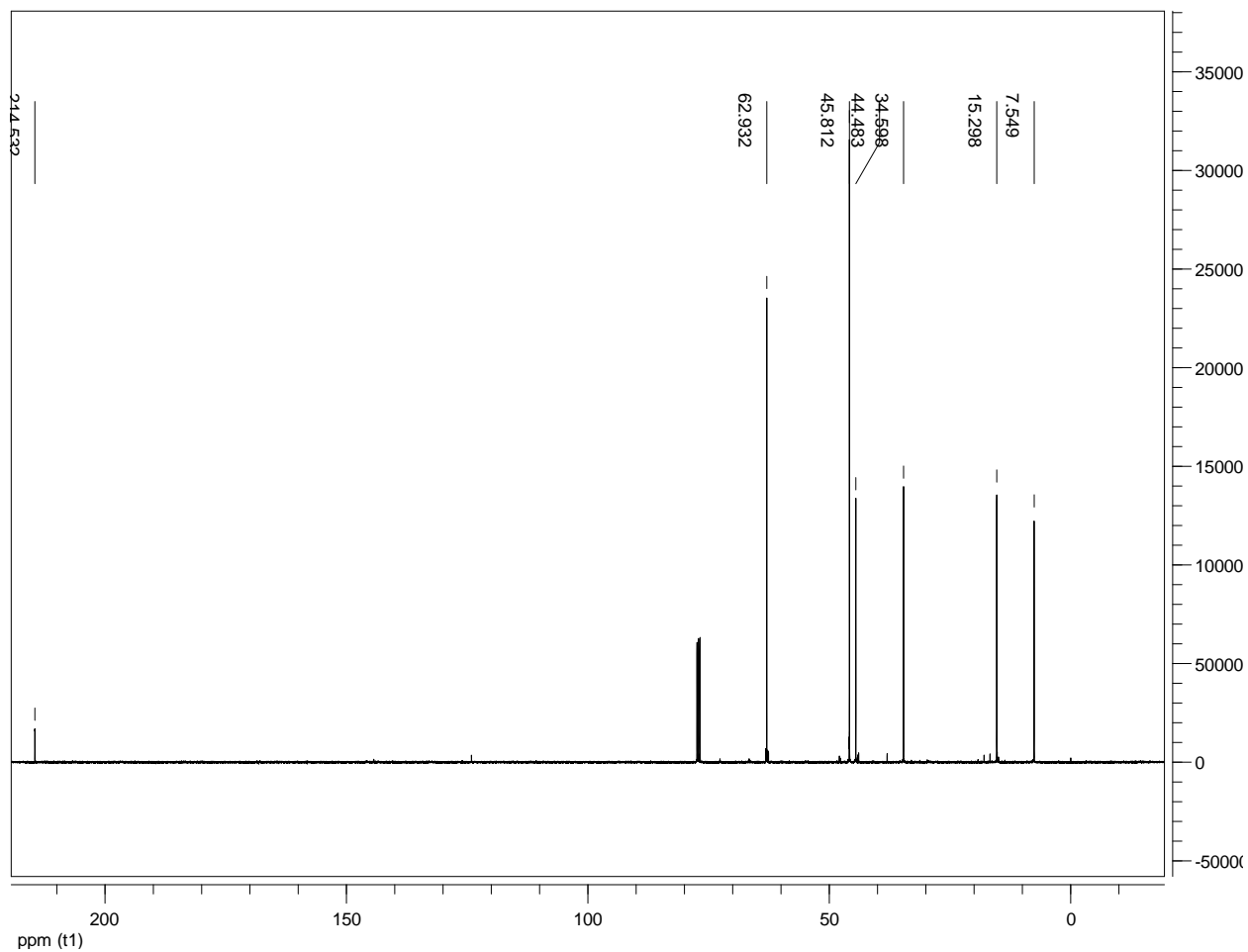


**1-(Dimethylamino)-2-methylpentan-3-one (27):** Synthesized following a modified procedure,<sup>123</sup> 3-pentanone (10.6 mL, 100 mmol), dimethylamine hydrochloride (8.16 g, 100 mmol) and paraformaldehyde (4.64 g, 150 mmol) were dissolved in 20 mL of absolute ethanol. Then 0.4 mL of concentrated hydrochloric acid was added and the mixture was refluxed overnight. The reaction was cooled to room temperature and a 4M solution of NaOH was added to basify the solution. The product was extracted three times with ether. The combined organic phases were washed with brine, dried over Na<sub>2</sub>SO<sub>4</sub>, filtered and evaporated. The product was obtained by distillation (Kugelrohr under vacuum at 120 °C) of the crude mixture. <sup>1</sup>H NMR (400 MHz, CDCl<sub>3</sub>) δ (ppm) 2.80-2.71 (m, 1H), 2.58 (dd, 1H, *J* = 8.7 Hz, *J* = 12.2 Hz), 2.50 (dq, 2H, *J* = 1.7 Hz, *J* = 7.2 Hz), 2.19 (s, 6H), 2.14 (dd, 1H, *J* = 6.0 Hz, *J* = 12.2 Hz), 1.07-1.02 (m, 6H).

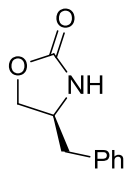


$^{13}\text{C}\{^1\text{H}\}$  NMR (100 MHz,  $\text{CDCl}_3$ )  $\delta$  (ppm) 214.5, 62.9, 45.8, 44.5, 34.6, 15.3, 7.5. MS (ESI+)  $m/z$  144.1 ( $\text{M}+\text{H}$ ); HRMS (ESI+)  $m/z$  calc'd for  $\text{C}_8\text{H}_{18}\text{NO}$  [ $\text{M}+\text{H}$ ] $^+$ : 144.1388; found: 144.1382.

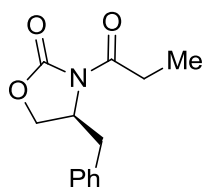




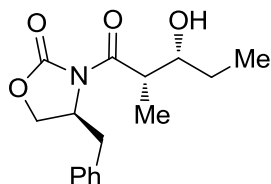
**(S)-2-Amino-3-phenylpropan-1-ol (10):** Synthesized following a reported procedure,<sup>124</sup> using 65 mmol of L-phenylalanine. 9.80 g (quantative yield) of a white solid was obtained. <sup>1</sup>H NMR (400 MHz, CDCl<sub>3</sub>) δ (ppm) 7.35-7.29 (m, 2H), 7.25-7.18 (m, 2H), 3.64 (dd, 1H, *J* = 3.9Hz, *J* = 10.6Hz), 3.38 (dd, 1H, *J* = 7.2Hz, *J* = 10.6Hz), 3.16-3.08 (m, 1H), 2.80 (dd, 1H, *J* = 5.2Hz, *J* = 13.5Hz), 2.53 (dd, 1H, *J* = 8.6Hz, *J* = 13.5Hz), 1.73 (s, 2H).



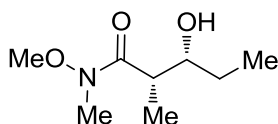
**(S)-4-Benzyloxazolidin-2-one (11):** (S)-2-amino-3-phenylpropan-1-ol (9.80 g, 65 mmol) and potassium carbonate (0.90 g, 6.5 mmol) were dissolved in dimethylcarbonate (11 mL, 130 mmol). The neat mixture was heated in a flask equipped with a short-path distillation apparatus. The mixture is refluxed and the methanol is distilled off. More dimethylcarbonate (20-40 mmol) is added until the excess dimethylcarbonate started to distill off. The mixture was cooled and then diluted in  $\text{CH}_2\text{Cl}_2$  and washed with 10%  $\text{NaHCO}_{3(\text{aq})}$ . The combined organic phases were washed with brine, dried over  $\text{Na}_2\text{SO}_4$ , filtered and evaporated. The crude mixture was recrystallized twice from hot ethylacetate and cold hexanes. 9.12 g (79%) of a white solid was obtained.  $^1\text{H NMR}$  (400 MHz,  $\text{CDCl}_3$ )  $\delta$  (ppm) 7.36-7.33 (m, 2H), 7.29 (d, 1H,  $J = 7.0\text{Hz}$ ), 7.18 (d, 2H,  $J = 7.4\text{Hz}$ ), 5.19 (s, 1H), 4.47 (t, 1H,  $J = 8.3\text{Hz}$ ), 4.16 (dd, 1H,  $J = 5.6\text{Hz}$ ,  $J = 8.5\text{Hz}$ ), 4.12-4.05 (m, 1H), 2.92-2.83 (m, 2H).  $^{13}\text{C}\{^1\text{H}\}$  NMR (100 MHz,  $\text{CDCl}_3$ )  $\delta$  (ppm) 159.0, 136.0, 129.1, 129.0, 127.3, 69.7, 53.8, 41.6.



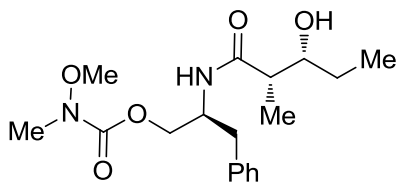
**(S)-4-Benzyl-3-propionyloxazolidin-2-one (12):** Synthesized following a reported procedure,<sup>125</sup> using 45 mmol of (S)-4-benzyloxazolidin-2-one. 8.96 g (85%) of a white solid was obtained.  $^1\text{H NMR}$  (400 MHz,  $\text{CDCl}_3$ )  $\delta$  (ppm) 7.36-7.32 (m, 2H), 7.30-7.28 (m, 1H), 7.22-7.20 (m, 2H), 4.68 (ddd, 1H,  $J = 3.3\text{Hz}$ ,  $J = 6.9\text{ Hz}$ ,  $J = 10.6\text{ Hz}$ ), 4.23-4.15 (m, 2H), 3.31 (dd, 1H,  $J = 3.3\text{ Hz}$ ,  $J = 13.4\text{ Hz}$ ), 3.03-2.90 (m, 2H), 2.77 (dd, 1H,  $J = 9.6\text{ Hz}$ ,  $J = 13.3\text{ Hz}$ ), 1.21 (t, 3H,  $J = 7.3\text{ Hz}$ ).  $^{13}\text{C}\{^1\text{H}\}$  NMR (100 MHz,  $\text{CDCl}_3$ )  $\delta$  (ppm) 174.3, 153.7, 135.6, 129.6, 129.2, 127.5, 66.4, 55.4, 38.1, 29.4, 8.5.



**(S)-4-Benzyl-3-((2S,3R)-3-hydroxy-2-methylpentanoyl)oxazolidin-2-one (13):** Synthesized following a reported procedure,<sup>126</sup> using 38 mmol of (S)-4-benzyl-3-propionyloxazolidin-2-one. 9.12 g (82%) of a white solid was obtained. <sup>1</sup>H NMR (400 MHz, CDCl<sub>3</sub>) δ (ppm) 7.37-7.28 (m, 3H), 7.22-7.20 (m, 2H), 4.71 (ddd, 1H, *J* = 3.4 Hz, *J* = 7.0 Hz, *J* = 12.8 Hz), 4.26-4.17 (m, 2H), 3.90-3.85 (m, 1H), 3.79 (ddd, 1H, *J* = 2.7 Hz, *J* = 7.0 Hz, *J* = 14.0 Hz), 3.26 (dd, 1H, *J* = 3.3 Hz, *J* = 13.4 Hz), 2.85-2.75 (m, 2H), 1.51 (m, 2H), 1.26 (d, 3H, *J* = 7.0 Hz), 0.98 (t, 3H, *J* = 7.4 Hz).

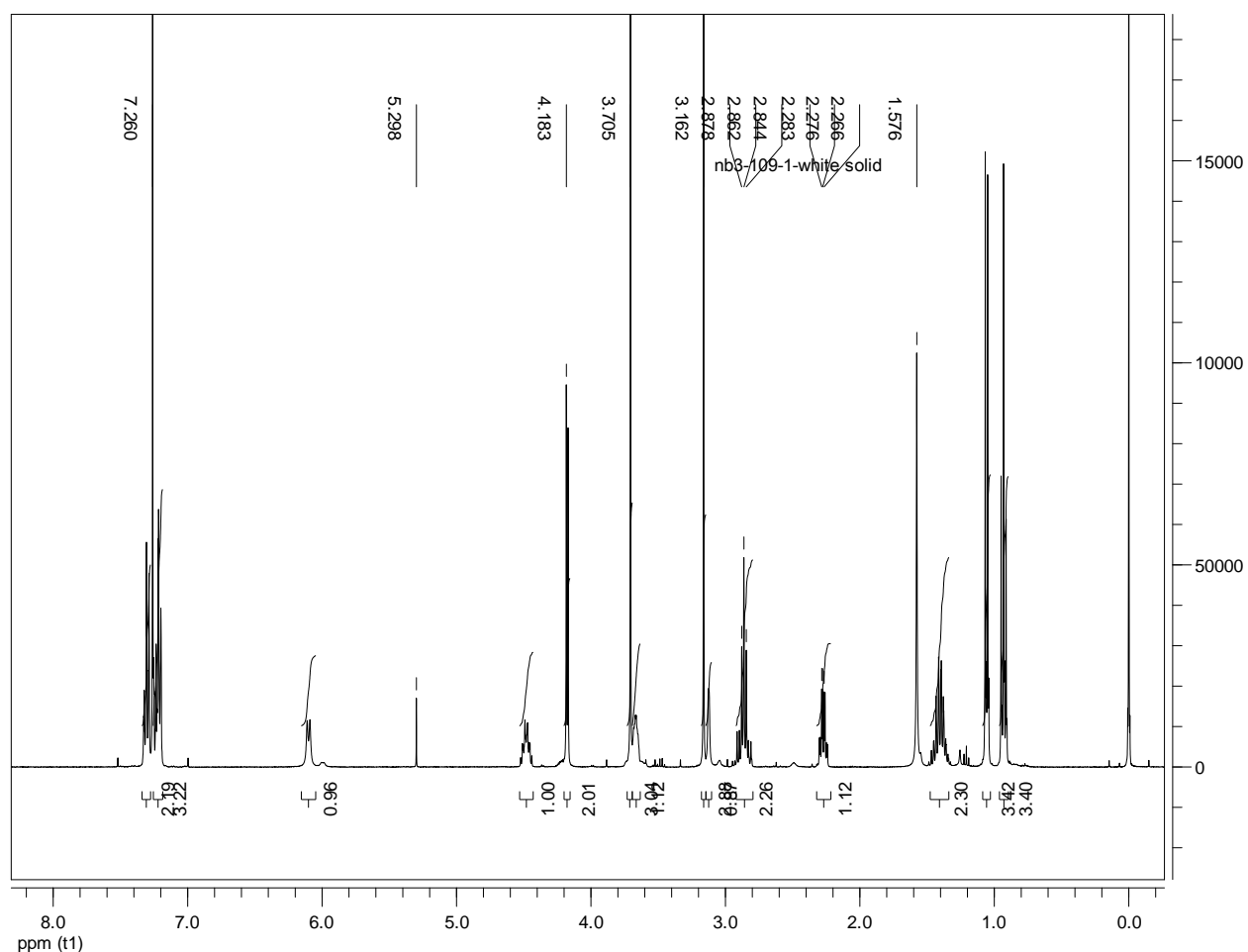


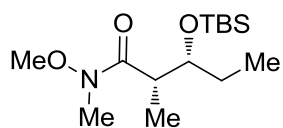
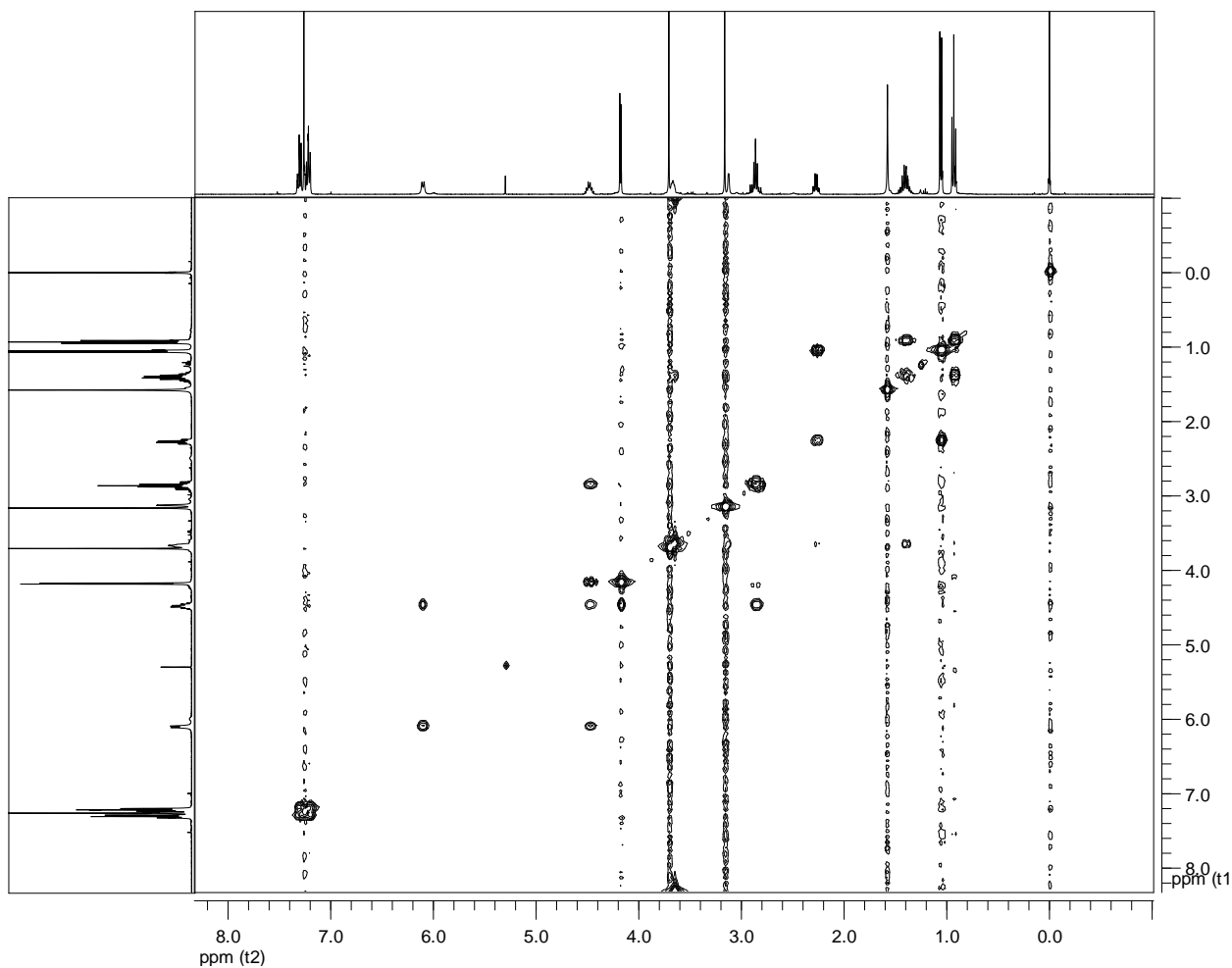
**(2S,3R)-3-Hydroxy-N-methoxy-N,2-dimethylpentanamide (14):** Synthesized following a reported procedure,<sup>127</sup> using 10.0 mmol of (S)-4-benzyl-3-((2S,3R)-3-hydroxy-2-methylpentanoyl)oxazolidin-2-one. 1.21 g (74%) (some material was lost) of a white solid was obtained. <sup>1</sup>H NMR (400 MHz, CDCl<sub>3</sub>) δ (ppm) 3.80-3.75 (m, 2H), 3.71 (s, 3H), 3.20 (s, 3H), 2.92 (s, 1H), 1.65-1.54 (m, 1H), 1.46-1.35 (m, 1H), 1.17 (d, 3H, *J* = 7.1 Hz), 0.97 (t, 3H, *J* = 7.4 Hz).



**(S)-2-((2S,3R)-3-Hydroxy-2-methylpentanamido)-3-phenylpropyl**

**methoxy(methyl)carbamate:** By-product obtained in the conversion of the oxazolidinone to the Weinreb amide (when using a large excess of reagents). >8g of a white solid was obtained.  $^1\text{H}$  NMR (400 MHz,  $\text{CDCl}_3$ )  $\delta$  (ppm) 7.33-7.28 (m, 2H), 7.25-7.19 (m, 3H), 6.11 (d, 1H,  $J = 8.2$  Hz), 4.52-4.44 (m, 1H), 4.18 (d, 2H,  $J = 5.2$  Hz), 3.71 (s, 3H), 3.69-3.64 (m, 1H), 3.16 (s, 3H), 3.13 (d, 1H,  $J = 2.6$  Hz), 2.91-2.80 (m, 2H), 2.27 (ddd, 1H,  $J = 2.9$  Hz,  $J = 7.2$  Hz,  $J = 14.3$  Hz), 1.47-1.33 (m, 2H), 1.06 (d, 3H,  $J = 7.2$  Hz), 0.93 (t, 3H,  $J = 7.4$  Hz).

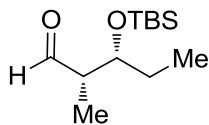




**(2S,3R)-3-((tert-Butyldimethylsilyl)oxy)-N-methoxy-N,2-dimethylpentanamide (15):**

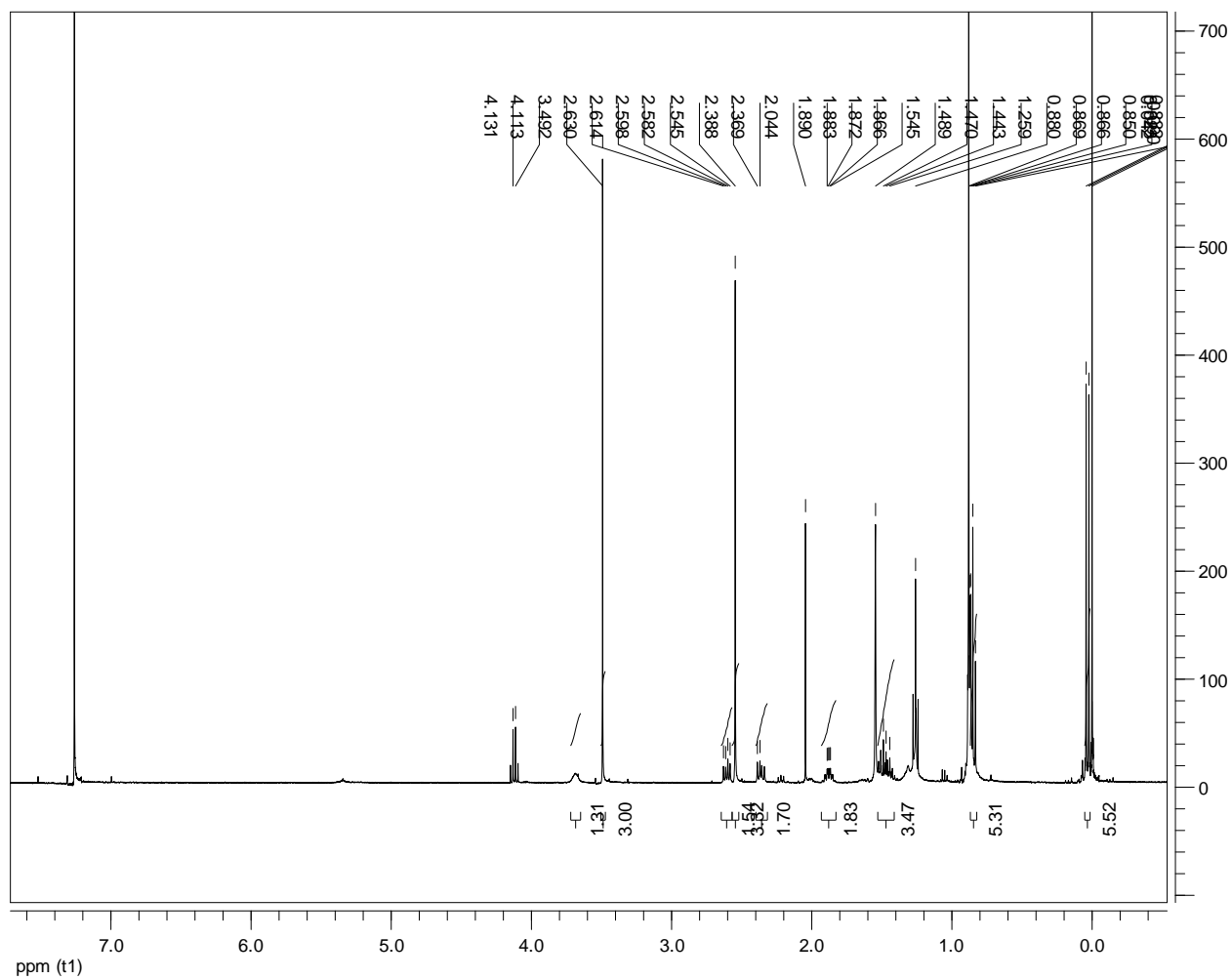
Synthesized following a reported procedure,<sup>128</sup> using 10.7 mmol of (2S,3R)-3-hydroxy-N-methoxy-N,2-dimethylpentanamide. 3.10 g (quantitative yield) of a colourless oil was obtained.

<sup>1</sup>H NMR (400 MHz, CDCl<sub>3</sub>) δ (ppm) 3.89 (td, 1H, *J* = 4.7 Hz, *J* = 8.2 Hz), 3.69 (s, 3H), 3.17 (s, 3H), 3.00 (s, 1H), 1.60-1.41 (m, 2H), 1.34 (t, 1H, *J* = 7.3 Hz), 1.15 (d, 3H, *J* = 6.9 Hz), 0.91-0.90 (m, 12H), 0.07 (s, 3H), 0.04 (s, 3H).

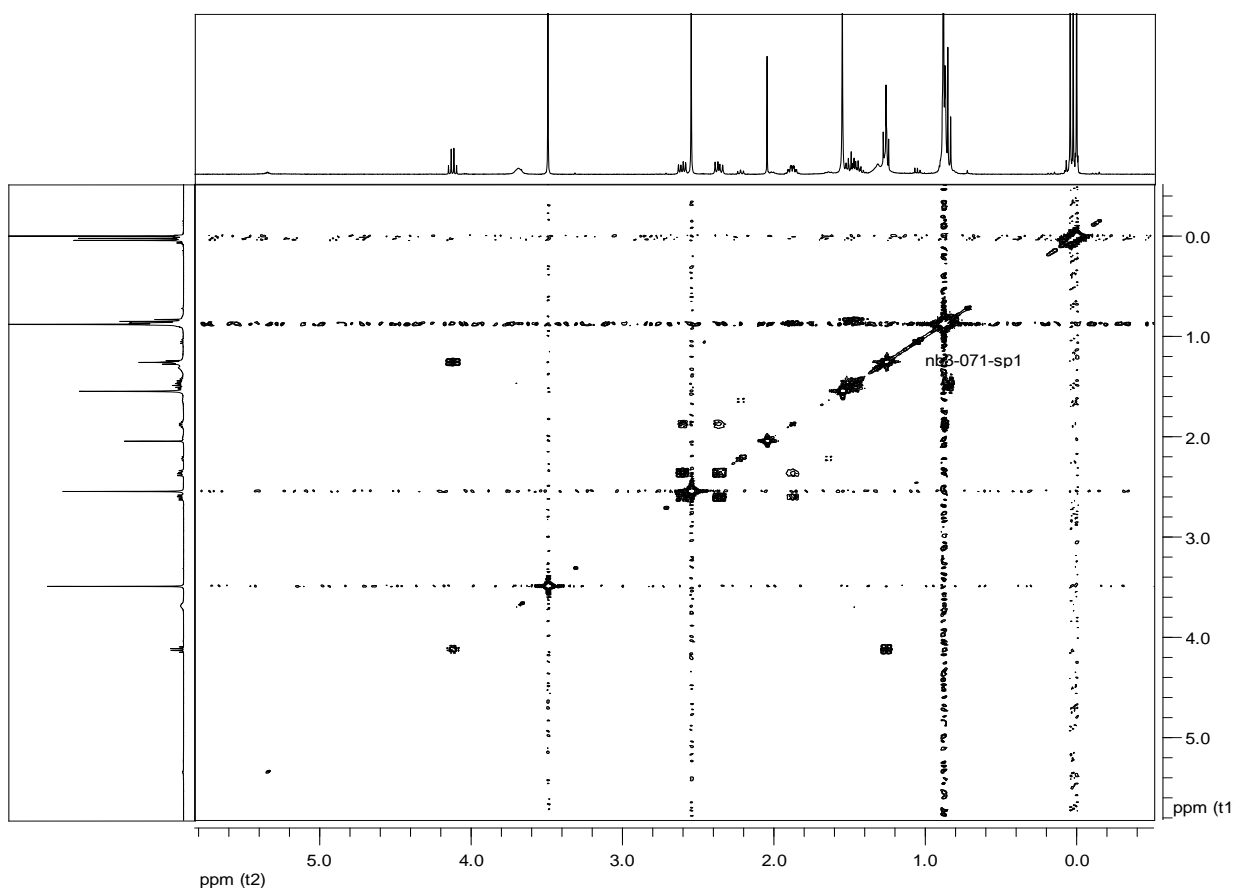
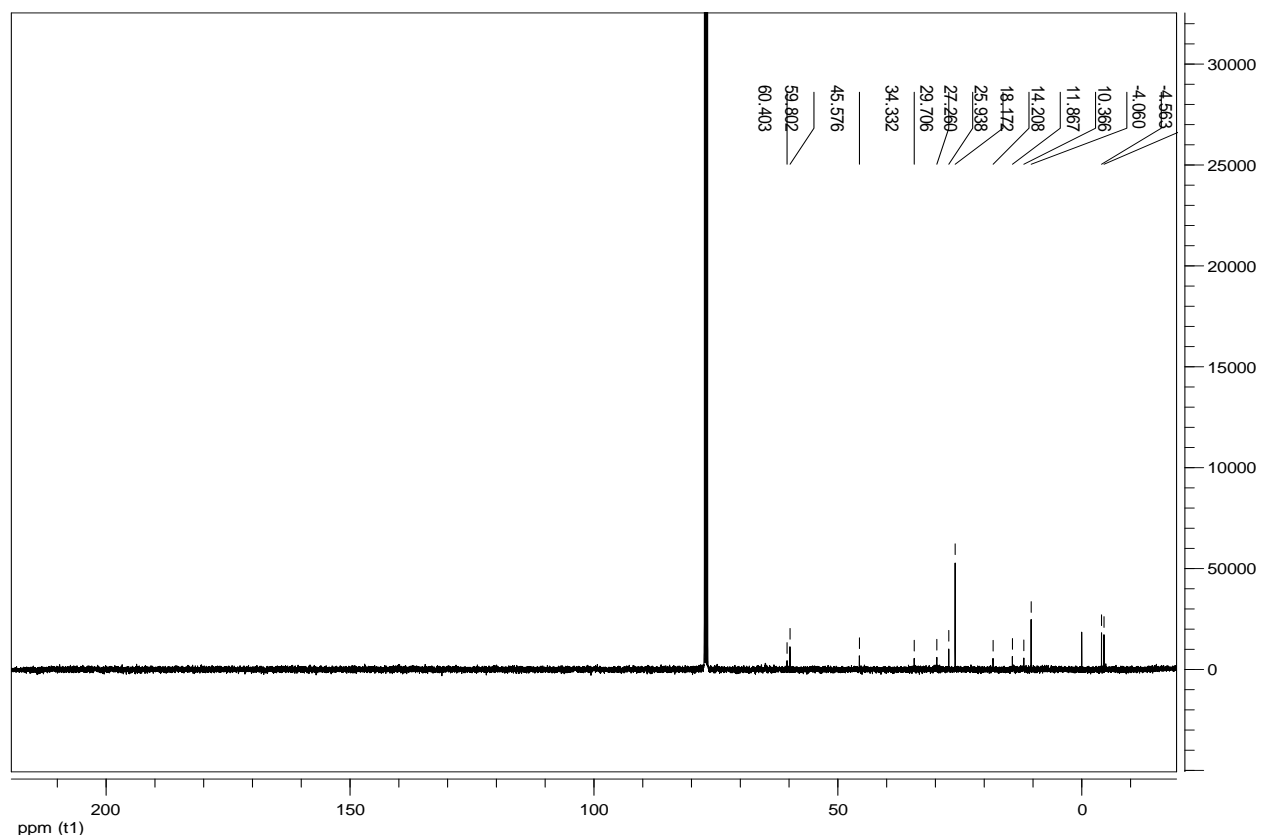


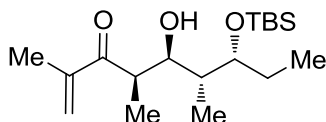


(400 MHz, CDCl<sub>3</sub>)  $\delta$  (ppm) 3.69 (s, 1H), 3.49 (s, 3H), 2.61 (dd, 1H,  $J = 6.4$  Hz,  $J = 12.5$  Hz), 2.55 (s, 3H), 2.36 (dd, 1H,  $J = 7.5$  Hz,  $J = 12.5$  Hz), 1.92-1.83 (m, 1H), 1.52-1.41 (m, 2H), 0.88 (s, 9H), 0.85 (t, 3H,  $J = 7.0$  Hz), 0.04 (s, 3H), 0.02 (s, 3H). <sup>13</sup>C{<sup>1</sup>H} NMR (100 MHz, CDCl<sub>3</sub>)  $\delta$  (ppm) 60.4, 59.8, 45.6, 34.3, 29.7, 27.2, 25.9, 18.2, 14.2, 11.9, 10.4, -4.1, -4.6.





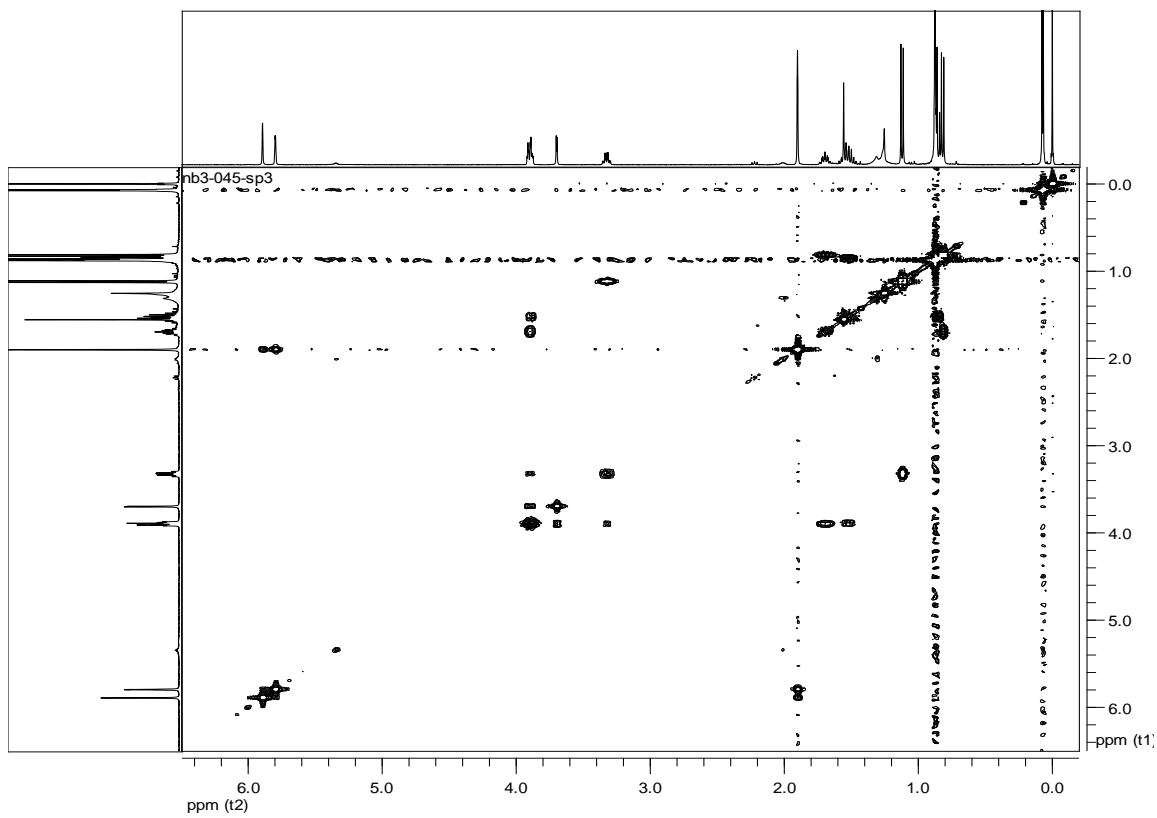
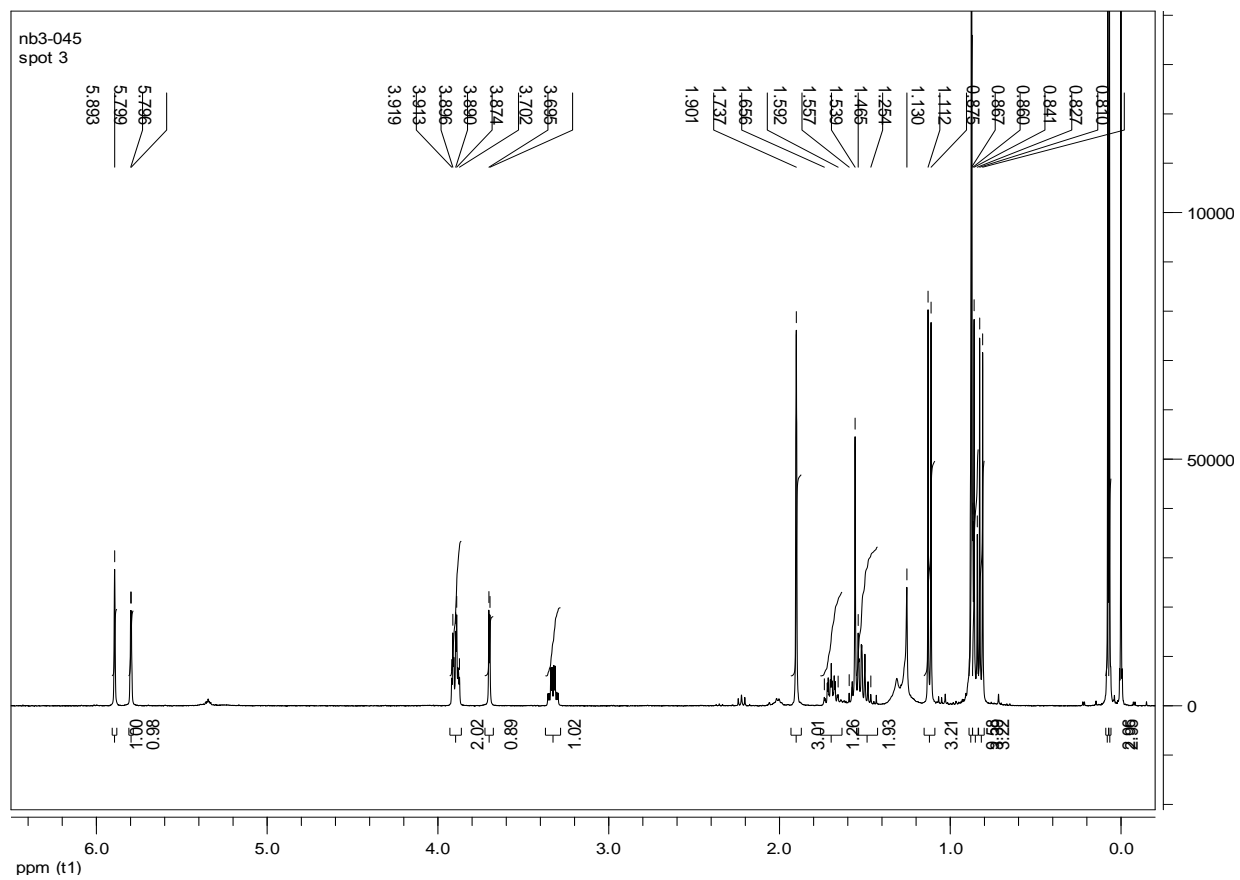


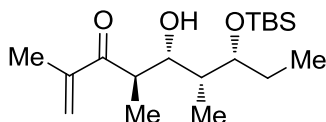


**(4R,5S,6R,7R)-7-((*tert*-Butyldimethylsilyl)oxy)-5-hydroxy-2,4,6-trimethylnon-1-en-3-one**

**(19)**: Under anhydrous conditions, hexamethyldisilazide (33  $\mu$ L, 0.155 mmol) was dissolved in 0.2 mL of dry tetrahydrofuran. At 0  $^{\circ}$ C, *n*-butyllithium (72  $\mu$ L of a 2.09M solution in hexanes, 0.15 mmol) was added dropwise. The reaction was stirred at room temperature for 30 mins under a nitrogen atmosphere. At -80  $^{\circ}$ C (dry ice and ether), 2-methylpent-1-en-3-one (15 mg, 0.15 mmol) was added and the flask was washed with 0.5 mL of dry tetrahydrofuran. This mixture was stirred at -80  $^{\circ}$ C for 30 mins. (2S,3R)-3-((*tert*-butyldimethylsilyl)oxy)-2-methylpentanal was then added in 0.5 mL of dry tetrahydrofuran. After stirring at -80 to -70  $^{\circ}$ C for 3h, the reaction was quenched at that temperature with 0.5 mL of a sat.  $\text{NH}_4\text{Cl}_{(\text{aq})}$  solution. The aqueous phase was extracted three times with ethyl acetate. The combined organic phases were dried over  $\text{Na}_2\text{SO}_4$ , filtered and evaporated. The crude product was purified by preparative TLC eluting with a gradient of 15% EtOAc/hexanes. 3.1 mg (10%) of a colourless oil was obtained.

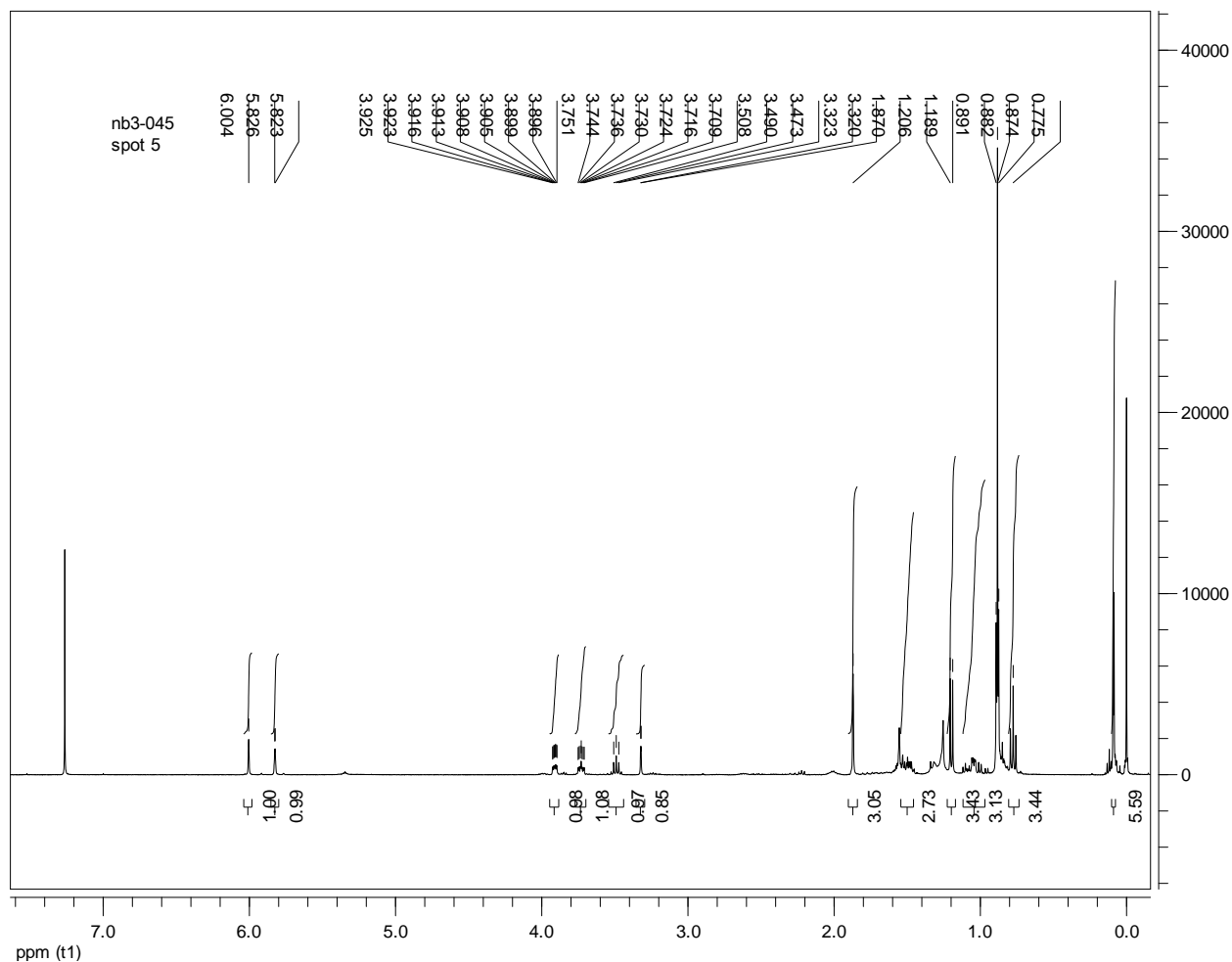
However, all four possible stereoisomers were isolated and characterized by  $^1\text{H}$  NMR and COSY. The anti/syn ratio was determined by the coupling constants of the  $\alpha$ - and  $\beta$ - protons, assuming a cyclic form via hydrogen bonding.  $^{130}\text{H}$  NMR (400 M Hz,  $\text{CDCl}_3$ )  $\delta$  (ppm) 5.89 (s, 1H), 5.80 (d, 1H,  $J = 1.1$  Hz), 3.92-3.87 (m, 2H), 3.70 (d, 1H,  $J = 2.5$  Hz), 3.33 (dq, 1H,  $J = 2.9$  Hz,  $J = 7.0$  Hz), 1.90 (s, 3H), 1.74-1.66 (m, 1H), 1.59-1.46 (m, 2H), 1.12 (d, 3H,  $J = 7.0$  Hz), 0.87 (s, 9H), 0.86 (t, 3H,  $J = 5.2$  Hz), 0.82 (d, 3H,  $J = 7.0$  Hz), 0.08 (s, 3H), 0.07 (s, 3H).  $^{13}\text{C}\{^1\text{H}\}$  NMR (100 M Hz,  $\text{CDCl}_3$ )  $\delta$  (ppm) MS (ESI+)  $m/z$  329 (M+H); HRMS (ESI+)  $m/z$  calc'd for  $\text{C}_{18}\text{H}_{37}\text{O}_3\text{Si}$  [M+H] $^+$ : 329.2512; found: 329.2512.

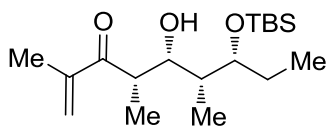
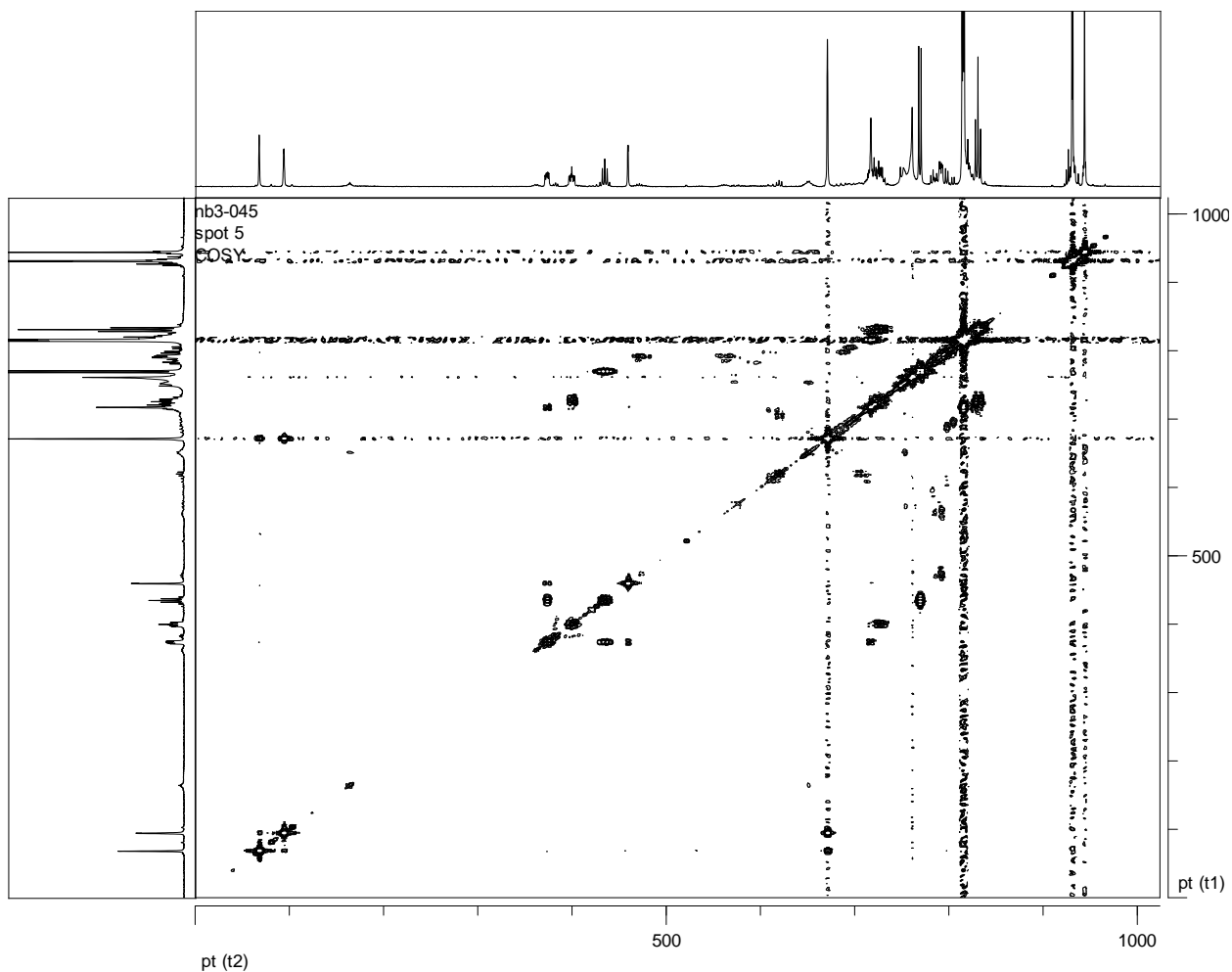




**(4R,5R,6R,7R)-7-((*tert*-Butyldimethylsilyl)oxy)-5-hydroxy-2,4,6-trimethylnon-1-en-3-one**

**(21)**: This product was isolated from the above procedure. 3.1 mg (10%) of a colourless oil was obtained.  $^1\text{H}$  NMR (400 M Hz,  $\text{CDCl}_3$ )  $\delta$  (ppm) 6.00 (s, 1H), 5.82 (d, 1H,  $J = 1.2$  Hz), 3.91 (ddd, 1H,  $J = 1.1$  Hz,  $J = 3.7$  Hz,  $J = 7.0$  Hz), 3.73 (ddd, 1H,  $J = 2.6$  Hz,  $J = 5.9$  Hz,  $J = 8.3$  Hz), 3.49 (p, 1H,  $J = 7.0$  Hz), 3.32 (d, 1H,  $J = 1.3$  Hz), 1.87 (s, 3H), 1.58-1.45 (m, 2H), 1.20 (d, 3H,  $J = 7.0$  Hz), 0.88 (m, 12H), 0.78 (t, 3H,  $J = 7.5$  Hz), 0.09 (s, 3H), 0.09 (s, 3H).  $^{13}\text{C}\{^1\text{H}\}$  NMR (100 M Hz,  $\text{CDCl}_3$ )  $\delta$  (ppm) MS (ESI+)  $m/z$  329 (M+H); HRMS (ESI+)  $m/z$  calc'd for  $\text{C}_{18}\text{H}_{37}\text{O}_3\text{Si}$  [M+H] $^+$ : 329.2512; found: 329.2520.

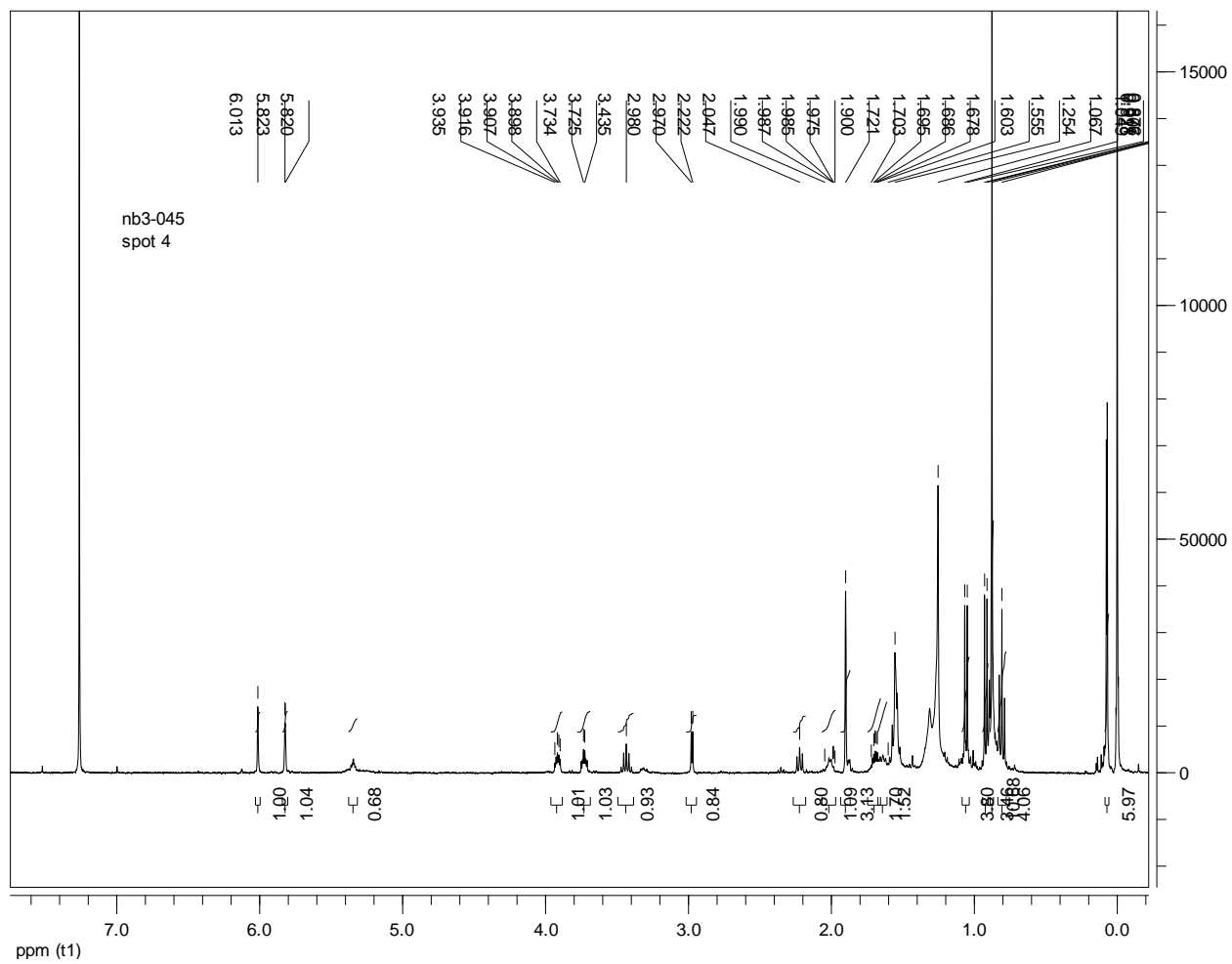


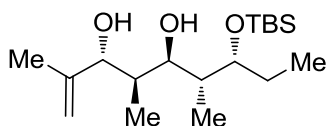
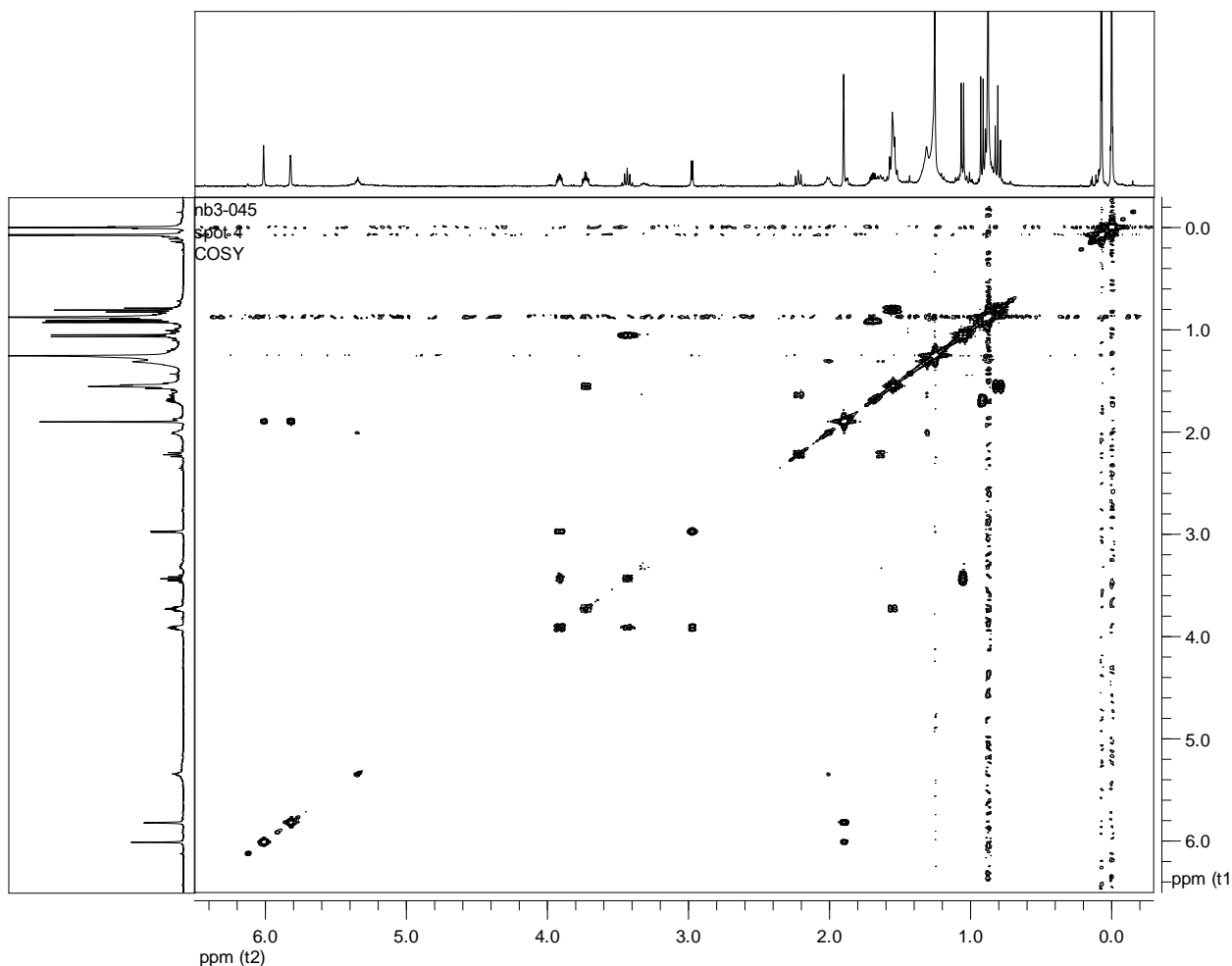


**(4S,5R,6R,7R)-7-((*tert*-Butyldimethylsilyl)oxy)-5-hydroxy-2,4,6-trimethylnon-1-en-3-one**

**(18)**: This product was isolated from the above procedure. A separate purification gave pure product for characterization.  $^1\text{H NMR}$  (400 MHz,  $\text{CDCl}_3$ )  $\delta$  (ppm) 5.99 (s, 1H), 5.83 (d, 1H,  $J = 1.2$  Hz), 4.01 (ddd, 1H,  $J = 1.7$  Hz,  $J = 6.3$  Hz,  $J = 7.9$  Hz), 3.69 (d, 1H,  $J = 8.9$  Hz), 3.57 (dt, 1H,  $J = 3.9$  Hz,  $J = 8.7$  Hz), 3.47 (dq, 1H,  $J = 4.0$  Hz,  $J = 7.1$  Hz), 1.88 (s, 3H), 1.61-1.42 (m, 3H), 1.24 (d, 3H,  $J = 7.1$  Hz), 0.88 (s, 9H), 0.82 (t, 3H,  $J = 7.5$  Hz), 0.75 (d, 3H,  $J = 6.9$  Hz), 0.09 (s, 3H), 0.07 (s, 3H).







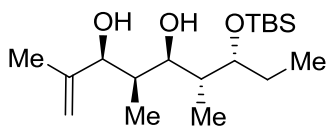
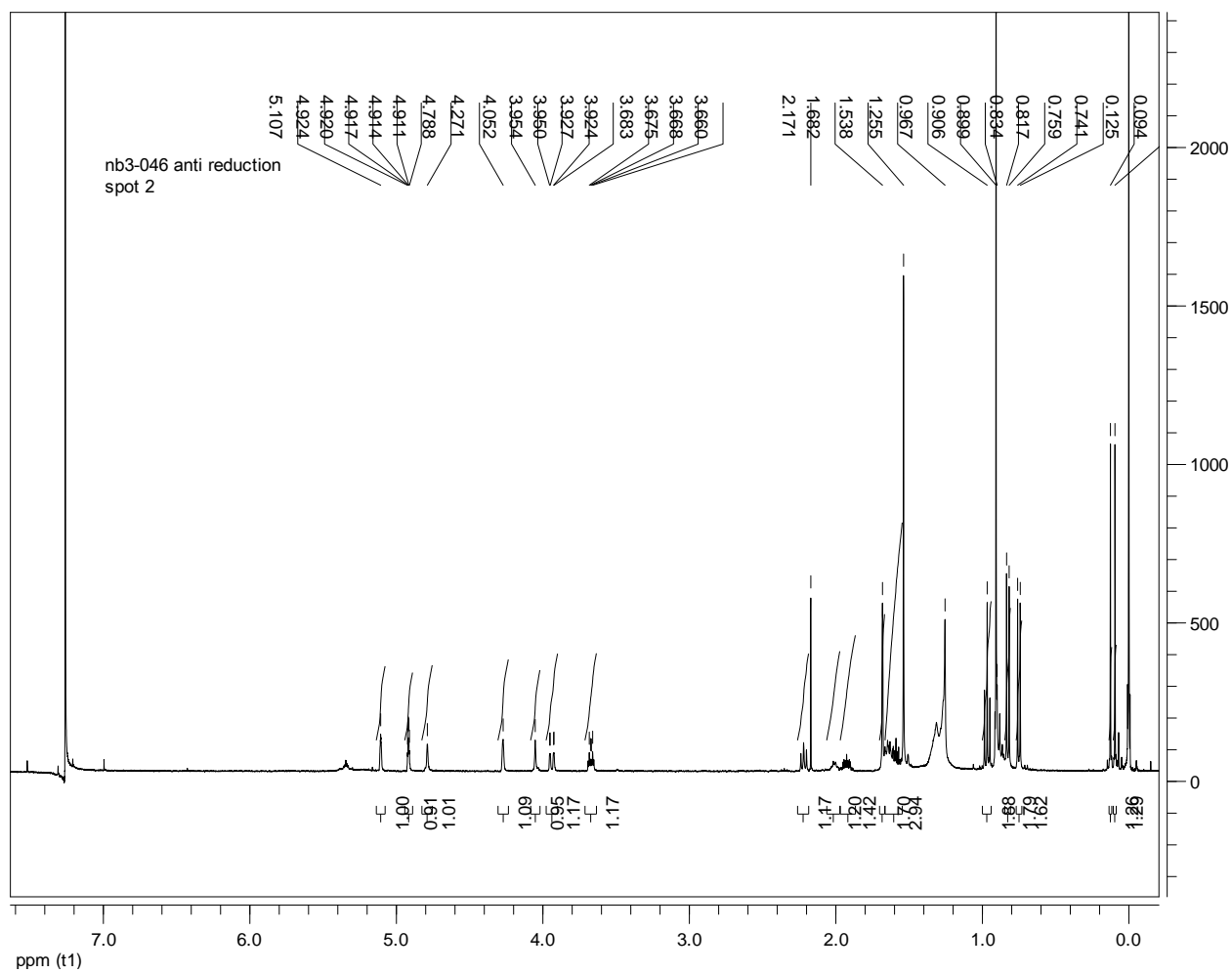
**(4R,5R,6R,7R)-7-((*tert*-Butyldimethylsilyl)oxy)-2,4,6-trimethylnon-1-ene-3,5-diol (34-anti):**

According to a modified procedure,<sup>131</sup> 0.009 mmol of (4R,5S,6R,7R)-7-((*tert*-butyldimethylsilyl)oxy)-5-hydroxy-2,4,6-trimethylnon-1-en-3-one yielded 1.9 mg (63%) of one diastereomer and 0.9 mg (30%) of a second diastereomer.

Anti diastereomer: <sup>1</sup>H NMR (400 M Hz, CDCl<sub>3</sub>) δ (ppm) 5.36-5.33 (m, 1H), 5.11 (s, 1H), 4.93-4.91 (m, 1H), 4.82 (s, 1H), 4.27 (s, 1H), 4.08 (s, 1H), 3.94 (dd, 1H, *J* = 1.7 Hz, *J* = 10.3 Hz), 3.67 (td, 1H, *J* = 3.2 Hz, *J* = 9.2 Hz), 2.21 (dd, 1H, *J* = 5.7 Hz, *J* = 13.5 Hz), 2.02-1.90 (m, 2H),



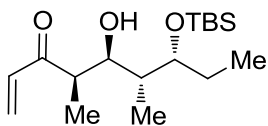
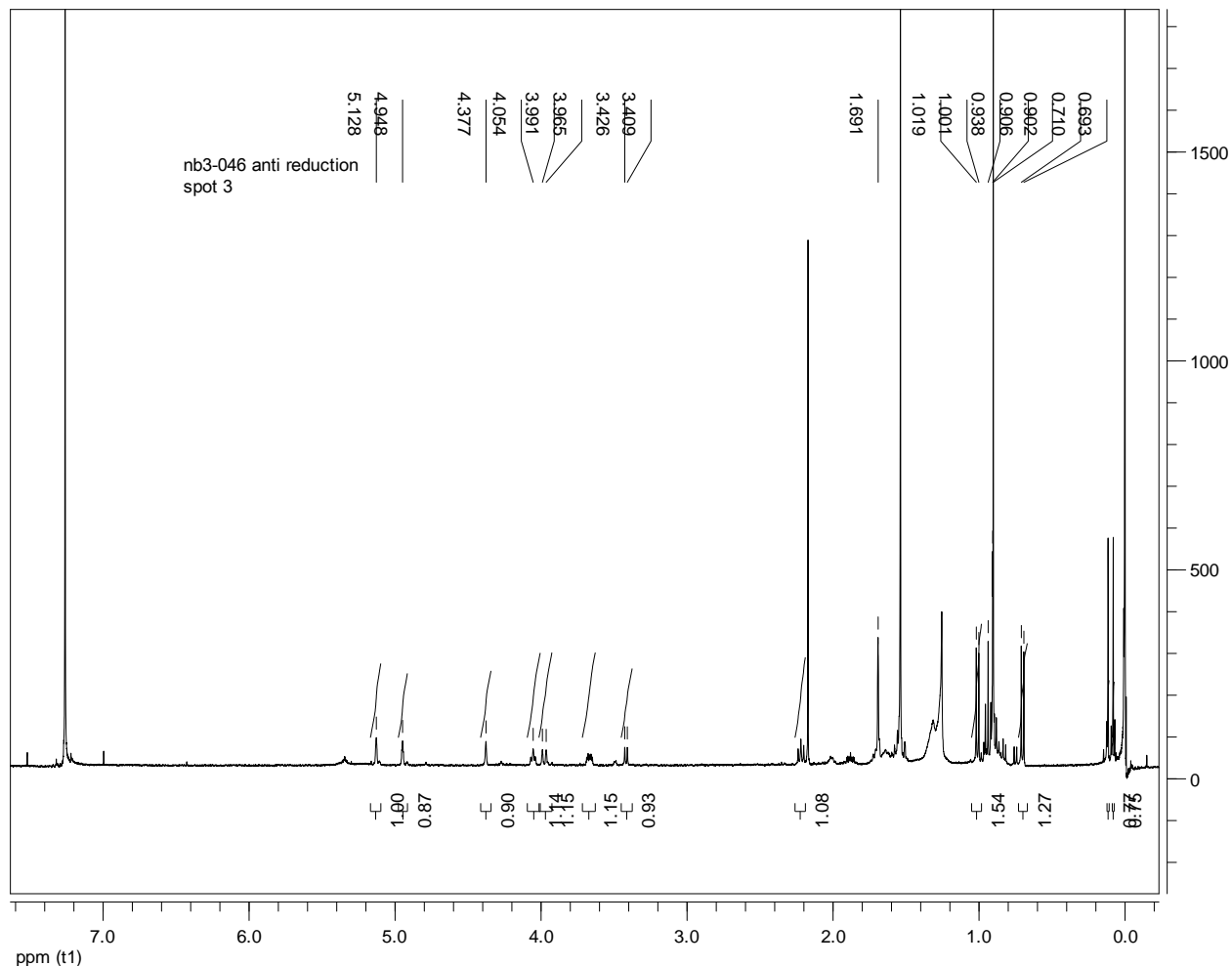
1.68 (s, 3H), 0.97 (t, 3H,  $J = 7.4$  Hz), 0.91 (d, 9H,  $J = 2.8$  Hz), 0.82 (d, 3H,  $J = 7.0$  Hz), 0.75 (d, 3H,  $J = 7.1$  Hz), 0.13 (s, 3H), 0.09 (s, 3H).



**(3S,4R,5R,6R,7R)-7-((*tert*-Butyldimethylsilyl)oxy)-2,4,6-trimethylnon-1-ene-3,5-diol (34-syn):**

Syn diastereomer:  $^1\text{H NMR}$  (400 M Hz,  $\text{CDCl}_3$ )  $\delta$  (ppm) 5.36-5.33 (m, 1H), 5.13 (s, 1H), 4.95 (s, 1H), 4.40 (s, 1H), 4.08-4.04 (m, 1H), 3.98 (d, 1H,  $J = 10.4$  Hz), 3.68-3.64 (m, 1H), 3.44 (d, 1H,  $J = 7.2$  Hz), 2.24-2.20 (m, 1H), 2.03-1.98 (m, 1H), 1.93-1.83 (m, 1H), 1.69 (s, 3H), 1.01 (d,

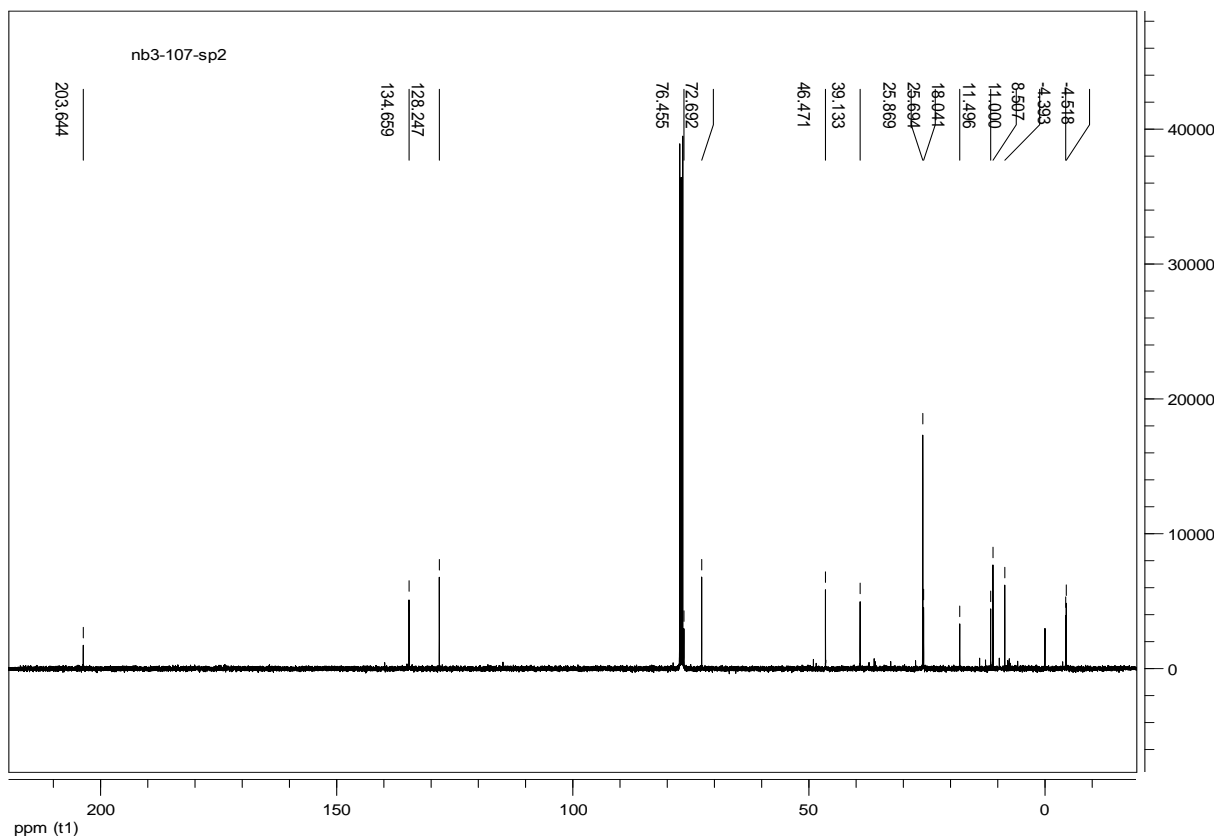
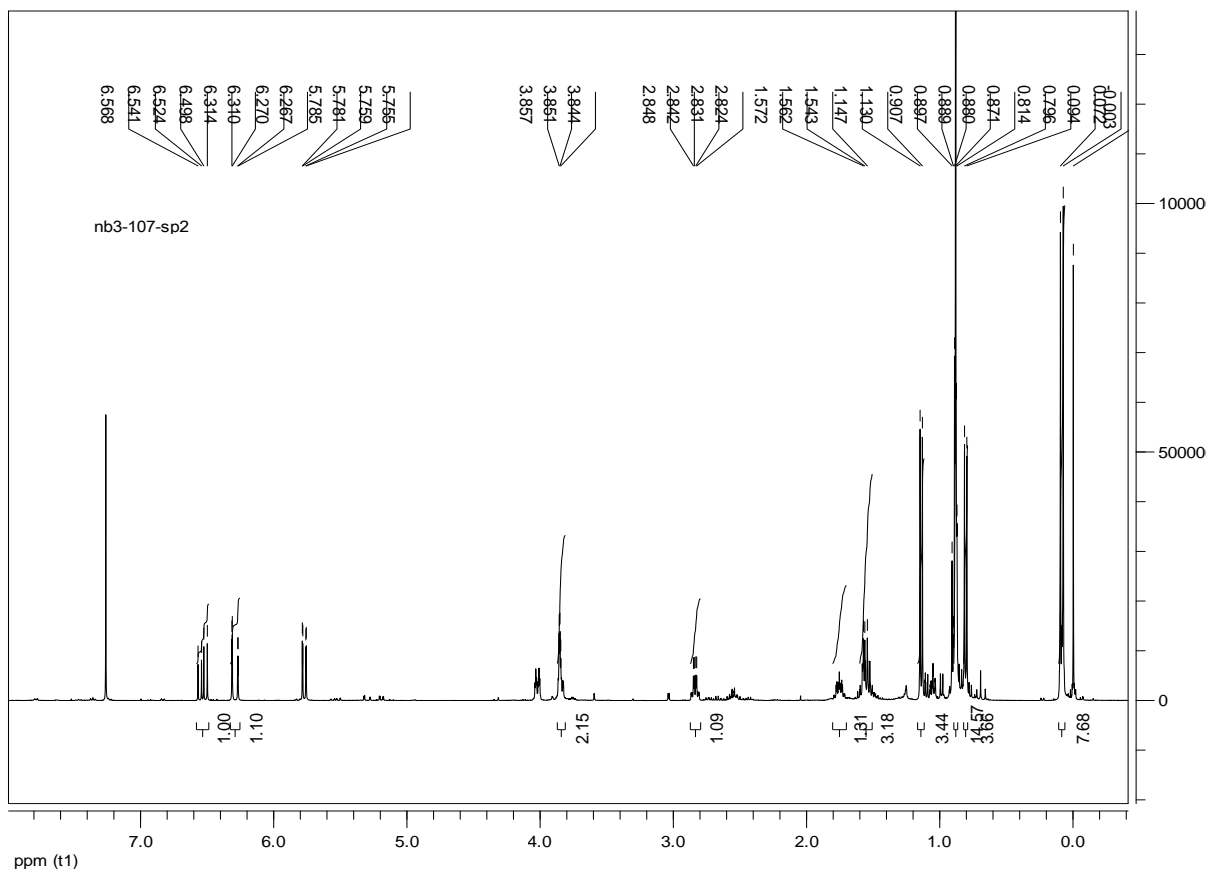
3H,  $J = 7.0$  Hz), 0.94 (t, 3H,  $J = 7.4$  Hz), 0.90 (s, 9H), 0.70 (d, 3H,  $J = 7.1$  Hz), 0.12 (s, 3H), 0.08 (s, 3H).

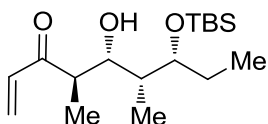
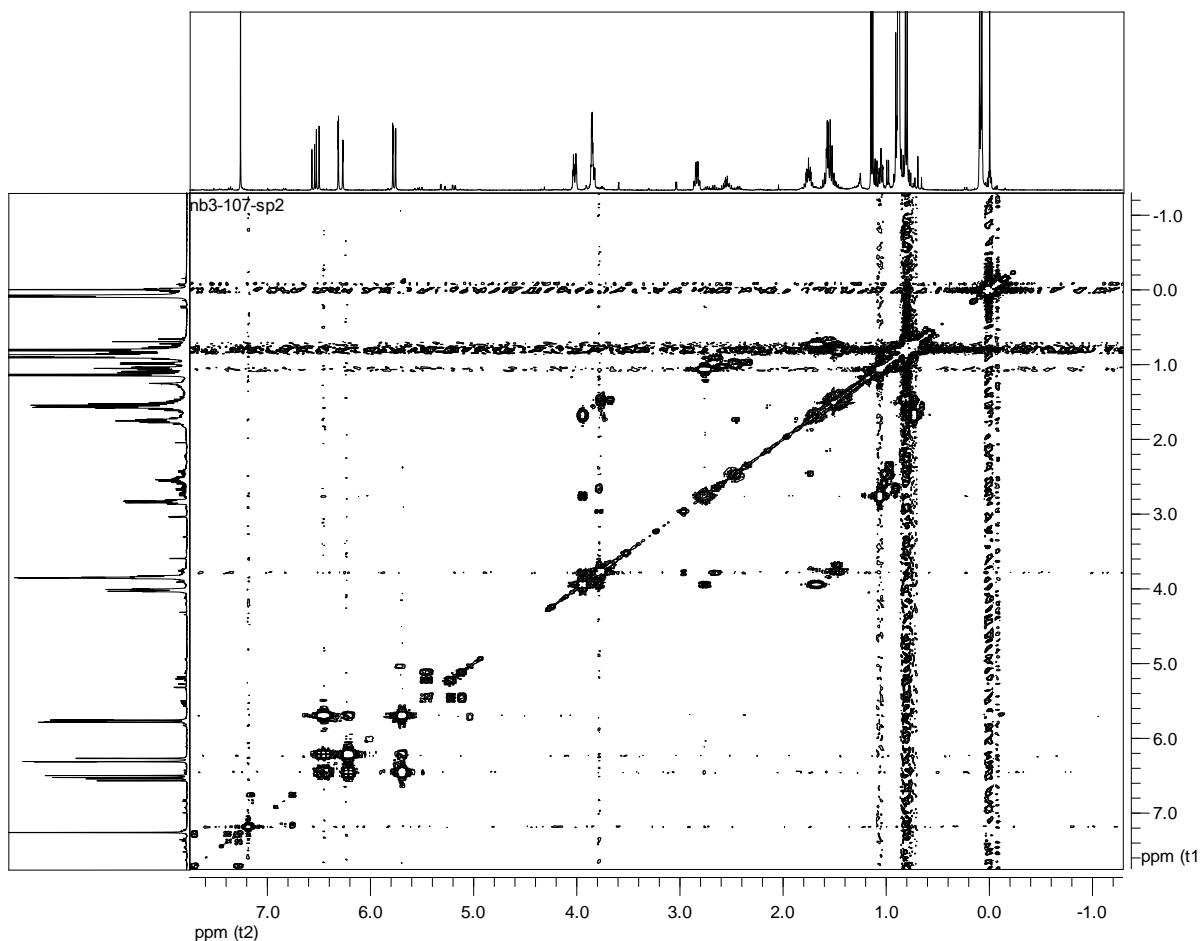


**(4R,5S,6R,7R)-7-((*tert*-Butyldimethylsilyl)oxy)-5-hydroxy-4,6-dimethylnon-1-en-3-one (30):**

According to a modified procedure<sup>132</sup>, under strictly anhydrous conditions, pent-1-en-3-one (178  $\mu$ L, 1.80 mmol) was dissolved in 18 mL of dry dichloromethane. At  $-78$   $^{\circ}$ C, dichlorophenylborane (distilled and stored in the glove box) (467  $\mu$ L, 3.60 mmol) was added followed by slow addition of anhydrous diisopropylethylamine (700  $\mu$ L, 4.05 mmol). The enolate formation was stirred at  $-78$   $^{\circ}$ C for 0.5 h and then at  $0$   $^{\circ}$ C for another 0.5 h. At  $-78$   $^{\circ}$ C, (2S,3R)-3-((*tert*-butyldimethylsilyl)oxy)-2-methylpentanal (0.225 g, 0.900 mmol) dissolved in 3

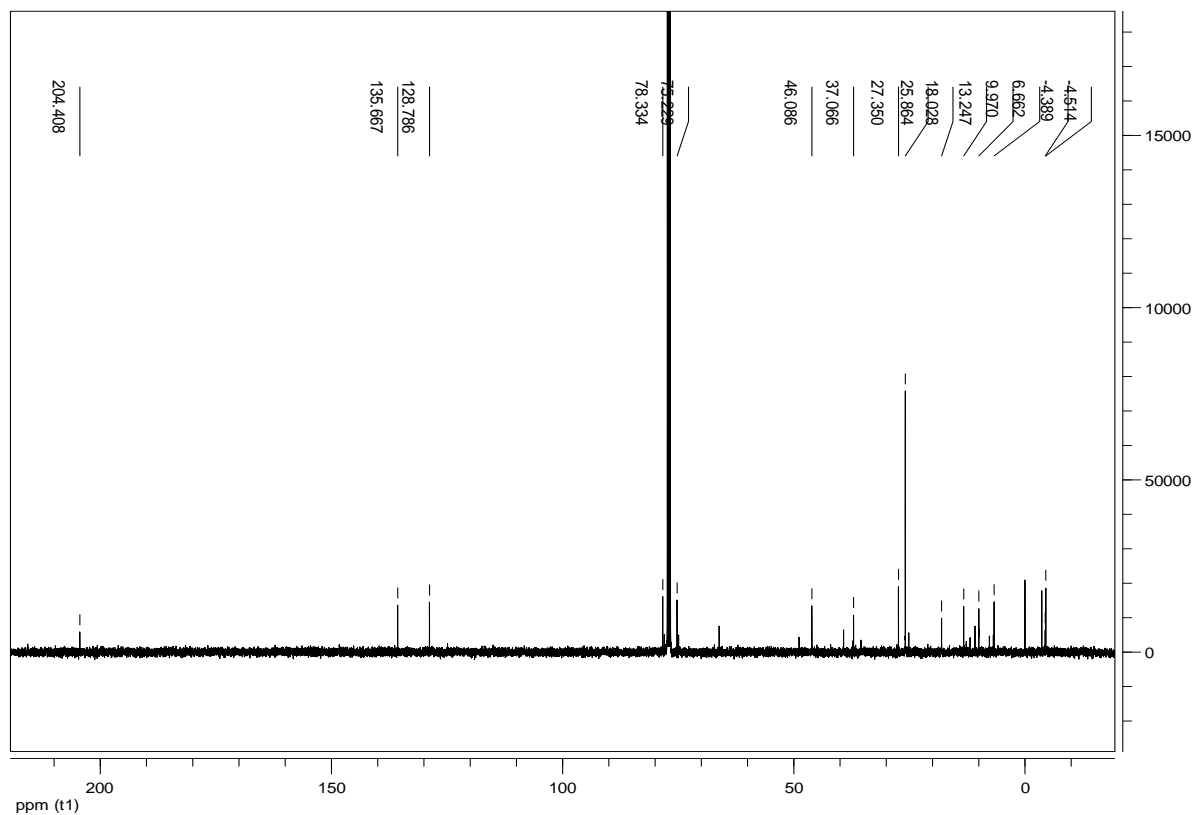
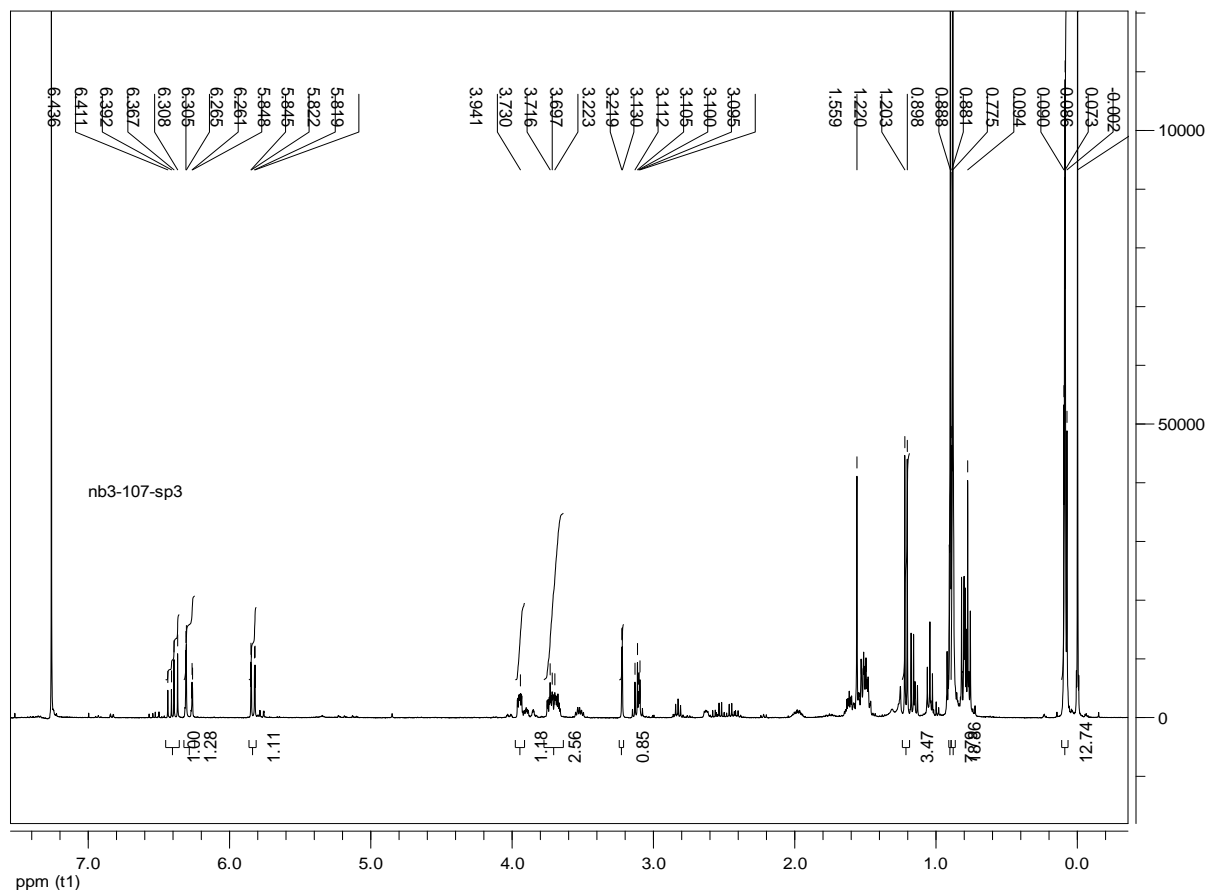
mL of dry dichloromethane was added via cannula to the enolate and was followed by two 0.5 mL washes. The reaction mixture was stirred at  $-78\text{ }^{\circ}\text{C}$  for 4 h and subsequently quenched at  $-78\text{ }^{\circ}\text{C}$  with 15 mL of a phosphate buffer at pH=7. Then, 5 mL of a 2:1 methanol/hydrogen peroxide mixture was added and stirred at room temperature for 4 h. The aqueous phase was extracted three times with dichloromethane. The combined organic phases were washed with brine. These aqueous phases were extracted three times with dichloromethane. The combined organic phases were dried over  $\text{Na}_2\text{SO}_4$ , filtered and evaporated. The crude product was purified by column chromatography with  $\text{Et}_3\text{N}$ -treated silica gel eluting with a 5%  $\text{Et}_2\text{O}$ /hexanes. 141.6 mg (50%) of a colourless oil was obtained. **Diastereoselectivity:** 2.2 : 1.  **$^1\text{H}$  NMR** (400 MHz,  $\text{CDCl}_3$ )  $\delta$  (ppm) 6.53 (dd, 1H,  $J = 10.4\text{ Hz}$ ,  $J = 17.4\text{ Hz}$ ), 6.29 (dd, 1H,  $J = 1.3\text{ Hz}$ ,  $J = 17.4\text{ Hz}$ ), 5.77 (dd, 1H,  $J = 1.3\text{ Hz}$ ,  $J = 10.5\text{ Hz}$ ), 4.02 (td, 1H,  $J = 2.4\text{ Hz}$ ,  $J = 9.5\text{ Hz}$ ), 3.88-3.81 (m, 2H), 2.84 (dq, 1H,  $J = 2.7\text{ Hz}$ ,  $J = 7.0\text{ Hz}$ ), 1.81-1.70 (m, 1H), 1.63-1.48 (m, 2H), 1.14 (d, 3H,  $J = 7.0\text{ Hz}$ ), 0.90-0.86 (m, 12H), 0.81 (d, 3H,  $J = 7.0\text{ Hz}$ ), 0.09 (s, 3H), 0.07 (s, 3H).  **$^{13}\text{C}\{^1\text{H}\}$  NMR** (100 MHz,  $\text{CDCl}_3$ )  $\delta$  (ppm) 203.6, 134.6, 128.2, 76.4, 72.7, 46.5, 39.1, 25.9, 25.7, 18.0, 11.5, 11.0, 8.5, -4.4, -4.5. **MS** (ESI+)  $m/z$  315 (M+H); **HRMS** (ESI+)  $m/z$  calc'd for  $\text{C}_{17}\text{H}_{35}\text{O}_3\text{Si}$  [M+H]<sup>+</sup>: 315.2356; found: 315.2350.

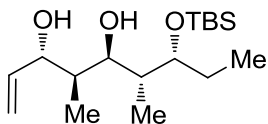
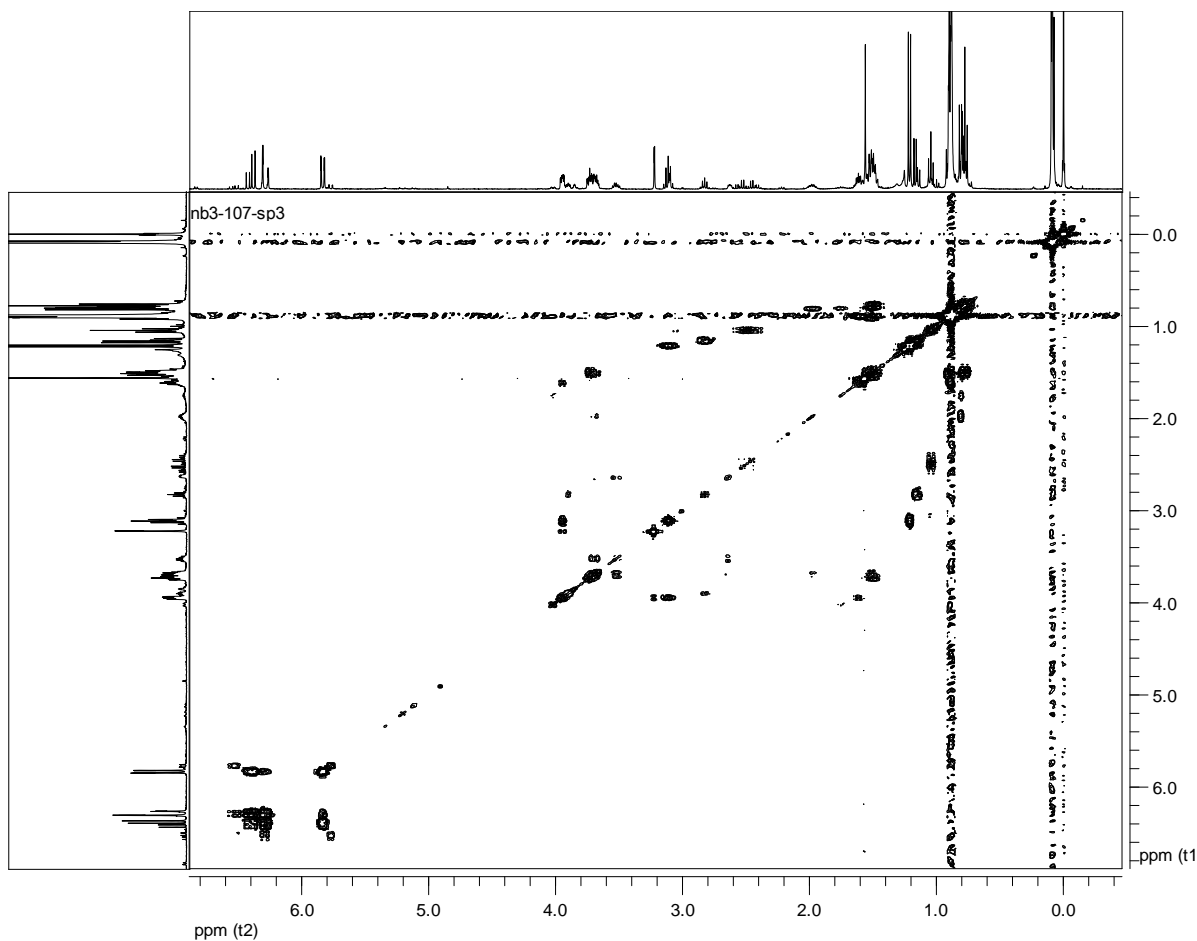




**(4R,5R,6R,7R)-7-((*tert*-Butyldimethylsilyl)oxy)-5-hydroxy-4,6-dimethylnon-1-en-3-one (31):**

According to the aldol protocol above, this diastereomer was obtained in varying yields.  $^1\text{H}$  NMR (400 MHz,  $\text{CDCl}_3$ )  $\delta$  (ppm) 6.40 (dd, 1H,  $J = 10.3$  Hz,  $J = 17.5$  Hz), 6.28 (dd, 1H,  $J = 1.4$  Hz,  $J = 17.5$  Hz), 5.83 (dd, 1H,  $J = 1.4$  Hz,  $J = 10.3$  Hz), 3.94 (ddd, 1H,  $J = 1.3$  Hz,  $J = 3.8$  Hz,  $J = 6.9$  Hz), 3.73 (ddd, 1H,  $J = 2.5$  Hz,  $J = 5.9$  Hz,  $J = 8.2$  Hz), 3.23 (d, 1H,  $J = 1.6$  Hz), 3.11 (p, 1H,  $J = 7.0$  Hz), 1.64-1.56 (m, 2H), 1.54-1.46 (m, 2H), 1.21 (d, 3H,  $J = 7.0$  Hz), 0.89 (d, 3H,  $J = 3.9$  Hz), 0.88 (s, 9H), 0.77 (t, 3H,  $J = 7.5$  Hz), 0.09-0.08 (m, 6H).  $^{13}\text{C}\{^1\text{H}\}$  NMR (100 MHz,  $\text{CDCl}_3$ )  $\delta$  (ppm) 204.4, 135.7, 128.8, 78.3, 75.2, 46.1, 37.1, 27.4, 25.9, 18.0, 13.2, 10.0, 6.7, -4.4, -4.5.

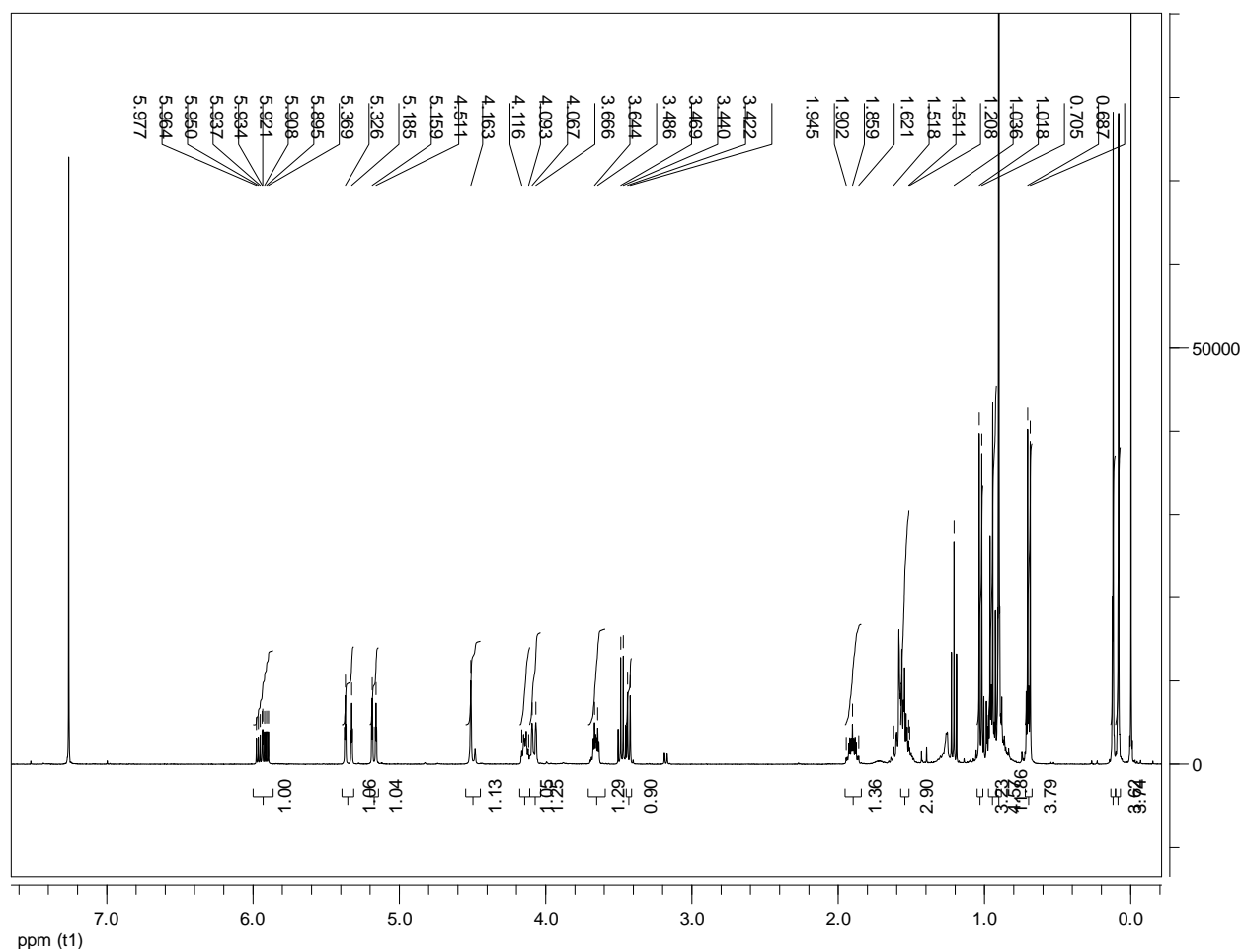




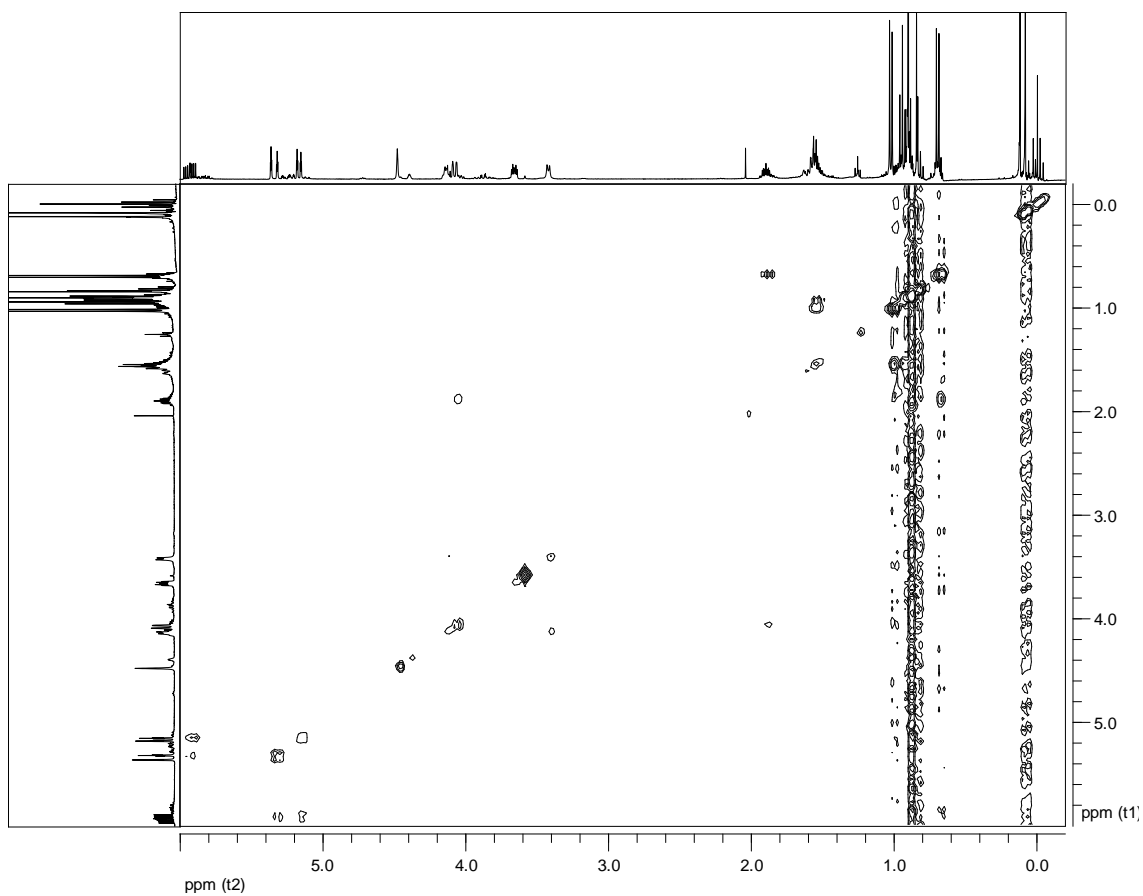
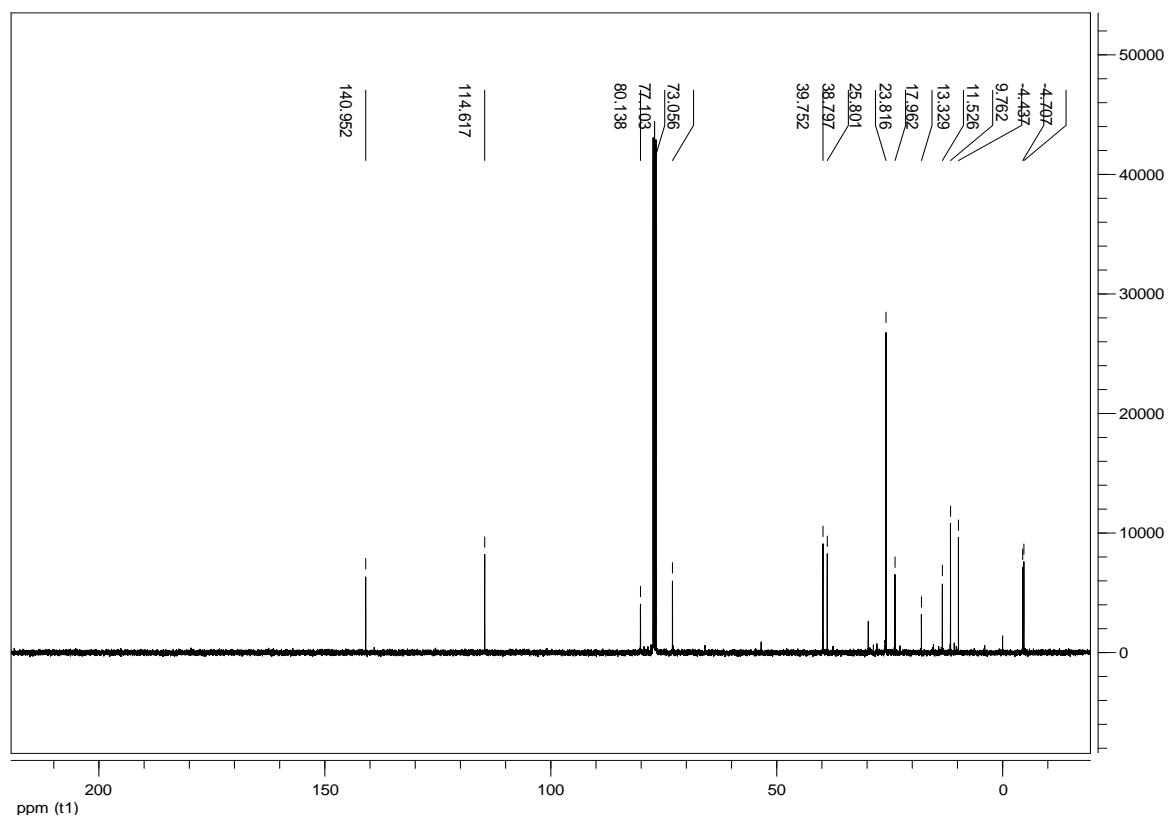
**(3S,4S,5R,6R,7R)-7-((*tert*-Butyldimethylsilyl)oxy)-4,6-dimethylnon-1-ene-3,5-diol (37-*anti*):**

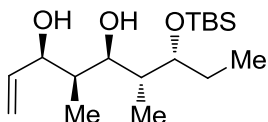
Under anhydrous reaction conditions, tetramethylammonium triacetoxyborohydride (847 mg, 3.22 mmol) was dissolved in 2.75 mL of dry acetonitrile and 2.75 mL of dry acetic acid. At  $-40^{\circ}\text{C}$  (ethylene glycol/ethanol bath), (4R,5S,6R,7R)-7-((*tert*-butyldimethylsilyl)oxy)-5-hydroxy-4,6-dimethylnon-1-en-3-one (219 mg, 0.696 mmol) in 1 mL of dry acetonitrile was slowly added via cannula, followed by a wash with 0.25 mL of acetonitrile. The reaction was stirred at  $-40^{\circ}\text{C}$  for 18 h. The reaction was quenched with 0.5 mL of 4-hydroxy-2-butanone (to consume unreacted borohydride). This mixture was stirred at room temperature for 0.5 h. Then, 8 mL of acetonitrile and 8 mL of glycerol were added and stirred for another 0.5 h. The reaction mixture was concentrated and basified with a 2M solution of sodium hydroxide. The aqueous phase was extracted three times with ether. The combined organic phases were dried over  $\text{Na}_2\text{SO}_4$ , filtered

and evaporated. The crude product was purified by column chromatography with Et<sub>3</sub>N-treated silica gel eluting with a 10% EtOAc/hexanes. 133 mg (61%) of a colourless oil was obtained. <sup>1</sup>H NMR (400 MHz, CDCl<sub>3</sub>) δ (ppm) 5.94 (ddd, 1H, *J* = 5.2 Hz, *J* = 10.5 Hz, *J* = 17.1 Hz), 5.35 (td, 1H, *J* = 1.7 Hz, *J* = 17.2 Hz), 5.17 (td, 1H, *J* = 1.7 Hz, *J* = 10.5 Hz), 4.51 (s, 1H), 4.17-4.12 (m, 1H), 4.08 (d, 1H, *J* = 10.3 Hz), 3.66 (td, 1H, *J* = 3.4 Hz, *J* = 8.8 Hz), 3.43 (d, 1H, *J* = 7.4 Hz), 1.94-1.86 (m, 1H), 1.62-1.51 (m, 2H), 1.03 (d, 3H, *J* = 7.0 Hz), 0.94 (t, 3H, *J* = 7.4 Hz), 0.90 (s, 9H), 0.70 (d, 3H, *J* = 7.1 Hz), 0.12 (s, 3H), 0.08 (s, 3H). <sup>13</sup>C{<sup>1</sup>H} NMR (100 MHz, CDCl<sub>3</sub>) δ (ppm) 141.0, 114.6, 80.1, 77.1, 73.1, 39.8, 38.8, 25.8, 23.8, 18.0, 13.3, 11.5, 9.8, -4.4, -4.7. MS (ESI+) *m/z* 317 (M+H); HRMS (ESI+) *m/z* calc'd for C<sub>17</sub>H<sub>37</sub>O<sub>3</sub>Si [M+H]<sup>+</sup>: 317.2512; found: 317.2510.





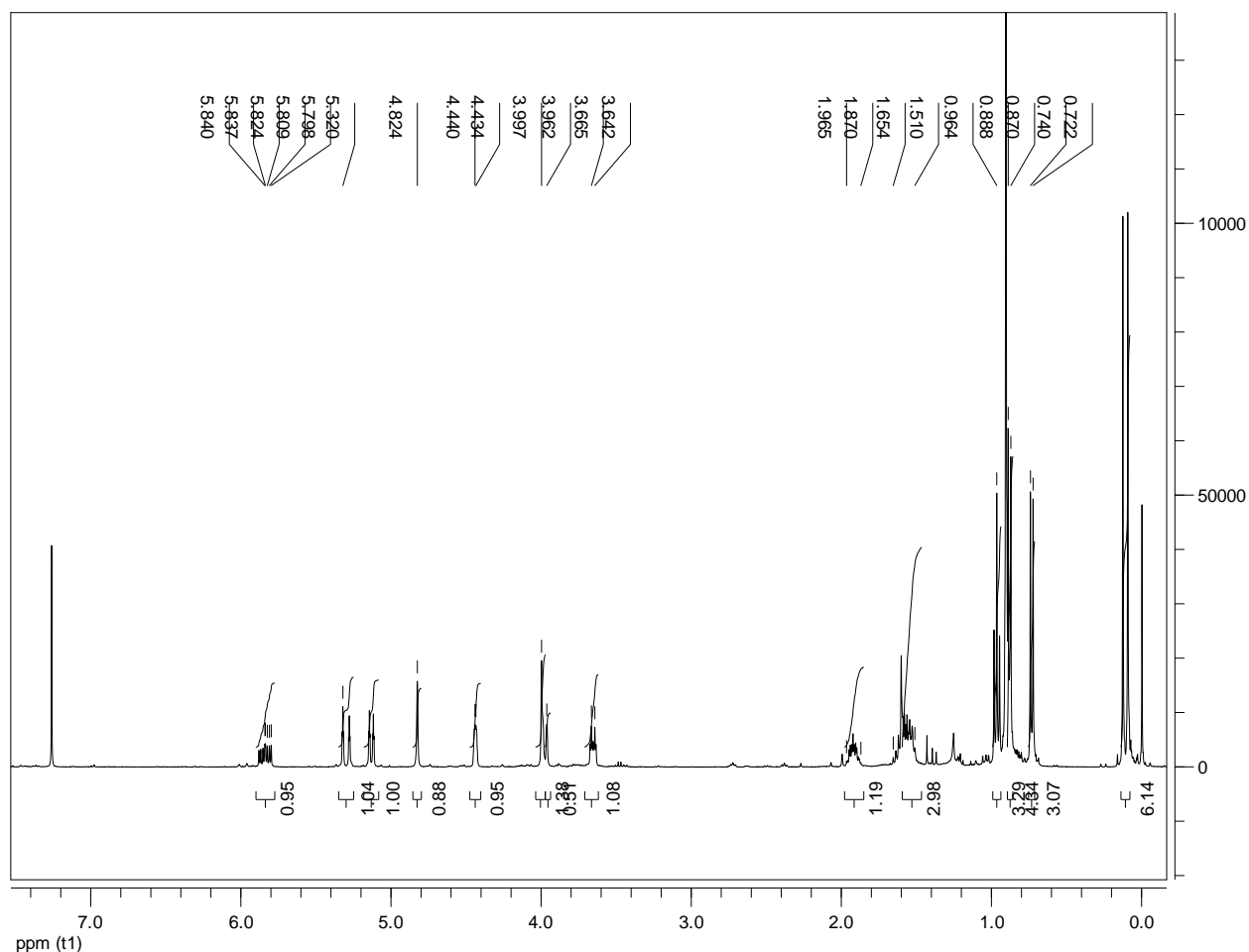


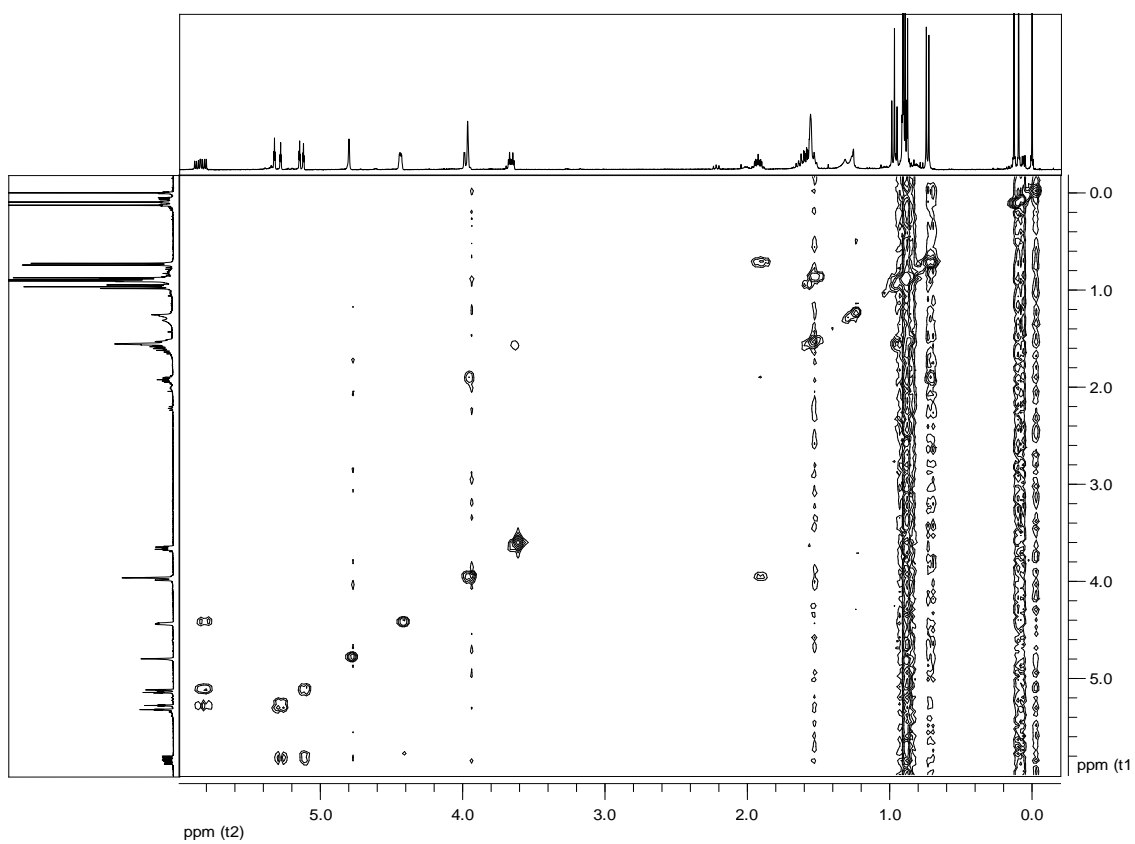
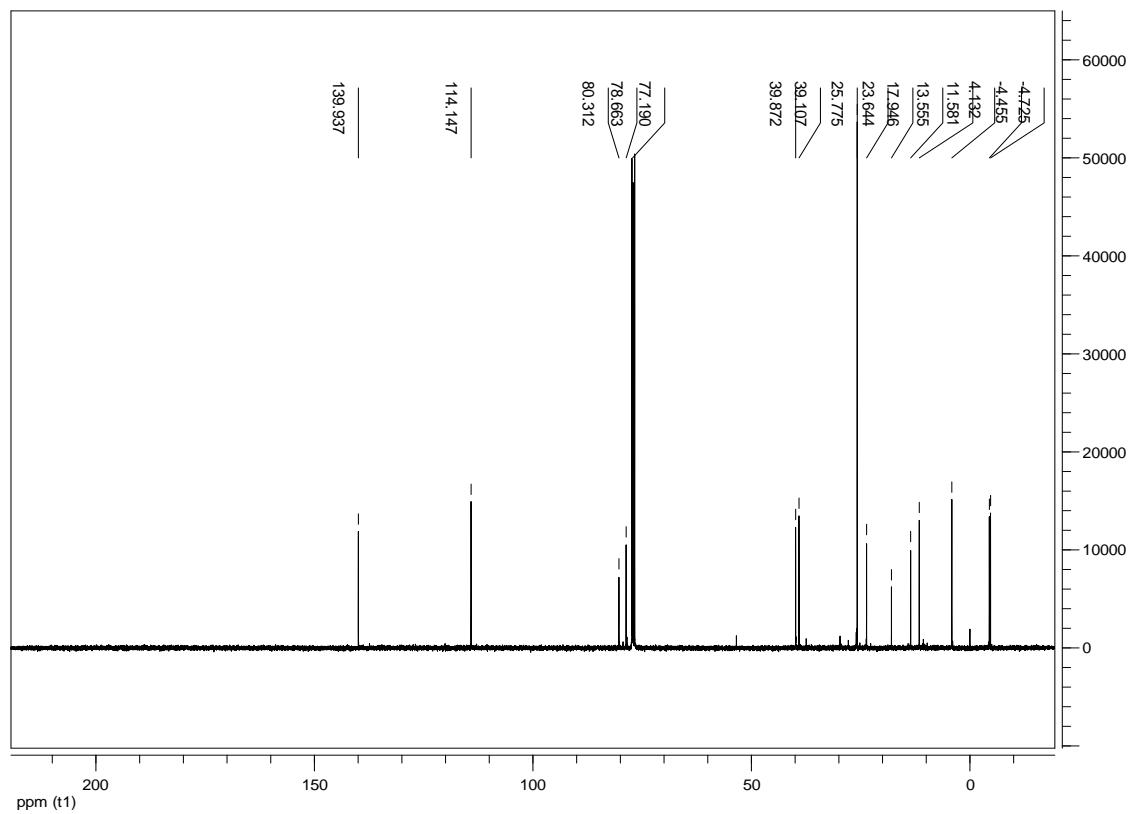


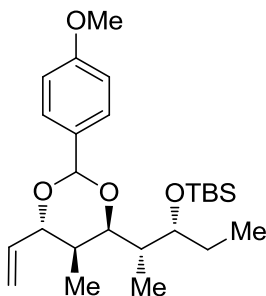
**(3R,4S,5R,6R,7R)-7-((*tert*-Butyldimethylsilyloxy)-4,6-dimethylnon-1-ene-3,5-diol (37-syn):**

According to the anti-reduction protocol above, 14.2 mg (6.5 %) of a colourless oil was obtained.

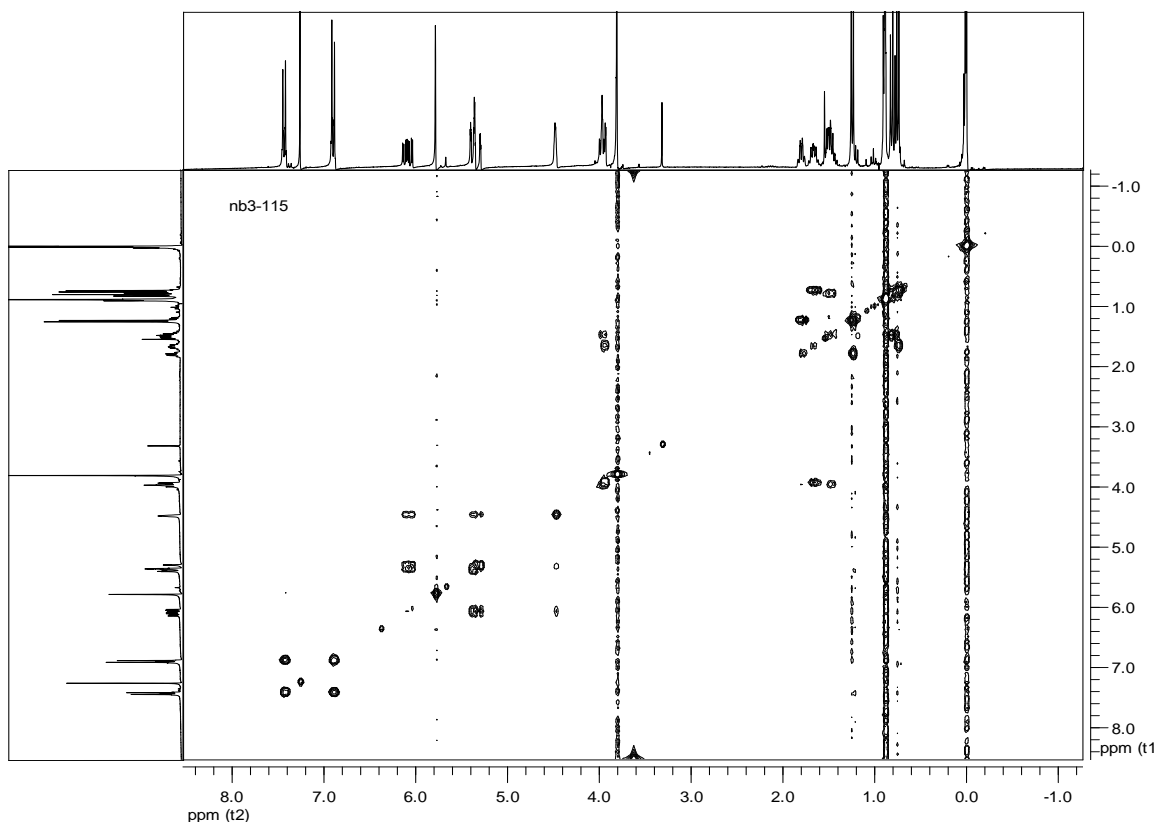
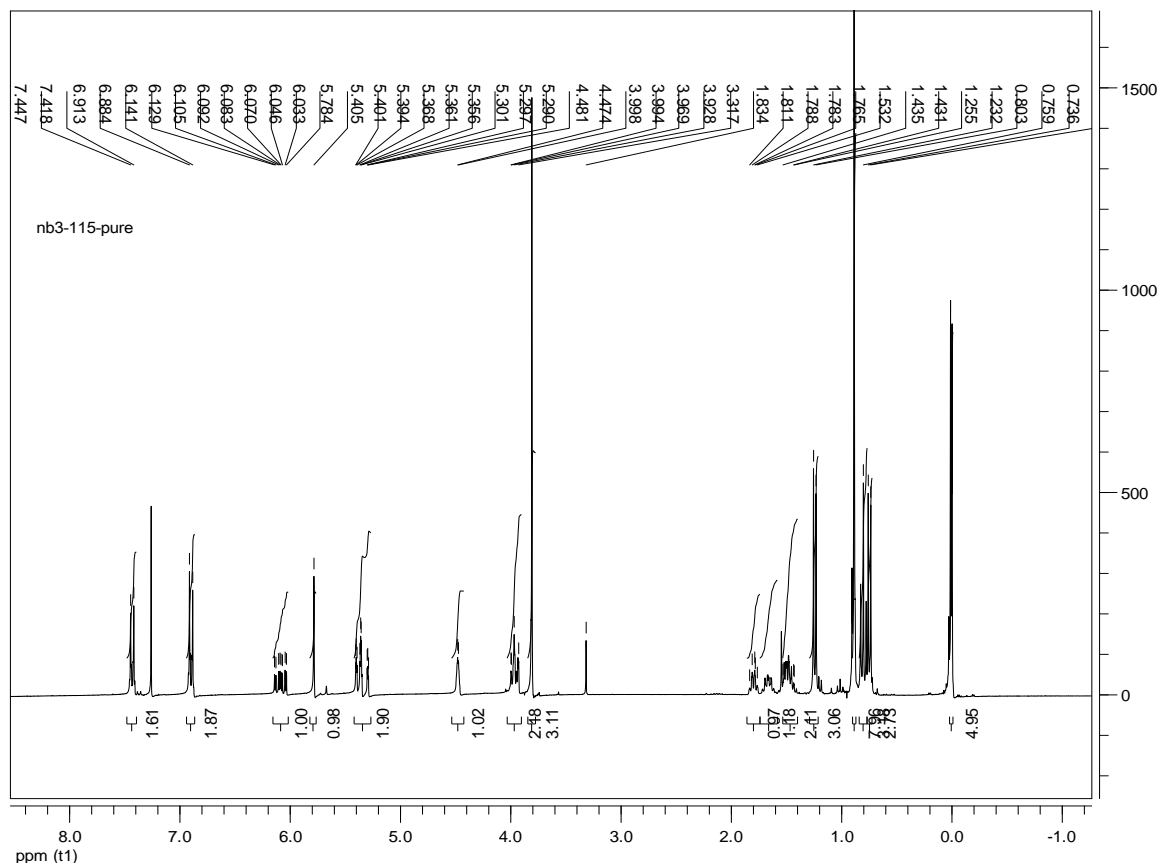
$^1\text{H NMR}$  (400 MHz,  $\text{CDCl}_3$ )  $\delta$  (ppm) 5.84 (ddd, 1H,  $J = 4.8$  Hz,  $J = 10.6$  Hz,  $J = 16.9$  Hz), 5.30 (td, 1H,  $J = 1.7$  Hz,  $J = 17.2$  Hz), 5.13 (td, 1H,  $J = 1.7$  Hz,  $J = 10.6$  Hz), 4.82 (s, 1H), 4.45-4.43 (m, 1H), 4.00 (s, 1H), 3.96 (s, 1H), 3.65 (td, 1H,  $J = 3.2$  Hz,  $J = 9.2$  Hz), 1.96-1.87 (m, 1H), 1.65-1.51 (m, 2H), 0.96 (t, 3H,  $J = 7.4$  Hz), 0.90 (s, 9H), 0.88 (d, 3H,  $J = 7.0$  Hz), 0.73 (d, 3H,  $J = 7.1$  Hz), 0.12 (s, 3H), 0.09 (s, 3H).  $^{13}\text{C}\{^1\text{H}\}$  NMR (100 MHz,  $\text{CDCl}_3$ )  $\delta$  (ppm) 140.0, 114.1, 80.3, 78.7, 77.2, 39.9, 39.1, 25.8, 23.6, 17.9, 13.6, 11.6, 4.1, -4.4, -4.7. **MS** (ESI+)  $m/z$  317 (M+H); HRMS (ESI+)  $m/z$  calc'd for  $\text{C}_{17}\text{H}_{37}\text{O}_3\text{Si}$  [M+H] $^+$ : 317.2512; found: 317.2513.

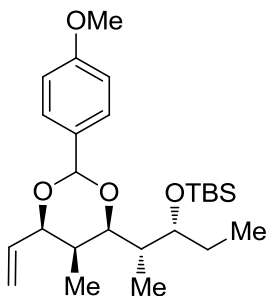




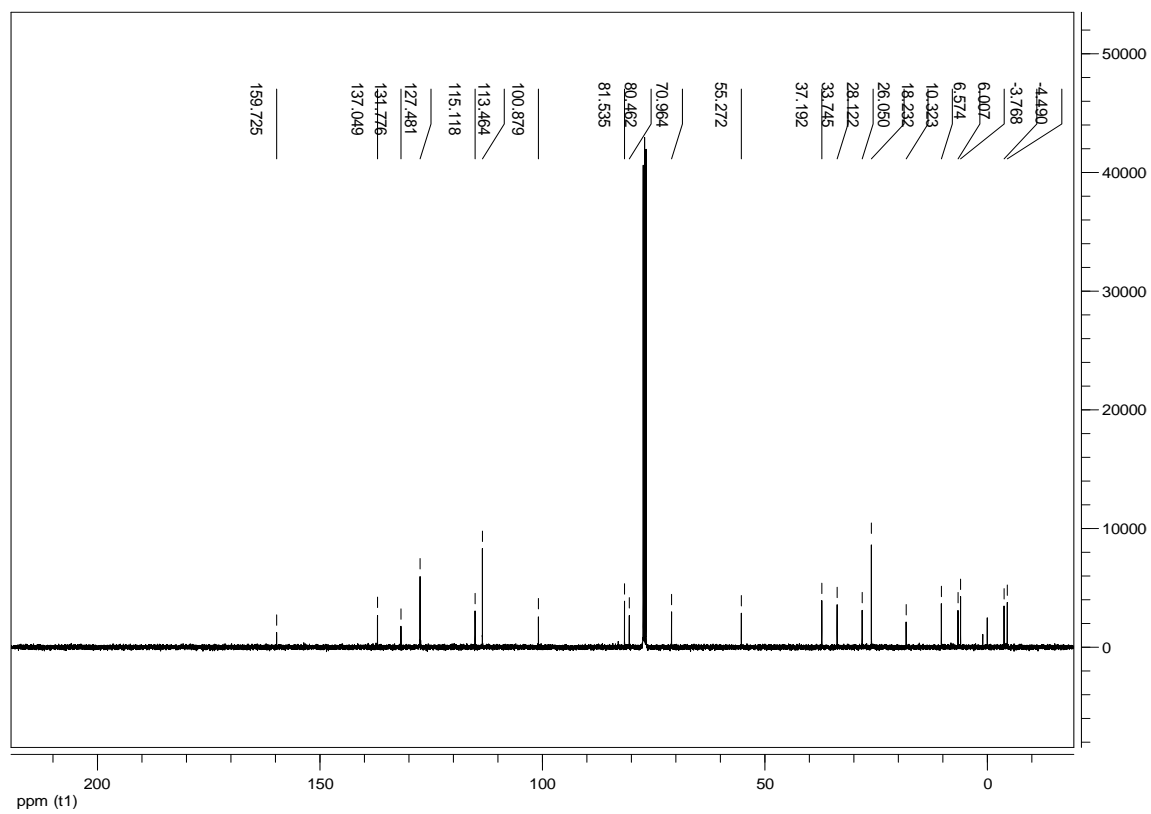
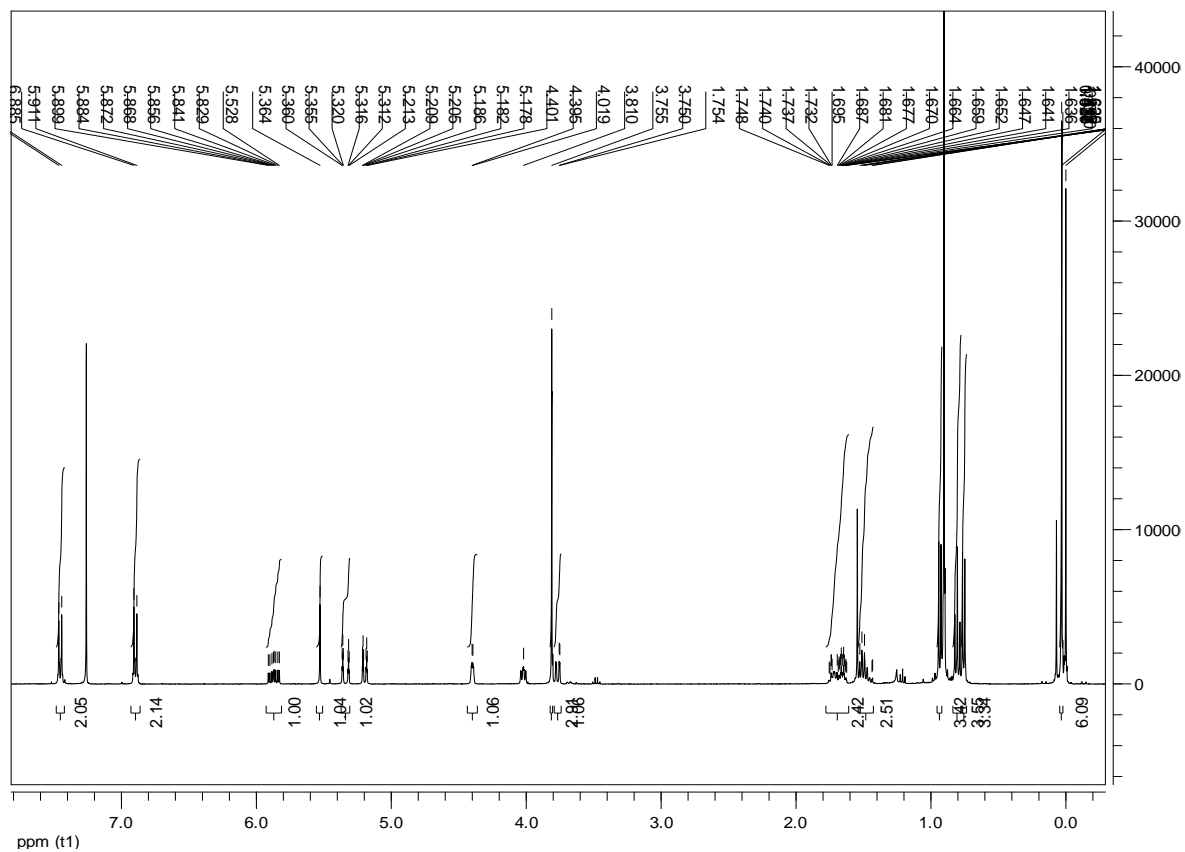


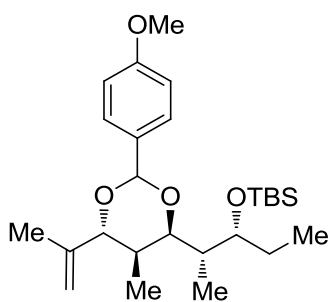
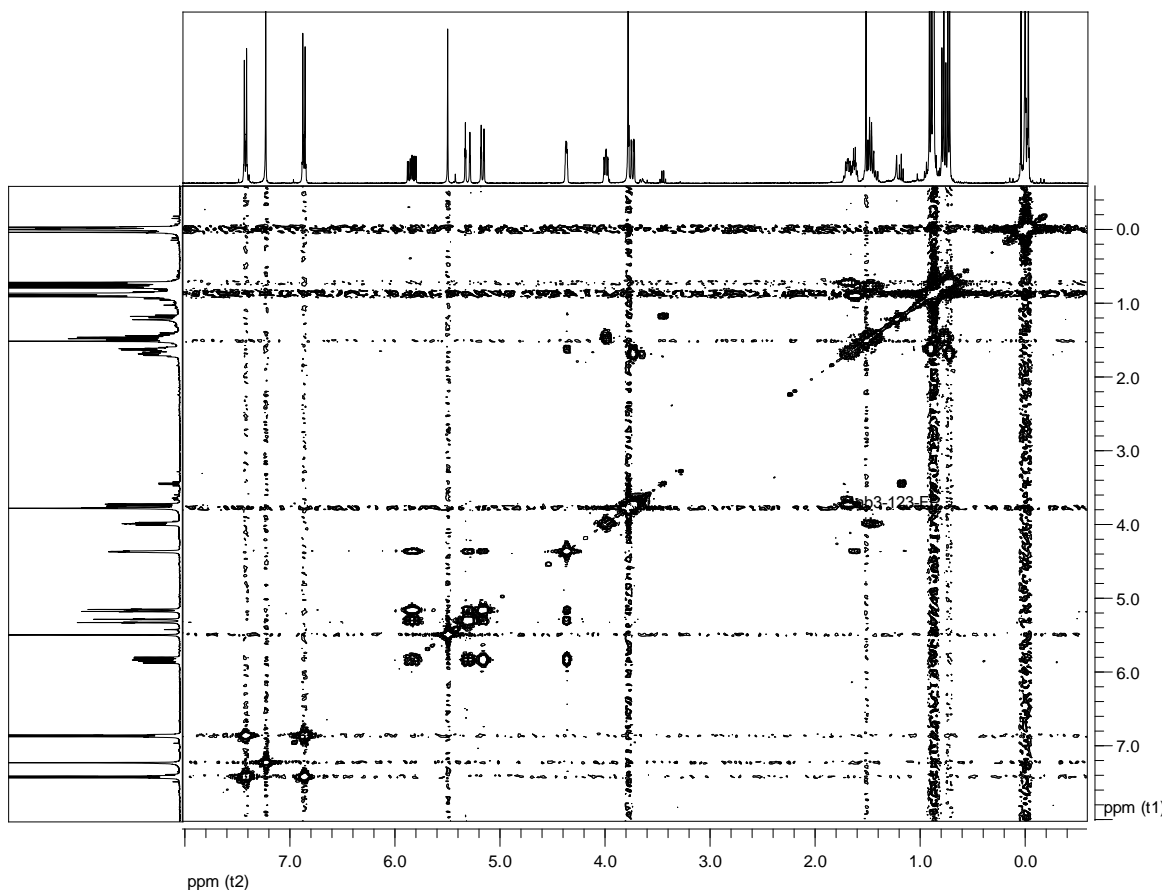
***tert*-Butyl(((2*R*,3*R*)-2-(((4*R*,5*S*,6*S*)-2-(4-methoxyphenyl)-5-methyl-6-vinyl-1,3-dioxan-4-yl)pentan-3-yl)oxy)dimethylsilane (38-*anti*):** According to a modified procedure,<sup>133</sup> under anhydrous conditions, (3*S*,4*S*,5*R*,6*R*,7*R*)-7-((*tert*-butyldimethylsilyl)oxy)-4,6-dimethylnon-1-ene-3,5-diol (123 mg, 0.388 mmol) was dissolved in 1 mL of dry dichloromethane. Then, at room temperature, pyridinium *p*-toluenesulfonate (5 mg, 0.02 mmol) was added followed by 1-(dimethoxymethyl)-4-methoxybenzene (99  $\mu$ L, 0.58 mmol). The reaction mixture was stirred at 35 °C for 15 h after which another equivalent of 1-(dimethoxymethyl)-4-methoxybenzene and PPTs were added. After a total of 29 h, the reaction was cooled to room temperature and passed through a plugged pipette with silica gel, eluting with dichloromethane. The crude mixture was evaporated and purified by column chromatography with Et<sub>3</sub>N-treated silica gel eluting with a 5% Et<sub>2</sub>O/hexanes. 162 mg (96%) of a colourless oil was obtained. <sup>1</sup>H NMR (400 MHz, CDCl<sub>3</sub>)  $\delta$  (ppm) 7.43 (d, 2H, *J* = 8.6Hz), 6.90 (d, 2H, *J* = 8.8Hz), 6.09 (ddd, 1H, *J* = 3.8 Hz, *J* = 11.0 Hz, *J* = 17.6 Hz), 5.78 (s, 1H), 5.41-5.29 (m, 2H), 4.48 (d, 1H, *J* = 2.1 Hz), 4.00-3.93 (m, 2H), 3.81 (s, 3H), 1.80 (qt, 1H, *J* = 2.0 Hz, *J* = 9.2 Hz), 1.67 (dq, 1H, *J* = 1.0 Hz, *J* = 6.7 Hz, *J* = 13.6 Hz), 1.53-1.43 (m, 2H), 1.24 (d, 3H, *J* = 6.9 Hz), 0.89 (s, 9H), 0.80 (t, 3H, *J* = 7.5 Hz), 0.75 (d, 3H, *J* = 6.9 Hz), 0.01 (s, 3H), 0.00 (s, 3H).





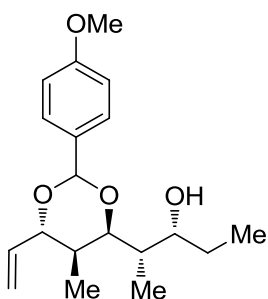
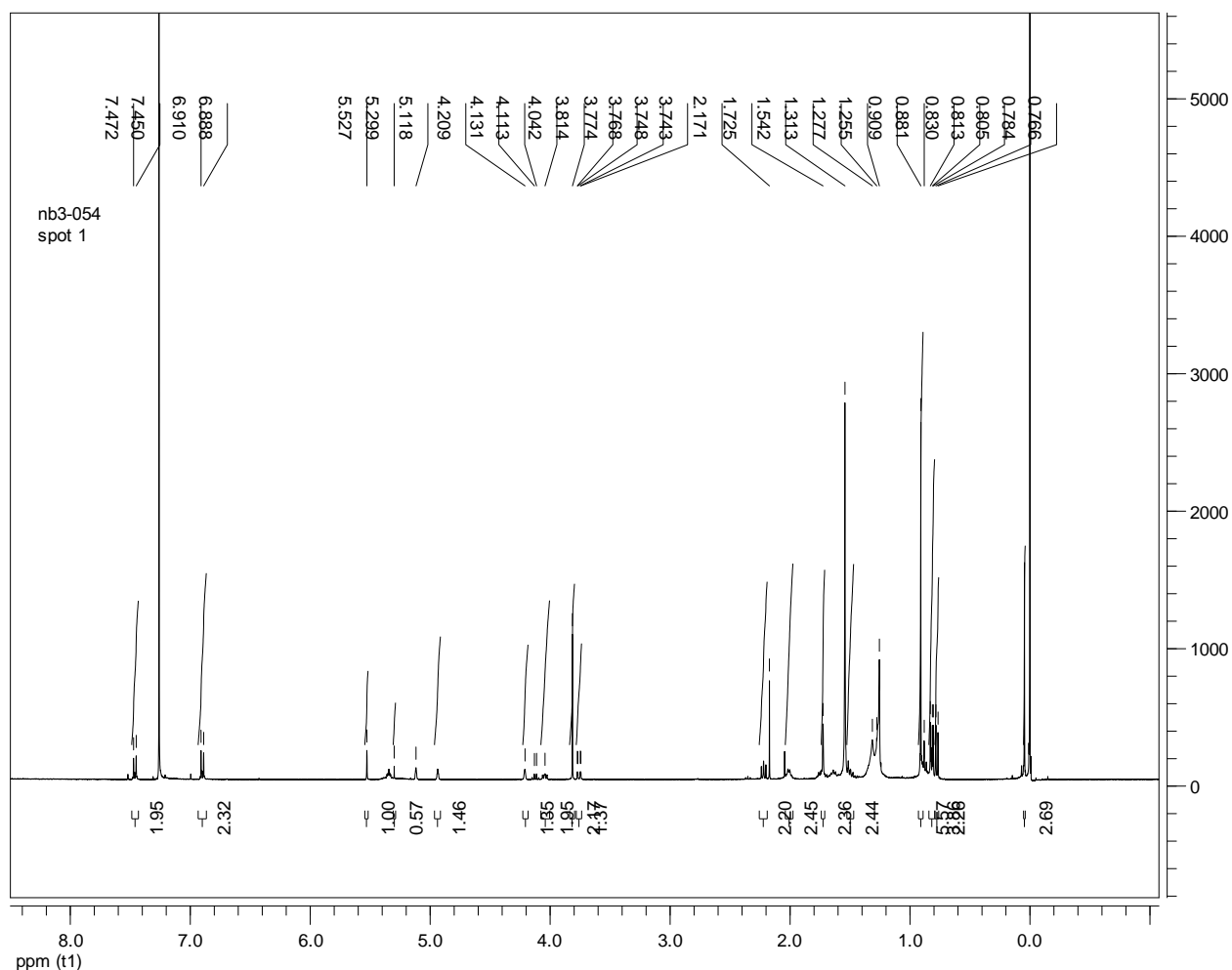
***tert*-Butyl(((2R,3R)-2-(((4R,5S,6R)-2-(4-methoxyphenyl)-5-methyl-6-vinyl-1,3-dioxan-4-yl)pentan-3-yl)oxy)dimethylsilane (38-syn):** According to the above procedure, 0.033 mmol of (3R,4S,5R,6R,7R)-7-((*tert*-butyldimethylsilyl)oxy)-4,6-dimethylnon-1-ene-3,5-diol yielded 7.7 mg (54%) of a colourless oil.  $^1\text{H NMR}$  (400 MHz,  $\text{CDCl}_3$ )  $\delta$  (ppm) 7.45 (d, 2H,  $J = 8.7$  Hz), 6.90 (d, 2H,  $J = 8.8$  Hz), 5.87 (ddd, 1H,  $J = 4.7$  Hz,  $J = 10.8$  Hz,  $J = 17.3$  Hz), 5.53 (s, 1H), 5.34 (td, 1H,  $J = 1.7$  Hz,  $J = 17.4$  Hz), 5.20 (td, 1H,  $J = 1.7$  Hz,  $J = 10.8$  Hz), 4.40 (dd, 1H,  $J = 2.2$  Hz,  $J = 4.5$  Hz), 4.02 (ddd, 1H,  $J = 1.1$  Hz,  $J = 5.9$  Hz,  $J = 8.3$  Hz), 3.81 (s, 3H), 3.77 (dd, 1H,  $J = 2.0$  Hz,  $J = 10.1$  Hz), 1.75-1.62 (m, 2H), 1.53-1.43 (m, 2H), 0.93 (d, 3H,  $J = 6.8$  Hz), 0.90 (s, 9H), 0.80 (t, 3H,  $J = 7.5$  Hz), 0.76 (d, 3H,  $J = 6.9$  Hz), 0.03 (s, 6H).  $^{13}\text{C}\{^1\text{H}\}$  NMR (100 MHz,  $\text{CDCl}_3$ )  $\delta$  (ppm) 159.7, 137.0, 131.8, 127.5, 115.1, 113.5, 100.9, 81.5, 80.5, 71.0, 55.3, 37.2, 33.7, 28.1, 26.0, 18.2, 10.3, 6.57, 6.0, -3.8, -4.5.





***tert*-Butyl(((2*R*,3*R*)-2-((4*R*,5*R*,6*R*)-2-(4-methoxyphenyl)-5-methyl-6-(prop-1-en-2-yl)-1,3-dioxan-4-yl)pentan-3-yl)oxy)dimethylsilane (35-*anti*):** According to the above procedure, 0.006 mmol of (4*R*,5*R*,6*R*,7*R*)-7-((*tert*-butyldimethylsilyl)oxy)-2,4,6-trimethylnon-1-ene-3,5-diol yielded 0.3 mg of a white solid.  $^1\text{H NMR}$  (400 MHz,  $\text{CDCl}_3$ )  $\delta$  (ppm) see spectrum.

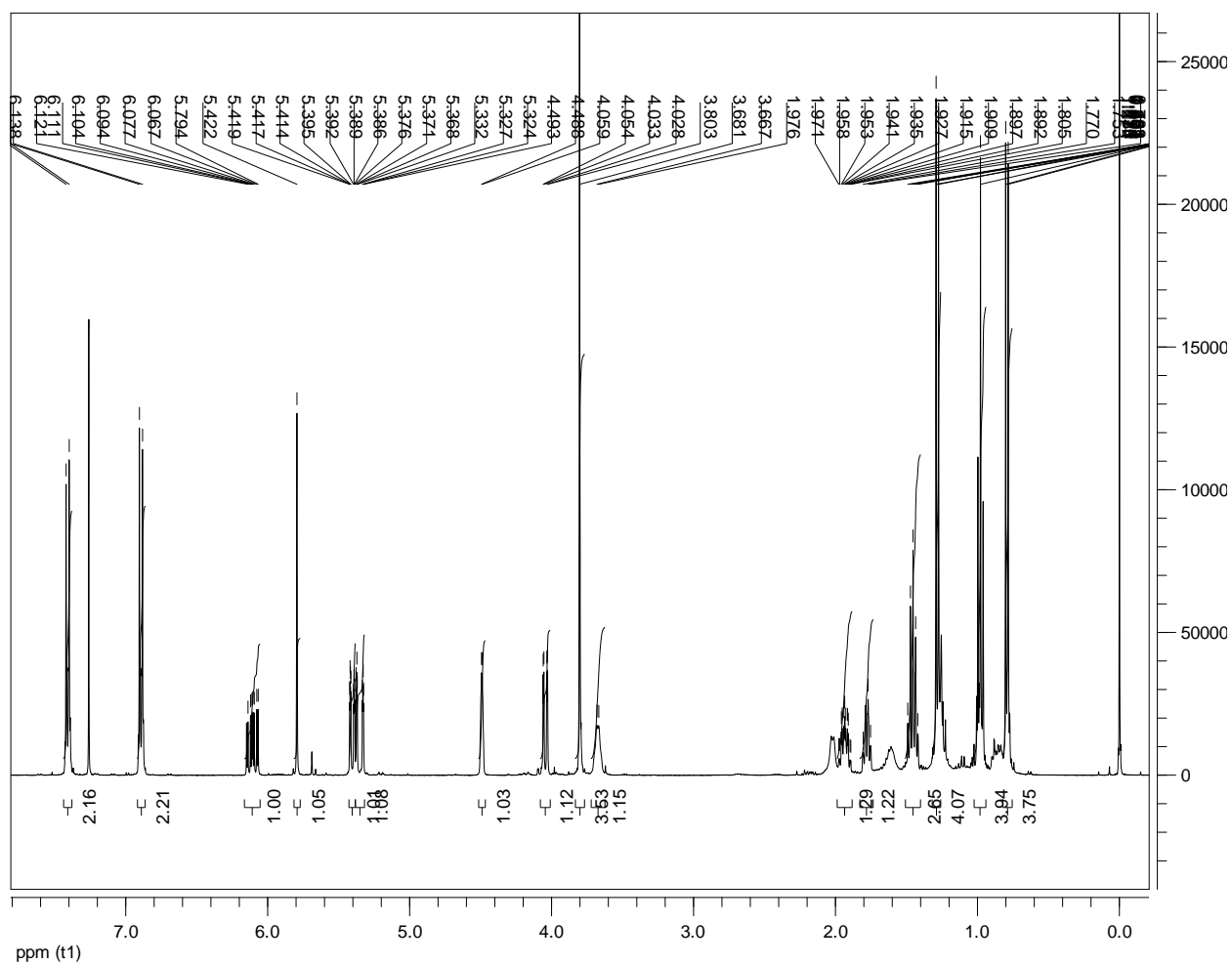


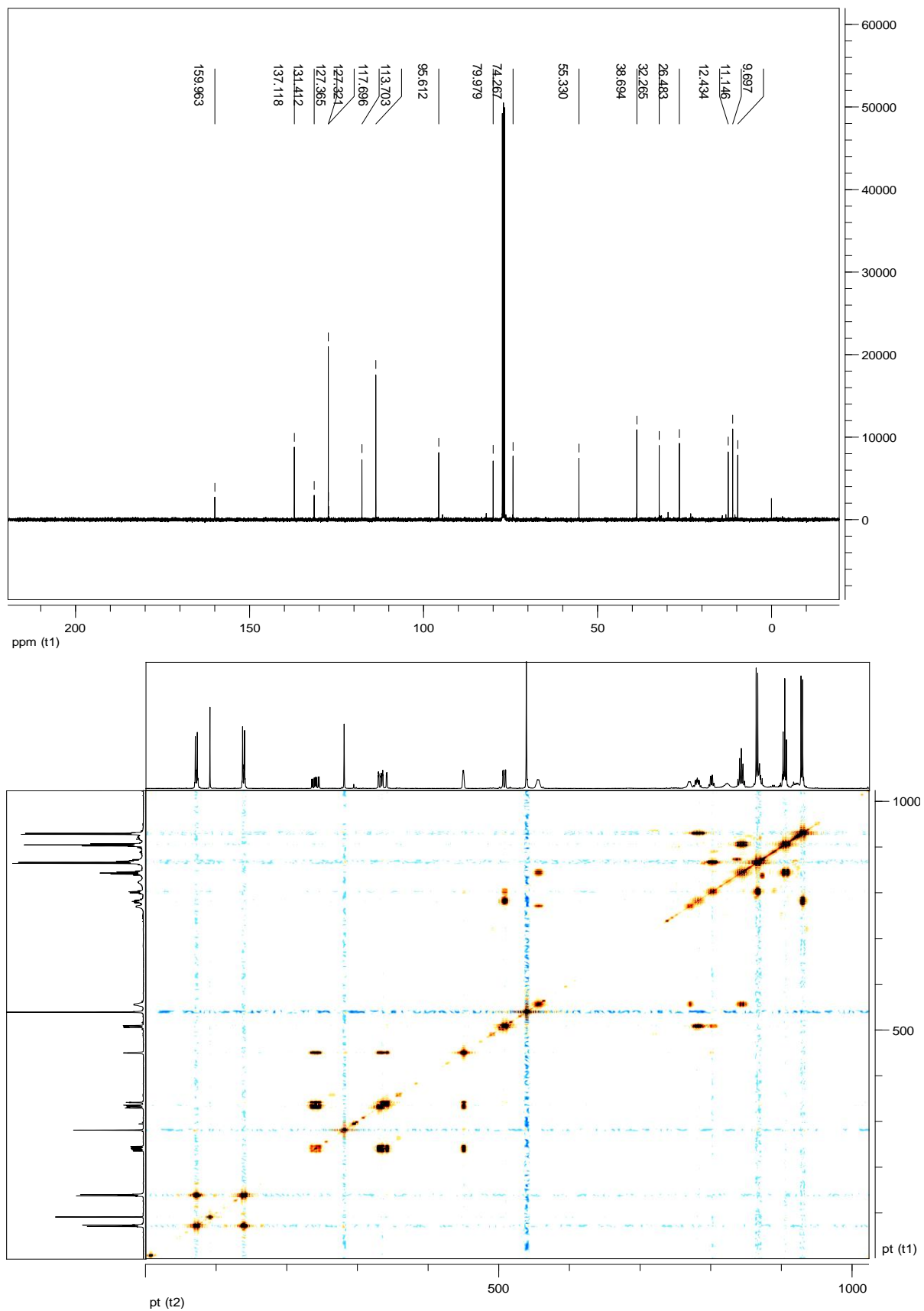


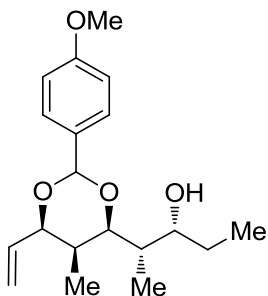
**(2S,3R)-2-((4S,5S,6S)-2-(4-Methoxyphenyl)-5-methyl-6-vinyl-1,3-dioxan-4-yl)pentan-3-ol**

**(39-anti):** According to a modified procedure,<sup>134</sup> under anhydrous conditions, *tert*-butyl(((2R,3R)-2-((4R,5S,6S)-2-(4-methoxyphenyl)-5-methyl-6-vinyl-1,3-dioxan-4-yl)pentan-3-yl)oxy)dimethylsilane (157 mg, 0.360 mmol) was dissolved in 7 mL of dry tetrahydrofuran. At 0 °C, a room temperature solution of *tert*-butylammonium fluoride (1.08 mL, 1M solution in THF) was added. This reaction mixture was stirred at room temperature for 15 mins and then heated to reflux for 18 h. The reaction mixture was cooled to room temperature and quenched with 6 mL

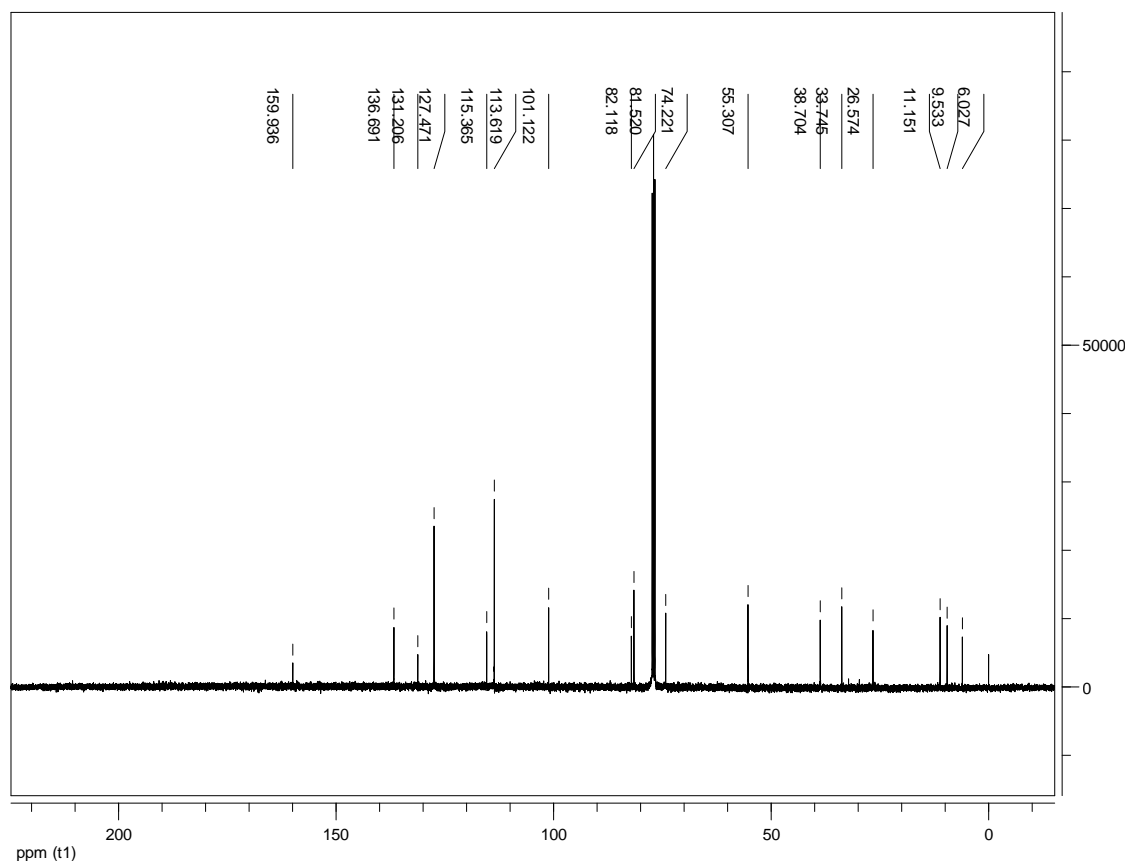
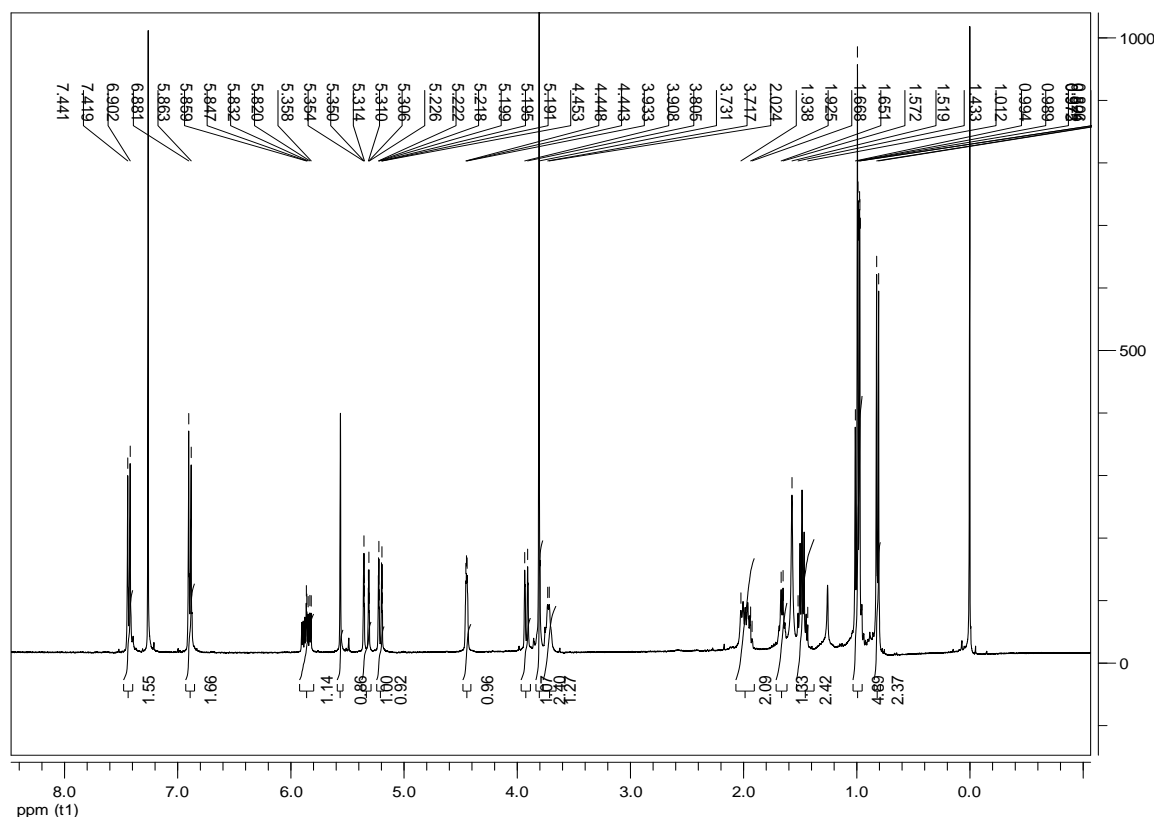
of a saturated solution of ammonium chloride. The aqueous phase was extracted three times with ether. The combined organic phases were dried over  $\text{Na}_2\text{SO}_4$ , filtered and evaporated. The crude product was purified by column chromatography with  $\text{Et}_3\text{N}$ -treated silica gel eluting with a 25%  $\text{Et}_2\text{O}$ /hexanes. 99.1 mg (86%) of a colourless oil was obtained.  $^1\text{H NMR}$  (400 MHz,  $\text{CDCl}_3$ )  $\delta$  (ppm) 7.41 (d, 2H,  $J = 8.7$  Hz), 6.89 (d, 2H,  $J = 8.8$  Hz), 6.11 (ddd, 1H,  $J = 3.9$  Hz,  $J = 11.0$  Hz,  $J = 17.6$  Hz), 5.79 (s, 1H), 5.40 (ddd, 1H,  $J = 1.2$  Hz,  $J = 2.2$  Hz,  $J = 11.0$  Hz), 5.35 (ddd, 1H,  $J = 1.3$  Hz,  $J = 2.0$  Hz,  $J = 17.6$  Hz), 4.49 (d, 1H,  $J = 2.1$  Hz), 4.04 (dd, 1H,  $J = 2.0$  Hz,  $J = 10.4$  Hz), 3.80 (s, 3H), 3.67 (d, 1H,  $J = 5.4$  Hz), 1.93 (ddd, 1H,  $J = 2.0$  Hz,  $J = 7.2$  Hz,  $J = 14.0$  Hz), 1.81-1.75 (m, 1H), 1.50-1.41 (m, 2H), 1.28 (d, 3H,  $J = 7.0$  Hz), 0.98 (t, 3H,  $J = 7.4$  Hz), 0.79 (d, 3H,  $J = 7.1$  Hz).  $^{13}\text{C}\{^1\text{H}\}$  NMR (100 MHz,  $\text{CDCl}_3$ )  $\delta$  (ppm) 160.0, 137.1, 131.4, 127.4, 127.3, 117.7, 113.7, 95.6, 80.0, 74.3, 55.3, 38.7, 32.3, 26.5, 12.4, 11.1, 9.7.

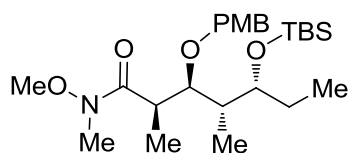
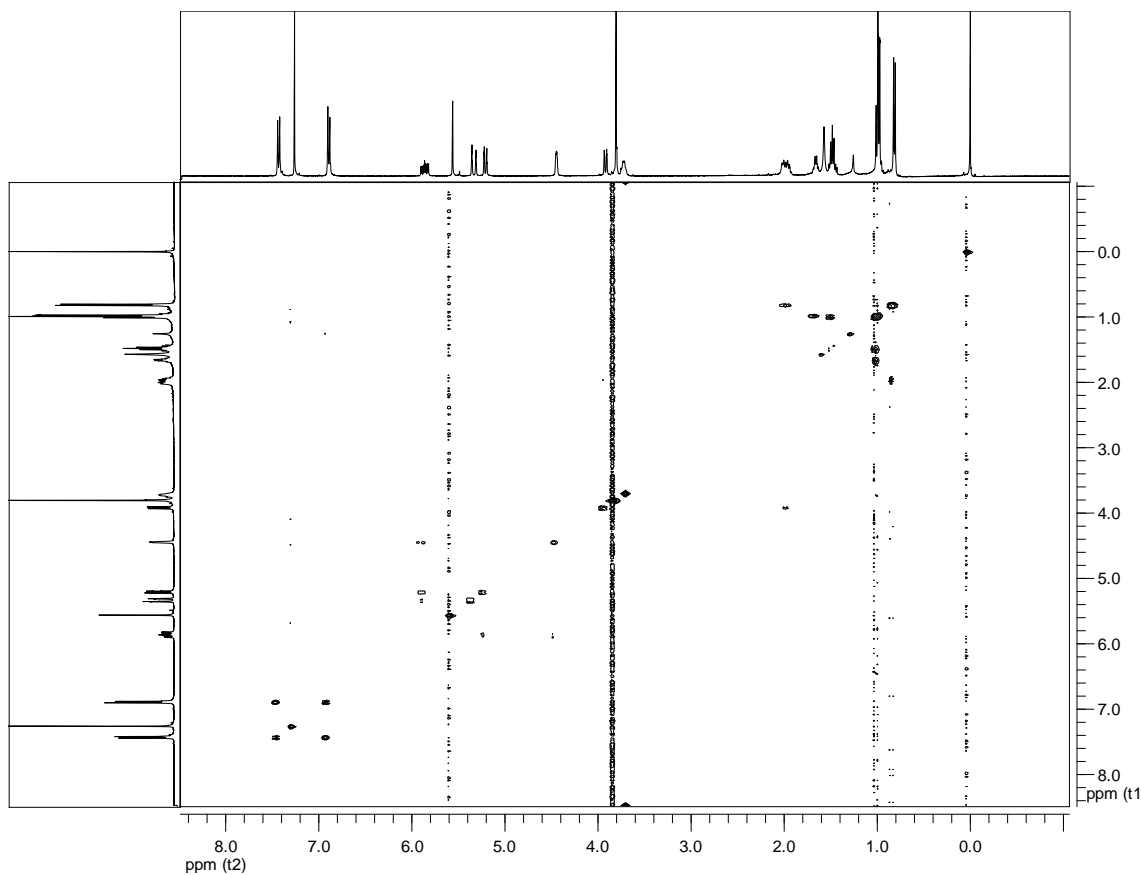






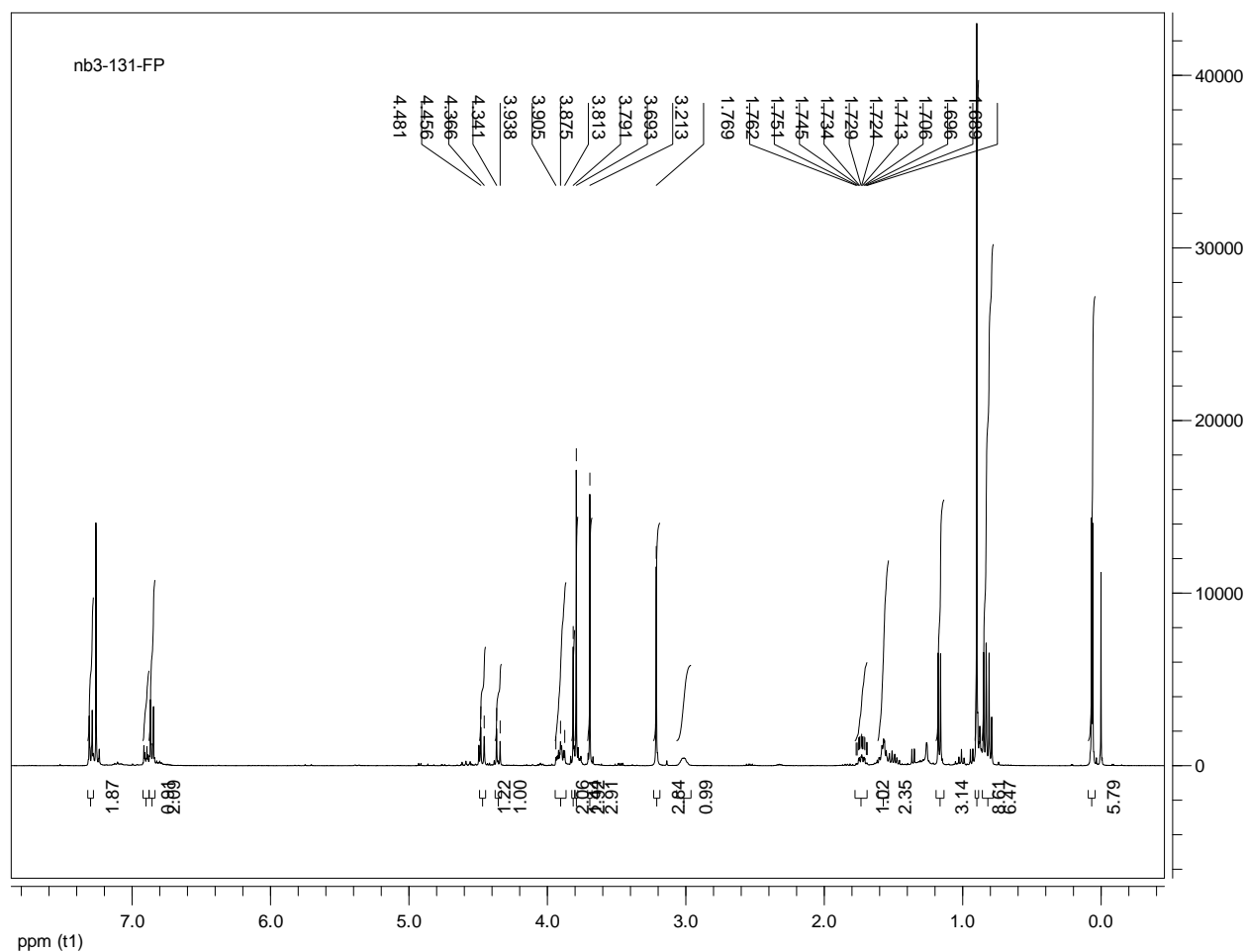
**(2S,3R)-2-((4S,5S,6R)-2-(4-Methoxyphenyl)-5-methyl-6-vinyl-1,3-dioxan-4-yl)pentan-3-ol (39-syn)**: According to the above procedure, 0.018 mmol of *tert*-butyl(((2R,3R)-2-((4R,5S,6R)-2-(4-methoxyphenyl)-5-methyl-6-vinyl-1,3-dioxan-4-yl)pentan-3-yl)oxy)dimethylsilane yielded 4.5 mg (79%) of a colourless oil.  $^1\text{H NMR}$  (400 MHz,  $\text{CDCl}_3$ )  $\delta$  (ppm) 7.43 (d, 2H,  $J = 8.7$  Hz), 6.89 (d, 2H,  $J = 8.7$  Hz), 5.86 (ddd, 1H,  $J = 4.7$  Hz,  $J = 10.8$  Hz,  $J = 17.3$  Hz), 5.56 (s, 1H), 5.33 (dt, 1H,  $J = 1.6$  Hz,  $J = 17.6$  Hz), 5.21 (dt, 1H,  $J = 1.6$  Hz,  $J = 10.8$  Hz), 4.46-4.43 (m, 1H), 3.92 (dd, 1H,  $J = 1.7$  Hz,  $J = 10.3$  Hz), 3.81 (s, 3H), 3.75-3.71 (m, 1H), 2.02-1.92 (ddd, 2H,  $J = 6.3$  Hz,  $J = 11.5$  Hz,  $J = 10.1$  Hz), 1.66 (ddd, 1H,  $J = 4.7$  Hz,  $J = 6.8$  Hz,  $J = 8.7$  Hz), 1.52-1.43 (m, 2H), 1.02-0.97 (m, 6H), 0.82 (d, 3H,  $J = 7.1$  Hz).  $^{13}\text{C}\{^1\text{H}\}$  NMR (100 MHz,  $\text{CDCl}_3$ )  $\delta$  (ppm) 159.9, 136.7, 131.2, 127.5, 115.4, 113.6, 101.1, 82.1, 81.5, 74.2, 55.3, 38.7, 33.7, 26.6, 11.2, 9.5, 6.0.

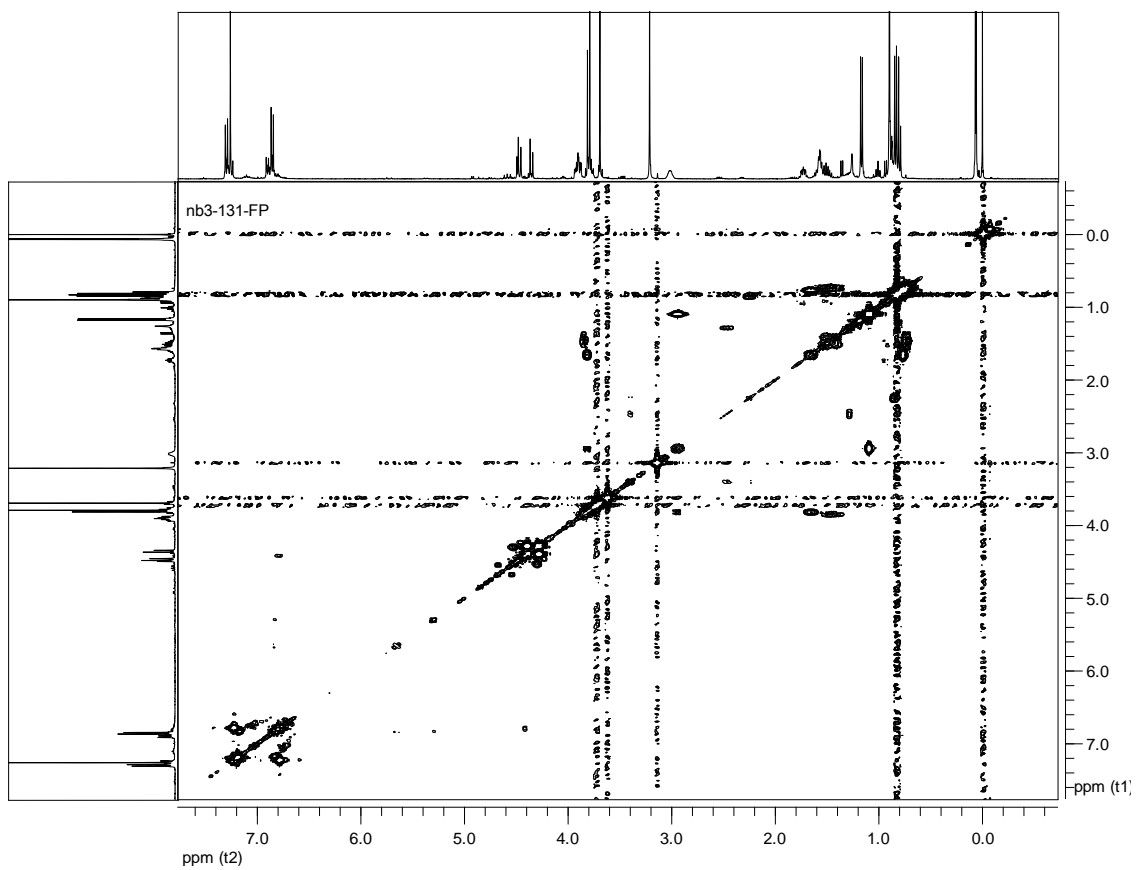
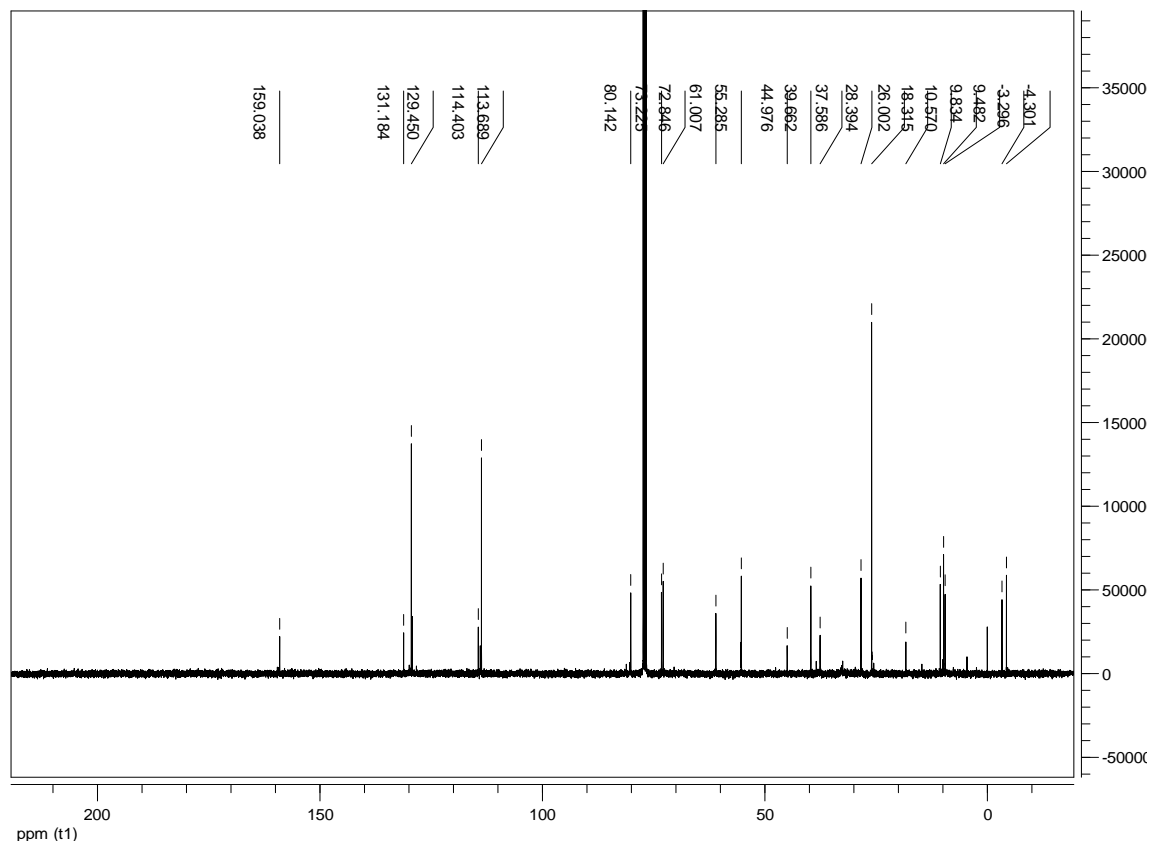




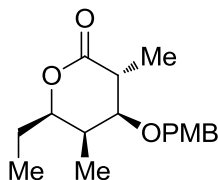
**(2R,3S,4R,5R)-5-((*tert*-Butyldimethylsilyl)oxy)-*N*-methoxy-3-((4-methoxybenzyl)oxy)-*N*,2,4-trimethylheptanamide (40):** According to a known procedure,<sup>135</sup> under anhydrous conditions, alcohol (21 mg, 0.0060 mmol) was dissolved in 0.5 mL of dry dichloromethane. At -78 °C, 4-methoxybenzyl 2,2,2-trichloroacetimidate (34 mg, 0.12 mmol) was added followed by boron trifluoride ethyl etherate (1.1  $\mu$ L, 0.009 mmol). The reaction mixture was stirred at -78 °C for 4 h when another equivalent of 4-methoxybenzyl 2,2,2-trichloroacetimidate and boron trifluoride ethyl etherate were added. The reaction mixture was stirred for a total of 8.5 h at -78 °C and was quenched with 0.5 mL of a saturated sodium bicarbonate solution. The aqueous phase was extracted three times with dichloromethane. The combined organic phases were dried over Na<sub>2</sub>SO<sub>4</sub>, filtered and evaporated. The crude product was first triturated with 5% EtOAc/hexanes to remove the insoluble trichloroacetamide. The filtrate was further purified by column

chromatography with Et<sub>3</sub>N-treated silica gel eluting with a 10% EtOAc/hexanes. 24.7 mg (88%) of a colourless oil was obtained. <sup>1</sup>H NMR (400 MHz, CDCl<sub>3</sub>) δ (ppm) 7.30 (d, 2H, *J* = 8.6 Hz), 6.86 (d, 2H, *J* = 8.6 Hz), 4.47 (d, 1H, *J* = 10.0 Hz), 4.35 (d, 1H, *J* = 10.2 Hz), 3.94-3.87 (m, 2H), 3.81 (s, 2H), 3.79 (s, 3H), 3.69 (s, 3H), 3.21 (s, 3H), 3.05-2.99 (m, 1H), 1.73 (ddd, 1H, *J* = 2.8 Hz, *J* = 7.0 Hz, *J* = 14.0 Hz), 1.60-1.45 (m, 2H), 1.17 (d, 3H, *J* = 6.9 Hz), 0.90 (s, 9H), 0.82 (m (t+d), 6H), 0.07 (s, 3H), 0.06 (s, 3H). <sup>13</sup>C{<sup>1</sup>H} NMR (100 MHz, CDCl<sub>3</sub>) δ (ppm) 159.0, 131.2, 129.4, 114.4, 113.7, 80.1, 73.2, 72.8, 61.0, 55.3, 45.0, 39.7, 37.6, 28.4, 26.0, 18.3, 10.6, 9.8, 9.5, -3.3, -4.3.

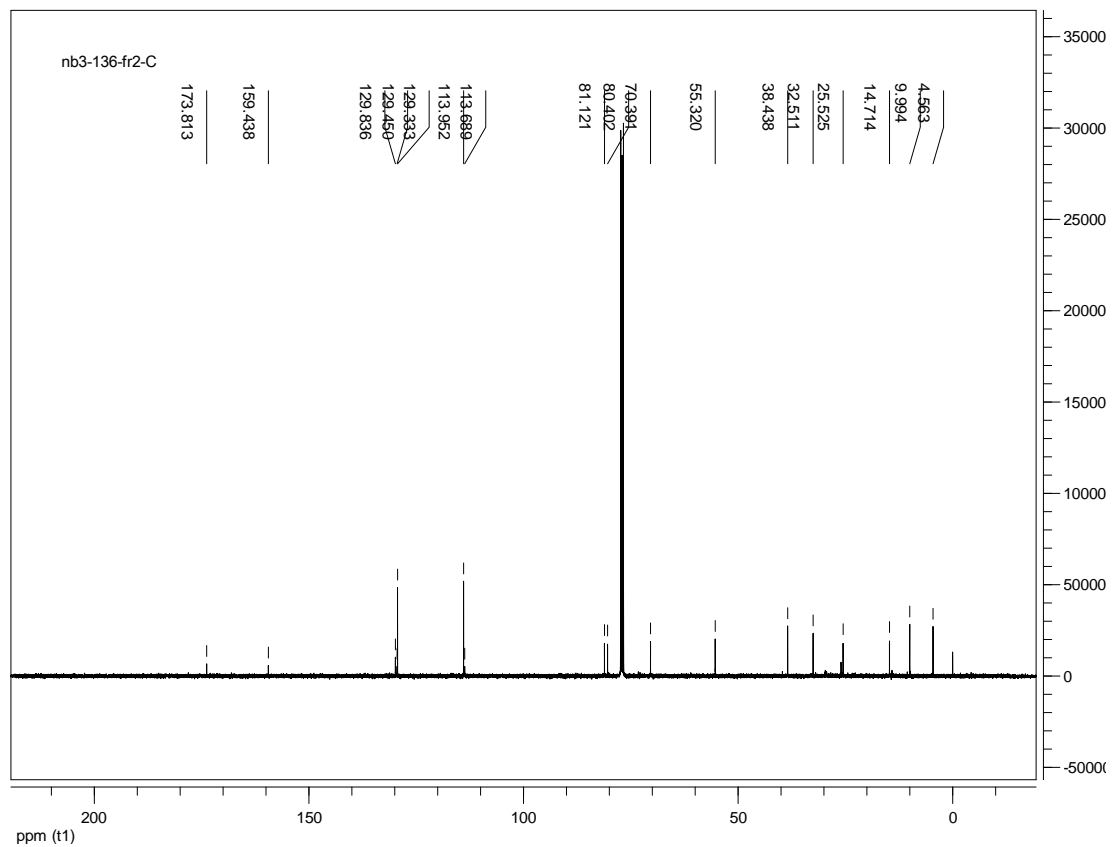
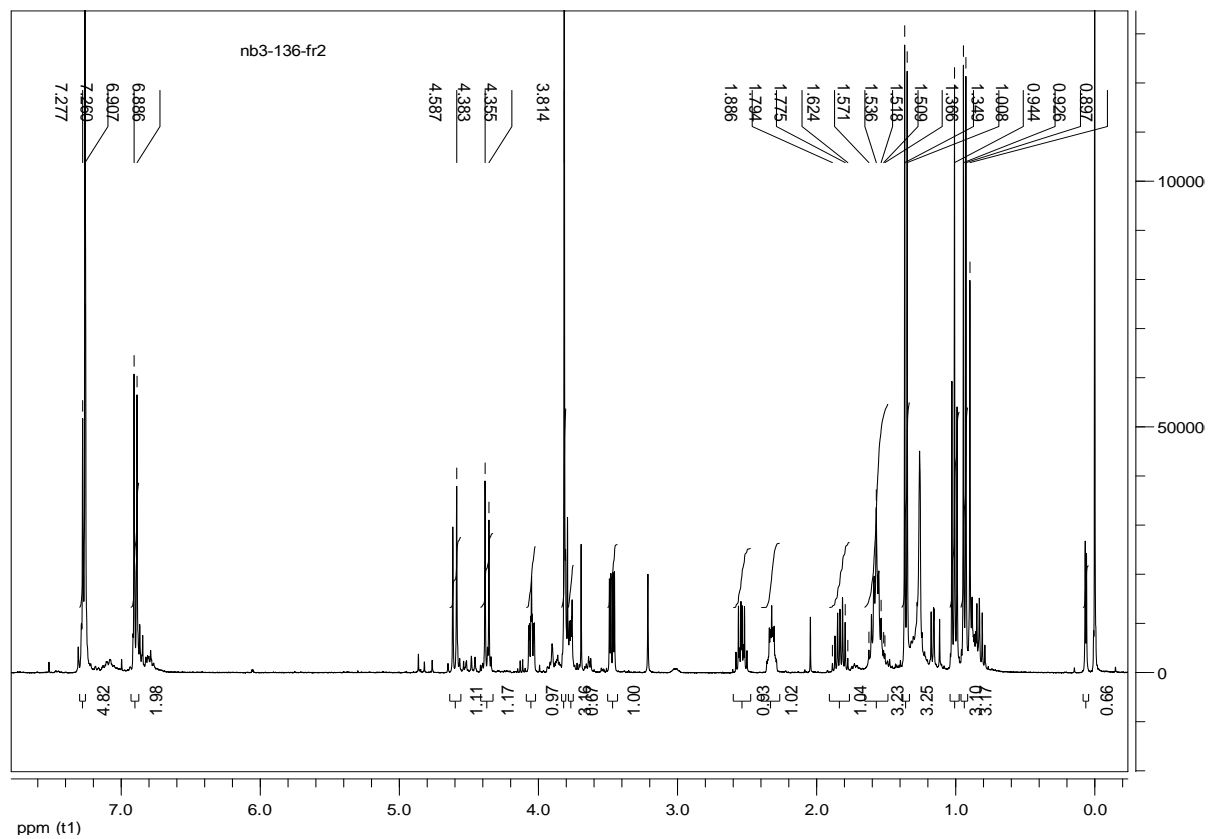


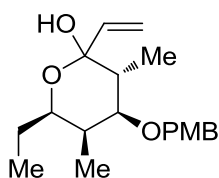
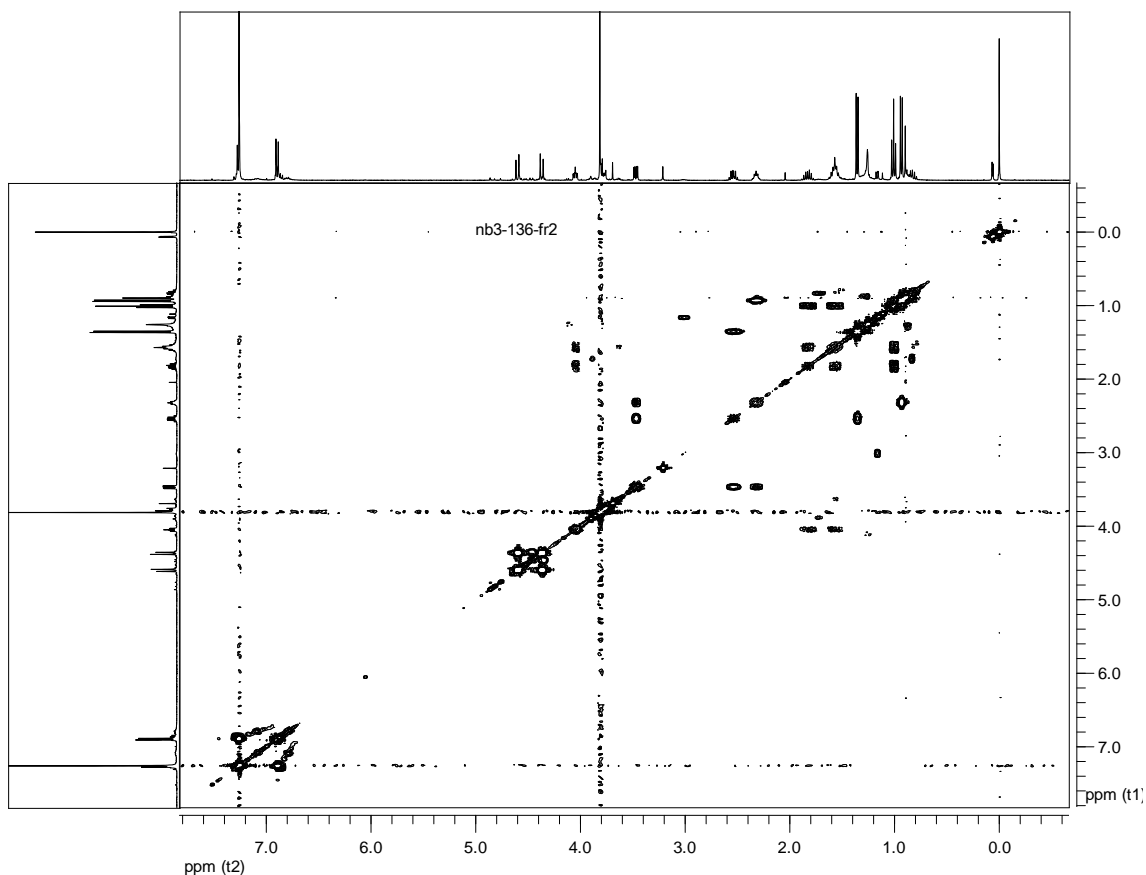






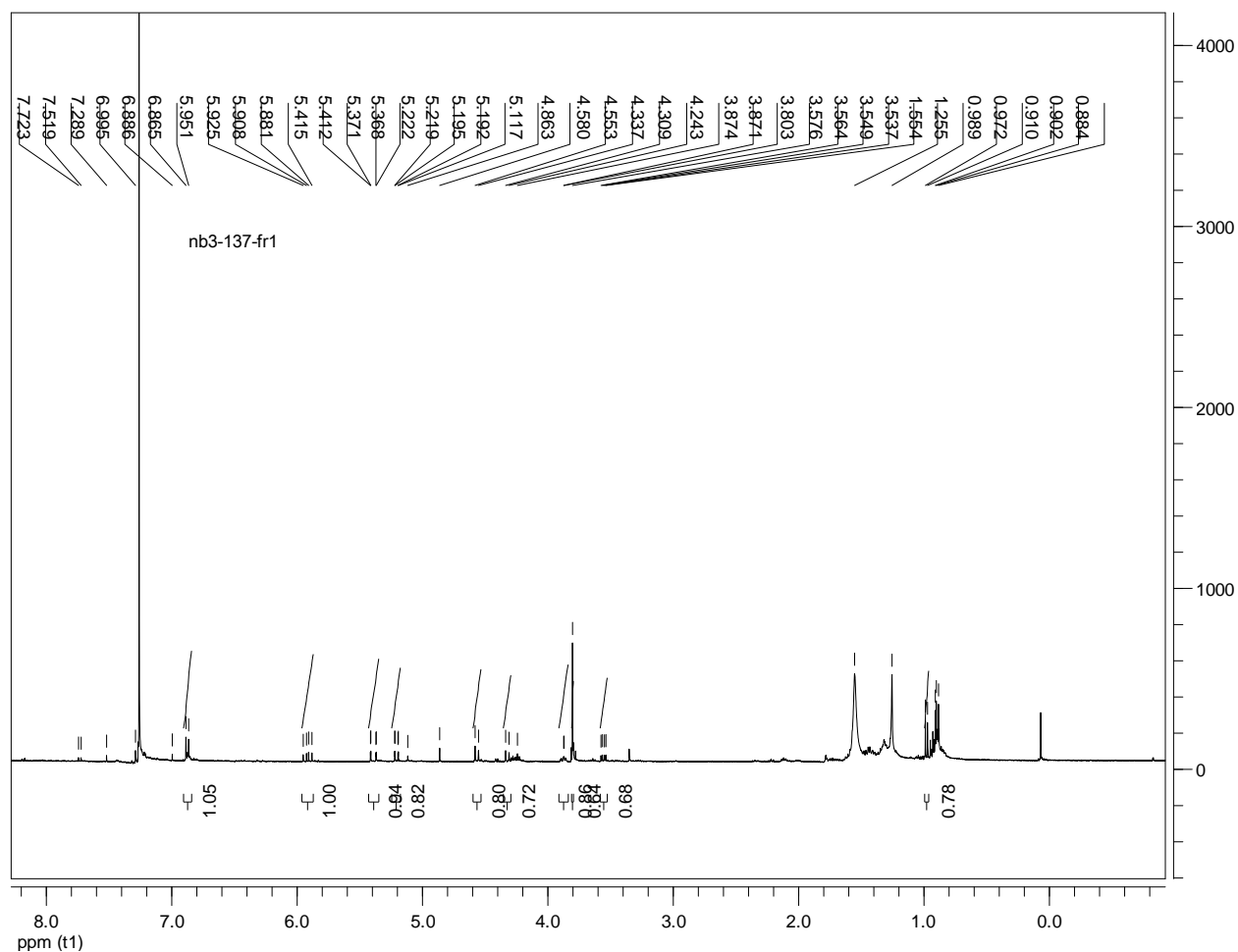
**(3R,4S,5S,6R)-6-Ethyl-4-((4-methoxybenzyl)oxy)-3,5-dimethyltetrahydro-2H-pyran-2-one (41):** In a flame dried flask, (2R,3S,4R,5R)-5-((*tert*-butyldimethylsilyl)oxy)-*N*-methoxy-3-((4-methoxybenzyl)oxy)-*N*,2,4-trimethylheptanamide (7.7 mg, 0.018 mmol) was dissolved in 1 mL of dry tetrahydrofuran. Then, a 1M solution of *tert*-butylammonium fluoride (53  $\mu$ L, 0.053 mmol) in tetrahydrofuran was added. The reaction was stirred at 65  $^{\circ}$ C for 24 h. The reaction was quenched with a saturated solution of ammonium chloride. The aqueous phase was extracted three times with ether. The combined organic phases were dried over Na<sub>2</sub>SO<sub>4</sub>, filtered and evaporated. The crude mixture was purified by a pipette column chromatography with Et<sub>3</sub>N-treated silica gel eluting with a 10% EtOAc/hexanes. 5.3 mg (28%) of a colourless oil was obtained. **<sup>1</sup>H NMR** (400 MHz, CDCl<sub>3</sub>)  $\delta$  (ppm) 7.27-7.25 (m, 2H), 6.90 (d, 2H,  $J$  = 8.6 Hz), 4.60 (d, 1H,  $J$  = 11.1 Hz), 4.37 (d, 1H,  $J$  = 11.1 Hz), 4.05 (ddd, 1H,  $J$  = 2.2 Hz,  $J$  = 6.1 Hz,  $J$  = 8.1 Hz), 3.81 (s, 3H), 3.47 (dd, 1H,  $J$  = 4.2 Hz,  $J$  = 10.3 Hz), 2.54 (qd, 1H,  $J$  = 7.1 Hz,  $J$  = 10.3 Hz), 2.32 (ddq, 1H,  $J$  = 2.3 Hz,  $J$  = 4.3 Hz,  $J$  = 6.9 Hz), 1.89-1.76 (m, 1H), 1.62-1.51 (m, 1H), 1.36 (d, 3H,  $J$  = 7.1 Hz), 1.01 (t, 3H,  $J$  = 7.5 Hz), 0.93 (d, 3H,  $J$  = 7.1 Hz). **<sup>13</sup>C{<sup>1</sup>H} NMR** (100 MHz, CDCl<sub>3</sub>)  $\delta$  (ppm) 173.8, 159.4, 129.8, 129.4, 129.3, 114.0, 113.7, 81.1, 80.4, 70.4, 55.3, 38.4, 32.5, 25.5, 14.7, 10.0, 4.6.

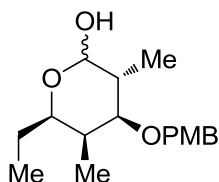
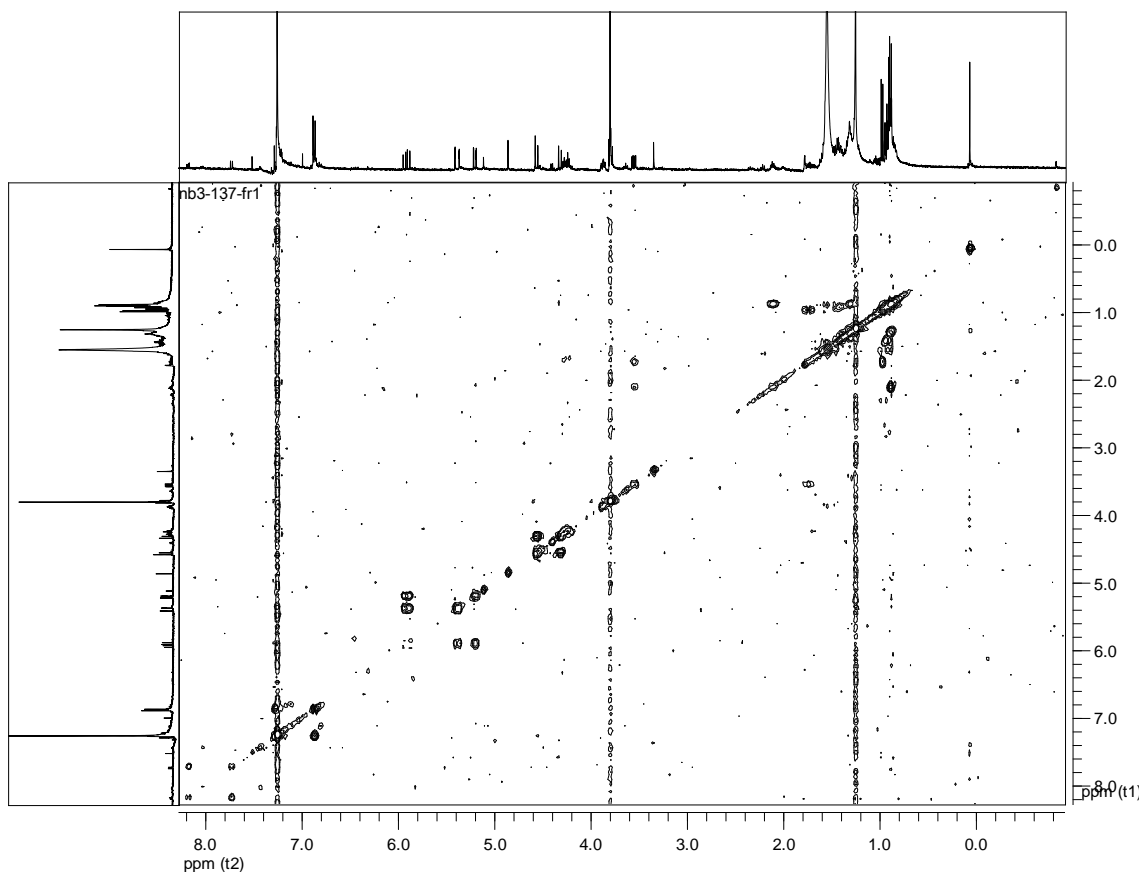




**(3R,4S,5S,6R)-6-Ethyl-4-((4-methoxybenzyl)oxy)-3,5-dimethyl-2-vinyltetrahydro-2H-pyran-2-ol (42):** According to a reported procedure<sup>136</sup>, the lactone (4.6 mg, 0.016 mmol) was dissolved in 0.1 mL of dry tetrahydrofuran. At -78 °C, a 1M solution of vinyl magnesium bromide (19  $\mu$ l, 0.019 mmol) was added dropwise via a microsyringe and the reaction was stirred first at -78 °C for 24 h, then at -40 °C for 12 h and finally at room temperature for another 12 h. The reaction was quenched with a saturated solution of ammonium chloride. The aqueous phase was extracted three times with ether. The combined organic phases were dried over Na<sub>2</sub>SO<sub>4</sub>, filtered and evaporated. The crude mixture was purified by a pipette column chromatography with Et<sub>3</sub>N-treated silica gel eluting with a 5% EtOAc/hexanes. 0.7 mg (14%) of a colourless oil was obtained. <sup>1</sup>H NMR (400 MHz, CDCl<sub>3</sub>)  $\delta$  (ppm) 7.28 (d, 2H,  $J$  = 8.7 Hz), 6.88 (d, 2H,  $J$  =

8.7 Hz), 5.92 (dd, 1H,  $J = 10.6$  Hz,  $J = 17.3$  Hz), 5.39 (dd, 1H,  $J = 1.2$  Hz,  $J = 17.3$  Hz), 5.21 (dd, 1H,  $J = 1.2$  Hz,  $J = 10.7$  Hz), 4.57 (d, 1H,  $J = 10.8$  Hz), 4.32 (d, 1H,  $J = 11.0$  Hz), 4.29-4.20 (m, 1H), 3.90-3.85 (m, 1H), 3.80 (s, 3H), 3.56 (dd, 1H,  $J = 4.7$  Hz,  $J = 10.9$  Hz), 2.22-2.10 (m, 1H), 1.78-1.64 (m, 2H), 1.46-1.34 (m, 2H), 0.98 (d, 3H,  $J = 6.7$  Hz), 0.92-0.88 (m, 5H).

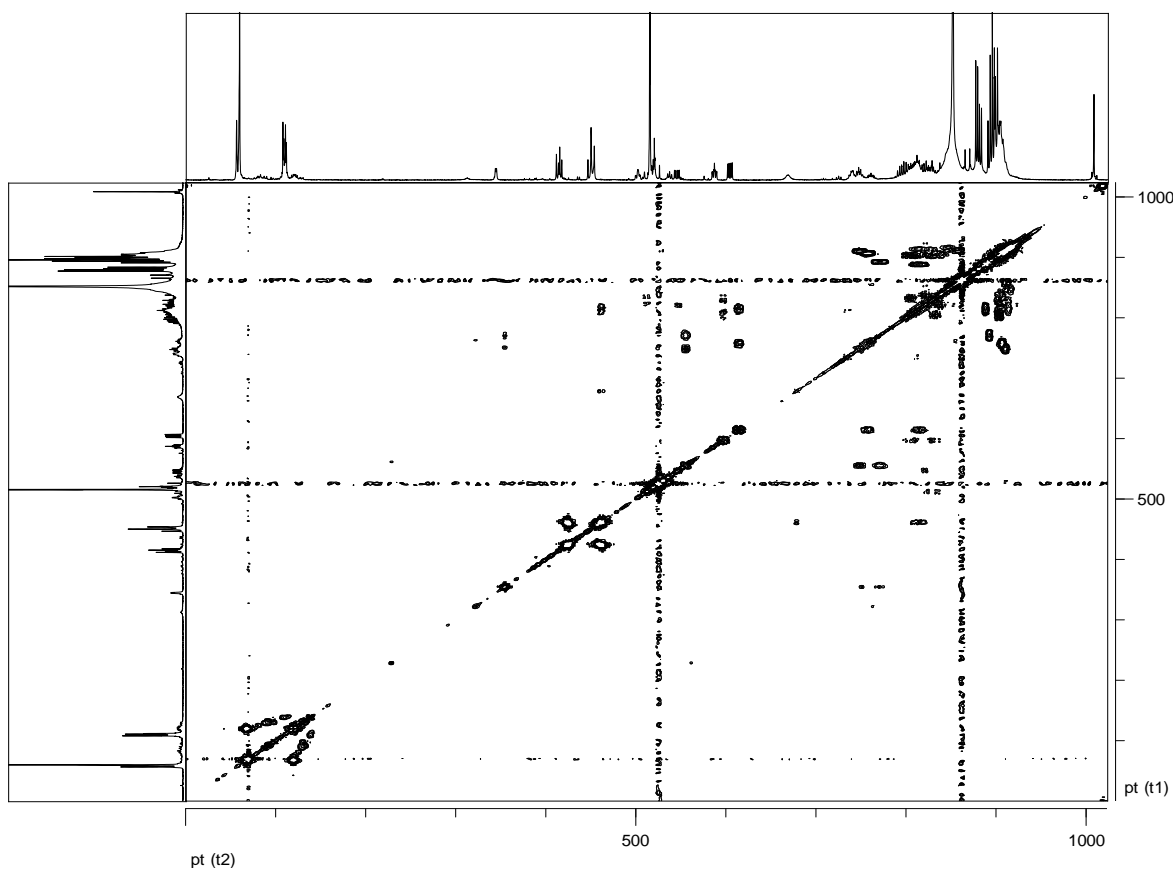
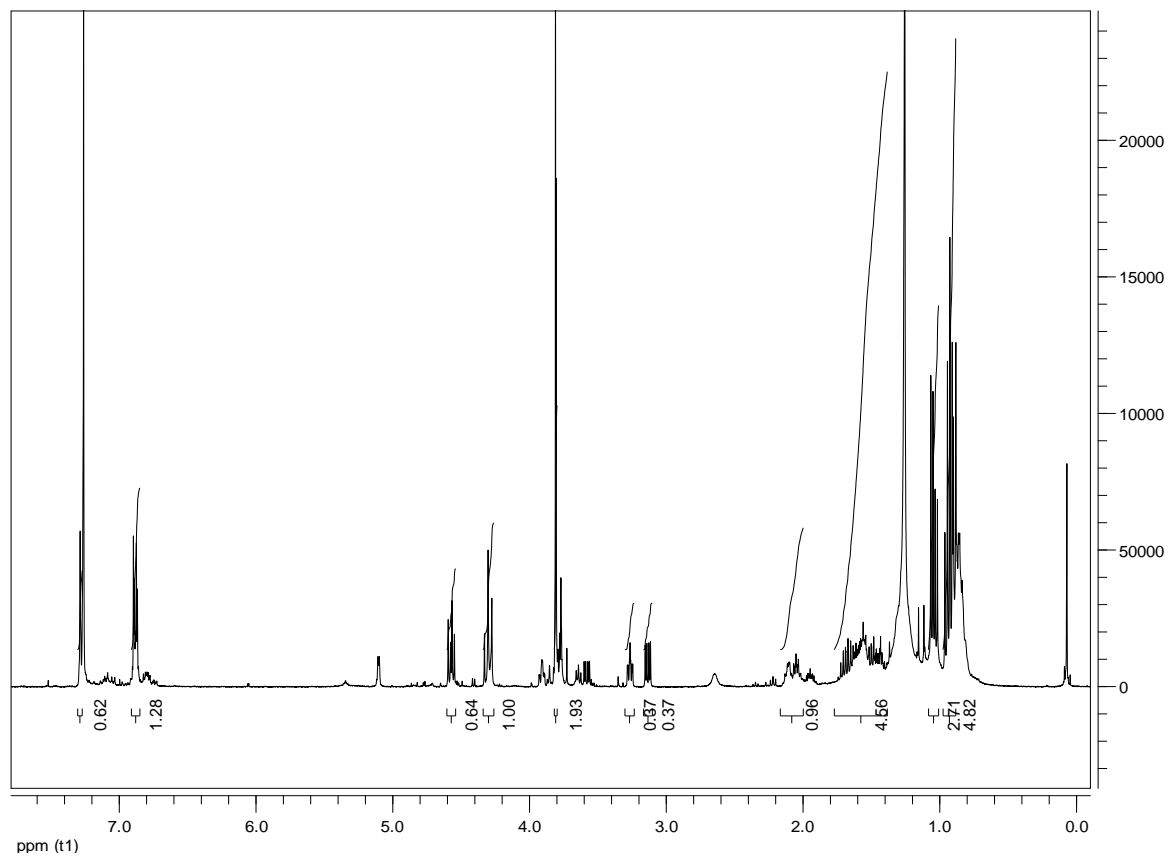




**(3R,4S,5S,6R)-6-Ethyl-4-((4-methoxybenzyl)oxy)-3,5-dimethyltetrahydro-2H-pyran-2-ol**

**(44)**: According to a known procedure,<sup>137</sup> the lactone (4.5 mg, 0.015 mmol) was dissolved in 0.2 mL of dry toluene. At  $-78\text{ }^{\circ}\text{C}$ , a 1M solution of diisobutylaluminium hydride (33  $\mu\text{L}$ , 0.033 mmol) was added and the reaction mixture was stirred at  $-78\text{ }^{\circ}\text{C}$  for 4 h. The reaction was quenched with a 20% Rochelle's salt solution and stirred for 2 h at room temperature. The aqueous phase was extracted three times with ether. The combined organic phases were dried over  $\text{Na}_2\text{SO}_4$ , filtered and evaporated. 4 mg (91%) of a colourless oil was obtained as the crude mixture.  $^1\text{H NMR}$ (400 MHz,  $\text{CDCl}_3$ )  $\delta$  (ppm) doubling of all peaks is observed at a ratio  $\sim 1:1$ .

See spectrum



## References

---

- <sup>1</sup> Yeung, C. S., Dong, V. M., *Chem. Rev.*, **2011**, *111*, 1215–1292
- <sup>2</sup> Stuart, D. R., Fagnou, K., *Science*, **2007**, *316*, 1172-1174
- <sup>3</sup> Stuart, D. R., Villemure, E., Fagnou, K., *J. Am. Chem. Soc.*, **2007**, *129*, 12072.
- <sup>4</sup> Potavathri, S., Dumas, A. S., Dwight, T. A., Naumiec, G. R., Hammann, J. M., DeBoef, B., *Tetrahedron Lett.*, **2008**, *49*, 4050.
- <sup>5</sup> Potavathri, S., Pereira, K. C., Gorelsky, S. I., Pike, A., LeBris, A. P., Deboef, B., *J. Am. Chem. Soc.*, **2010**, *132*, 14676.
- <sup>6</sup> Stuart, D. R., Villemure, E., Fagnou, K., *J. Am. Chem. Soc.*, **2007**, *129*, 12072.
- <sup>7</sup> Dwight, T. A., Rue, N. R., Charyk, D., Josselyn, R., DeBoef, B., *Org. Lett.*, **2007**, *9*, 3137
- <sup>8</sup> Malakar, C. C., Schmidt, D., Conrad, J., Beifuss, U., *Org. Lett.*, **2011**, *13*, 1378
- <sup>9</sup> Xi, P., Yang, F., Qin, S., Zhao, D., Lan, J., Gao, G., Hu, C., You, J., *J. Am. Chem. Soc.*, **2010**, *132*, 1822
- <sup>10</sup> Wang, Z., Li, K., Zhao, D., Lan, J., You, J., *Angew. Chem. Int. Ed.*, **2011**, *50*, 5365.
- <sup>11</sup> Xi, P., Yang, F., Qin, S., Zhao, D., Lan, J., Gao, G., Hu, C., You, J., *J. Am. Chem. Soc.*, **2010**, *132*, 1822
- <sup>12</sup> Han, W., Mayer, P., Ofial, A. R., *Angew. Chem. Int. Ed.*, **2011**, *50*, 2178
- <sup>13</sup> For examples of *N*-oxides in two fold C–H bond activation, see: (a) Xi, P., Yang, F., Qin, S., Zhao, D., Lan, J., Gao, G., Hu, C., You, J., *J. Am. Chem. Soc.*, **2010**, *132*, 1822, (b) Wang, Z., Li, K., Zhao, D., Lan, J., You, J., *Angew. Chem. Int. Ed.*, **2011**, *50*, 5365, (c) Han, W., Mayer, P., Ofial, A. R., *Angew. Chem. Int. Ed.*, **2011**, *50*, 2178, (d) Cho, S. H., Hwang, S. J., Chang, S., *J. Am. Chem. Soc.*, **2008**, *130*, 9254, (e) Gong, X., Song, G., Zhang, H., Li, X., *Org. Lett.*, **2011**, *13*, 1766, (f) Yamaguchi, A. D., Mandal, D., Yamaguchi, J., Itami, K., *Chem. Lett.*, **2011**, *40*, 555.

- 
- <sup>14</sup> Wei, Y., Su, W., *J. Am. Chem. Soc.*, **2010**, *132*, 16377
- <sup>15</sup> He, C.-Y., Fan, S., Zhang, X., *J. Am. Chem. Soc.*, **2010**, *132*, 12850
- <sup>16</sup> Hull, K. L., Sanford, M. S., *J. Am. Chem. Soc.*, **2007**, *129*, 11904
- <sup>17</sup> Li, B.-J., Tian, S.-L., Fang, Z., Shi, Z.-J., *Angew. Chem. Int. Ed.*, **2008**, *47*, 1115.
- <sup>18</sup> Brasche, G., García-Fortanet, J., Buchwald, S. L., *Org. Lett.*, **2008**, *10*, 2207
- <sup>19</sup> Wang, X., Leow, D., Yu, J.-Q., *J. Am. Chem. Soc.*, **2011**, *133*, 13864
- <sup>20</sup> Karthikeyan, J., Cheng, C.-H., *Angew. Chem. Int. Ed.*, **2011**, *123*, 10054–10057
- <sup>21</sup> Liégault, B., Lee, D., Huestis, M. P., Stuart, D. R., Fagnou, K., *J. Org. Chem.*, **2008**, *73*, 5022
- <sup>22</sup> Sridharan, V., Martín, M. A., Menéndez, J. C., *Eur. J. Org. Chem.*, **2009**, 4614-4621
- <sup>23</sup> Liégault, B., Lee, D., Huestis, M. P., Stuart, D. R., Fagnou, K., *J. Org. Chem.*, **2008**, *73*, 5022
- <sup>24</sup> (a) Dwight, T. A., Rue, N. R., Charyk, D., Josselyn, R., DeBoef, B., *Org. Lett.*, **2007**, *9*, 3137,  
(b) ref 23
- <sup>25</sup> Ackermann, L., Jeyachandran, R., Potukuchi, H. K., Novák, P., Büttner, L., *Org. Lett.*, **2010**, *12*, 2056
- <sup>26</sup> Pintori, D. G., Greaney, M. F., *J. Am. Chem. Soc.*, **2011**, *133*, 1209-1211
- <sup>27</sup> Kalyani, D., Sanford, M. S. *Org. Lett.*, **2005**, *7*, 4149-4152
- <sup>28</sup> Desai, L. V., Malik, H. A., Sanford, M. S. *Org. Lett.*, **2006**, *8*, 1141-1144
- <sup>29</sup> Kalberer, E. W., Whitfield, S. R., Sanford, M. S. *J. Mol. Catal. A.*, **2006**, *251*, 108-113
- <sup>30</sup> Desai, L. V., Stowers, K. J., Sanford, M. S. *J. Am. Chem. Soc.*, **2008**, *130*, 13285-13293
- <sup>31</sup> Jintoku, T., Nishimura, K., Takaki, K., Fujiwara, Y., *Chem. Lett.*, **1990**, 1687 (for corrected yields see: *Chem. Lett.* **1991**, 193)
- <sup>32</sup> Zhang, Y.-H., Yu, J.-Q., *J. Am. Chem. Soc.*, **2009**, *131*, 14654-14655



- 
- <sup>33</sup> Azumaya, I., Kagechika, H., Fujiwara, Y., Itoh, M., Yamaguchi, K., Shudo, K., *J. Am. Chem. Soc.*, **1991**, *113*, 2833 - 2838
- <sup>34</sup> Yeung, C. S., Xhao, X., Borduas, N., Dong, V. M., *Chem. Sci.*, **2010**, *1*, 331-336
- <sup>35</sup> Sun, H.-Y., Gorelsky, S. I., Stuart, D. R., Campeau, L.-C., Fagnou, K. *J. Org. Chem.*, **2010**, *75*, 8180–8189
- <sup>36</sup> Franckevicius, V., Cuthbertson, J. D., Pickworth, M., Pugh, D.S., Taylor, R. J. K., *Org. Lett.*, **2011**, *13*, 4264 - 4267
- <sup>37</sup> Dam, J. H., Osztrovsky, G., Nordstrom, L. U., Madsen, R., *Chem.--A Eur. J.*, **2010**, *16*, 6820 - 6827
- <sup>38</sup> T. Yang, C. Lin, H. Fu, Y. Jiang and Y. Zhao, *Bioorg. Chem.*, 2005, *33*, 386.
- <sup>39</sup> D. H. Hey and R. A. J. Long, *J. Chem. Soc.*, **1959**, 4110.
- <sup>40</sup> B. L. Fox and R. J. Doll, *J. Org. Chem.*, **1973**, *38*, 1136.
- <sup>41</sup> P. Grammaticakis, *Bull. Soc. Chim. Fr.*, **1965**, *3*, 848.
- <sup>42</sup> D. Crich and J.-T. Hwang, *J. Org. Chem.*, **1988**, *63*, 2765.
- <sup>43</sup> A. Correa and C. Bolm, *Angew. Chem. Int. Ed.*, **2007**, *46*, 8862.
- <sup>44</sup> R. Yamasaki, A. Tanatani, I. Azumaya, S. Saito, K. Yamaguchi and H. Kagechika, *Org. Lett.*, **2003**, *5*, 1265.
- <sup>45</sup> Liegault, B., Lee, D., Huestis, M. P., Stuart, D. R., Fagnou, K., *J. Org. Chem.*, **2008**, *73*, 5022 – 5028
- <sup>46</sup> Zhang, L., Su, S., Wu, H., Wang, S., *Tetrahedron*, **2009**, *65*, 10022 - 10024
- <sup>47</sup> Ganton, M. D., Kerr, M. A. *Org. Lett.*, **2005**, *7*, 4777 - 4779
- <sup>48</sup> Nordstrom, L. U., Vogt, H., Madsen, R., *J. Am. Chem. Soc.*, **2008**, *130*, 17672 - 17673

- 
- <sup>49</sup> He, C., Chen, C., Cheng, J., Liu, C., Liu, W., Li, Q., Lei, A., *Angew Chem Int Ed*, **2008**, *47*, 34
- <sup>50</sup> Huang, Z., Reilly, J. E., Buckle, R. N. *Synlett*, **2007**, 1026 - 1030
- <sup>51</sup> Harayami, T., Akiyama, T., Nakano, Y., Nishioka, H., Abe, H., Takeuchi, Y., *Chem. Pharm. Bull.*, **2002**, *50*, 519.
- <sup>52</sup> Lenz, G. R., *J. Org. Chem.*, **1974**, *39*, 2846.
- <sup>53</sup> González-López de Turiso, F., Curran, D. P., *Org. Lett.*, **2005**, *7*, 151.
- <sup>54</sup> Cahiez, G., Moyeux, A., Burndia, J., Duplais, C., *J. Am. Chem. Soc.*, **2007**, *129*, 13788.
- <sup>55</sup> Yeung, C. S., Zhao, X., Borduas, N., Dong, V. M., *Chem. Sci.*, **2010**, *1*, 331-336.
- <sup>56</sup> For a review on palladacycles and their use in catalysis, see: (a) Dupont, J., Consorti, C. S., Spencer, J., *Chem. Rev.*, **2005**, *105*, 2527-2571, (b) Lyons, T. W., Sanford, M. S., *Chem. Rev.*, **2010**, *110*, 1147–1169 and references there in. For a review on Pd(II)-catalyzed C—H activation, see: (c) Chen, X., Engle, K. M., Wang, D.-H., Yu, J.-Q., *Angew. Chem. Int. Ed.*, **2009**, *48*, 5094 – 5115.
- <sup>57</sup> Bercaw, J. E., Durrell, A. C., Gray, H. B., Green, J. C., Hazari, N., Labinger, J. A., Winkler, J. R., *Inorg. Chem.* **2010**, *49*, 1801-1810
- <sup>58</sup> For examples of TFA-bridged Pd-dimers, see: (a) Aloui, F., Hassine, B. B., *Tetrahedron Lett.*, **2009**, *50*, 4321-4323; (b) Roiban, D., Serrano, E., Soler, T., Grosu, I., Cativiela, C., Urriolabeitia, E. P., *Chem. Commun.*, **2009**, *31*, 4681-4683; (c) Frech, C. M., Leitus, G., Milstein, D., *Organometallics*, **2008**, *27*, 894-899; (d) Bedford, R. B., Betham, M., Charmant, J. P. H., Haddow, M. F., Orpen, A. G., Pilarski, L. T., *Organometallics*, **2007**, *26*, 6346-6353; (e) Ruddock, P. L., Williams, D. J., Reese, P. B., *Steroids*, **2004**, *69*, 193-199; (f) Stromnova, T. A., Paschenko, D. V., Boganova, L. I., Daineko, M. V., Katser, S. B., Chukarov, A. V., Kuz'mina, L. G., Howard, J. A. K., *Inorganica Chim. Acta*, **2003**, *350*, 283-288; (g) Schwarz, I., Rust, J., Lehmann, C. W., Braun, M., *J. Organomet. Chem.*, **2000**, *605*, 109-116; (h) Stromnova, T. A.,

---

Orlova, S. T., Kazyl'kin, D. N., Stolyarov, I. P., Eremenko, I. L., *Russ. Chem. Bull.*, **2000**, *49*, 150-153; (i) Vitagliano, A., Åkermark, B., Hansson, S., *Organometallics*, **1991**, *10*, 2592-2599; (j) Goddard, R., Krüger, C., Mynott, R., Neumann, M., Wilke, G., *J. Organomet. Chem.*, **1993**, *454*, C20-C25; (k) Trost, B. M., Metzner, P. J., *J. Am. Chem. Soc.*, **1980**, *102*, 3572-3577. For trimeric Pd( $\mu$ -TFA) structures see: (l) Podobedov, R. E., Stromnova, T. A., *Russ. J. Coord. Chem.*, **2008**, *34*, 780-782.

<sup>59</sup> Bercaw, J. E., Durrell, A. C., Gray, H. B., Green, J. C., Hazari, N., Labinger, J. A., Winkler, J. R., *Inorg. Chem.* **2010**, *49*, 1801-1810

<sup>60</sup> Otwinowski, Z., Minor, W., *Methods in Enzymology, Macromolecular Crystallography*, Part A edited by C. W. Carter & R. M. Sweet. London: Academic press., **1997**, *276*, 307-326

<sup>61</sup> Blessing, R. H., *Acta Cryst.*, **1995**, *A51*, 33-38.

<sup>62</sup> Sheldrick, G. M., *Acta Cryst.*, **2008**, *A64*, 112-122

<sup>63</sup> Yeung, C. S., Xhao, X., Borduas, N., Dong, V. M., *Chem. Sci.*, **2010**, *1*, 331-336

<sup>64</sup> Effenberger, F., Kottmann, H., *Tetrahedron*, **1985**, *41*, 4171-4182

<sup>65</sup> Chen, F., Yang, J., Zhang, H., Guan, C., Wan, J., *Syn. Commun.*, **1995**, *25*, 3163 – 3172.

<sup>66</sup> Kim, Y. H., Choi, H. C., *Phosphorus, Sulfur Silicon Relat. Elem.*, **1997**, *120*, 327-328

<sup>67</sup> Whang, J. P., Yang, S. G., Kim, Y. H., *Chem. Commun.*, **1997**, *15*, 1355 – 1356.

<sup>68</sup> Yang, S. G., Hwang, J. P., Park, M. Y., Lee, K., Kim, Y. H., *Tetrahedron*, **2007**, *63*, 5184–5188

<sup>69</sup> Zhang, Y.-H., Yu, J.-Q. *J. Am. Chem. Soc.*, **2009**, *131*, 14654–14655

<sup>70</sup> Alonso, D. A., Najera, C., Pastor, I. M., Yus, M. *Chem. Eur. J.*, **2010**, *16*, 5274 – 5284

<sup>71</sup> a) Ueda, S., Nagasawa, H., *Angew. Chem. Int. Ed.*, **2008**, *47*, 6411-6413; b) Ueda, S., Nagasawa, H., *J. Org. Chem.*, **2009**, *74*, 4272-4277

- 
- <sup>72</sup> Yang, S. G., Hwang, J. P., Park, M. Y., Lee, K., Kim, Y. H., *Tetrahedron*, **2007**, *63*, 5184–5188
- <sup>73</sup> Yeung, C. S., Xhao, X., Borduas, N., Dong, V. M., *Chem. Sci.*, **2010**, *1*, 331–336
- <sup>74</sup> Butler, A., Walker, J. V., *Chem. Rev.*, **1993**, *93*, 1937–1944.
- <sup>75</sup> Crampton, M. R. *Organic Reaction Mechanisms*, Knipe, A. C., Watts, W. E., Eds., Wiley: New York, NY, **2003**, 275–286.
- <sup>76</sup> (a) Taylor, R. *Electrophilic Aromatic Substitution*, Wiley: New York, NY, **1990**; (b) De la Mare, P. B. *Electrophilic Halogenation*, Cambridge University: Cambridge, **1976**, Chapter 5
- <sup>77</sup> Snieckus, V. *Chem. Rev.*, **1990**, *90*, 879–933
- <sup>78</sup> Dick, A. R., Kampf, J. W., Sanford, M. S., *J. Am. Chem. Soc.*, **2006**, *128*, 4972–4973
- <sup>79</sup> Kalyani, D., Dick, A. R., Anani, W. K., Sanford, M. S., *Tetrahedron*, **2006**, *62*, 11483–11498
- <sup>80</sup> a) Hirano, M., Monobe, H., Yakabe, S., Morimoto, T., *J. Chem. Research*, **1998**, 662–663, b) Hirano, Yakabe, S., M., Monobe, H., Clark, J. H., Morimoto, T., *J. Chem. Soc., Perkin Trans. I*, **1997**, 3081–3085
- <sup>81</sup> Wan, X., Ma, Z., Li, B., Zhang, K., Cao, S., Zhang, S., Shi, Z., *J. Am. Chem. Soc.*, **2006**, *128*, 7416–7417
- <sup>82</sup> Dick, A. R., Hull, K. L., Sanford, M. S., *J. Am. Chem. Soc.*, **2004**, *126*, 2300–2301
- <sup>83</sup> Kalyani, D., Dick, A. R., Anani, W. Q., Sanford, M. S., *Tetrahedron*, **2006**, *62*, 11483–11498
- <sup>84</sup> Bedford, R. B., Mitchell, C. J., Webster, R. L., *Chem. Commun.*, **2010**, *46*, 3095–3097
- <sup>85</sup> Bedford, R. B., Haddow, M. F., Mitchell, C. J., Webster, R. L., *Angew. Chem. Int. Ed.*, **2011**, *50*, 5524–5527
- <sup>86</sup> Wan, X., Ma, Z., Li, B., Zhang, K., Cao, S., Zhang, S., Shi, Z., *J. Am. Chem. Soc.*, **2006**, *128*, 7416–7417

- 
- <sup>87</sup> Mulzer, J., *Angew. Chem. Int. Ed.*, **1991**, *30*, 1452-1454
- <sup>88</sup> Khosla, C., Tang, Y., Chen, A. Y., Schnarr, N. A., Cane, D.E. *Annu. Rev. Biochem.*, **2007**, *76*, 195-221
- <sup>89</sup> Staunton, J., Wilkinson, B., *Chem. Rev.*, **1997**, *97*, 2611-2629
- <sup>90</sup> Staunton, J., Wilkinson, B., *Chem. Rev.*, **1997**, *97*, 2611-2629
- <sup>91</sup> Masamune, S., Hiramama, M., Mori, S., Ali, S. A., Garvey, D. S., *J. Am. Chem. Soc.*, **1981**, *103*, 1568-1571
- <sup>92</sup> Myles, D. C., Danishefsky, S. J., *J. Org. Chem.*, **1990**, *55*, 1636-1648
- <sup>93</sup> Evans, D. A., Kim, A. S., Metternich, R., Novack, V. J., *J. Am. Chem. Soc.*, **1998**, *120*, 5921-5942
- <sup>94</sup> Stang, E. M., White, M. C., *Nature Chem.*, **2009**, *1*, 547-551
- <sup>95</sup> Crimmins, M. T., Slade, D. J., *Org. Lett.*, **2006**, *8*, 2191-2194
- <sup>96</sup> Stang, E. M., White, M. C., *Nature Chem.*, **2009**, *1*, 547-551
- <sup>97</sup> Zheng, J., Taylor, C. A., Piasecki, S. K., Keatinge-Clay, A. T. *Structure*, **2010**, *18*, 913-922
- <sup>98</sup> Pohl, N. L., Gokhale, R. S., Cane, D. E., Khosla, C., *J. Am. Chem. Soc.*, **1998**, *120*, 11206-11207
- <sup>99</sup> For selected examples of syn-aldol anti-Felkin selectivity see: a) Lister, T., Perkins, M. V., *Angew. Chem. Int. Ed.*, **2006**, *45*, 2560-2564, b) Perkins, M. V., Sampson, R. A., Joannou, J., Taylor, M. R., *Tetrahedron Lett.*, **2006**, *47*, 3791-3795, c) Sampson, R. A., Perkins, M. V., *Org. Lett.*, **2002**, *4*, 1655-1658, d) Yang, G., Myles, D. C., *Tetrahedron Lett.*, **1994**, *35*, 1313-1316, e) Paterson, I., Chen, D. Y.-K., Coster, M. J., Acena, J. L., Bach, J., Gibson, K. R., Keown, L. E., Oballa, R. M., Trieselmann, T., Wallace, D. J., Hodgson, A. P., Norcross, R. D., *Angew. Chem. Int. Ed.*, **2001**, *40*, 4055-4060

---

<sup>100</sup> (a) Stiles, M., Winkler, R. R., Chang, Y.-L., Traynor, L., *J. Am. Chem. Soc.* **1964**, *86*, 3337-3342; (b) House, H. O., Crumrine, D. S., Teranishi, A. Y., Olmstead, H. D., *J. Am. Chem. Soc.* **1973**, *95*, 3310-3324; (c) Heathcock, C. H., Buse, C. T., Kleschick, W. A., Pirrung, M. C., Sohn, J. E., Lampe, J., *J. Org. Chem.*, **1980**, *45*, 1066-1081; (d) Mukaiyama, T., Banno, K., Narasaka, K., *J. Am. Chem. Soc.* **1974**, *96*, 7503-7509

<sup>101</sup> a) Toshima, K., Jyojima, T., Miyamoto, N., Katohno, M., Nakata, M., Matsumura, S., *J. Org. Chem.*, **2001**, *66*, 1708-1715, b) Toshima, K., Yamaguchi, H., Jyojima, T., Noguchi, Y., Nakata, M., Matsumura, S., *Tetrahedron Lett.*, **1996**, *37*, 1073-1076, c) Evans, D. A., Calter, M. A., *Tetrahedron Lett.*, **1993**, *34*, 6871-6874

<sup>102</sup> Woodward and coworkers, *J. Am. Chem. Soc.*, **1981**, *103*, 3213-3215

<sup>103</sup> Jin, J., Chen, Y., Li, Y., Wu, J., Dai, W.-M., *Org. Lett.*, **2007**, *9*, 2585 and references therein.

<sup>104</sup> For examples of attempted RCM's to form tri-substituted olefins, see: a) Hoye, T. R., Zhao, H. *Org. Lett.*, **1999**, *1*, 169. b) Andrus, M. B., Meredith, E. L., Hicken, E. J., Simmons, B. L., Glancey, R. R., Ma. W. *J. Org. Chem.*, **2003**, *68*, 8162. c) Wilson, M. S., Woo, J. C. S., Dake, G. R. *J. Org. Chem.*, **2006**, *71*, 4237. d) Helmboldt, H., Köhler, D., Hiersemann, M. *Org. Lett.*, **2006**, *8*, 1573.

<sup>105</sup> a) Jin, J., Chen, Y., Li, Y., Wu, J., Dai, W.-M., *Org. Lett.*, **2007**, *9*, 2585, b) Xu, Z., Johannes, C. W., Houri, A. F., La, D. S., Cogan, D. A., Hofilena, G. E., Hoveyda, A. H. *J. Am. Chem. Soc.*, **1997**, *11*, 10302, c) May, S. A., Grieco, P. A. *Chem. Commun.*, **1998**, 1597, d) Smith, A. B., III, Mesaros, E. F., Meyer, E. A. *J. Am. Chem. Soc.*, **2006**, *128*, 5292.

<sup>106</sup> Kalaitzakis, D., Kambourakis, S., Rozzell, D. J., Smonou, I., *Tetrahedron: Assym.*, **2007**, *18*, 2418-2426

<sup>107</sup> Magdziak, D., Lalic, G., Lee, H. M., Fortner, K. C., Aloise, A. D., Shair, M. D. *J. Am. Chem. Soc.*, **2005**, *127*, 7284-7285

- 
- <sup>108</sup> Niwayama, S., Cho, H., Lin, C., *Tetrahedron Letters*, **2008**, *49*, 4434-4436
- <sup>109</sup> Niwayama, S., Cho, H., Lin, C., *Tetrahedron Letters*, **2008**, *49*, 4434-4436
- <sup>110</sup> Niwayama, S., Cho, H., Lin, C., *Tetrahedron Letters*, **2008**, *49*, 4434-4436
- <sup>111</sup> Brandaenge, S., Leijonmarck, H., Oelund, J., *Acta Chem. Scand.*, **1989**, *43*, 193-195
- <sup>112</sup> Bohman, B., Unelius, C. R., *Tetrahedron*, **2009**, *65*, 8697-8701
- <sup>113</sup> Christoffers, J., Kauf, T., Werner, T., Roessle, M., *Eur. J. Org. Chem.*, **2006**, *11*, 2601-2608
- <sup>114</sup> Danieli, B., Lesma, G., Palmisano, G., Passarella, D., Silvani, A., *Tetrahedron*, **1994**, *50*, 6941-6954
- <sup>115</sup> Brandaenge, S., Leijonmarck, H., Oelund, J., *Acta Chem. Scand.*, **1989**, *43*, 193-195
- <sup>116</sup> Zhang, Y.-H., Song, K., Zhu, N.-Y., Yang, D., *Chem. Eur. J.*, **2010**, *16*, 577-587
- <sup>117</sup> *Organic Syntheses*, **1985**, *63*, 1-5
- <sup>118</sup> Hughes, A. J., Keatinge-Clay, A. T., *Chemistry & Biology*, **2011**, *18*, 165-176
- <sup>119</sup> Pohl, N. L., Gokhale, R. S., Cane, D. E., Khosla, C., *J. Am. Chem. Soc.*, **1998**, *120*, 11206-11207
- <sup>120</sup> Sung, K., Wu, S. Y., *Synth. Commun.*, **2001**, *31*, 3069-3074
- <sup>121</sup> Samsung Total Petrochemicals, Patent US**2010**/298509 A1
- <sup>122</sup> Glufke, U., Hanselmann, P., Patent: US2003/171622, A1, **2003**
- <sup>123</sup> Hagiwara, T., Mochizuki, H., Fuchikami, T., *Synlett*, **1997**, 587
- <sup>124</sup> Boije af Genn, G., Talman, V., Aitio, O., Ekokoski, E., Finel, M., Tuominen, R. K., Yli-Kauhaluoma, J., *J. Med. Chem.*, **2009**, *52*, 3969-3981
- <sup>125</sup> May, A. E., Willoughby, P. H., Hoye, T. R., *J. Org. Chem.*, **2008**, *73*, 3292-3294

- 
- <sup>126</sup> Gage, J. R., Evans, D. A., *Org. Syn.*, **1990**, *168*, 83-88
- <sup>127</sup> Cane, D. E., Tan, W., Ott, W. R., *J. Am. Chem. Soc.*, **1993**, *115*, 527-535
- <sup>128</sup> Cane, D. E., Tan, W., Ott, W. R., *J. Am. Chem. Soc.*, **1993**, *115*, 527-535
- <sup>129</sup> Cane, D. E., Tan, W., Ott, W. R., *J. Am. Chem. Soc.*, **1993**, *115*, 527-535
- <sup>130</sup> (a) Stiles, M., Winkler, R. R., Chang, Y.-L., Traynor, L., *J. Am. Chem. Soc.* **1964**, *86*, 3337-3342; (b) House, H. O., Crumrine, D. S., Teranishi, A. Y., Olmstead, H. D., *J. Am. Chem. Soc.* **1973**, *95*, 3310-3324; (c) Heathcock, C. H., Buse, C. T., Kleschick, W. A., Pirrung, M. C., Sohn, J. E., Lampe, J., *J. Org. Chem.*, **1980**, *45*, 1066-1081; (d) Mukaiyama, T., Banno, K., Narasaka, K., *J. Am. Chem. Soc.* **1974**, *96*, 7503-7509
- <sup>131</sup> Mandal, A. K., *Org. Lett.*, **2002**, *4*, 2043-2045
- <sup>132</sup> Toshima, K., Jyojima, T., Miyamoto, N., Katohno, M., Nakata, M., Matsumura, S., *J. Org. Chem.*, **2001**, *66*, 1708- 1715
- <sup>133</sup> Evans, D. A., Trenkle, W. C., Zhang, J., Burch, J. D., *Org. Lett.*, **2005**, *7*, 3335-3338
- <sup>134</sup> Evans, D. A., Kim, A. S., Metternich, R., Novack, V. J., *J. Am. Chem. Soc.*, **1998**, *120*, 5921-5942
- <sup>135</sup> Chandra, B., Fu, D., Nelson, S. G., *Angew. Chem. Int. Ed.*, **2010**, *49*, 2591-2594
- <sup>136</sup> Cai, X.-C., Wu, X., Sinder, B. B., *Org. Lett.*, **2010**, *12*, 1600-1603
- <sup>137</sup> Berkenbusch, T., Brueckner, R., *Chem.-A Eur. J.*, **2004**, *10*, 1545-1557